COASTAL STRUCTURES HANDBOOK SERIES

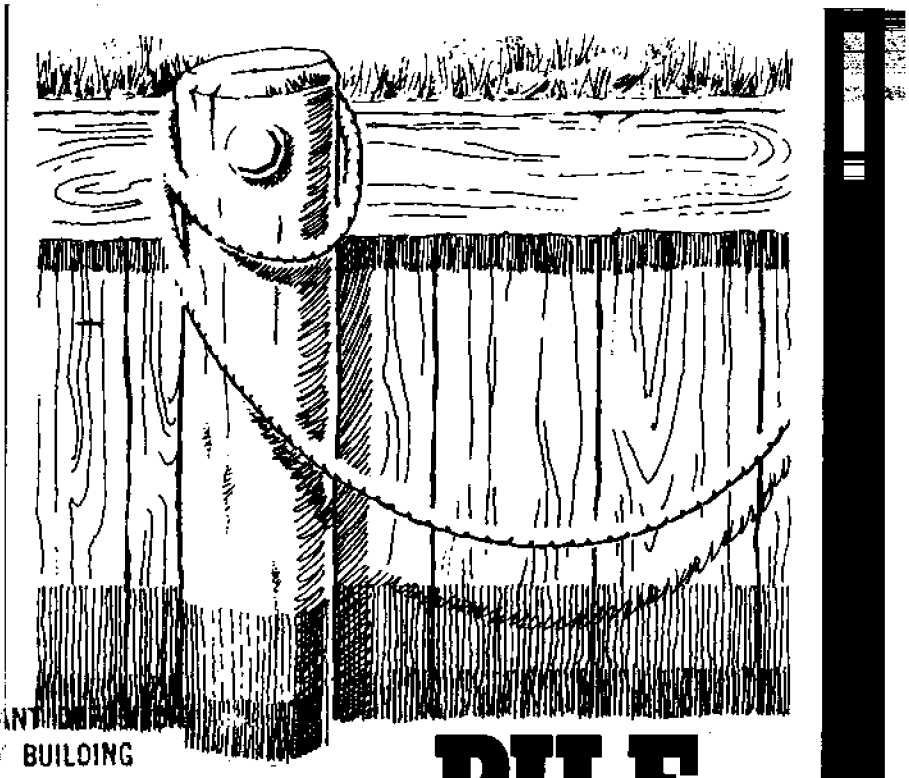

PILE FOUNDATIONS

Francis K.-P. Cheung
and Fred H. Kulhawy

NEW YORK SEA GRANT INSTITUTE

FIRST IMPRESSION

This manual is part of the Coastal Structures Handbook Series. The series is being prepared for the New York Sea Grant Institute by the Geotechnical Engineering group at Cornell University, coordinated by Fred H. Kulhawy.

COVER DESIGN: DICK GORDON

Communications
New York Sea Grant Institute
State University of New York
and Cornell University
411 State Street
Albany, New York 12246

COASTAL STRUCTURES HANDBOOK SERIES
PILE FOUNDATIONS

Francis K.-P. Cheung

and

Fred H. Kulhawy

School of Civil and Environmental Engineering

Cornell University

Ithaca, New York

1982

This research was sponsored by the New York Sea Grant Institute under a grant (NA81AA-D-00027) from the Office of Sea Grant, National Oceanic and Atmospheric Administration (NOAA), US Department of Commerce.

ABSTRACT

This study focuses primarily on the design and construction of pile foundations in the coastal regime. The discussions are separated into four parts. In the first part, an assessment is made of the nature and intensities of loads acting on piles. Second, the design principles and methodologies for the various types of loads (compressive, uplift and lateral) are outlined. Considerations are also given to scour, pile buckling, bent piles and downdrag. Third, the three materials (concrete, steel and wood) commonly used for piles are discussed, concentrating on the potential problems in their use and the appropriate preventive measures. Finally, the methods of installation of piles are described. The emphasis of this study is on conventional design procedures and practical techniques.

TABLE OF CONTENTS

LIST OF TABLES

LIST OF FIGURES

LIST OF SYMBOLS

English Letters

A	- cross-sectional area of pile
A_p	- area of pile point or tip
A_s	- area of pile shaft embedded in soil
B_g	- width of pile group
B'_g	- equivalent width of pile group
C	- seismic coefficient
C_D	- drag coefficient
C_L	- lift coefficient
C_M	- inertial coefficient
$\bar{c}$	- effective cohesion
c_f	- end-restraint coefficient
c_u	- undrained shear strength of soil
c_α	- pile-soil adhesion strength
D	- diameter of pile
d	- distance between still water level and mudline
E_p	- Young's modulus of pile material
E_u	- undrained Young's modulus of soil
e	- distance of lateral loads above the ground-line
$\bar{e}$	- eccentricity of loading
F_D	- total horizontal drag force on pile
F_i	- total horizontal inertial force on pile
F_m	- maximum total wave force on pile
F_{Dm}	- maximum total horizontal drag force on pile
F_{im}	- maximum total horizontal inertial force on pile

F_{Lm} - maximum total lift force on pile

FS - factor of safety

f - total horizontal force per unit length of pile

f_D - drag force per unit length of pile

f_i - inertial force per unit length of pile

f_L - lift force per unit length of pile

f_m - maximum wave force per unit length of pile

f_s - average ultimate shaft resistance per unit area

G_s - shear modulus of soil

g - gravitational acceleration

H - wave height

H_b - breaking wave height

I_p - moment of inertia of cross-section of pile

I_r - rigidity index

I_{rr} - reduced rigidity index

J_R - dimensionless parameter for unsupported portion of piles in soils with constant modulus

J_T - dimensionless parameter for unsupported portion of piles in soils with linearly increasing modulus

K - soil stress coefficient

K_D - dimensionless parameter for total drag force

K_i - dimensionless parameter for total inertial force

K_o - soil stress coefficient at rest

K_p - passive soil stress coefficient

K_u - soil stress coefficient for uplift

K^* - energy-absorbing capacity of structure for earthquakes

K_{Dm} - dimensionless parameter for maximum total drag force

K_{im} - dimensionless parameter for maximum total inertial force

k - energy-absorbing coefficient for ship impact; $k_h D$

k_h - horizontal subgrade modulus

L - wavelength; length of embedment of pile

L_A - Airy approximation of wavelength

L_c - critical depth

L_e - equivalent length of the pile

L_g - length of pile group

L_o - deepwater wavelength

L_s - equivalent length of embedded portion of pile

L_u - length of unsupported portion of pile

ΔL - distance between two points on a pile

ℓ_{max} - dimensionless length parameter for fully embedded piles in soils with constant modulus

M_D - moment of drag force about the mudline

M_i - moment of inertial force about the mudline

M_m - maximum total moment about the mudline

M_{Dm} - maximum moment about the mudline because of drag force component

M_{im} - maximum moment about the mudline because of inertial force component

M_{max} - maximum bending moment in a pile

M_{yield} - yield moment of pile

m - number of piles in a row

m_s - mass of ship

N_c - bearing capacity factor with respect to cohesion

N_q - bearing capacity factor with respect to overburden stress

N_σ - bearing capacity factor with respect to mean normal effective stress

N_γ - bearing capacity factor for pile foundations with pile cap in contact with ground

n - number of rows of piles in a pile group

n_h - coefficient of modulus variation

OCR - overconsolidation ratio

P - lateral load

P_e - horizontal earthquake excitation force

P_s - ship impact force

P_{ult} - ultimate lateral load

p - soil reactive stress

p_{all} - allowable soil reaction stress

p_{max} - maximum soil reaction along the deflected pile

Q - compressive load

Q_d - downdrag load

Q_p - ultimate point resistance

Q_s - ultimate shaft resistance

Q_{cr} - critical buckling load

Q_{all} - allowable compressive load

Q_{ult} - ultimate compressive load

q_ℓ - limiting value on unit point resistance below the critical depth for piles in sand

q_p - average ultimate point resistance per unit area

R - $\sqrt[5]{E_p I_p / k_h D}$

R_e - Reynolds Number

S_D - dimensionless parameter for moment of drag force

S_i - dimensionless parameter for moment of inertial force

S_R - dimensionless parameter for embedded portion of piles in soils with constant modulus

S_T - dimensionless parameter for embedded portion of piles in soils with linearly increasing modulus

S_{Dm} - dimensionless parameter for moment of maximum drag force

S_{im} - dimensionless parameter for moment of maximum inertial force

s - center to center spacing of piles

T - wave period; $\sqrt[5]{E_p I_p / n_h}$

T_n - natural period of vibration

T_{ult} - ultimate uplift load

t - time

t_{100} - time duration for consolidation settlement

U_{cr} - dimensionless buckling parameter for fully embedded piles in soils with constant modulus

u - horizontal water particle velocity

u_{max} - maximum horizontal velocity at still water level

$\bar{u}_{max}$ - average maximum horizontal velocity over the submerged length of the pile

V_{cr} - dimensionless buckling parameter for fully embedded piles in soils with linearly increasing modulus

v_s - speed of ship at impact

W - $C_M D/C_D H$

W_p - net weight of pile

W_T - total effective weight of structure

x - horizontal coordinate axis in the direction of wave propagation

y - pile deflection

y_o - pile deflection at ground-line

y_{max} - maximum pile deflection

Z - section modulus of the cross-section of pile

z - vertical coordinate axis, origin at still water level, positive upwards; distance below ground-line

z_{max} - dimensionless length parameter for fully embedded piles in soils with linearly increasing modulus

Greek Letters

α - empirical coefficient for adhesion in terms of c_u

α_m - coefficient for determination of maximum total moment about the mudline

β - K tan δ; $\sqrt[4]{k_h D/4E_p I_p}$

γ - unit weight of water

$\bar{\gamma}_s$ - submerged unit weight of soil

δ - angle of friction between pile and soil

η - efficiency factor; $\sqrt[5]{n_h/E_p I_p}$

θ - $\frac{2\pi x}{L} - \frac{2\pi t}{T}$

θ_a - inclination of pile at point a

θ_b - inclination of pile at point b

λ - empirical coefficient for adhesion in terms of $\bar{\sigma}_v + 2c_u$

υ - kinematic viscosity of water

ξ_v - volume change factor

$\bar{\sigma}_o$ - mean normal effective stress

$\bar{\sigma}_v$ - effective vertical stress

$\bar{\sigma}_{vp}$ - effective vertical stress at the pile tip

σ_{max} - yield stress of pile material

τ_a - limiting pile-soil adhesion

ϕ - arc tan (D/s)

$\bar{\phi}$ - effective angle of internal friction of soil

ϕ_m - coefficient for determination of maximum total wave force

Δ - average volumetric strain in the plastic zone at failure

LIST OF CONVERSION FACTORS

To Convert From	To	Multiply By
t_F	t_c	$t_c = \frac{5}{9}(t_F - 32°)$
inch	mm	25.4
feet	meter	0.3048
lb	Newton	4.448
lb/in^2	kN/m^2	6.895
lb/ft	N/m	14.59
lb/ft^2	kN/m^2	0.0479
lb/ft^3	kN/m^3	0.1571
lb-ft	N-m	1.356
ft^2/sec	m^2/sec	0.0929

CHAPTER 1

INTRODUCTION

The expansion of man's activities has led to an increase in coastal construction along the shoreline. Waterfront structures that are commonly seen include docks, piers, bulkheads, seawalls and other elevated structures that provide commercial as well as recreational facilities. The foundations for these types of structures often take the form of piling. A few examples on the use of piles in the coastal region are illustrated in Fig. 1.1.

Piles are structural members used to transmit surface loadings to the subsoil. They may act singly (e.g., fender piles) or in groups (e.g., pier); they may be fully embedded (e.g., retaining structures) or partially embedded (e.g., dolphin). Furthermore, advancement in installation equipment has allowed these members to be driven in any desired orientation. The versatility of pile foundations has made them adaptable to most types of conditions and requirements.

The use of pile foundations dates back to prehistoric times, long before the birth of soil mechanics. Construction was largely based on experience with little theoretical considerations. In recent years, a large volume of technical literature has been published with regard to this subject matter.

Loadings that may act upon a waterfront structure include, but are not limited to, waves, currents, ice, earthquakes, wind and ship impact (Fig. 1.2). These various forms of loadings

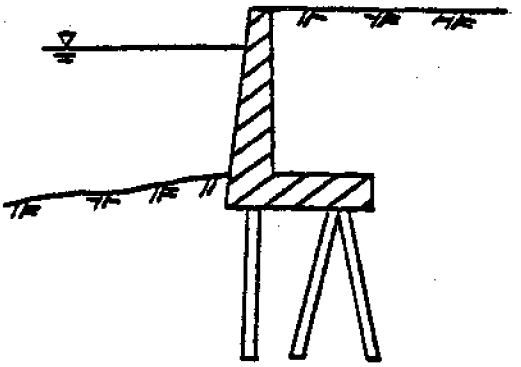

(a) retaining structure

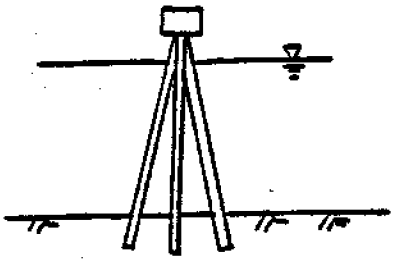

(b) dolphin

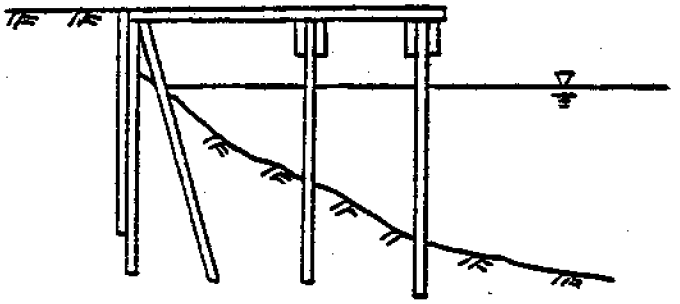

(c) dock, pier or wharf

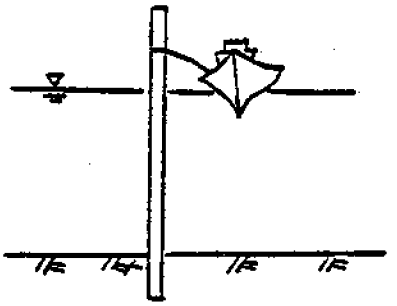

(d) ship mooring

Fig. 1.1 Examples of Use of Piles in the Coastal Region

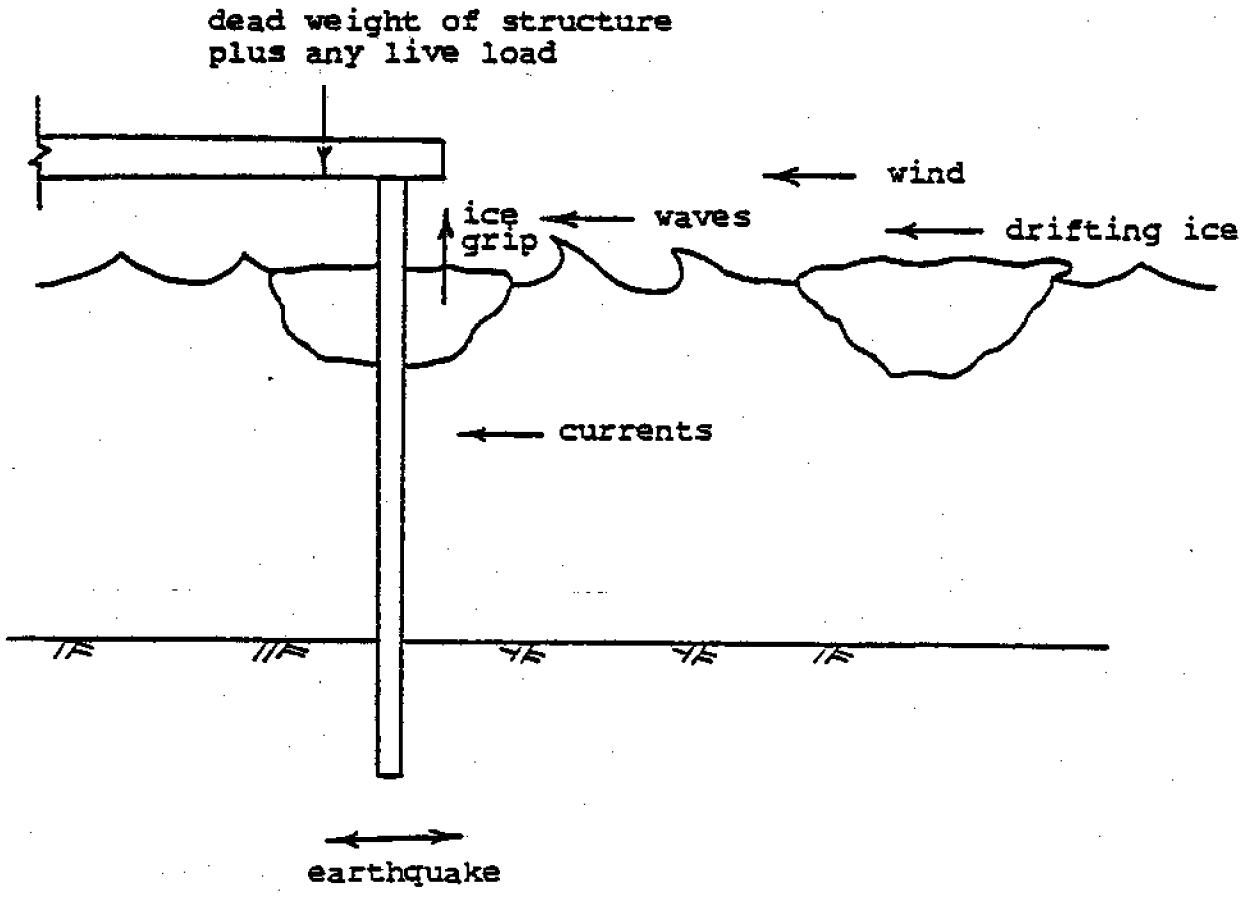

Fig. 1.2 Potential Forces on a Waterfront Structure

produce compressive, lateral and uplift forces that may strongly influence the design and construction of the structure. Furthermore, the cost of the structure is directly proportional to the magnitude of the design load. Therefore, an understanding of the nature of these loadings is essential to achieve a proper design.

The ultimate capacities of pile foundations are determined at least by the following factors:

1) in-situ properties of the soil mass
2) dimensions and material properties of the pile
3) methods of installation
4) loading conditions

Each of these factors should be examined carefully. The extent to which they will influence the strength of the foundation depends largely on the size of the structure and the site location.

The most reliable method to determine the load capacities of piles is through pile load tests. They are commonly performed for major projects where no prior information on behavior of deep foundations at the site is available. Pile load tests are usually expensive and may not be feasible for small-scale construction. They will not be emphasized herein.

Current methodologies to assess the capacities of pile foundations are largely based on empirical correlation of field data with basic soil parameters. Rigorous theoretical analysis is still in the preliminary stage and often requires many simplifying assumptions. Numerical solutions (e.g., fi-

nite element methods), with the advent of high speed digital computers, have shown promise on this aspect. However, the computer cost required is likely to be high and unless the in-situ soil parameters are known to a high degree of accuracy, these methods may not be justifiable. In this report, emphasis will be placed on conventional design procedures and practical techniques.

Besides the various forms of loadings mentioned earlier, the design of piles for coastal structures may require consideration of:

1) effect of scour on pile foundations
2) capacity of bent piles
3) pile buckling
4) negative skin friction

These phenomena are further depicted in Fig. 1.3 and will be discussed later.

Piles used in the coastal environment are subject to adverse conditions that often result in material deterioration. Various forms of attack are illustrated in Fig. 1.4. Three commonly used materials (concrete, steel and wood) will be considered. The mechanism of corrosion as well as possible preventive measures will be presented.

In the last section of this report, a brief description on installation of piles will be outlined. It should be noted that the method of installation has a profound effect on load capacities and should not be overlooked in the design phase.

Finally, example problems will be given in the Appendix to illustrate the design methodologies outlined in various

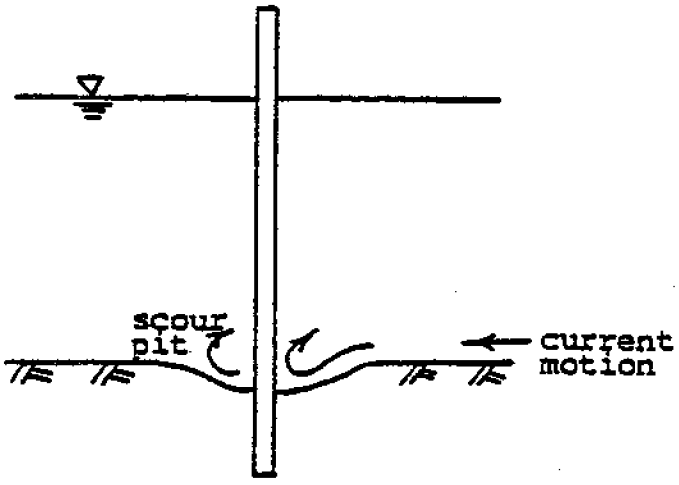

(a) scour

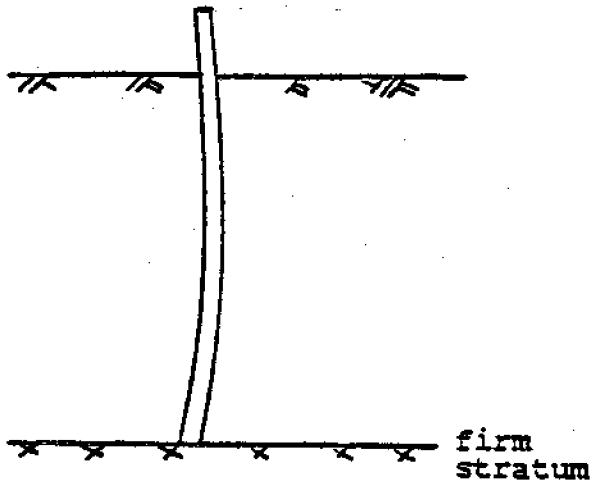

(b) bent pile

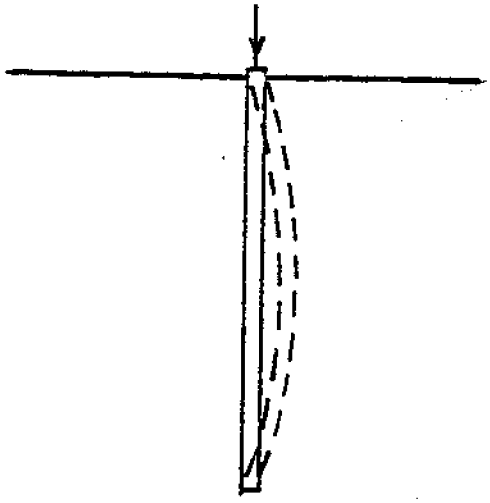

(c) pile buckling

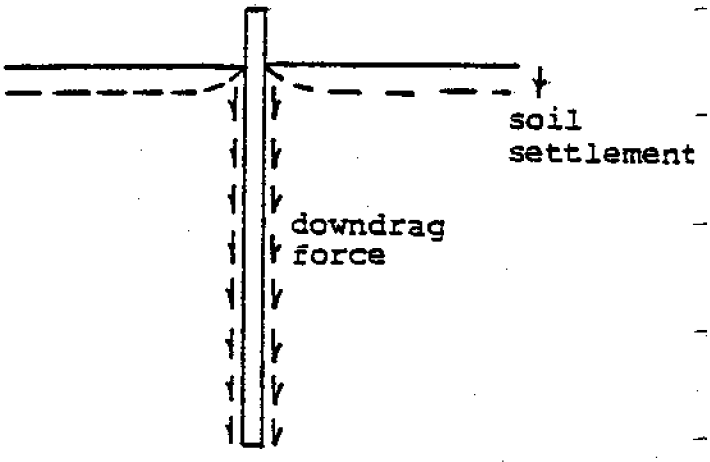

(d) negative skin friction

Fig. 1.3 Typical Considerations for the Design of Pile Foundations

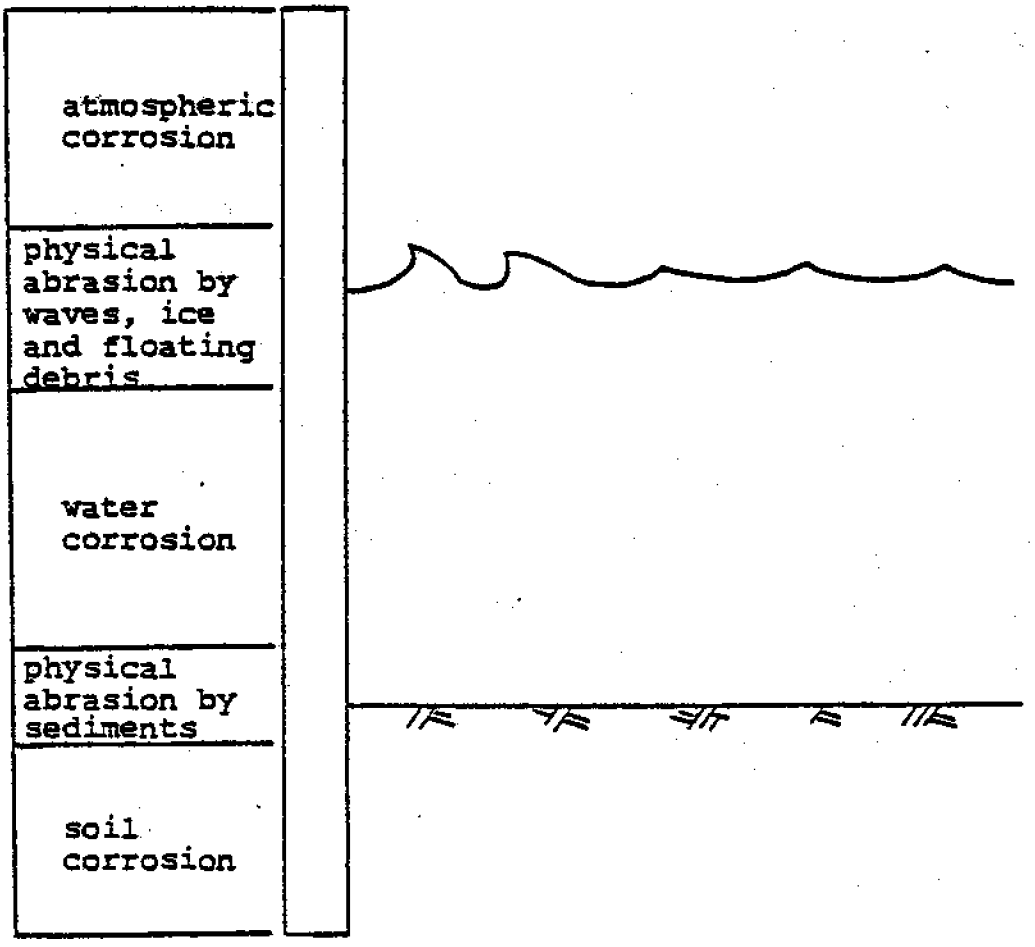

Fig. 1.4 Various Forms of Material Deterioration in the Coastal Environment

chapters. The problems are solely for demonstration purposes and will be kept simple. It should be understood that other factors may also affect the solutions to these problems. Although it is impossible to discuss all these factors in the example problems, the idea that design incorporates considerations from every aspect should always be kept in mind.

Overall, this report is intended to serve as a guide for the design and construction of pile foundations in the coastal regime. The flow chart in Fig. 1.5 illustrates the sequence under which this may be done. The design procedures along with their inherent assumptions will be described. However, one should not view the procedures as "the standard rules"; rather, one should approach the problem intelligently to develop a rational and economic design.

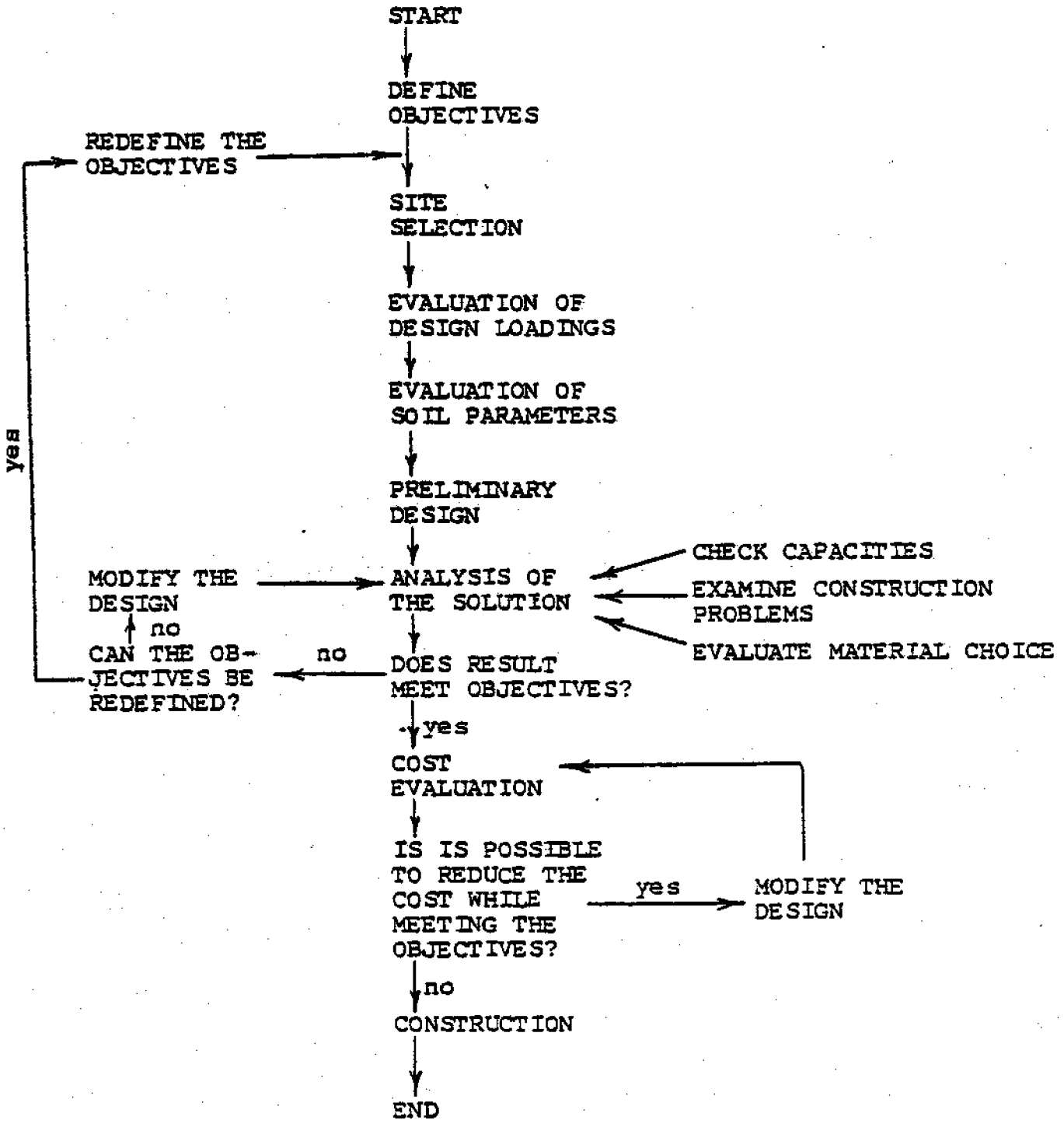

Fig. 1.5 Typical Sequence for Use in the Design of Pile Foundations

CHAPTER 2

LOADINGS ON PILES

One of the first steps in the design of any structure is an evaluation of the nature and intensity of the loads that may act on the structure throughout its design life. This requires a thorough understanding of the design objectives as well as the site characteristics.

Piles used for waterfront structures are subjected to a large number of forces which may act either axially or laterally. They may induce bending moments and, in some instances, may even cause uplift or downdrag of piles. Forces may act directly on piles or they may be transmitted to the piles through another medium. For example, ice and waves may act directly on exposed piles, while earthquake loads are considered to be applied to the piles through the soils. In most cases, piles that are fully embedded take forces indirectly, usually through the superstructure above (e.g., seawall) or the soil below.

Loads may be broadly classified into three categories:

1) In the first category, the separation is into dead and live loads. Dead load is a gravity load and is always acting. The weight of the structure, including any permanent attachments, are considered as dead loads. The magnitude and distribution of these loads are usually known accurately, but not until the design has been completed. Therefore, the dead load has to be estimated in the preliminary de-

sign stage and revised after an analysis is made. Live loads may vary in magnitude and location. These forces are important for structures such as piers where movable equipment, human occupants, vehicles, etc., may form a substantial portion of the total load. Minimum values of live loads for design are often prescribed by local building codes; these are usually conservative.

2) Secondly, loads can be gradually applied or they can be in constant motion. The former is a static load and the latter is a dynamic load. Static loads can be dead loads or live loads. Their influence on the structure is restricted to the magnitude of force that is applied. In contrast, dynamic loads will fluctuate with time and the response of the structure is dependent upon the inertial and damping characteristics of the system. By definition, all dynamic loads are live loads. The dynamic response of the structure can be evaluated by a dynamic analysis or, for ordinary design, by using a conservative value for the specified load values.

3) Thirdly, the duration of loading can be long (sustained) or short (transient). The major difference between these two types of loadings lies essentially in the way in which the soil behaves. For sustained loads in clays, two distinct types of soil behavior can be identified — undrained and drained. However, for transient loads (e.g., earthquake, blasting), the short duration of load application prohibits the dissipation of excess pore-water pressure and

undrained conditions will exist, regardless of soil properties.

Sometimes there is no clear line of demarcation between dead load vs. live load, static load vs. dynamic load or sustained load vs. transient load. In that case, the decision must be based upon the judgment of the designer. However, he or she should understand the inherent assumptions made in selecting an appropriate design load.

Loadings that will be discussed in this chapter are:

1) waves
2) currents
3) ice
4) earthquakes
5) ship impact

These forces are not by all means inclusive, but they represent the common and likely loading conditions for piles used in coastal regions. The direct effects of forces resulting from wind on piles are small, but its influence on wave and ice action should not be overlooked. Consideration should also be given to loadings caused by floating debris, if applicable. Loadings from tides are likely to be small and will not be considered here.

The relative importance of the forces mentioned above depends upon the regional climatic and geologic conditions. Vital factors at one particular site may not be applicable to others. Moreover, the effects of these forces are not necessarily cumulative. Although wind and waves are likely

to occur at the same time and in the same direction, impact forces from ice sheets will not occur simultaneously with the most severe wave action. It is impractical and uneconomical to design a structure to withstand all these forces at their maximum amplitudes.

The action of these loadings, especially those that are produced by the environment, should be anticipated to come from any direction unless specific conditions make a different assumption more justifiable.

In reality, most of the forces mentioned above are dynamic in nature. The intensities as well as the directions of the forces will vary with time. Theoretically, a dynamic analysis that takes into account the inertial and damping characteristics of the system will be more appropriate. While this may be necessary for design of deep water offshore platforms, it is of little relevance for simpler small-scale construction. In such cases, it is adequate to consider the loads in terms of their static equivalents. The validity of such assumptions depends upon both the form of the structure and the nature of the load. In cases where the fluctuating components of the applied force deviate drastically from the mean load, or the natural frequency of the structure approaches the frequency of the predominant force component, a dynamic analysis of the problem may become mandatory. In this study, only static analysis will be presented. Dynamic response of structures is beyond the scope of this study.

2.1 Waves

Piles used in the coastal environment are likely to be subjected to some forms of wave action, whether directly on the piles or indirectly through the superstructure. Wave loads on wall-type structures are discussed by Hubbell and Kulhawy (1979) and will not be presented here. This section will concentrate on behavior of piles under direct wave action.

Waves can be generated by many means, e.g., moving vessels, earthquake, wind, etc.. The one that has the most influence for waterfront structures is the wind-generated wave. Although seismic-generated waves may have high orders of magnitude, it is not feasible to include them in normal design practice except in regions where seismic-generated waves occur frequently or a loss of life is anticipated.

The severity of wave action on piles depends largely upon site conditions. In sheltered waters where most of the wave energy has been attenuated, wave forces will not have any strong influence on the design.

Wave types vary from non-breaking to breaking and broken waves, with each of these producing different magnitudes of forces on a structure. An unbroken wave is essentially a wave of oscillation, which breaks when the forward velocity of the crest particles exceeds the velocity of propagation of the wave itself (Quinn, 1972). The procedures for determination of non-breaking wave forces on piles will be outlined below. Wave forces resulting from the action of broken waves are usually negli-

gible and will not be considered.

2.1.1 Non-Breaking Waves on Vertical Piles

Methods currently in use for determination of wave forces on piles are based on Morison's equation (Morison, et al., 1950), which assumes that forces exerted by wave-associated flows on piles result from the sum of two components:

1) inertial force

2) drag force

Morison's equation is semi-empirical and is given as:

$$f = f_i + f_D \tag{2.1}$$

in which: f = total horizontal force per unit length of pile

f_i = inertial force per unit length of pile

f_D = drag force per unit length of pile

Inertial forces result from constant acceleration or retardation of water particles in the form of ideal nonviscous flow. This is based on the assumption that the wave height is small in comparison with depth and the water is incompressible and frictionless (ideal fluid). The inertial force component can be expressed as:

$$f_i = C_M \frac{\gamma}{g} \frac{\pi D^2}{4} \frac{\partial u}{\partial t} \tag{2.2}$$

in which: C_M = inertial coefficient

γ = weight density of fluid

= 62.4 lb/ft^3 (9.8 kN/m^3) for fresh water

= 64.0 lb/ft^3 (10.0 kN/m^3) for salt water

D = diameter of pile

$\frac{\partial u}{\partial t}$ = horzontal watar particle acceleration at the axis

of the pile (assuming the pile does not exist)

g = acceleration due to gravity
= 32.2 ft/sec^2 (9.8 m/sec^2)

Drag forces result from the constant velocity of water particles in the form of real viscous flow and can be expressed as:

$$f_D = C_D \frac{1}{2} \frac{\gamma}{g} u |u| D \qquad (2.3)$$

in which: C_D = drag coefficient

u = horizontal water particle velocity at the axis of the pile (assuming the pile does not exist)

The factor $\frac{1}{2}$ does not have any physical meaning and results from the manner in which the measurements of the empirical coefficient, C_D, were reported (Nair, 1969). $u|u|$ is used instead of u^2 to indicate that the force is always acting in the same direction as the velocity. A definition sketch of wave forces on a vertical cylindrical pile is shown in Fig. 2.1.

The design diameters of the piles, D, as used in Equations 2.2 and 2.3, do not have to be equal to the actual diameters of the members. Due consideration must be given to the possibility of marine growth or ice collar, which may increase the dimensions of the piles and therefore the magnitude of wave forces.

For high waves in shallow water, the drag force is predominant and the maximum force against the pile occurs at or near the crest of the waves. For low waves in deep water, the inertial force is predominant and the maximum force occurs when the water surface at the pile is close to the still water sur-

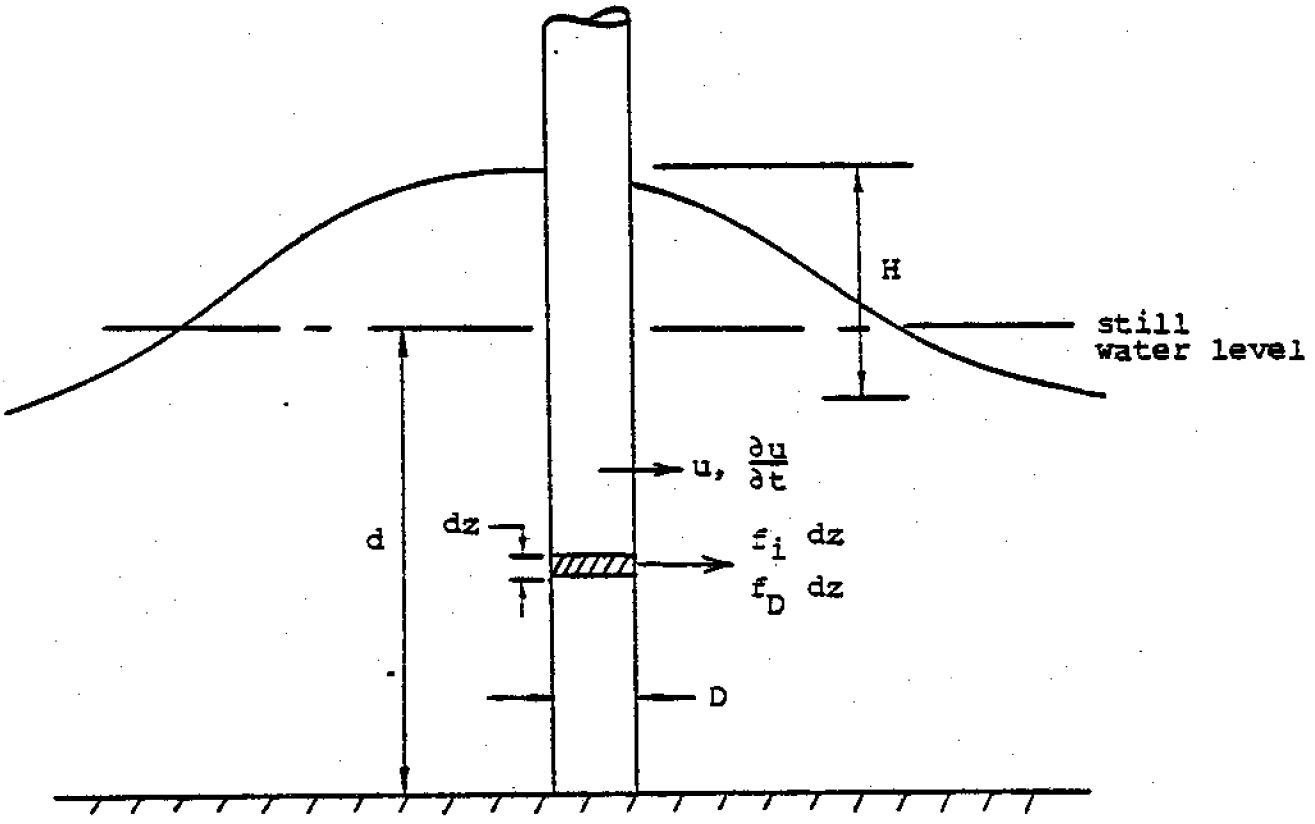

Fig. 2.1 Definition Sketch of Wave Forces on a Vertical Pile

face (Quinn, 1972).

It should be realized that the linear ertial and drag forces as used in Equation any rigorous theoretical basis. The admis of drag force violates the principles on w force is derived. Three other major assum Morison's equation are given as follows:

1) flow is unidirectional.

2) the presence of the pile will not water flow pattern.

3) the pile is rigid and will not def Although the above assumptions may limit t cation of Morison's equation under some si no simple alternative at the present time.

The second assumption implies that th be small compared with the wavelength of t of this, CERC (1977) suggested the applica equation to be limited to cases where:

$$\frac{D}{L_A} < 0.05$$

in which: L_A = Airy approximation of wavel Fig. 2.2 can be used for determination of mensionless parameter, $\frac{d}{gT^2}$, in which: d = water level and the mudline, and T = wave

The restriction as imposed by Equatic fied in most cases except for piles that a meter. In that case, a wave diffraction a

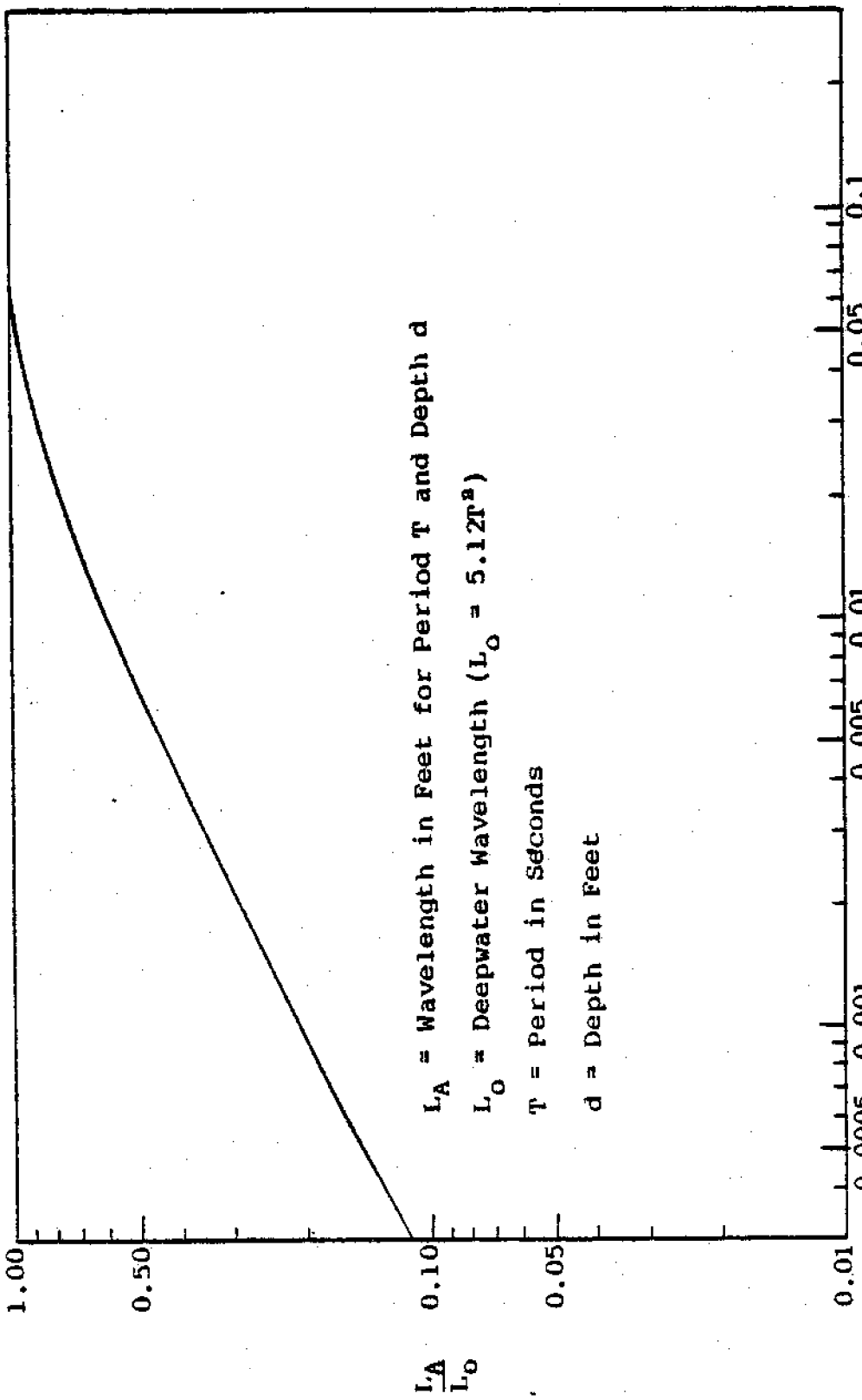

Fig. 2.2 Relative Wavelength Versus d/gT^2 (Airy Wave Theory) (after CERC, 1977)

It will not be discussed here because it is doubtful that it is of any value for the design of small-scale structures.

Using Morison's equation, the evaluation of wave-pile interaction forces can be separated into two phases:

1) the selection of an appropriate wave theory to predict the flow fields.
2) the determination of the two hydrodynamic coefficients, C_M and C_D.

Actual wave motion is complex and difficult to model mathematically. In spite of this, numerous wave theories have been presented in the literature to describe this natural phenomenon. It is beyond the scope of this study to cover the development and capabilities of all these theories. The readers should refer to Wiegel (1964) or CERC (1977) for a more comprehensive review of this subject matter.

The most fundamental wave theory is the Airy theory, also called the linear or small-amplitude theory. Based on this mathematical model, the horizontal water particle velocities and accelerations at any time t are given respectively as:

$$u = \frac{H}{2} \frac{gT}{L} \frac{\cosh[2\pi(z+d)/L]}{\cosh[2\pi d/L]} \cos\left(\frac{2\pi t}{T}\right) \tag{2.5}$$

$$\frac{\partial u}{\partial t} = \frac{g\pi H}{L} \frac{\cosh[2\pi(z+d)/L]}{\cosh[2\pi d/L]} \sin\left(-\frac{2\pi t}{T}\right) \tag{2.6}$$

in which: H = wave height

z = vertical coordinate axis, origin at still water level, positive upwards

L = wavelength

This theory is simple and relatively easy to use. However, this theory is unable to predict more complicated wave motion and fails to realize that wave crests may deviate further from the still water level than do the troughs. In general, the use of higher order theory (also called non-linear or finite amplitude theory) can better describe the actual wave characteristics. However, its use will involve tedious computations, and access to a computer or computer-generated design charts is necessary. In predicting the velocity and acceleration fields for use in Morison's equation, any defensible established wave theory can be used. However, the designer should have a thorough understanding of the inherent assumptions and limitations associated with various wave theories.

Development of these wave theories is built upon many simplifying assumptions, with some of the more common ones given as follows (CERC, 1977):

1) the fluid is homogeneous and incompressible.
2) surface tension force is minimal.
3) coriolis effect can be neglected.
4) pressure at the free surface is uniform and constant.
5) the fluid is ideal and nonviscous.
6) there is no interaction with other wave motions.
7) the vertical velocity at the bed is zero.
8) wave amplitude is small and wave form is invariant in time and space.
9) waves are two-dimensional.

The designer should examine the impact of these assumptions on

the problem and interpret the results carefully for application to actual design.

The two hydrodynamic coefficients, C_M and C_D, are empirical coefficients that can be determined from previous recorded data, model tests or full-scale field experiments. These two values depend upon the dimensions of the piles, wave characteristics, and the choice of wave theory. Published values for these two coefficients show a lot of scatter.

Based on the results of many investigators, CERC (1977) recommended the following guidelines for determination of the two coefficients.

Inertial coefficients (C_M):

$$C_M = 2.0 \qquad \text{when } R_e < 2.5X10^5 \tag{2.7}$$

$$C_M = 2.5 - \frac{R_e}{5X10^5} \qquad \text{when } 2.5X10^5 < R_e < 5X10^5 \tag{2.8}$$

$$C_M = 1.5 \qquad \text{when } R_e > 5X10^5 \tag{2.9}$$

Drag coefficient (C_D):

Variation of C_D with Reynolds number is shown in Fig. 2.3. In both cases, the coefficients are given as a function of the Reynolds number, defined as:

$$R_e = \frac{u_{max} D}{\nu} \tag{2.10}$$

in which: R_e = Reynolds number

u_{max} = maximum horizontal velocity at still water level

ν = kinematic viscosity of the fluid

= $1X10^{-5}$ ft^2/sec ($9.3X10^{-7}$ m^2/sec) at 20°C for water

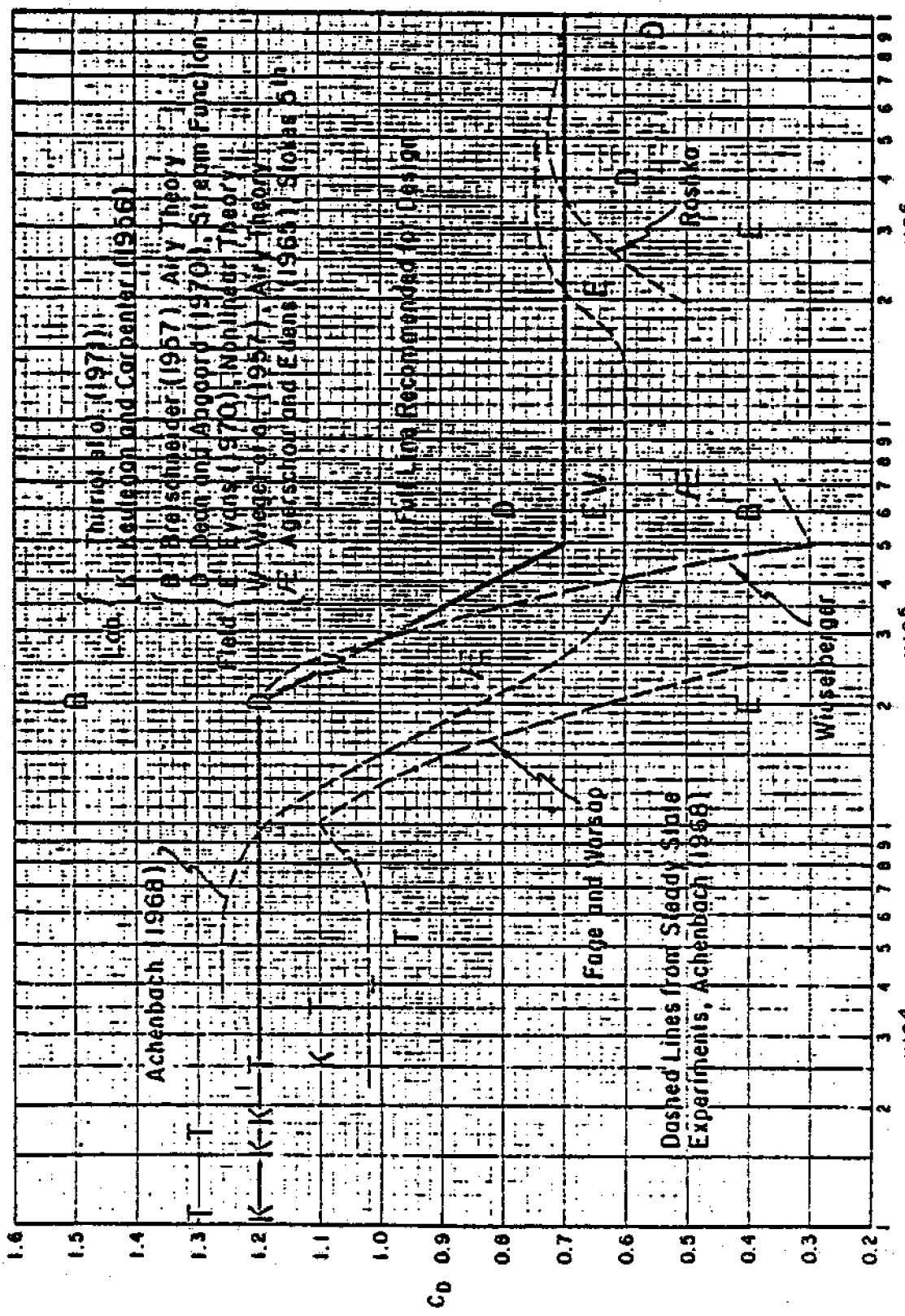

Fig. 2.3 Variation of Drag Coefficient, C_D, with Reynolds Number, R_e (CERC, 1977)

Given the flow fields, dimensions of the pile and the two hydrodynamic coefficients, Equations 2.2 and 2.3 can be used to compute the inertial and drag forces, respectively, at any location along the pile. The force distributions can be obtained by successive applications of Equations 2.2 and 2.3 over the entire length of the pile.

The total inertial and drag force components that act on the pile can be obtained by integration of Equations 2.2 and 2.3 along the whole length of the member that is submerged under water. Assuming the two hydrodynamic coefficients to be constant with depth, the total horizontal force components can be expressed as:

$$F_I = C_M \gamma \frac{\pi D^2}{4} H K_I \tag{2.11}$$

$$F_D = C_D \frac{1}{2} \gamma D H^2 K_D \tag{2.12}$$

in which: F_I = total horizontal inertial force on pile

K_I = dimensionless parameter for total inertial force

F_D = total horizontal drag force on pile

K_D = dimensionless parameter for total drag force

and the moments of these forces about the mudline can be expressed as:

$$M_I = F_I \, d \, S_I \tag{2.13}$$

$$M_D = F_D \, d \, S_D \tag{2.14}$$

in which: M_I = moment of inertial force about the mudline

S_I = dimensionless parameter for moment of inertial force

d = distance between still water level and mudline

M_D = moment of drag force about the mudline

S_D = dimensionless parameter for moment of drag force

Thus, dXS_i and dXS_D can be considered as the moment arms for the inertial and drag forces respectively.

The values of the four dimensionless parameters K_i, K_D, S_i and S_D are functions of the velocity and acceleration fields of the wave-induced flows. Therefore, these parameters are directly related to the choice of wave theory. As the velocity and acceleration fields will change as the wave propagates, the parameters K_i, K_D, S_i, S_D (and thus F_i, F_D, M_i, M_D) will all vary with time. However, for design of individual piles, the maximum values of these components are of primary interest to the designer.

The maximum values of the force and moment components can be expressed as:

$$F_{im} = C_M \gamma \frac{\pi D^2}{4} H K_{im} \tag{2.15}$$

$$F_{Dm} = C_D \frac{1}{2} \gamma D H^2 K_{Dm} \tag{2.16}$$

$$M_{im} = F_{im} d S_{im} \tag{2.17}$$

$$M_{Dm} = F_{Dm} d S_{Dm} \tag{2.18}$$

in which: F_{im} = maximum total horizontal inertial force on pile

F_{Dm} = maximum total horizontal drag force on pile

M_{im} = maximum moment about the mudline because of inertial force component

M_{Dm} = maximum moment about the mudline because of drag force component

If the inertial and drag force components are in phase (i.e., their maximum amplitudes occur at the same time), the maximum force acting on a pile will be the sum of the two values; otherwise, the maximum total force will be somewhat less than the sum of the two components. The time lag between these two quantities depends upon the wave parameters and the choice of wave theory. In the case of Airy wave theory, the force variations are given as:

$$F_I = F_{Im} \sin \theta \tag{2.19}$$

$$F_D = F_{Dm} \cos\theta \, |\cos\theta| \tag{2.20}$$

in which: $\theta = \frac{2\pi x}{L} - \frac{2\pi t}{T}$

x = horizontal coordinate axis in direction of wave propagation (relative to wave crest)

Charts for determination of K_{Im}, K_{Dm}, S_{Im} and S_{Dm} based on Dean's stream function theory are shown in Figs. 2.4, 2.5, 2.6 and 2.7 respectively. The use of these figures requires the determination of the dimensionless water depth, $\frac{d}{gT^2}$, and the degree of nonlinearity of the design wave. The degree of nonlinearity is expressed by the ratio of design wave height (H) to breaking wave height (H_b). The breaking wave height can be estimated from Fig. 2.8 using the breaking limit line on the graph.

As indicated above, the maximum inertial force may not be in phase with the maximum drag force and this prohibits the linear addition of these two quantities to obtain the maximum total force. Again, based on stream function theory, charts shown in

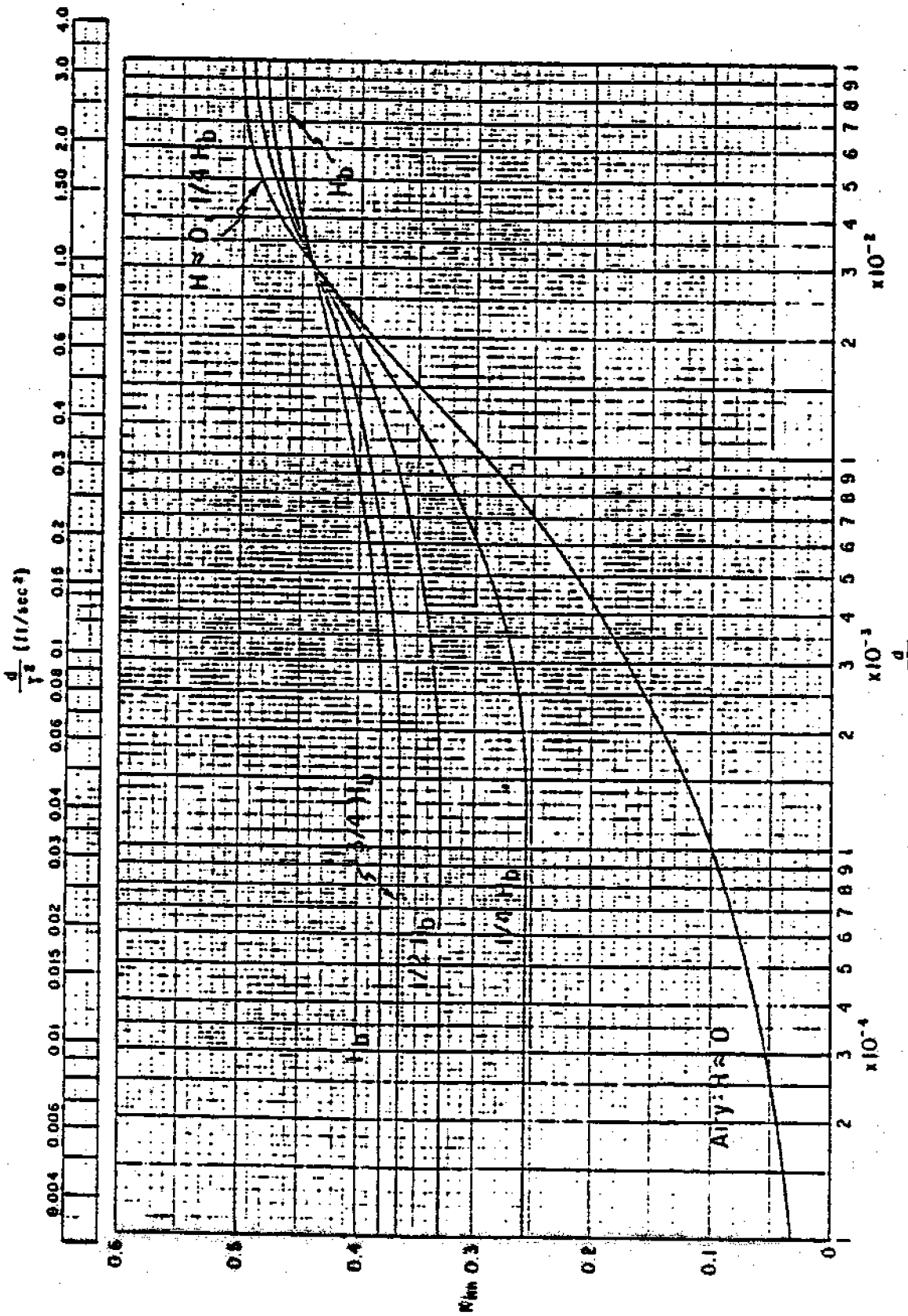

Fig. 2.4 K_{im} Versus Relative Depth, d/gT^2 (CERC, 1977)

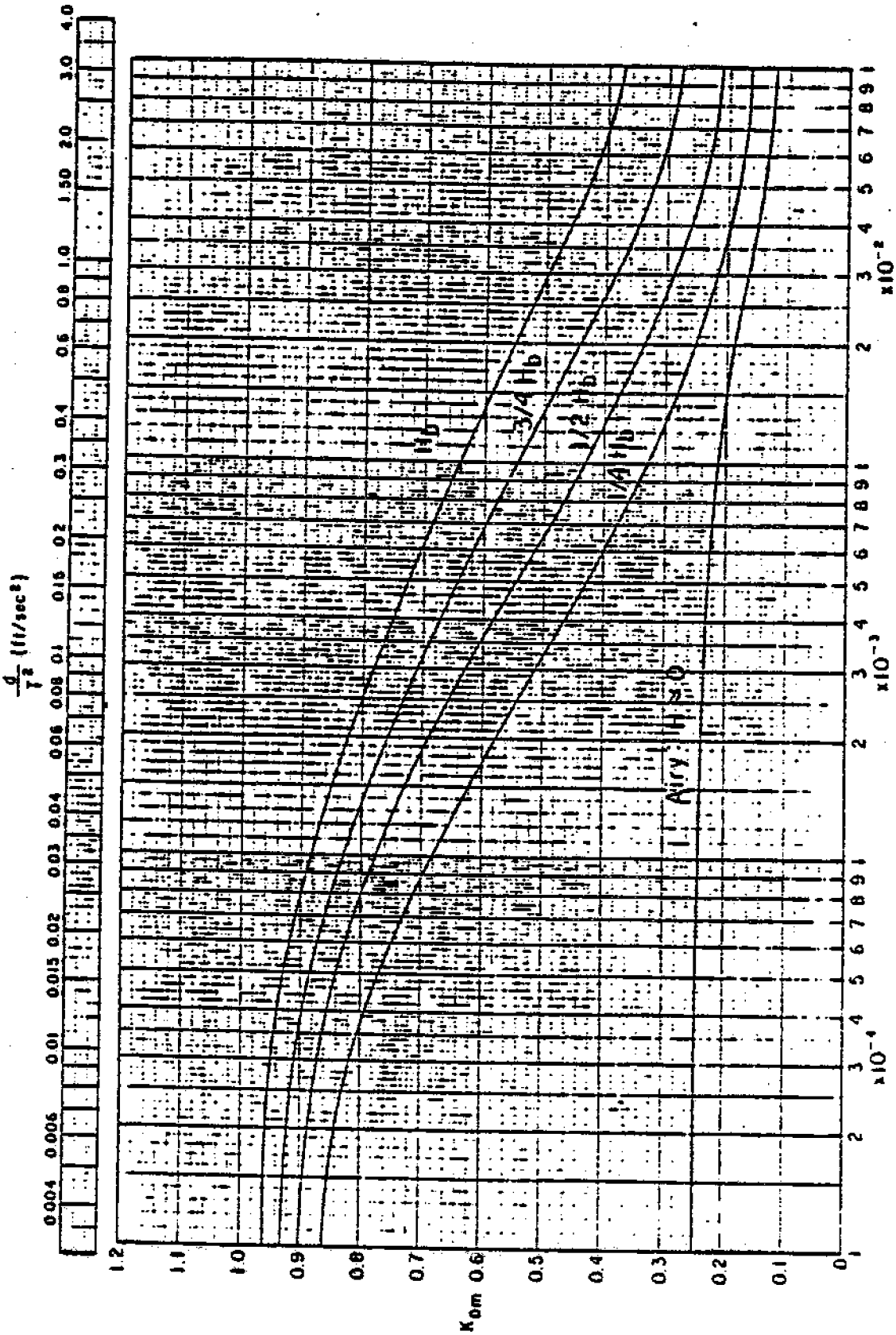

Fig. 2.5 K_{Dm} Versus Relative Depth, d/gT^2 (CERC, 1977)

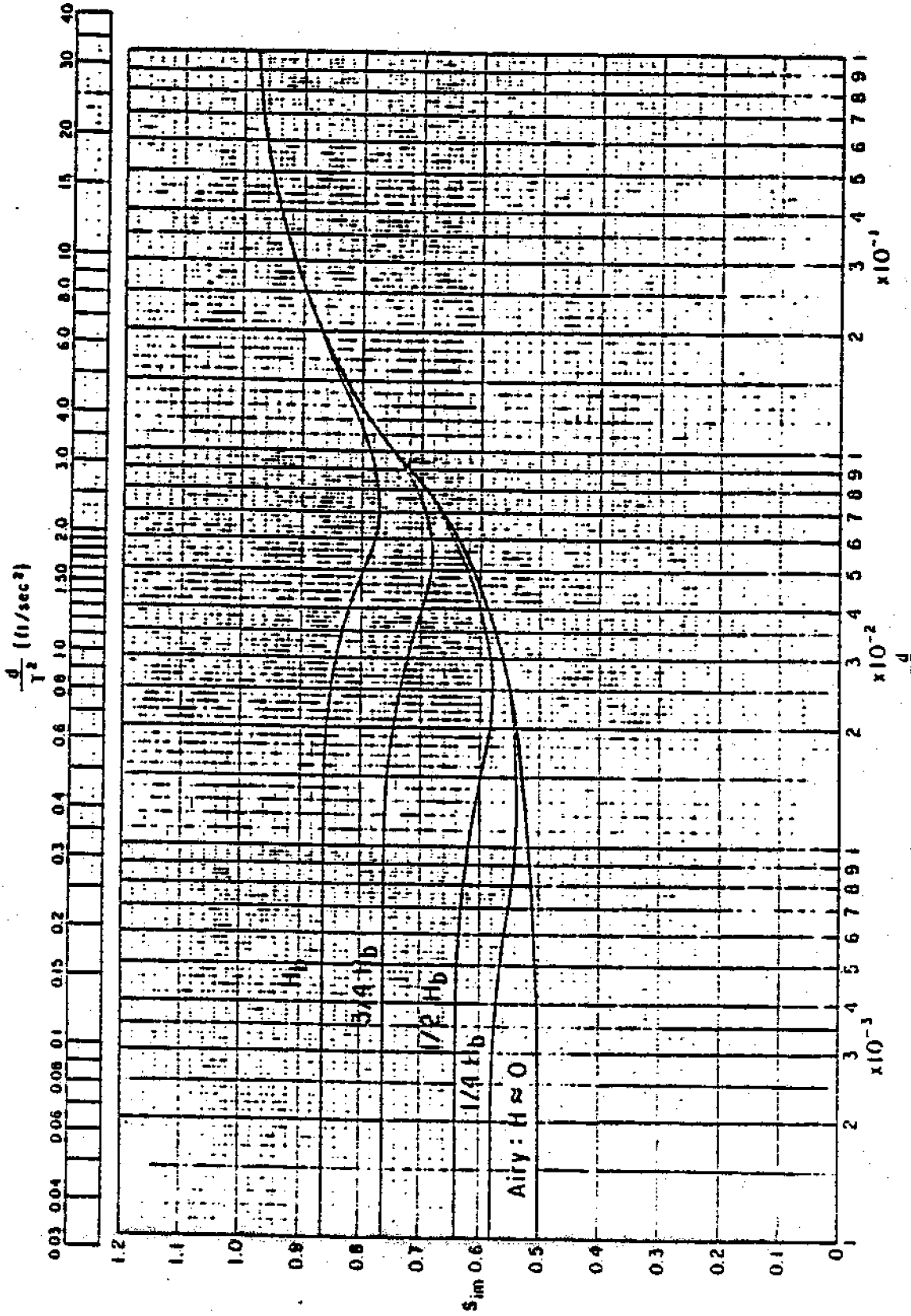

Fig. 2.6 Inertia Force Moment Arm, S_{im}, Versus Relative Depth, d/gT^2 (CERC, 1977)

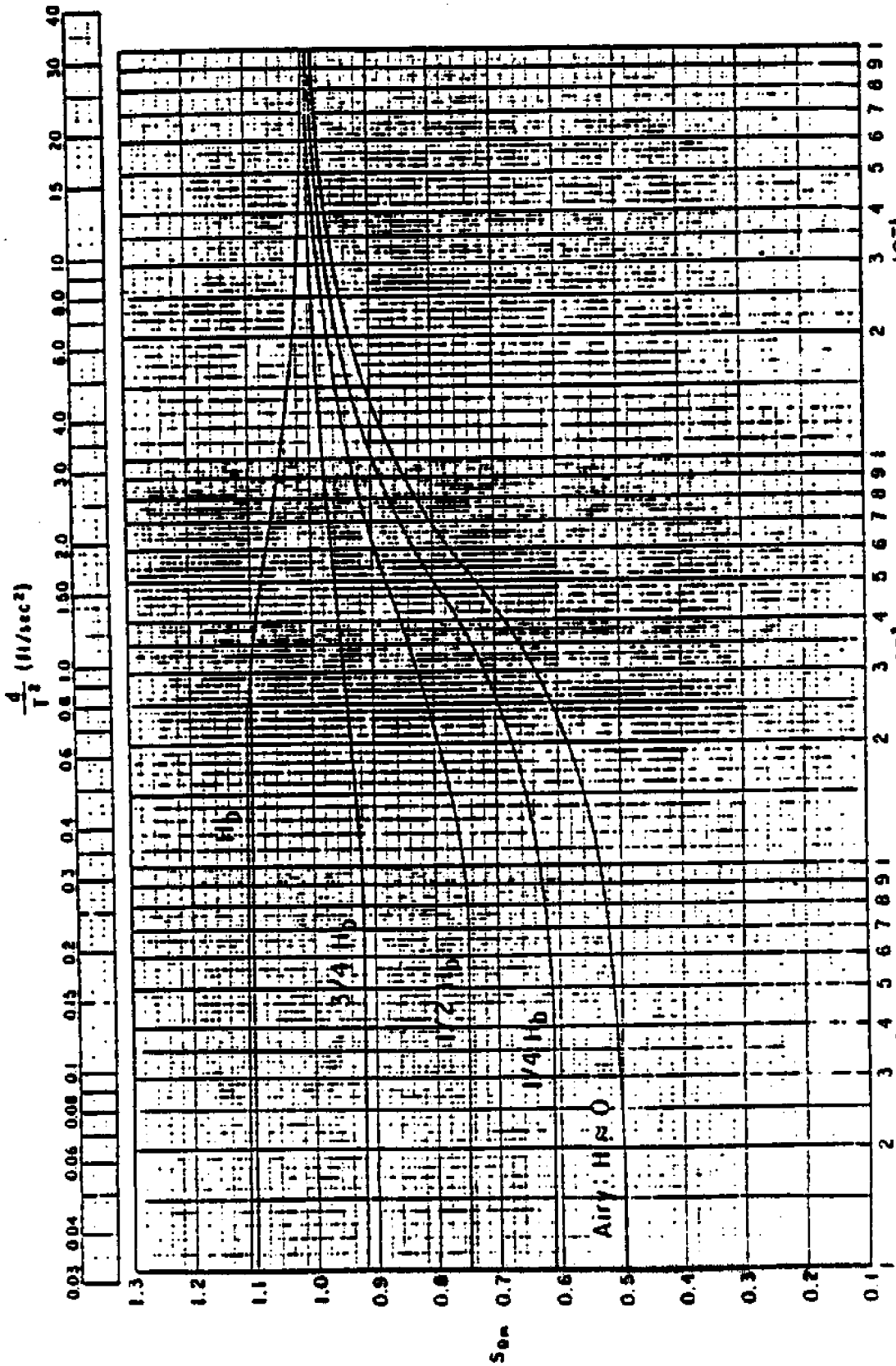

Fig. 2.7 Drag Force Moment Arm, S_{Dm}, Versus Relative Depth, d/gT^2 (CERC, 1977)

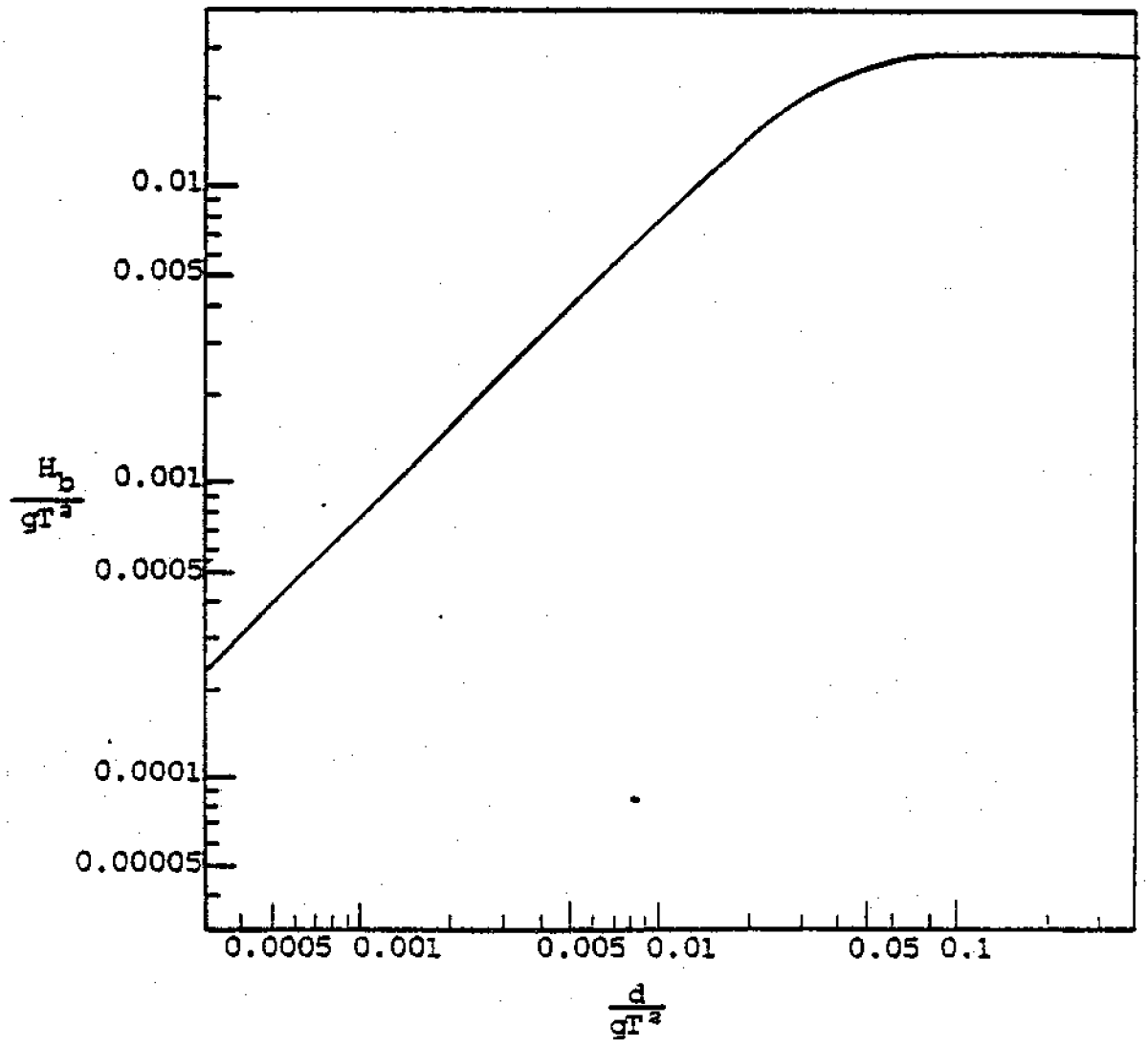

Fig. 2.8 Breaking Wave Height (after CERC, 1977)

Figs. 2.9, 2.10, 2.11 and 2.12 can be employed to estimate the maximum total horizontal force associated with wave-induced flows. The appropriate chart to be used is determined by the dimensionless parameter, W, defined as:

$$W = \frac{C_M D}{C_D H} \tag{2.21}$$

and the maximum total force can be obtained from:

$$F_m = \phi_m \gamma C_D H^2 D \tag{2.22}$$

where ϕ_m is the coefficient read from the figure. In a similar manner, the maximum total moment about the mudline can be computed from:

$$M_m = \alpha_m \gamma C_D H^2 D \tag{2.23}$$

where α_m is the coefficient given by Figs. 2.13, 2.14, 2.15 and 2.16 using procedures similar to that adopted for determination of ϕ_m. In most cases, it is necessary to interpolate between different figures to obtain the appropriate ϕ_m and α_m factors.

2.1.2 Non-Breaking Waves on Groups of Vertical Piles

Piles are often used in groups for coastal structures. If the spacings between the piles are large compared with the wavelength, the existence of one pile will have no influence on the others and each pile can be designed according to procedures described earlier. However, as the distance between the piles gets smaller, the piles will influence one another by modifying the flow pattern of waves around each pile. Muga and Wilson (1970) have identified three major influences associated with group effects: sheltering, solidification and synchronization.

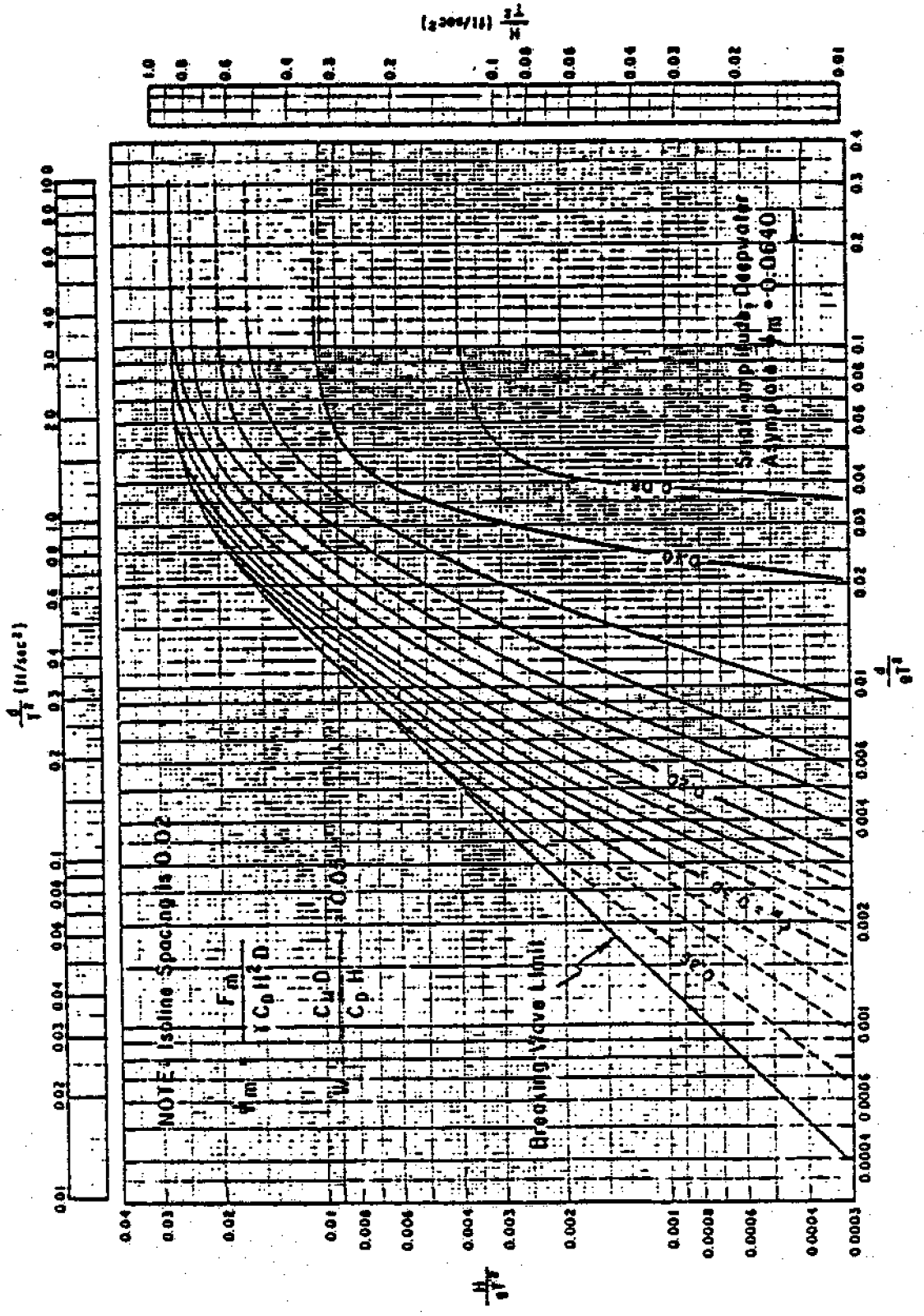

Fig. 2.9 Isolines of ϕ_m Versus H/gT^2 and d/gT^2 ... (W=0.05) (CERC, 1977)

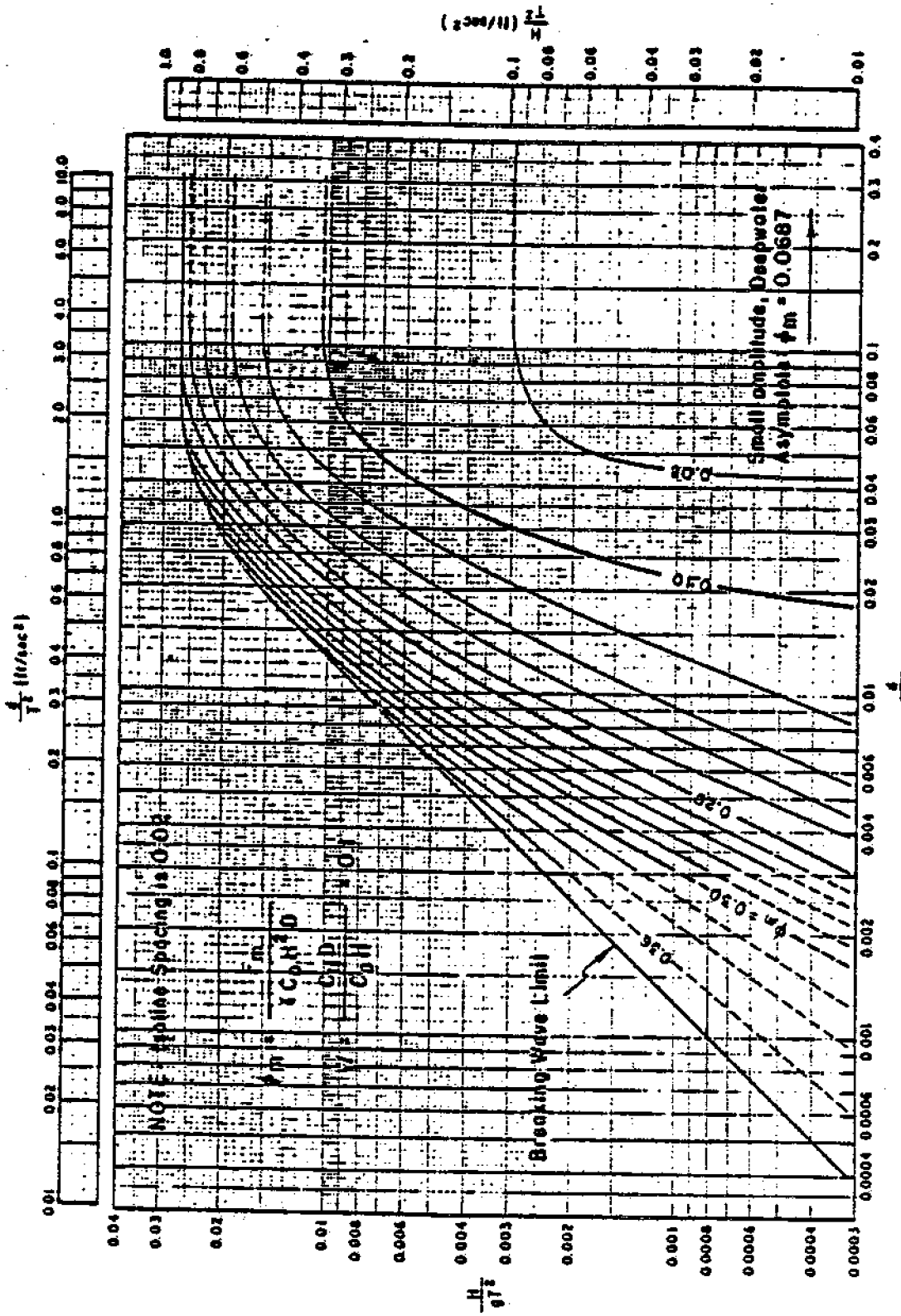

Fig. 2.10 Isolines of ϕ_m Versus H/gT^2 and d/gT^2 ... (W=0,1) (CERC, 1977)

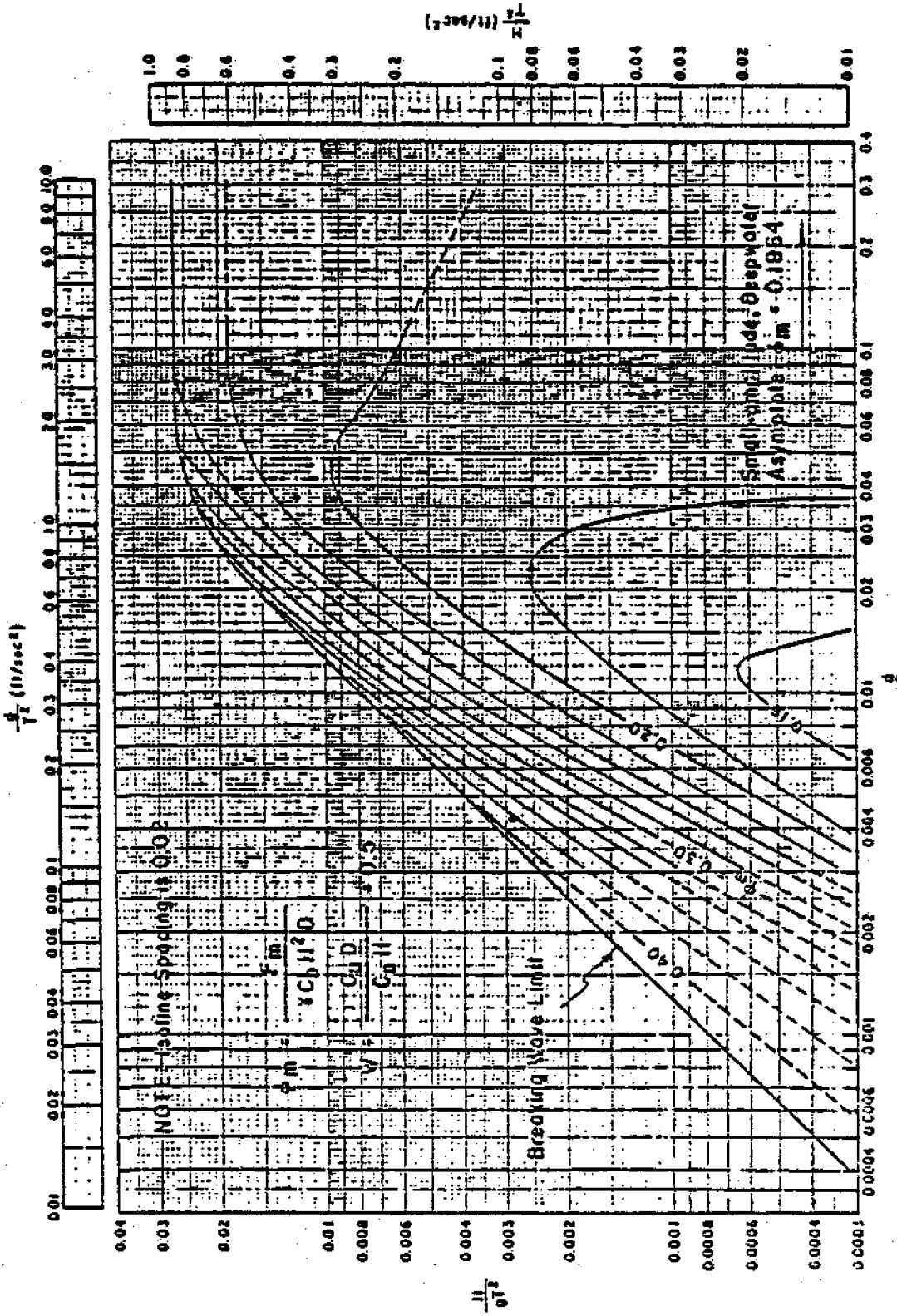

Fig. 2.11 Isolines of ϕ_m Versus H/gT^2 and d/gT^2 ... (W=0.5) (CERC, 1977)

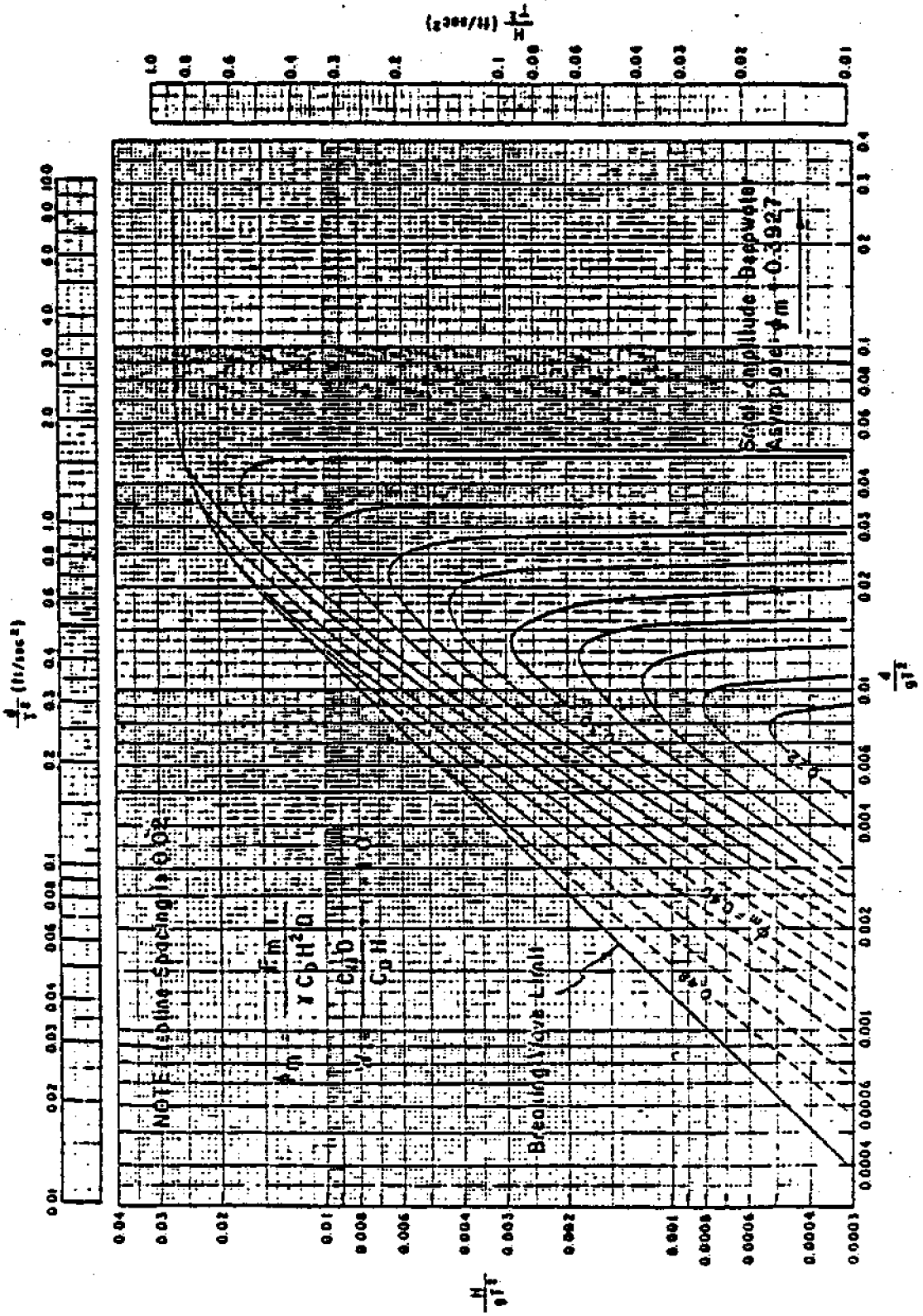

Fig. 2.12 Isolines of ϕ_m Versus H/gT^2 and d/gT^2 ... (W=1.0) (CERC, 1977)

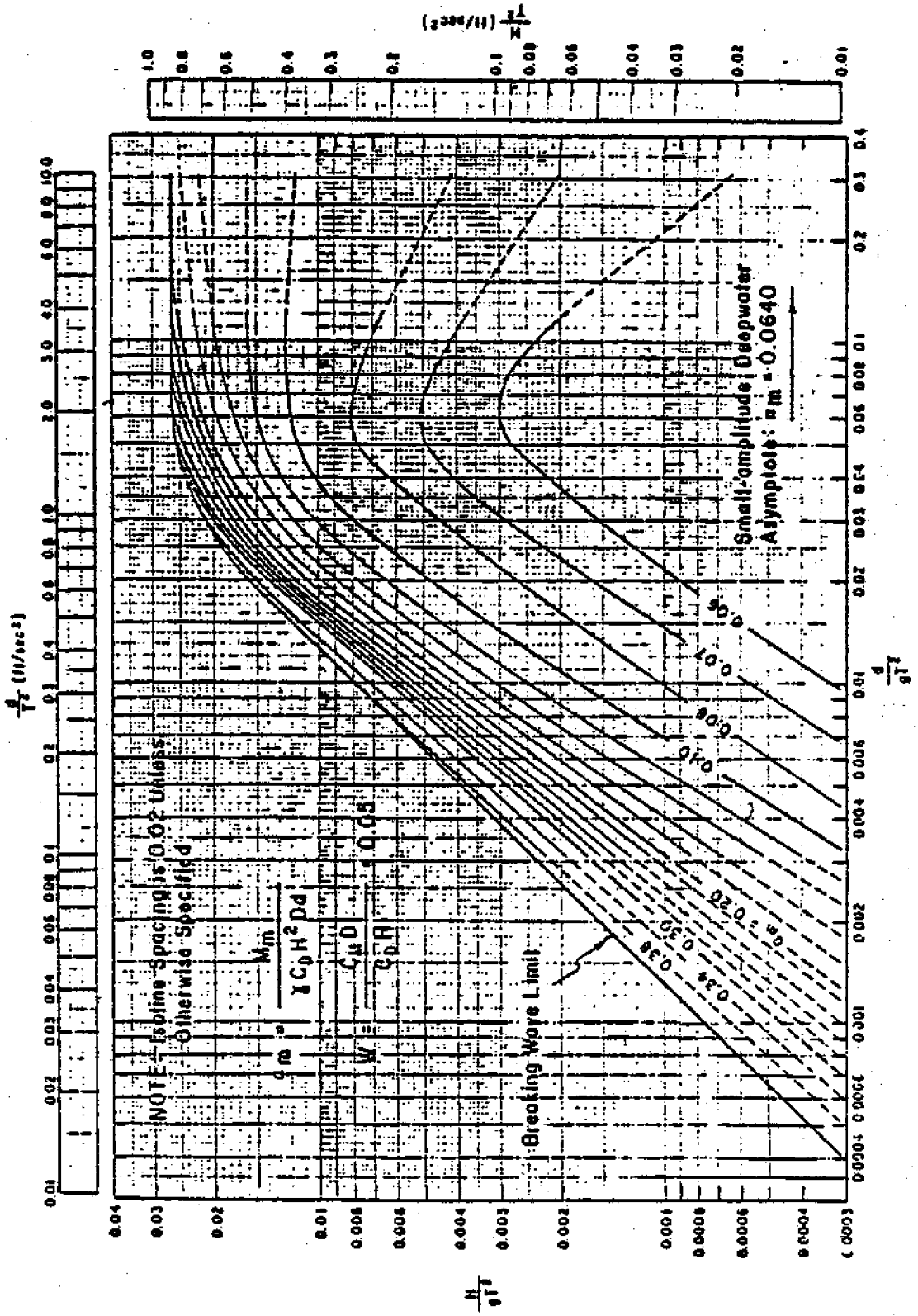

Fig. 2.13 Isolines of α_m Versus H/gT^2 and d/gT^2 ... (W=0.05) (CERC, 1977)

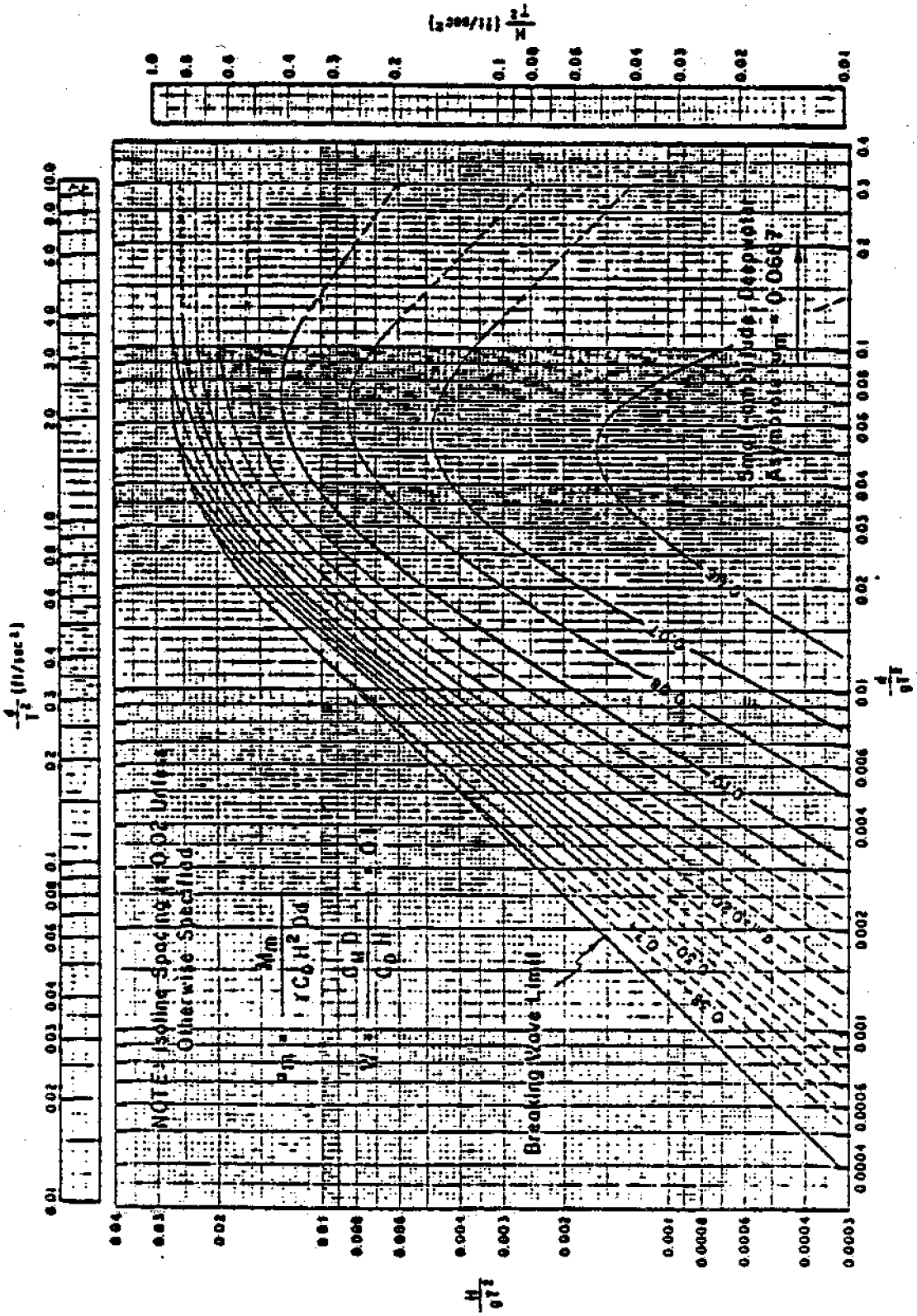

Fig. 2.14 Isolines of α_m Versus H/gT^2 and d/gT^2 ... (W=0.1) (CERC, 1977)

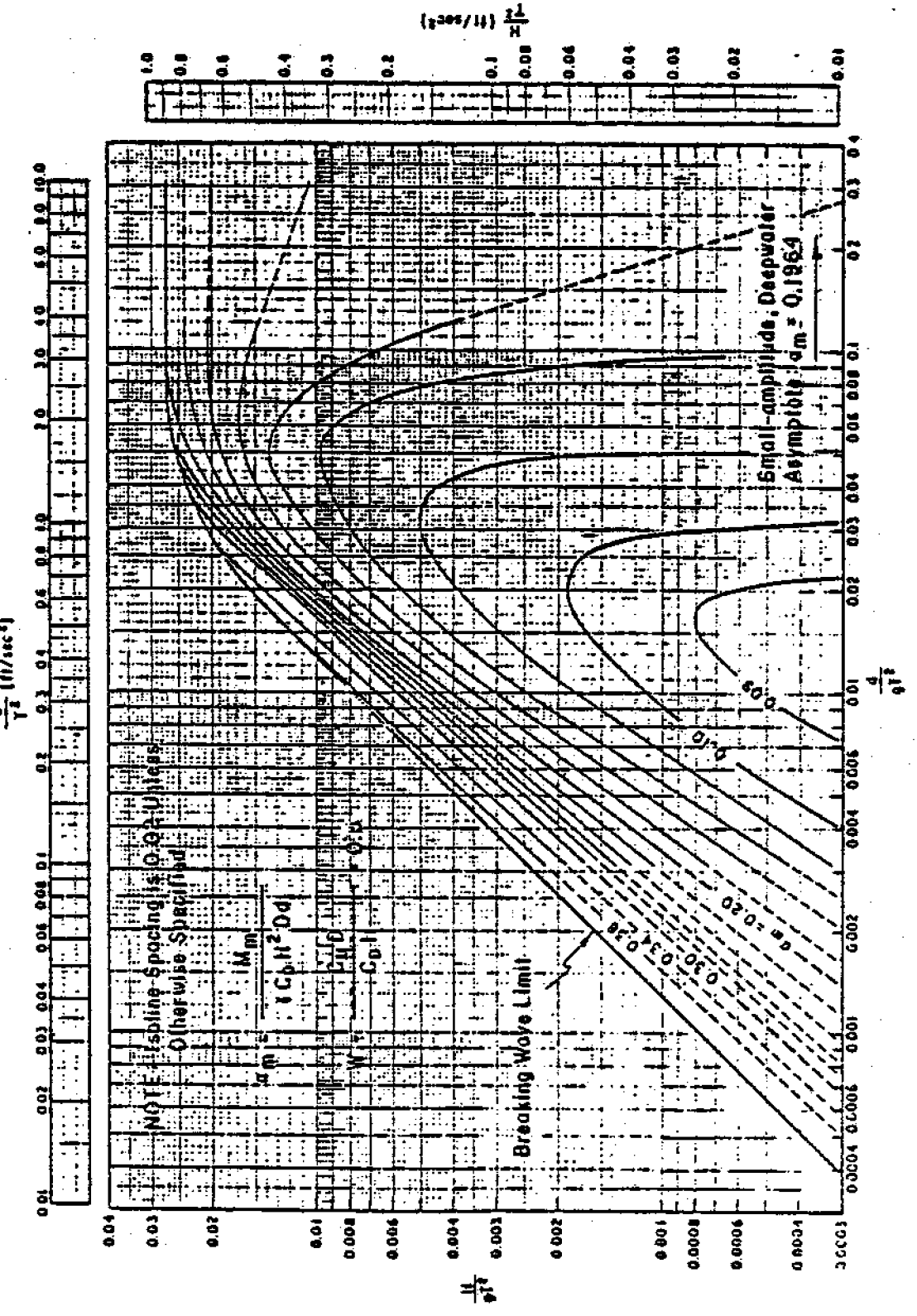

Fig. 2.15 Isolines of α_m Versus H/gT^2 and d/gT^2 ... (W=0.5) (CERC, 1977)

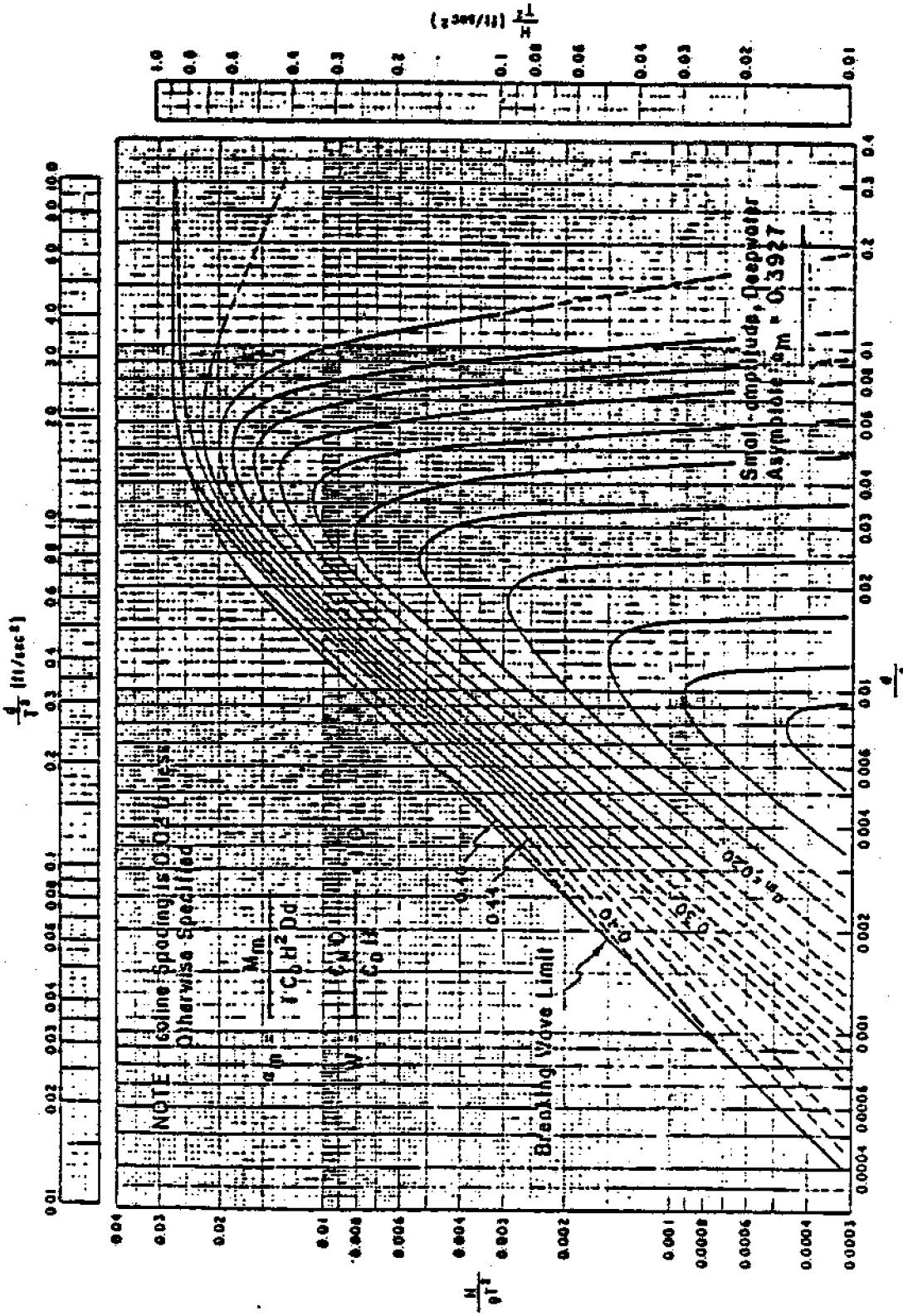

Fig. 2.16 Isolines of α_m Versus H/gT^2 and d/gT^2 ... (W=1.0) (CERC, 1977)

The effect of solidification is important only for pile groups that consist of large diameter piles and the effect of synchronization is significant only for cases where the piles are flexible. Both of these effects will not be described here. A more detailed discussion of these two effects can be found in Muga and Wilson (1970).

The effect of sheltering is illustrated in Fig. 2.17. The upstream pile (or other form of obstruction) increases the turbulence intensity of the flow toward the downstream pile. This leads to a lowering of the drag coefficient for the downstream pile, and the forces and moments acting on it may be substantially reduced. Correction factors to reduce wave loads on piles in the sheltered regions have been developed (e.g., Chappelear, 1959) in light of this effect. However, some authorities (e.g., Newmark, 1956; Quinn, 1972) recommended that this sheltering effect be disregarded in actual design. In fact, if we design the piles to withstand wave forces from all possible directions, this shielding effect will not play a significant role except for members that are completely surrounded.

The stability of a pile-supported structure with respect to wave forces is directly related to the maximum total force and moment that will be acting on the entire group of piles, rather than that on individual piles. When all these piles are arranged in a row perpendicular to the direction of wave propagation, the maximum total force and moment for the whole group of piles can be obtained by summation of the maximum total force and moment acting on each individual pile. Ignoring the shel-

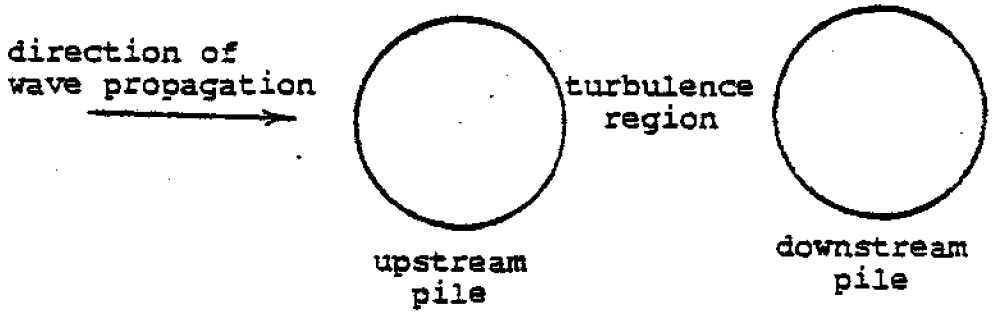

Fig. 2.17 Sheltering Effect

tering effect, this procedure is also valid for piles that are spaced a whole number of wavelengths (1,2,3,4,....) apart in the direction of wave propagation. In all other cases, the maximum total force and moment that can be acting on a group of piles will be smaller than the sum of the maximum values of each individual pile. This is because the maximum total forces and moments on each pile will not occur at the same time. Nevertheless, the time lag can be assumed to be negligible if the spacings between piles are small compared with the wavelength. In that case, the summation of the maximum values for each member will provide an approximate upper bound solution.

The procedures to compute the maximum wave force and moment on a group of piles are rather tedious and are demonstrated in the Appendix on Example Problems.

2.1.3 Non-Breaking Waves on Inclined Piles .

The use of inclined piles (also called batter or raking piles) is very common in the coastal zone, as they are more effective in taking lateral loads. Also, cross-bracing between vertical piles may also be randomly oriented through the velocity and acceleration fields of the flows. Morison's equation has also been widely used in this situation. However, there is no one well-established method of evaluating the variables associated with this equation because the water particle kinematic vectors are no longer perpendicular to the member. Several approaches have been adopted by the offshore industry. A review of these approaches is given by Wade and Dwyer (1976). The authors cited a variation of at least 22% in forces and mo-

ments among the various methods considered.

For piles that are oriented in the direction of wave propagation, CERC (1977) recommended that the force acting at any arbitrary location on an inclined pile be taken as the horizontal force acting on a fictitious vertical pile at the same location, as illustrated in Fig. 2.18. The limits to which the above recommendation are valid have not yet been established. Nevertheless, it can serve as an approximation until more up-to-date information is available.

2.1.4 Lift Forces on Vertical Piles

In addition to inertial forces that are initiated by water particle acceleration and drag forces that are initiated by water particle velocity, transverse forces may develop because of eddies forming alternately on each side of the piles. The nature of these forces is not very well understood. Analogous to the drag force, lift forces can be expressed as:

$$f_L = C_L \frac{\gamma}{g} D \frac{u^2}{2} \qquad (2.24)$$

in which: f_L = lift force per unit length of pile

C_L = lift coefficient

These forces act in a direction that is perpendicular to both the pile axis and the direction of wave propagation.

For a flexible member, Laird (1962) observed that if the eddy shedding period is close to the natural period of vibration of the pile, lift forces could be 4.5 times greater than the drag forces based on the same velocity under steady uniform flow. The amplification is because of dynamic interaction be-

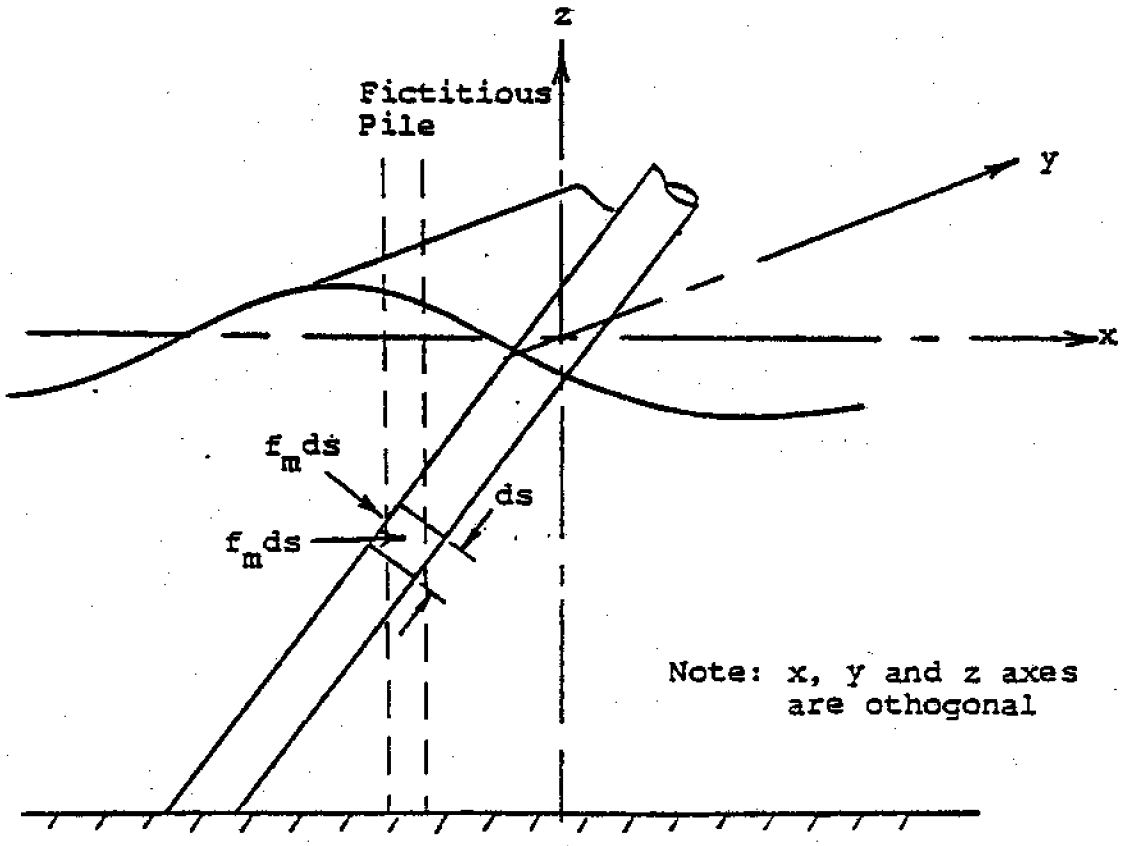

Fig. 2.18 Replacement of an Inclined Pile by a Fictitious Vertical Pile for the Calculation of Wave Forces

tween the member and waves. However, for rigid piles, Laird discovered that lift forces are of the same order of magnitude as the corresponding drag forces in uniform steady flow.

CERC (1977) indicated that, for rigid piles, the values of drag forces can be used as an upper limit for lift forces and suggested the following equation to estimate the maximum value of lift forces:

$$F_{Lm} = C_L \frac{1}{2} \gamma D H^2 K_{Dm} \qquad (2.25)$$

in which: F_{Lm} = maximum total lift force on pile
The lift coefficient, C_L, is found to be dependent upon the Carpenter number, $\bar{u}_{max}T/D$ where $\bar{u}_{max}$ is the average maximum horizontal velocity over the submerged length of the pile. This is shown in Fig. 2.19.

2.1.5 Breaking Waves on Vertical Piles

For waves breaking in deep water, CERC (1977) pointed out that wave forces can be predicted using the same procedures as for non-broken waves. The difference is that only the breaking wave limit line ($H = H_b$) in Figs. 2.4 through 2.16 will be relevant for this situation.

Breaking wave conditions are more common in shallow water. As indicated earlier, the predominant wave force component in shallow water results from drag and CERC (1977) suggested a drag coefficient of 1.75 for design. This recommendation is based on experimental results obtained by Hall (1958) on small-scale model tests. The higher value of C_D is probably because of dynamic effects involved in waves breaking.

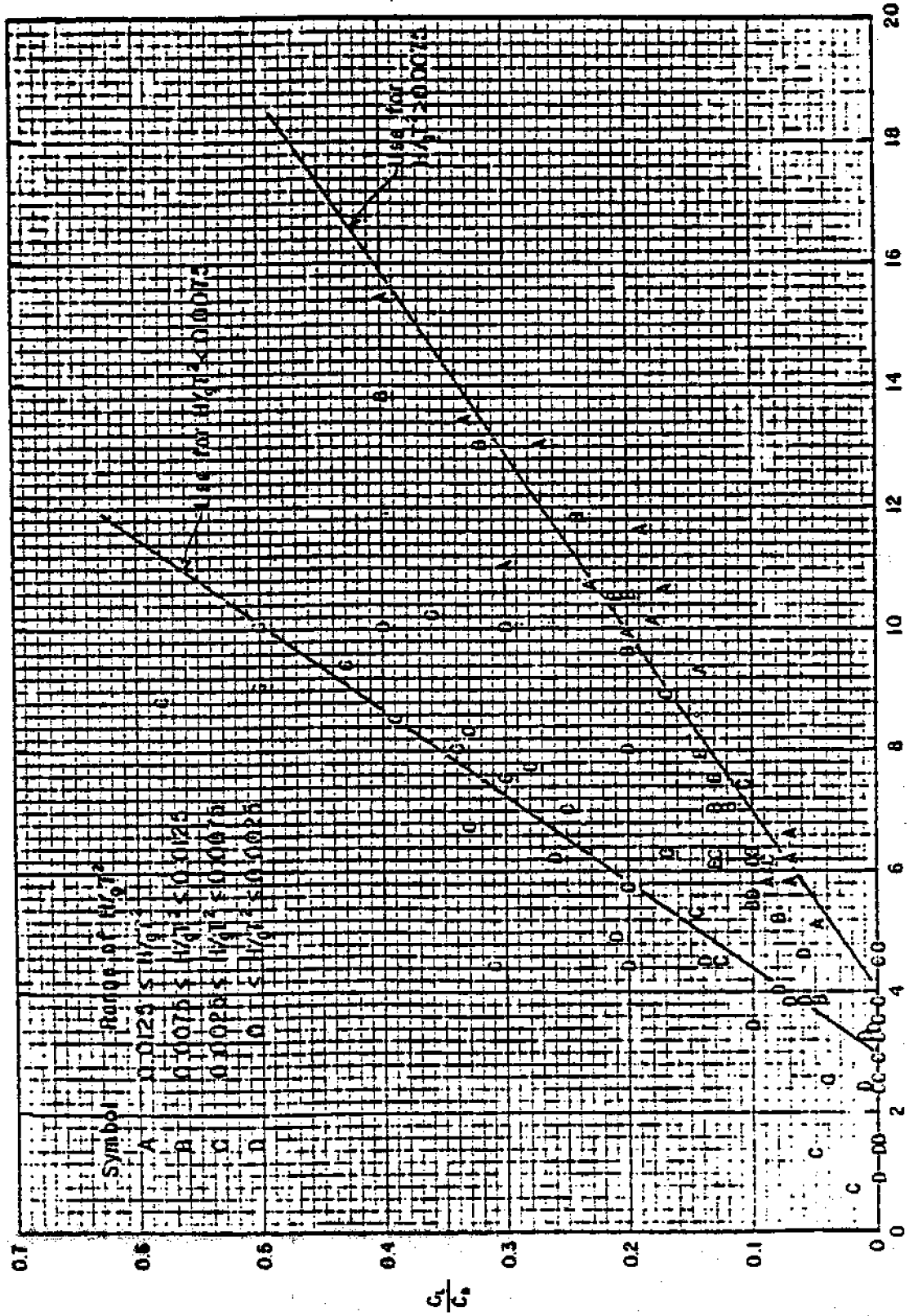

Fig. 2.19 Variation of C_L/C_D with Carpenter Number and H/gT^2 (CERC, 1977)

2.2 Currents

The natural phenomenon of current has been discussed by Hubbell and Kulhawy (1979). It should be realized that direct current action on piles may constitute only a small portion of the total influence; consideration must also be given to its effect on moored vessels or other floating objects in the shore area.

Current forces exerted on piles can be expressed as:

$$f_D = C_D \frac{1}{2} \frac{\gamma}{g} D\, u\, |u| \qquad (2.26)$$

The drag coefficient, C_D, can be obtained from Fig. 2.3 with a knowledge of the Reynolds number (R_e). Again, the lift forces may be significant if the pile is flexible and it vibrates under the action of shedding eddies.

Current velocity to be used in design is largely dependent upon the topographic and meteorological conditions at the site. It can be measured directly at the site with any appropriate device. In cases where this information is not available, Chellis (1961) recommended a value of about 7 ft/sec (2 m/sec) for ordinary design.

In cases where current and waves may exist together, it is necessary to superimpose the current velocity with the water particle velocity vectorially to arrive at the total drag forces acting on the member.

2.3 Ice

The characteristics of ice depend largely upon the climatic conditions at the site. In sheltered waters where wave action will not be severe, ice loads may be a controlling fac-

tor in design. In cold regions, appreciable damage of waterfront structures because of ice action has been reported.

The formation of ice may enlarge existing cracks in concrete piles, and moving ice floes may cause severe abrasion of pile surfaces at the water level. In addition, expansion of water because of freezing in an enclosed area can produce static ice stress against a structure. A value of up to 30,000 psi (207 MN/m^2) was cited by CERC (1977).

In general, the two most common forms of loadings associated with ice formation can be categorized into the following:

1) vertical loads resulting from ice grip

2) lateral loads resulting from ice impact

Vertical loads on piles by ice are made possible by ice grip on the member. In regions where the water level changes gradually, this is not likely to occur. However, in areas where ice forms undisturbed for a long time, thick ice sheets may adhere to the piles and a sudden rise of water level may result in considerable uplift forces. Similarly, a sudden drop of water level will leave the ice hanging around the pile, resulting in downdrag of piles. Impact force from ice sheets is caused by momentum of the moving ice blocks carried by wind or current.

These two forms of loadings caused by ice have been discussed by Hubbell and Kulhawy (1979), who discuss appropriate procedures to estimate the magnitude of these forces.

2.4 Earthquakes

Earthquakes, even though they may occur infrequently, can result in disastrous destruction. Thus, earthquake design must

always be considered in an active seismic zone. Stronger earthquakes in the United States from historical times through 1970 are listed in the following U.S. Department of Commerce's (1973) publication: *Earthquake History of the United States* . Further information can be obtained in the annual report: *United States Earthquakes* , published jointly by the U.S. Department of Commerce and U.S. Department of the Interior. A seismic risk map of the United States is shown in Fig. 2.20. It should be noted that earthquake design often leads to costly solutions which may not be justifiable for small-scale structures. Therefore, the consequences of an earthquake should always be examined before an analysis is performed.

The procedures for determination of earthquake loads on retaining structures are outlined by Hubbell and Kulhawy (1979) using methods proposed by Seed and Whitman (1970). This section will discuss some of the earthquake problems associated with pile-supported structures. It should be emphasized that earthquake analysis is a very complex dynamic problem and can be a separate subject in itself; therefore only general guidelines will be provided here.

All structures have a natural period of vibration. In active seismic zones, this period should be computed to avoid resonance with the period caused by earthquake excitation. For the case of a single pile, Chellis (1961) presented the following equation to estimate the natural period of vibration:

$$T_n = c_f \sqrt{\frac{W_p}{E_p I_p / L_e^3}} \qquad (2.23)$$

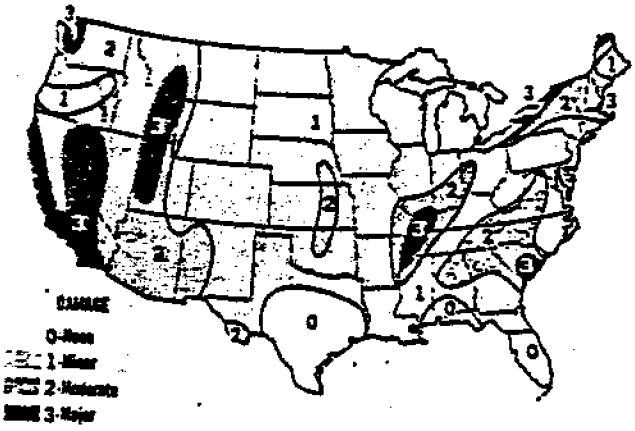

Fig. 2.20 Seismic Risk Map for Continental United States (U.S. Department of Commerce, 1973)

in which: T_n = natural period of vibration

W_p = effective weight of pile

E_p = Young's modulus of pile material

I_p = moment of inertia of pile cross-section

L_e = length of pile down to point of apparent fixity (see Section 6.2)

c_f = coefficient depending on end restraint condition of pile

= 0.18 for full fixity at bottom and no restraint at top

= 0.09 for full fixity at both top and bottom (see Section 6.2 for details on end conditions)

For a group of piles, the following equation is suggested:

$$T_n = c_f \sqrt{\frac{\Sigma W_p}{\Sigma (E_p I_p / L_e^3)}} \qquad (2.24)$$

It is believed (Chellis, 1961) that resonance will not be a problem under normal earthquake conditions if the natural period of vibration of the structure is kept above 2 seconds.

An earthquake consists of horizontal and vertical ground motions. The vertical motion is of much smaller magnitude than the horizontal motion and is usually neglected in design. The horizontal motion will give rise to lateral forces acting on the structure, the magnitude of which depends upon the stiffness, inertial and damping characteristics of the system, and the size of the earthquake.

The Structural Engineers Association of California (SEAOC) simplifies the seismic response of structures and recommends

the following equation to estimate the magnitude of horizontal excitation forces during an earthquake (Degenkolb, 1970):

$$P_e = K^* C W_T \qquad (2.25)$$

in which: P_e = horizontal excitation force

K^* = coefficient to indicate capacity of structure to absorb energy (may vary from 0.67 to 3.00)

C = seismic coefficient

$= 0.05/\sqrt[3]{T_n}$

W_T = total effective weight of structure

The development of the SEAOC equation is based on the idea that as the ground under the structure moves, the inertia of the structure will tend to resist this movement, as illustrated in Fig. 2.21.

It should be noted that methods outlined in this section may have severe limitations in assessing the seismic response of structures. Many of relevant parameters have been omitted in the development of the equations. Therefore, the results should be interpreted carefully.

2.5 Ship Impact

Direct ship impact with docks or piers is undesirable and some forms of protective device should be used to absorb the energy of impact. Fender piles are often employed for this purpose since they are relatively cheap and easy to replace. Thus, ship impact constitutes one of the most influential factors for design of fender piles.

Unlike other types of loading, ship impact forces are not

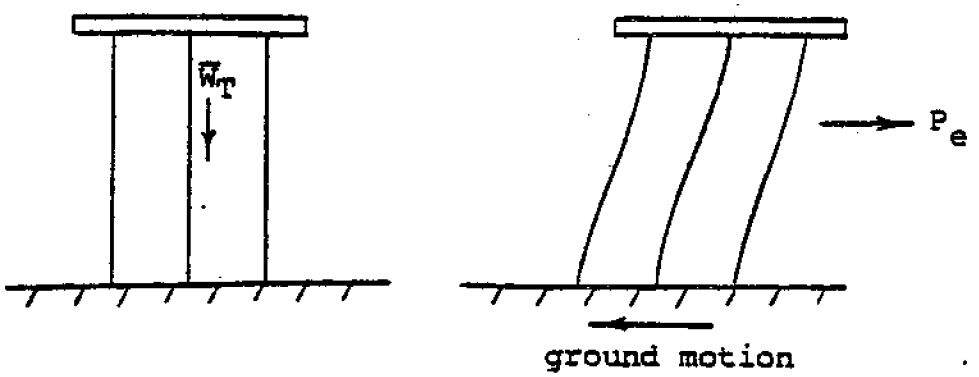

Fig. 2.21 Forces Developed by Earthquakes

natural phenomenon. Although it may not be avoided, it can be controlled to some degree. The magnitude of the force is a function of the weight of the vessel (including any load that it may carry), the speed at impact and the energy-absorbing capability of the system.

The speed at impact is determined by the skill of the pilot as well as the meteorological and oceanographic conditions. Quinn (1972) suggested an impact speed of 0.25 to 0.50 ft/sec (0.076 to 0.152 m/sec) for design. The energy-absorbing capability of the system depends largely upon the degree of rigidity of the pile. A rigid pile will undergo small deflection and result in a large magnitude of impact force. Conversely, a flexible pile will experience larger deflection with smaller impact force. Based on the energy conservation equation, the impact force can be given as:

$$P_s = \frac{1}{2} \frac{(km_s)v_s^2}{y} \tag{2.26}$$

in which: P_s = ship impact force

k = energy-absorbing coefficient

m_s = mass of ship (including load if applicable)

v_s = speed of ship at impact

y = deflection of pile

The energy-absorbing coefficient, k, is used to account for the fact that not all the energy is imparted to the pile; kinematic energy is also absorbed through deformation of the ship hull, deformation of the ground, rebound of the ship, etc.. Quinn (1972) recommended a k value of 0.5 for design.

2.6 Summary

Various forms of loadings that can affect pile-supported structures in the coastal regime have been described. Most of these loads are produced by the environment and therefore they will fluctuate with time. This point has been ignored and it is assumed that these dynamic loads can be represented by their static equivalents. The validity of such assumptions has been discussed at the beginning of the chapter.

Procedures for evaluation of waves, currents, ice, earthquakes and ship impact loads on piles are outlined. The direct effects of forces resulting from wind, tides, etc., are likely to be small, but their interaction with other forms of loadings should not be ignored. As the final cost of the structure is directly related to the magnitude of the design loads, good judgment must be exercised in the selection of these load values.

The extent of influence of all forms of loadings depends largely upon the site conditions. In well-protected areas where most of the loads can be attenuated, the design load may be substantially reduced. Protection can be natural or man-made. Natural protection (e.g., sheltered bays) is provided by the topographic features at the site and may be available by a careful evaluation of various selected sites. Man-made protection (e.g., breakwaters, ice breakers) is constructed to suit site conditions and specific requirements. The resulting benefits should at least offset the cost required to set up the protective device.

Finally, it should be emphasized that the forces acting on

a structure depend not only on the sources of loadings; instead, they are functions of both the sources of loadings and the structure itself. Modification of the structural orientation and/or configuration may very often change the magnitude of the loads. Therefore, different options should be constantly examined in the design phase.

CHAPTER 3

DESIGN OF PILES FOR COMPRESSIVE LOADS

Compressive forces are exerted by the weight of the structure, which includes the weight of pilings, decks, stiffeners, connectors and other attachments that will remain throughout the life of the structure. In cases where the structure is partially submerged in water, the buoyancy force for the submerged portion should be deducted from the total dead load to obtain the net compressive force.

For structures such as docks or piers, it is also necessary to include live loads (e.g., movable equipment, human occupants, vehicles) in design. The magnitude of the live loads depends upon the use of the structure and the amount of traffic anticipated. Minimum values are often prescribed by local building codes.

In addition to the dead and live loads mentioned above, consideration must also be given to installation loads during the construction stage, especially if the use of heavy construction equipment is necessary.

3.1 Ultimate Capacity of Single Piles

The ultimate load on a pile is defined as the load that causes failure of either the pile or the soil. Under most circumstances, this is governed by soil failure, unless the pile is founded on dense sand or rock. The following discussions will be limited to cases where failure of soil is the critical failure mode. However, the structural capacity of the pile

should always be checked (See Sections 6.2 and 6.3.).

The determination of the ultimate axial capacity of single piles gives us an estimation on the maximum load a pile can carry for a given depth of embedment, or restated in another way, it provides a method by which we can determine the depth of penetration required for a particular job. Evaluation of compressive load capacity is required for the design of pile foundations. However, one should realize that the design of any foundation may be governed by settlement (although rare for the case of deep foundations), as well as bearing capacity. Discussions on pile settlements will be presented in Section 3.3.

Computation of ultimate axial capacity is difficult, mainly because of the large numbers of parameters involved and the uncertainties associated with these parameters. Moreover, installation of piles alters the soil properties to an extent that may differ considerably from the original ground conditions.

The ultimate axial load capacity of a single pile is determined at least by the following factors:

1) in-situ properties of the soil mass
2) dimensions and material properties of the pile
3) methods of installation
4) loading conditions
5) time effects

The extent to which these factors influence the final capacity is a function of the size of the pile and the ground conditions. For small scale construction work, the method of installation

is probably the most important consideration that can influence the ultimate capacity. Therefore, the person that supervises the installation process should have a sound understanding of the assumptions made in the design phase.

For design purposes, the ultimate capacity of deep foundations under compressive loading is conventionally separated into two components:

1) shaft resistance or skin friction

2) point resistance or base resistance

A free-body diagram of an axially loaded pile is shown in Fig. 3.1. In algebraic form, the ultimate compressive load that can be carried by the pile-soil system is given as:

$$Q_{ult} = Q_s + Q_p - \bar{W}_p = f_s A_s + q_p A_p - \bar{W}_p \qquad (3.1)$$

in which: Q_{ult} = ultimate compressive load

Q_s = ultimate shaft resistance

Q_p = ultimate point resistance

$\bar{W}_p$ = net weight of pile = weight of pile - hydrostatic uplift

f_s = average ultimate shaft resistance per unit area

q_p = average ultimate point resistance per unit area

A_s = area of pile shaft embedded in soil

A_p = area of pile point or tip

The value of $\bar{W}_p$ is usually small compared with Q_{ult} and therefore is often disregarded in Equation 3.1. Methods to evaluate f_s and q_p will be presented later. The areas of the pile shaft and pile point are given respectively as:

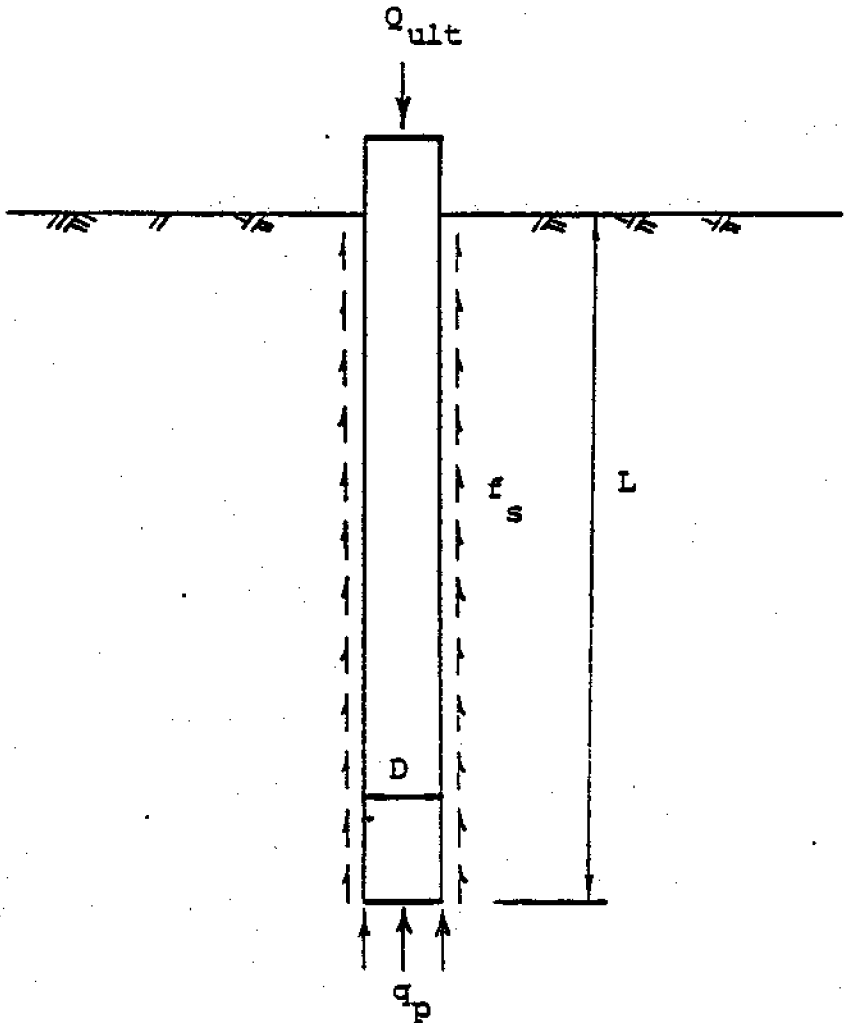

Fig. 3.1 Free-Body Diagram of a Pile under Compressive Loads

$$A_s = \pi \int_0^L D\, dz = \pi D L \text{ for a constant cross-section} \quad (3.2)$$

$$A_p = \pi D^2/4 \quad (3.3)$$

in which: L = length of embedment of pile

D = diameter of pile

The allowable compressive load can be computed from the following:

$$Q_{all} = Q_{ult}/FS \quad (3.4)$$

in which: Q_{all} = allowable compressive load

FS = factor of safety

The choice of the factor of safety should reflect our confidence in the parameters involved in the design process. It also depends upon the nature of the project and the financial loss in case of failure. A factor of safety that ranges from 3 to 4 is generally used for designing piles under compressive loadings, when subsurface information is reasonably well-known.

Based on the mechanism of load transfer, piles can be classified into two types: 1) piles that transmit the major portion of the surface loads to the subsoil through shaft resistance are called friction piles and, 2) piles that derive their load capacities primarily from point resistance are referred to as end-bearing piles.

It should be noted that Equation 3.1 assumes the shaft resistance and point resistance to be independent of one another. This is not true in reality. The shaft and point resistances are not mobilized simultaneously. Pile movement required to mobilize shaft resistance is around 1/4 to 1/2 inch (6.4 to

12.7 mm), while a displacement on the order of 0.08 to 0.10 D is normally needed to mobilize the point resistance for driven piles (Murphy, 1974). Therefore, in general, ultimate point resistance will not be developed until after the ultimate shaft resistance is fully mobilized (Fig. 3.2). However, for design purposes, our main concern is in the total value of ultimate load.

Although methodologies to evaluate the ultimate load capacities of piles classify the soil material into clay and sand, the behavior of these two materials are the same in principle. The difference lies in the critical condition with respect to drainage that each material will experience under load. Drained (long-term) conditions will normally govern for cohesionless soils, while undrained (short-term) conditions normally are the critical mode of failure for normally consolidated and lightly overconsolidated cohesive materials (For more information, see Sections 3.3 and 8.7.). In reality, procedures used to determine ultimate load capacities for piles in clay are also applicable to sand and vice versa. The appropriate choice of method depends upon the conditions present.

Since large numbers of technical papers have reported pile capacities on the basis of clay (undrained) and sand (drained) materials, the following discussions will be broadly separated into these two categories. In many practical situations, the soil profile is likely to contain both clay and sand layers. In that case, the appropriate parameters and approaches can be used for each layer to obtain the ultimate capacity for the

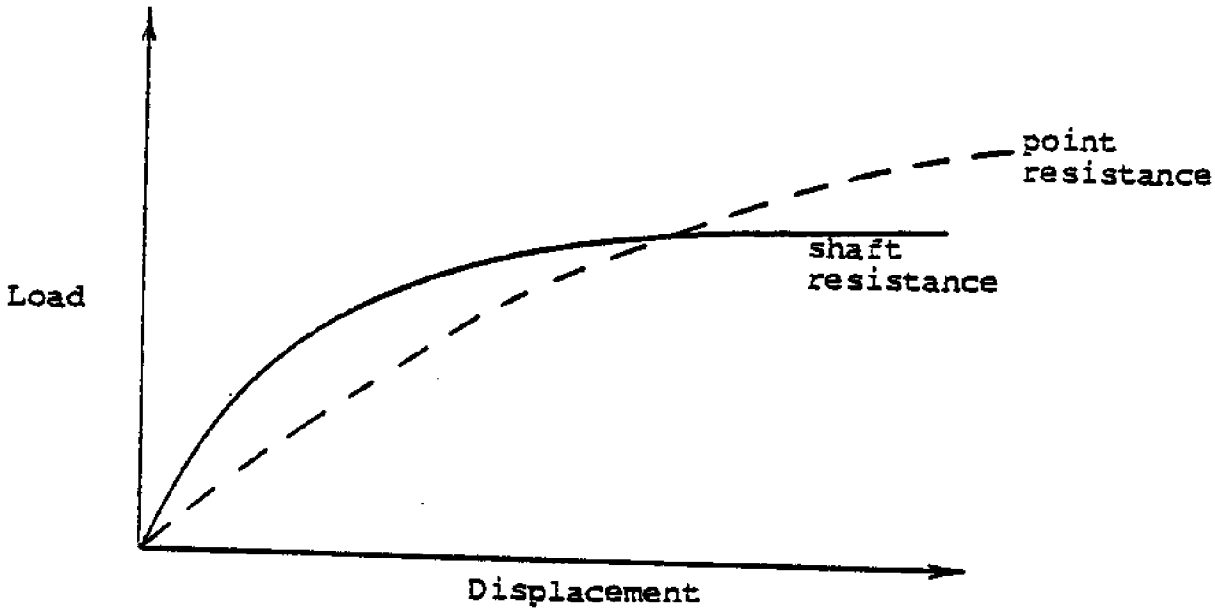

Fig. 3.2 Relative Movement for Mobilization of Point and Shaft Resistances

whole pile.

In the discussions that follow, the loading conditions are assumed to be static and long-term. Dynamic and transient loadings on piles are beyond the scope of this study.

3.1.1 Piles in Clay

For piles driven in normally consolidated and lightly overconsolidated clays (contractive soils), undrained loading is generally considered as the critical mode of failure. On the other hand, for piles driven in heavily overconsolidated clays (dilative soils), the drained case is believed to govern the design.

The type of clay that we frequently encounter in the coastal regime is normally consolidated, although overconsolidated clay may be found in regions that have been subjected to a great deal of erosion or that have been preloaded.

In general, for piles driven entirely into clay, point resistance is small as compared with shaft resistance and the displacement required to mobilize shaft resistance is smaller than that required to mobilize point resistance. This is especially the case for small diameter piles driven into soft clay. Therefore, point resistance is sometimes omitted in the design of pile foundations in clays.

Three major approaches have been proposed to estimate the compressive load capacity of piles in clays: α-method, β-method and λ-method. The α-method uses parameters associated with undrained loading and thus is often called a total stress approach. The β-method is based on drained parameters and is

sometimes called an effective stress approach. The λ-method was developed on the basis of soil stress theory for the undrained case. Each of these three methods will be described. The α and λ-methods are largely based on empiricism in which the coefficients α and λ were back-calculated from load test results. The β-method has some theoretical basis since the β-coefficient can be computed directly from basic soil parameters.

3.1.1.1 α-method

This method has been widely used to compute the compressive load capacity of piles in clay. It considers failure under undrained conditions to be the critical mode of failure and thus parameters associated with undrained loading are used. For this case, the unit point resistance can be computed from:

$$q_p = N_c \, c_u \tag{3.5}$$

in which: N_c = bearing capacity factor with respect to cohesion

c_u = undrained shear strength of the soil

and the average shaft resistance per unit area is given as:

$$f_s = c_\alpha \tag{3.6}$$

in which: c_α = pile-soil adhesion per unit area

The determination of the ultimate point resistance involves the evaluation of N_c, c_u and A_p, where the parameters are defined earlier. A_p is directly related to the geometry of the pile and c_u can be measured in the field or laboratory. These two quantities can be obtained with no great difficulties. For the determination of N_c, Meyerhof (1951) derived the following equation:

$$N_c = \frac{4}{3} \{ \ln \frac{1}{3} (E_u/c_u) + 1.75 \} \quad (3.7)$$

in which: E_u = undrained Young's modulus of soil

As reported by D'Appolonia, et al. (1971), values of E_u/c_u for many types of normally consolidated and lightly overconsolidated clays with plasticity index less than 30% are larger than 400. This corresponds to a N_c value of greater than 9. Therefore, the use of N_c equal to 9 sets a lower limit for the point resistance. They also pointed out that E_u/c_u would decrease with increasing overconsolidation ratio and increasing plasticity index. For heavily overconsolidated clays, it is possible that N_c may go down to as low as 5 or 6.

At present, the value of N_c that has been widely accepted in practice is 9, although values between 5 and 25 have been suggested. Meyerhof's equation is not widely used because of difficulty in evaluation of the undrained Young's modulus of soils. Besides, the point resistance constitutes only a small portion of the ultimate load capacity, so prediction of point resistance assuming a N_c value of 9 will provide sufficient accuracy for most practical purposes. In fact, a N_c value of 9 in normally consolidated clays has been confirmed by full scale load tests carried out by Clark and Meyerhof (1973).

The adhesion parameter, c_α, in Equation 3.6 indicates how well the pile and soil adhere together. Its value depends upon a number of factors, which include the pile material, soil properties and method of installation. The best way to determine c_α is from full scale pile-load tests; however, this normally

is not economically feasible for small-scale structures. Empirical values or past data are often used. Numerous attempts have been made to correlate c_a to c_u, the undrained shear strength of soil, and therefore, c_a is often expressed as:

$$c_a = \alpha\, c_u \tag{3.9}$$

in which: α = adhesion coefficient

Vesić (1967) presented a summary of the relationship between c_a and c_u based on the work on many investigators (Fig. 3.3). The figure includes values for both driven and bored piles. His results indicated that α is consistent and is approximately equal to one for soft clay with an undrained shear strength of less than 1000 psf (48 kN/m^2). On the other hand, the values of α for stiff clay are scattered with values that go down to as low as 0.3.

As illustrated by Vesić's results (Fig. 3.3), it is not surprising that there has been little disagreement on the use of α equal to one for soft clay with an undrained shear strength of less than 1000 psf (48 kN/m^2). However, the choice of α for stiff clay is not as clear. McClelland (1974) compiled the recommendations made by several investigators for driven piles in clays and this is shown in Fig. 3.4.

Although the recommended values of α for stiff clay vary, there is a general trend of a decrease in α with increasing shear strength of the soil. This phenomenon, as well as the large scatter of data for stiff clay, may be explained by the existence of natural fissures under in-situ conditions or the

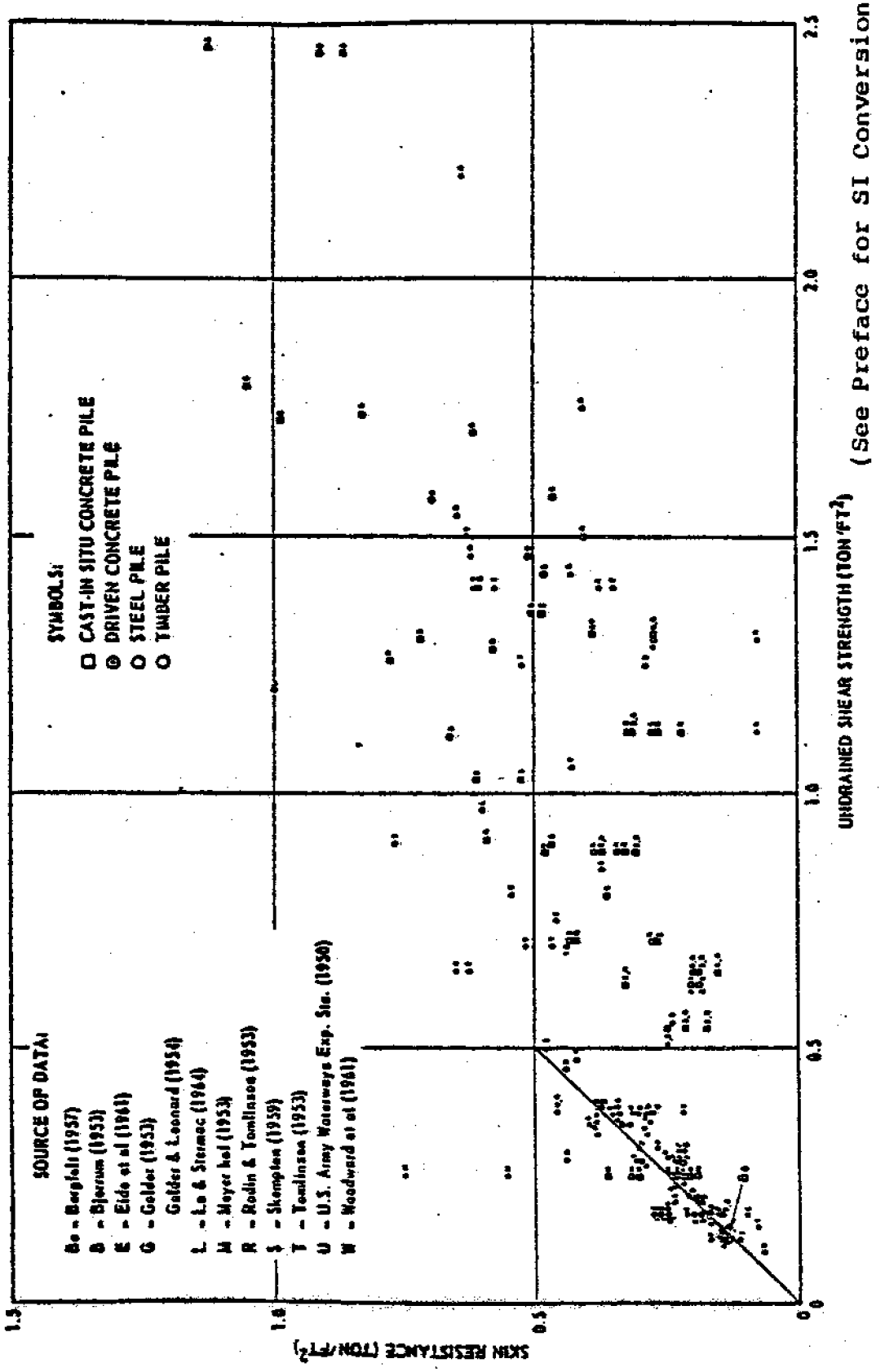

(See Preface for SI Conversions)

Fig. 3.3 Comparison between Skin Resistance of Piles in Clay and Undrained Shear Strength (Vesić, 1967)

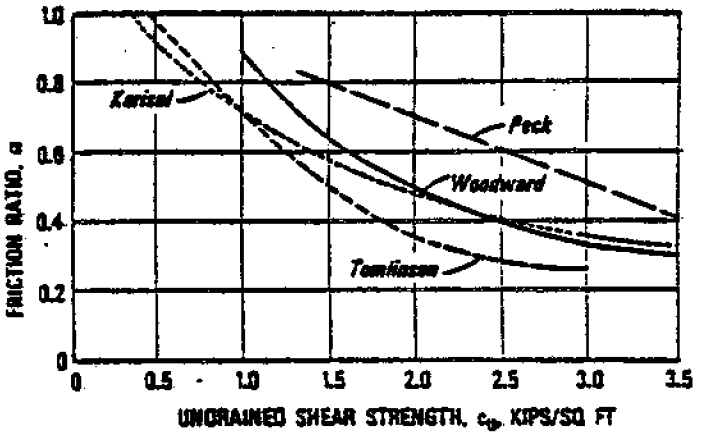

(See Preface for SI Conversions)

Fig. 3.4 Correlations of α with c_u (McClelland, 1974)

formations of cracks caused by pile driving.

Tomlinson (1977) attributed the scattering of α for stiff clay to soil strata overlying the stiff clay layer and suggested the α-values given in Fig. 3.5. Two of the notable features in Tomlinson's proposal are that it takes into account the effect of length/diameter ratio and the effect of the sequence of soil layers through which the piles pass.

3.1.1.2 β-method

For long-term conditions in which the excess pore-water pressure induced by installation and loading of the piles is negligible compared with the effective overburden stress, the ultimate axial capacity of a pile may be expressed in terms of effective stress parameters. This drained condition may very well be the critical case for piles driven into heavily overconsolidated clays.

Chandler (1968) described very clearly this effective stress approach for obtaining the ultimate capacity. He suggested that the horizontal effective stresses in the ground may control the magnitude of shaft resistance if the rate of loading is slow enough to ensure that drained conditions exist along the pile shaft. These conditions, according to him, can be met in maintained load tests and in long-term, in-service conditions. To be consistent with the implicit assumption that drained conditions govern, the unit point resistance for this approach should be computed as for sands and the average shaft resistance per unit area is given as:

$$f_s = \bar{c} + K \bar{\sigma}_v \tan \delta \qquad (3.10)$$

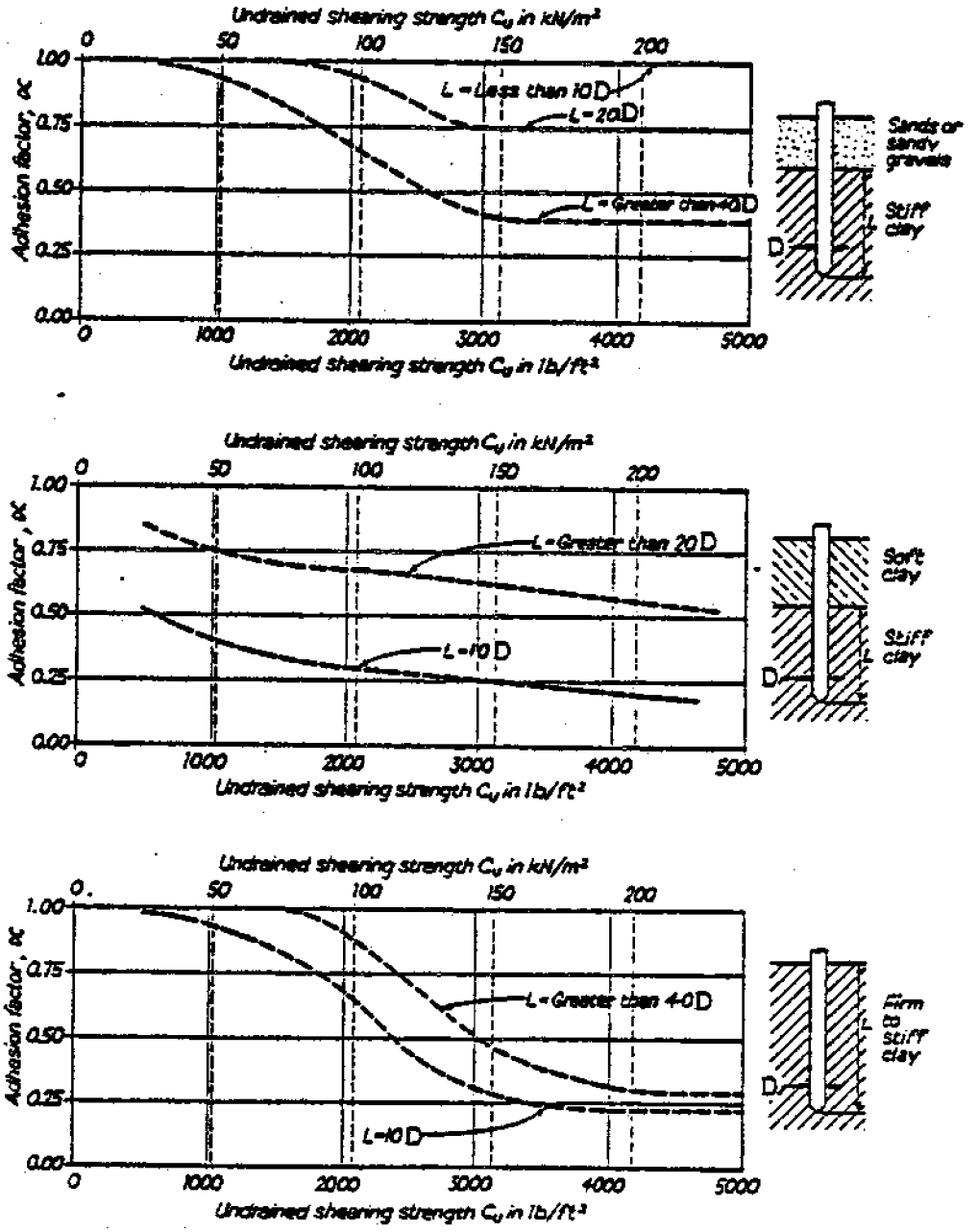

Fig. 3.5 Design Curves for α-coefficient for Piles Driven into Clay (Tomlinson, 1977)

in which: $\bar{c}$ = effective cohesion $\tilde{=}$ 0

K = horizontal stress coefficient

$\bar{\sigma}_v$ = effective vertical stress

δ = angle of friction between pile and soil

Burland (1973) advocated that this effective stress approach is applicable for all design cases. He suggested that, at the pile-soil interface, the rate of dissipation of excess pore water pressure can be so rapid that undrained conditions are almost non-existent. The assumptions of this effective stress approach, as stated in Burland's paper, are given as follows:

1) before loading, the excess pore water stress set up during installation is essentially dissipated.
2) the zone of disturbance around the shaft is relatively narrow and loading takes place under drained conditions.
3) the soil has no effective cohesion because of remolding during installation.
4) the horizontal stress is proportional to the vertical effective overburden stress.

Adopting Chandler's (1968) procedures, Burland (1973) expressed Equation 3.10 in the form:

$$f_s = \beta \bar{\sigma}_v \qquad (3.11)$$

in which: β = skin friction coefficient = K tan δ

The magnitude of the horizontal stress coefficient, K, depends upon the properties of the soil and the method of installation. It should be slightly larger than the soil stress co-

efficient at rest (K_o) for small displacement piles (e.g., H pile, pipe pile) and may approach the passive soil stress coefficient (K_p) for large displacement piles. Since the evaluation of K is very difficult, Burland (1973) suggested the use of K equal to K_o to establish a lower limit on shaft resistance. For normally consolidated clays, K_o can be estimated from Jáky's expression:

$$K_o = 1 - \sin \bar{\phi} \qquad (3.12)$$

in which: K_o = soil stress coefficient at rest

$\bar{\phi}$ = effective angle of internal friction of soil

In reality, the angle of friction between the pile and the soil is likely to be less than the drained angle of internal friction of soil (except for rough concrete piles). However, it can be assumed that failure takes place in the remolded soil close to the pile shaft instead of along the pile-soil interface, so that δ may be taken as $\bar{\phi}$ (Tomlinson, 1971).

By setting $K = K_o$ and $\delta = \bar{\phi}$, Burland (1973) noted that the values of β vary only between narrow limits for a wide range of $\bar{\phi}$ (Fig. 3.6). For typical values of $\bar{\phi}$ that range from 20° to 30°, β lies only between 0.24 and 0.29. This agrees with values of β back-calculated from load test results on piles driven in normally consolidated clays (Fig. 3.7). The β values from these tests range from 0.25 to 0.4 with an average value of about 0.32. Burland recommended the use of 0.3 for β in design. This important finding implies that the shaft resistance is determined largely by the shaft area and the effective vertical stress along the pile shaft.

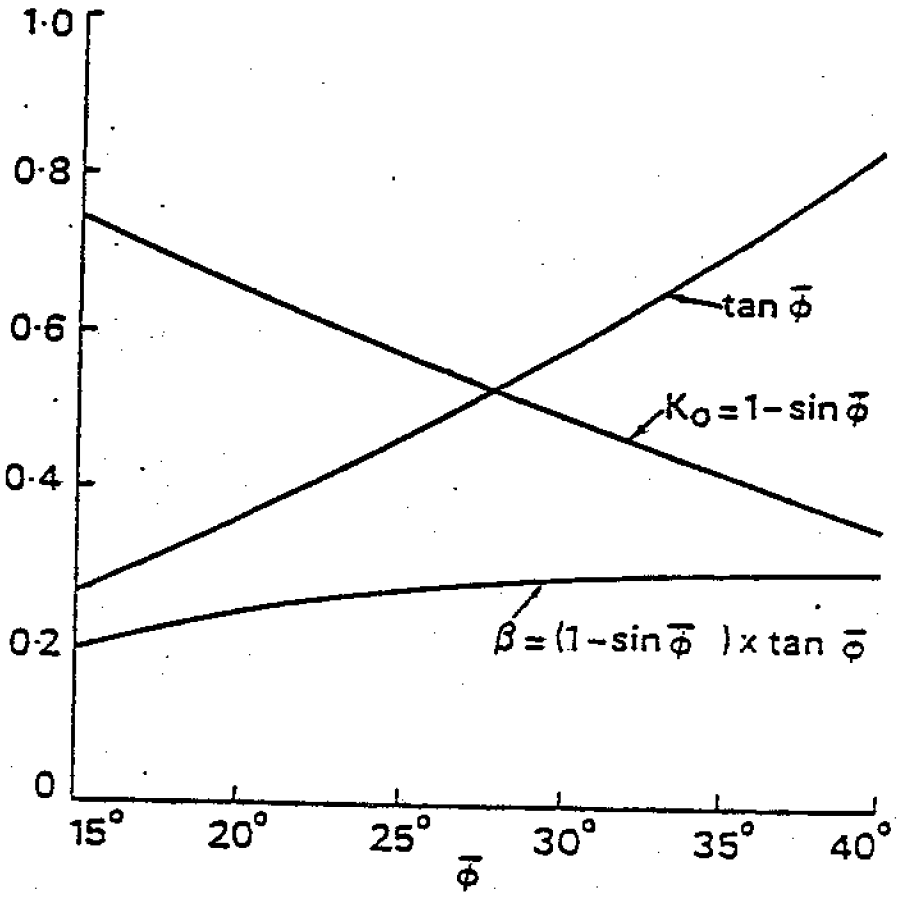

Fig. 3.6 Variation of β with $\bar{\phi}$ (Burland, 1973)

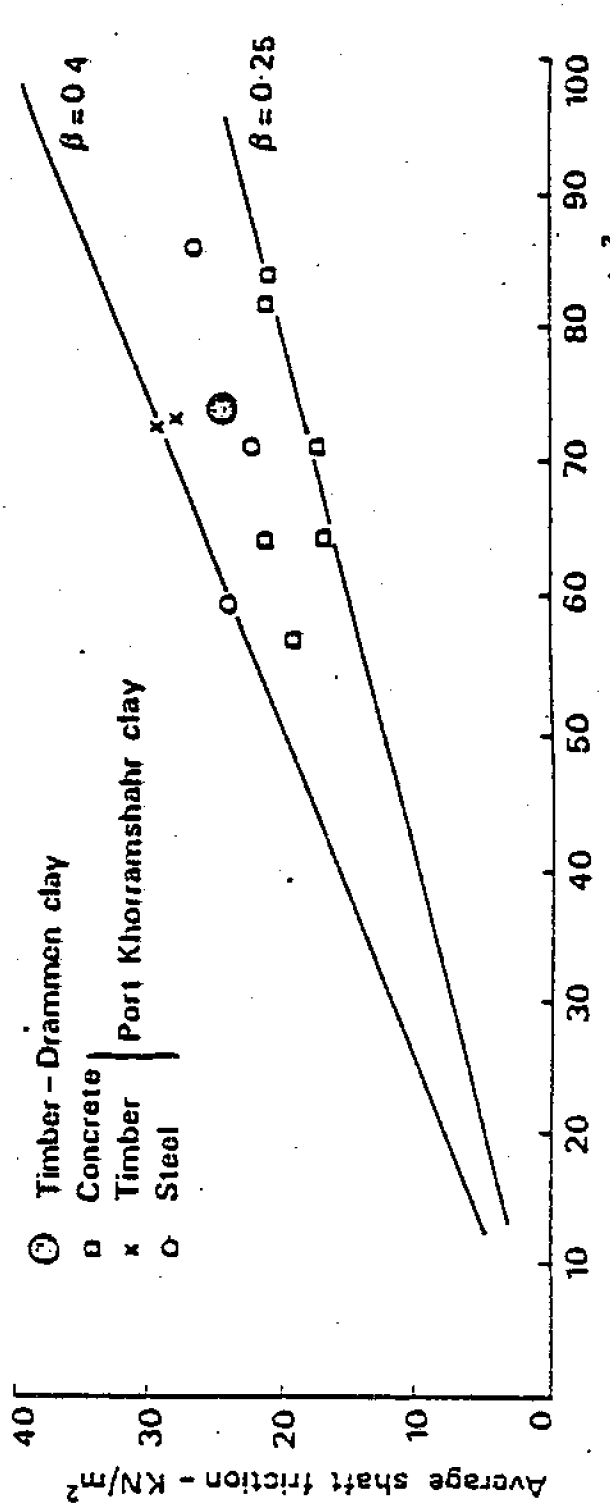

(See Preface for English Units Conversions)

Fig. 3.7 Values of β Back-calculated from Load Test Results (Burland, 1973)

For stiff overconsolidated clay, Equation 3.12 does not apply and difficulty lies in estimating the value of soil stress coefficient at rest, K_o. Meyerhof (1976) suggested that K_o can be roughly estimated from the following expression:

$$K_o = (1 - \sin \bar{\phi}) \sqrt{OCR} \qquad (3.13)$$

in which: OCR = overconsolidation ratio

The validity of Equation 3.13 has been verified by Flaate and Selnes (1977). They demonstrated that the correction factor $\sqrt{OCR}$ applied to overconsolidated clay does give results that are similar to those for normally consolidated clay. This is shown in Fig. 3.8.

3.1.1.3 λ-method

Vijayvergiya and Focht (1972) presented an alternative approach to evaluate the pile capacity in cohesive soils. Based on the classical Rankine passive soil stress theory for undrained conditions, they evaluated the shaft resistance of piles using the effective vertical stress as well as the undrained shear strength. These parameters were related to the shaft resistance through an empirically determined coefficient, λ. Using this method, the point resistance may be computed in the same way as the α-method and the average shaft resistance per unit area is expressed as:

$$f_s = \lambda \, (\bar{\sigma}_v + 2c_u) \qquad (3.14)$$

in which: λ = adhesion coefficient

The λ-coefficient was determined from 47 load tests on steel pipe piles summarized by the investigators. It is given as a function of depth of pile penetration (Fig. 3.9).

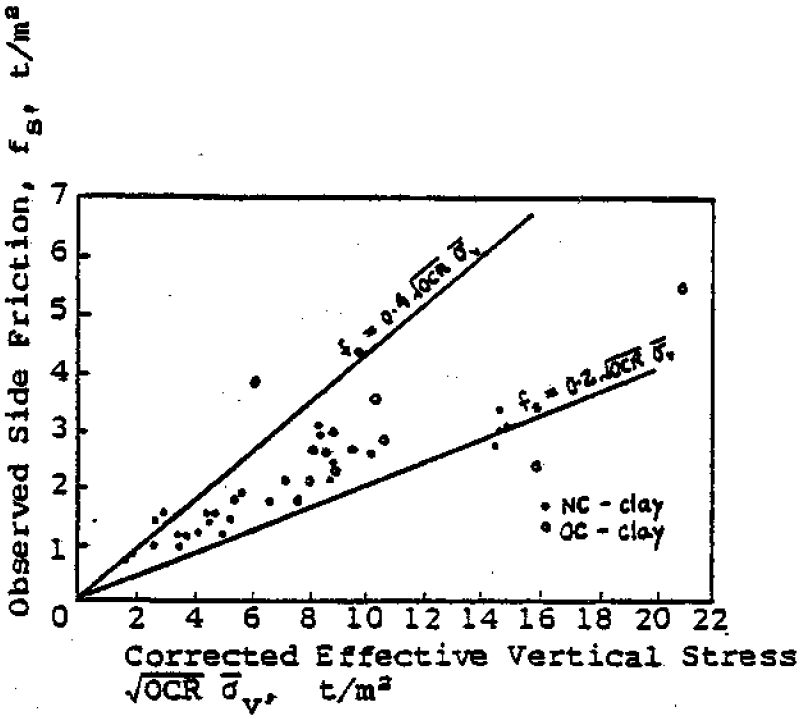

Fig. 3.8 Observed Shaft Resistance Versus Adjusted Effective Vertical Stress (Flaate and Selnes, 1977)

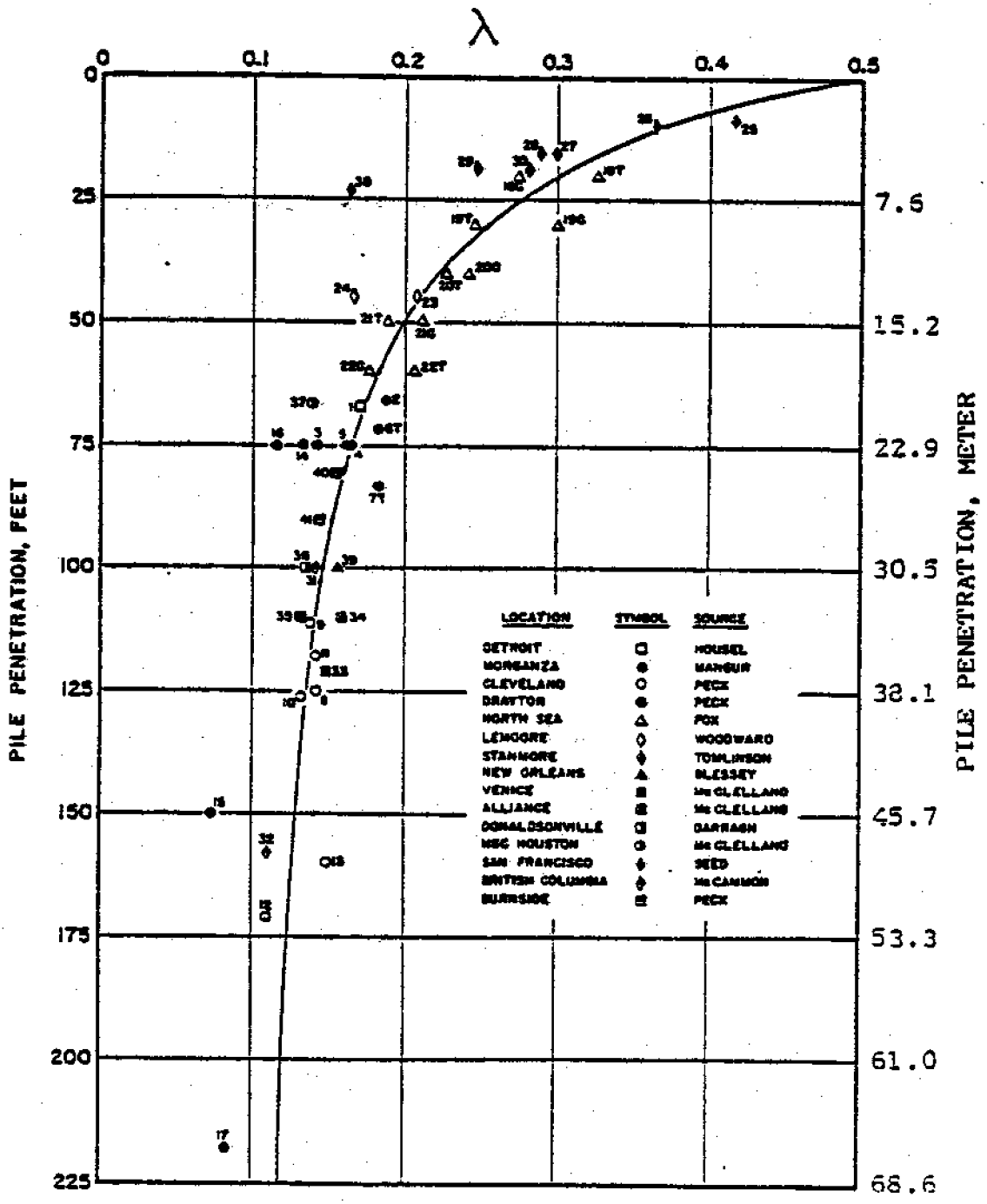

Fig. 3.9 λ-coefficient Versus Pile Penetration (Vijayvergiya and Focht, 1972)

One distinct feature of the λ-method is that it indicates the possibility of decreasing shaft resistance with increasing pile length. This is confirmed by Meyerhof's (1976) finding that β may decrease with increasing pile penetration.

The λ-approach has been questioned by several investigators. Flaate and Selnes (1977) reported that the λ-method generally overestimates the shaft resistance and the correlation is poor (Fig. 3.10). Esrig and Kirby (1979) argued that the data base used to determine the coefficient λ may be biased. They pointed out that the data from short piles are generally piles that are driven into stiff overconsolidated clay, while the data from very long piles are generally piles that are driven into soft clay.

This method has been widely used by the offshore industry to predict the load capacities of heavily-loaded steel pipe piles. It should be realized that although the Rankine theory can be rigorously derived, the λ-method itself is purely empirical. Rankine theory is applicable only for plane strain cases (e.g., long retaining structures) and its use for circular shafts does not have any theoretical justification.

3.1.2. Piles in Sand

Because of the fast rate of excess pore water stress dissipation, piles driven in sand are dominated by drained conditions and drained parameters are to be used in the analysis. Unlike piles embedded in clay, the point resistance may have an appreciable value and should not be omitted in design.

For the drained case, the unit point resistance can be ex-

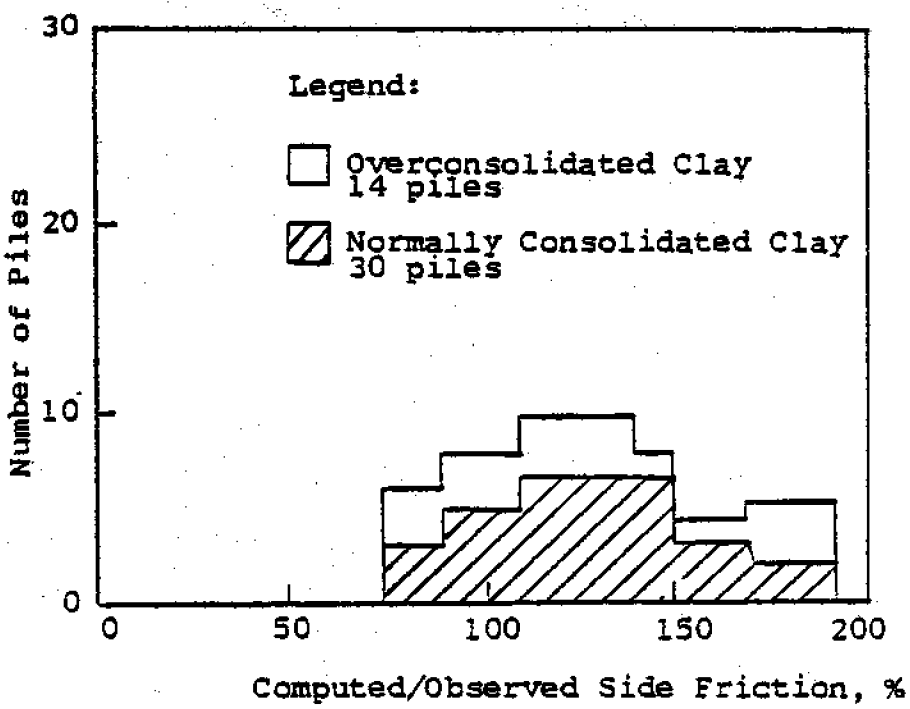

Fig. 3.10 Frequency Curves for Computed/Observed Shaft Resistance Using the λ-method (after Flaate and Selnes, 1977)

pressed as:

$$q_p = N_q \, \bar{\sigma}_{vp} \tag{3.15}$$

in which: N_q = bearing capacity factor with respect to overburden stress

$\bar{\sigma}_{vp}$ = effective vertical stress at the pile point

and the average shaft resistance per unit area can be computed from:

$$f_s = K \, \bar{\sigma}_v \tan \delta \tag{3.16}$$

Based on the assumption that the soil is a perfectly plastic material, a wide scatter of N_q variations have been proposed by various authorities (Fig. 3.11). Of the solutions shown in Fig. 3.11, that of Berezantzev, et al. (1961) is considered to be most reliable (Nordlund, 1963; Vesić, 1965; Tomlinson, 1977). Tomlinson (1977) refined Berezantzev, et al.'s results and suggested N_q values given in Fig. 3.12.

Meyerhof (1976) suggested the use of an upper limit value for unit point resistance below the critical depth (L_c). The unit point resistance should then be expressed as:

$$q_p = N_q \, \bar{\sigma}_{vp} \leq q_\ell \tag{3.17}$$

in which: q_ℓ = limiting value on unit point resistance below the critical depth for piles in sand

According to Meyerhof (1976), the critical depth ratio can be estimated from Fig. 3.13. Equation 3.15 is applicable only for piles with $\frac{L}{D}$ less than $\frac{L_c}{D}$, where L_c is the critical depth. Beyond the critical depth ratio, q_p may be taken as q_ℓ, which is constant with depth and equal to the value of q_p at $\frac{L_c}{D}$.

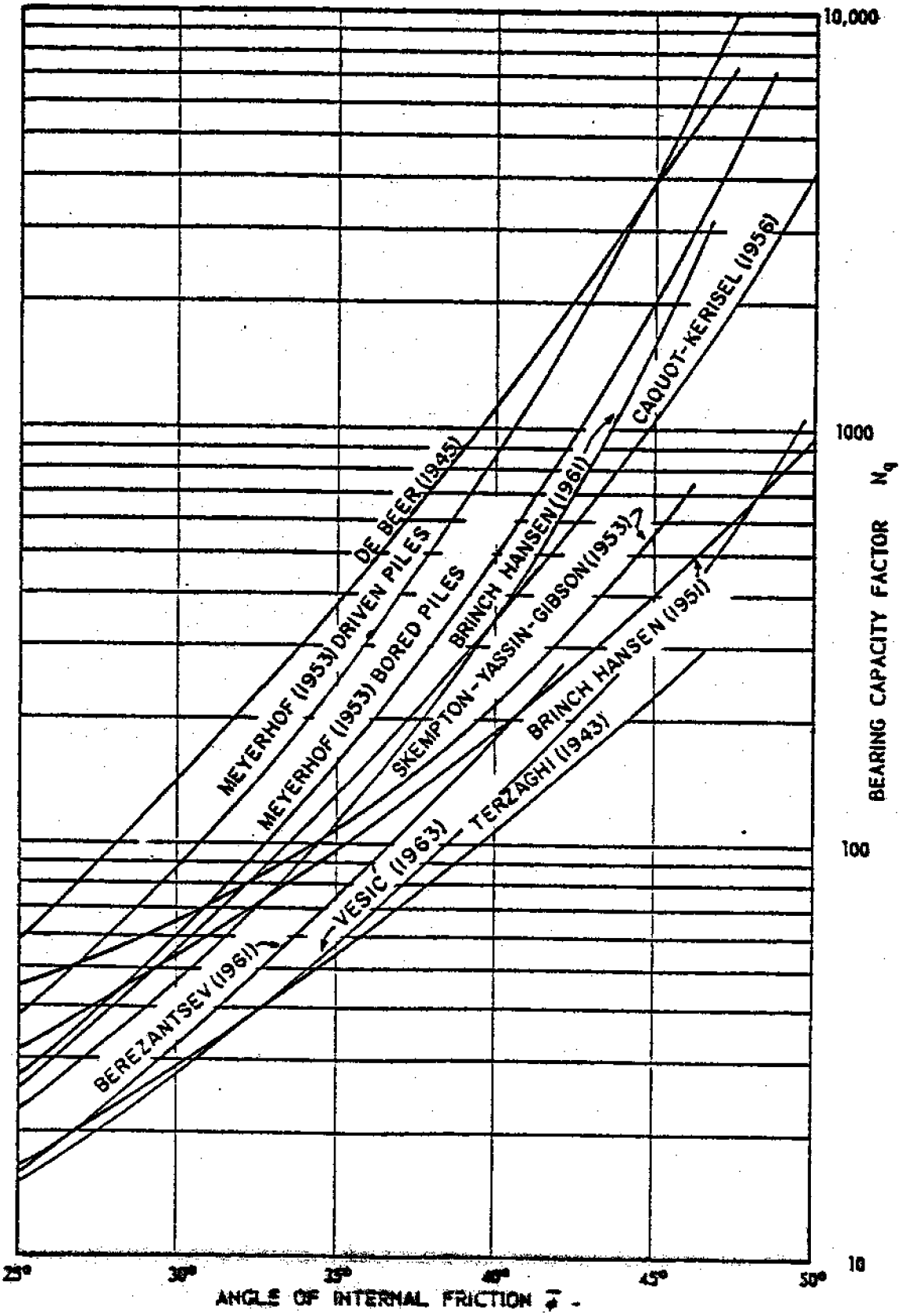

Fig. 3.11 Bearing Capacity Factors With Respect To Overburden Stress (Vesić, 1965)

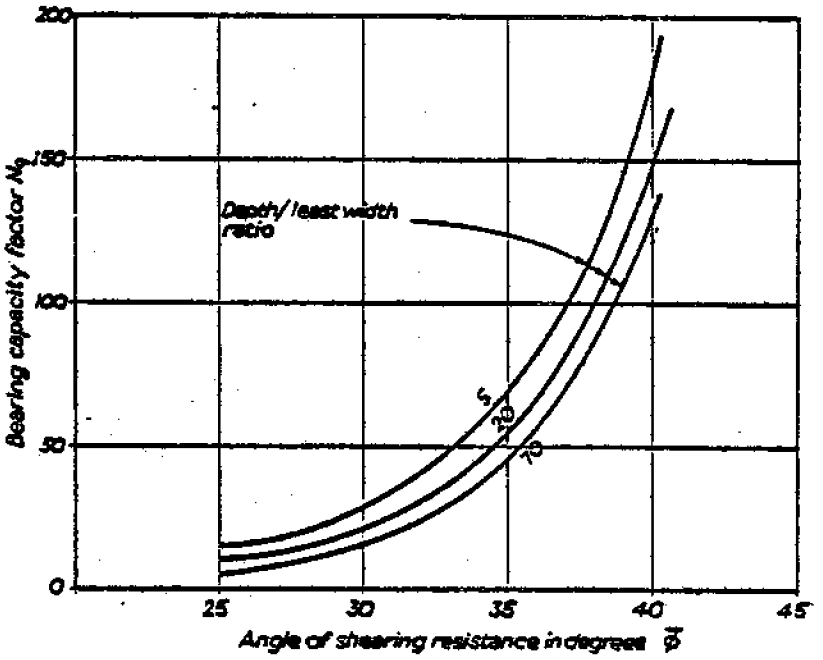

Fig. 3.12 Berezantzev's Values of N_q Refined by Tomlinson (Tomlinson, 1977)

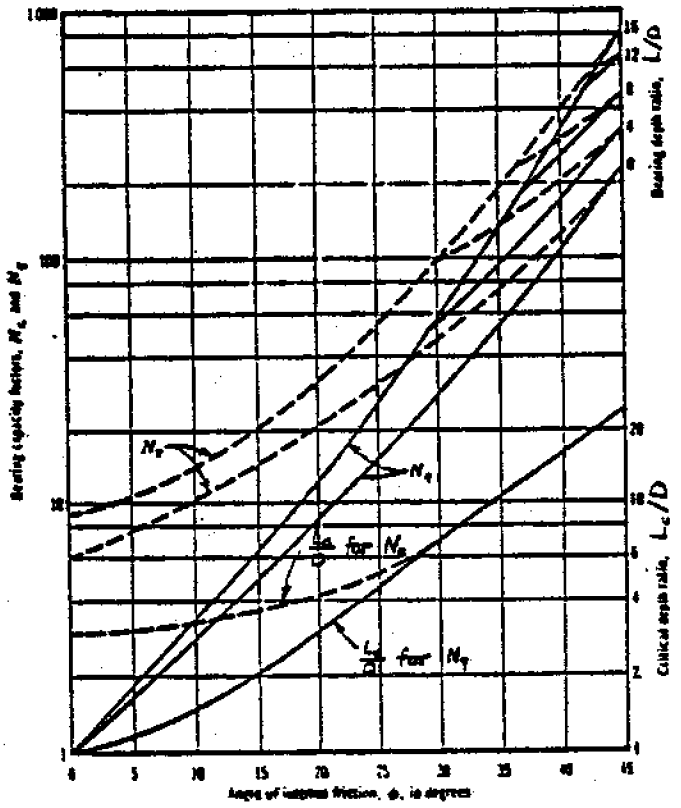

Fig. 3.13 Bearing Capacity Factors and Critical Depth Ratios for Driven Piles (Meyerhof, 1976)

Vesić (1977) took a different view and expressed the point resistance of pile foundations in sand in terms of the mean normal effective stress rather than the vertical effective stress. This is given as:

$$q_p = N_\sigma \bar{\sigma}_o \tag{3.18}$$

in which: N_σ = bearing capacity factor with respect to mean normal effective stress

$\bar{\sigma}_o$ = mean normal effective stress = $\frac{1+2K_o}{3} \bar{\sigma}_{vp}$

By considering the expansion of a spherical cavity in an infinite soil mass, Vesić (1977) derived values of N_σ taking into account the effect of compressibility of the soil and the volume changes of the soil mass. The mass is assumed to behave as an ideal elastic-plastic solid.

The compressibility of the soil is expressed in terms of a rigidity index, I_r, given as:

$$I_r = \frac{G_s}{\bar{c} + \bar{\sigma}_o \tan \bar{\phi}} \tag{3.19}$$

in which: G_s = shear modulus of soil

Vesić (1977) compiled typical values of rigidity index for different soil types and these are shown in Table 3.1. In general, the stiffer the soil, the higher will be the value of the rigidity index.

Vesić (1977) defined the volume change of the sand mass to be the average volumetric strain at failure in the plastic zone surrounding the tip of the foundation (Fig. 3.14). He introduced a volume change factor, ξ_v, which is defined as:

TYPICAL VALUES OF RIGIDITY INDEX, I_r

(a) sands and silts

Soil	Relative density D_r	Mean Normal stress level σ_o (kg/cm^2)	Rigidity index I_r	Source
Chattahoochee sand	80%	0.1 1 10 100	200 118 52 12	Vesić and Clough (1968)
	20%	0.1 1	140 65	
Ottawa sand	82% 21%	0.05 0.05	265 89	Roy (1966)
Piedmont silts		0.70	10-30	Vesić (1972)

(b) clays (undrained conditions)

Soil	Plasticity index I_p	Water content	OC ratio	Effective stress level σ_o (kg/cm^2)	Rigidity index	Source
Weald clay	25	23.1% 22.5%	1 24	2.1 0.35	99 10	Ladanyi (1963)
Drammen clay	19	24.9% 25.1% 27.2%	1	1.5 2.5 4.0	267 259 233	
Lagunillas clay	50	65%*	1	6.5 4.0	390 300	

*prior to consolidation

Table 3.1 Typical Values of Rigidity Index (Vesič, 1977)

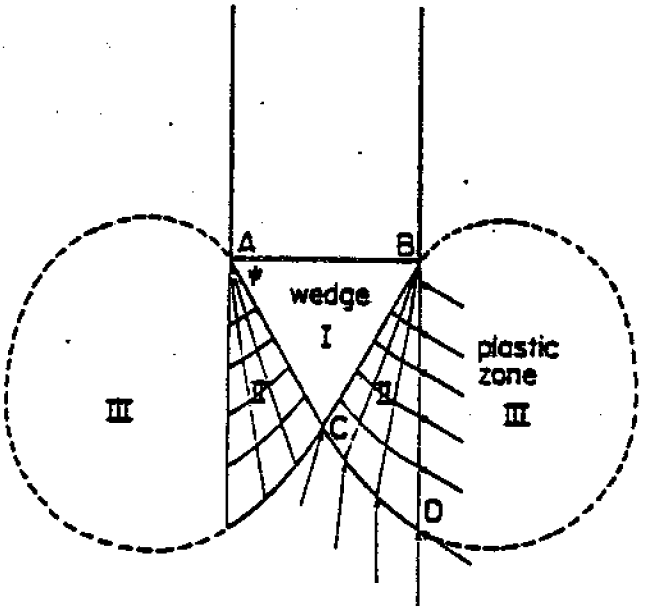

Fig. 3.14 Assumed Failure Pattern under Pile Point (Vesič, 1977)

$$\xi_v = \frac{1}{1 + I_r \Delta} \tag{3.20}$$

in which: ξ_v = volume change factor

Δ = average volumetric strain in the plastic zone at failure

The corrected rigidity index, I_{rr}, that takes into account the effect of volume change is then given as:

$$I_{rr} = \xi_v I_r \tag{3.21}$$

in which: I_{rr} = reduced rigidity index

In the case of no volume change (undrained condition), ξ_v can be taken as one and I_{rr} will then be equal to I_r.

The variation of N_σ with I_{rr} and $\bar{\phi}$ is shown in Fig. 3.15. The plot indicates that the rigidity index is as significant as the angle of internal friction in the determination of N_σ.

Although Vesić (1977) did not mention the existence of a critical depth, the increase in $\bar{\sigma}_o$ with depth will lead to a reduction in N_σ and it is possible that the unit point resistance may reach a limiting value.

It has been reported by Vesić (1965) that $\bar{\sigma}_{vp}$ and $\bar{\sigma}_v$ in Equations 3.15 and 3.16 cannot increase indefinitely with depth. He pointed out that the effective vertical stress reaches a limiting value at a depth of about 10 diameters for very loose sand to about 20 diameters for very dense sand. Accordingly, the point and shaft resistances will reach a peak value at these depths. An illustration of the variation of unit point and shaft resistances with depth is shown in Fig. 3.16. Vesić (1965) attributed this behavior to the effect of arching in the

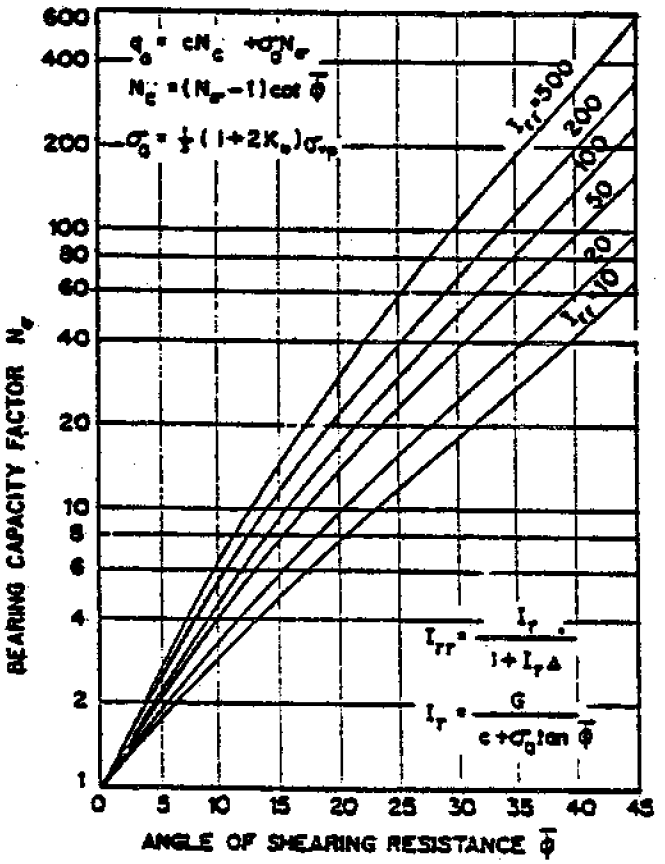

Fig. 3.15 Variation of N_σ with I_{rr} and $\bar{\phi}$ (Vesić, 1977)

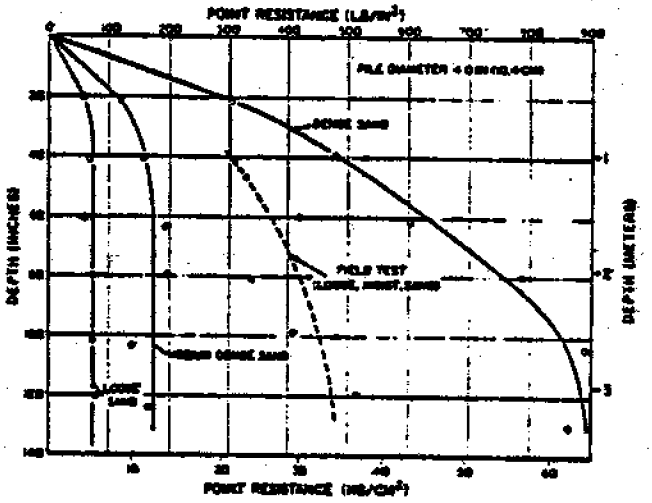

Fig. 3.16a Variation of Point Resistance with Pile Length (Vesić, 1965)

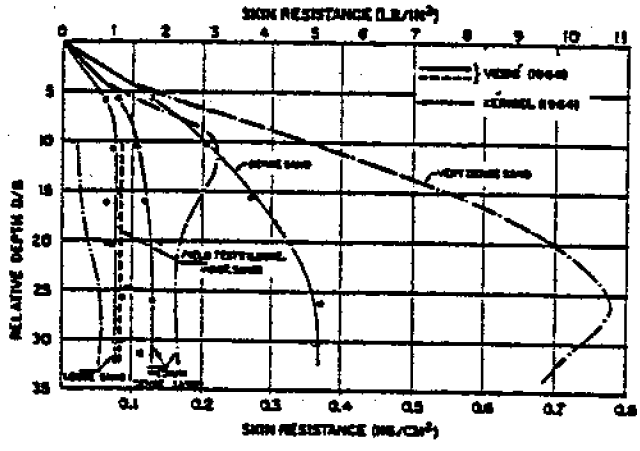

Fig. 3.16b Variation of Shaft Resistance with Pile Length (Vesić, 1965)

sand above the pile tip. However, subsequent research does not seem to support this concept. At present, this is still a debatable question. No solid evidence can be found either for or against this effect. In spite of this, the idea of a limiting value of vertical effective stress is still extensively used in practice because it is on the conservative side.

Values of K and δ, as used in Equation 3.16, have been suggested by Broms (1966). This is shown in Table 3.2.

In the case of a tapered pile, an increase in shaft resistance should be anticipated. The method to evaluate the ultimate load capacity of tapered piles in sands will not be described here. However, the reader can refer to the work of Nordlund (1963) for procedures to estimate the ultimate compressive capacity of tapered piles.

3.2 Ultimate Capacity of Pile Groups

Piles are commonly used in groups, with spacings of a few diameters apart. Like the design of a single pile, the design of a pile group must conform to two basic criteria: bearing capacity and settlement. Evaluation of group bearing capacity will be discussed in this section and group settlement will be presented in Section 3.3.

The methods for estimation of single pile load capacity have been presented earlier. Determination of the load carrying capacity of a pile group requires an estimation of single pile capacity, together with a judgment on the effect of interaction between piles in a group.

The ultimate capacity of a group of piles which derive

Pile Type	K	δ
Steel	0.5 to 1.0	20°
Concrete	1.0 to 2.0	$\frac{3}{4}\bar{\phi}$
Timber	1.5 to 4.0	$\frac{2}{3}\bar{\phi}$

Table 3.2 Values of K and δ for Piles in Sand (Broms, 1966)

most of their load carrying capacities through point resistance can generally be taken as the sum of ultimate load capacities of individual piles. However, for piles that transmit most of their loads through shaft resistance, group effects must be taken into consideration. For piles in which shaft and point resistances are equally important, it is recommended that groups effects be considered only for shaft resistance (Chellis, 1961; Vesić, 1969).

For piles that derive most of their capacities from shaft resistance, the load carrying capacity of the group is generally less than that of a single pile multiplied by the total number of piles in a group. This reduction is often expressed in terms of an efficiency factor, η, given as:

$$\eta = \frac{\text{ultimate load capacity of group}}{\text{sum of ultimate load capacities of individual piles}} \quad (3.22)$$

The efficiency factor of a pile group depends primarily on the soil properties and spacings of piles rather than the material of the pile. In general, η is equal to one at relatively large spacings, but decreases as the spacing decreases.

3.2.1 Groups in Clay

Several empirical formulae have been proposed to determine the group efficiency factor. Some of the more common ones are given as follows:

1) Converse-Labarre formula

$$\eta = 1 - \phi \left\{\frac{(n-1)m+(m-1)n}{90mn}\right\} \quad (3.23)$$

in which: ϕ = arc tan (D/s)

n = number of rows

m = number of piles in a row

s = center to center spacing of piles

2) Feld's rule

The calculated load capacity of each pile in a group is reduced by 1/16 for each adjacent pile around it and no consideration is made to pile spacing or pile diameter.

A more comprehensive review of these empirical formulae can be found in Chellis (1961). These empirical formulae are mainly related to the geometry of the group with no consideration given to the physical properties of the soil or the length of piles embedded. In fact, Chellis (1961) showed great variations in η for a given pile group using various empirical formulae. These formulae may be misleading and may not be applicable to all types of design conditions. However, they can provide a quick estimate on pile group efficiency and may serve as a check. Results from model tests carried out by Whitaker (1957) and Sowers, et al. (1961) seem to favor the Converse-Labarre efficiency equation.

Besides the use of empirical formulae, model tests have been conducted by various investigators to determine the group efficiency factors of pile groups in clays. de Mello (1969) summarized the works from Whitaker (1957), Saffery and Tate (1961) and Sowers, et al. (1961) and this is reproduced in Fig. 3.17. The figure includes results for free-standing pile groups of 2x2 to 9x9 piles with lengths 12D to 48D. From the figure, it can be seen that for spacings commonly used in practice (2D to 4D), η is on the order of 0.7 to 0.9 and that high-

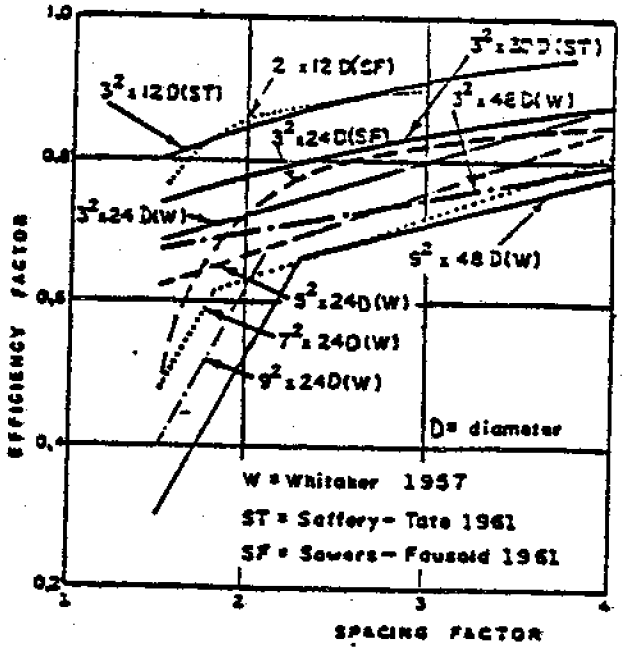

Fig. 3.17 Relationship between Pile Spacing and Efficiency Factor for Free-Standing Groups by Model Tests (de Mello, 1969)

er efficiency factors occur for larger spacings, piles having smaller length/diameter ratios and pile groups having the smallest number of piles.

One of the most widely used methods to estimate group load capacity is that proposed by Terzaghi and Peck (1967). They suggested that the group capacity is the lesser of:

1) the sum of the ultimate capacities of individual piles in the group
2) the ultimate capacity of the block defined by the exterior piles in the group

For a block with plan dimension B_g X L_g, the block capacity can be expressed as:

$$Q_{ult} = B_g L_g c_u N_c + 2L\ (B_g + L_g) c_u \qquad (3.24)$$

The concept of block failure is further depicted in Fig. 3.18.

These two types of failure have been confirmed by Whitaker (1957), who demonstrated that for any pile group, there is a critical value of spacing below which failure occurs as if the whole block of piles acts as a very large foundation.

3.2.2 Groups in Sand

Unlike pile groups in clays, pile groups in sands may have an efficiency factor less than or exceeding unity, depending on the relative density of the sand mass, pile roughness and spacings of piles in the group. When groups of piles are driven into loose sand, the soil around the piles becomes highly compacted. If the pile spacing is close enough, this will increase the frictional resistance along the pile shafts and hence the ultimate group capacity may exceed the sum of ultimate capaci-

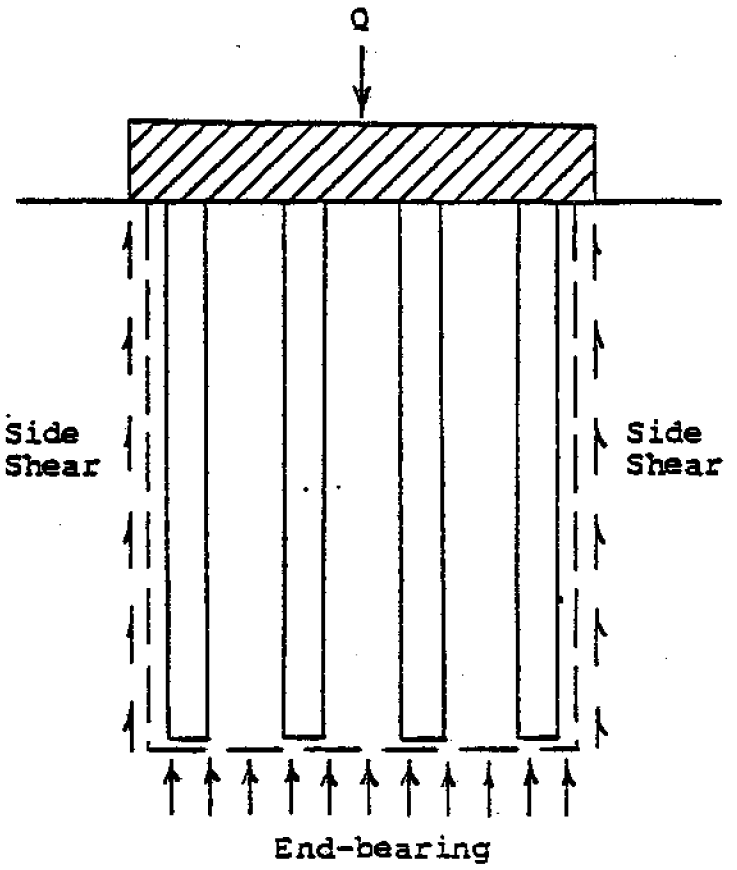

Fig. 3.18 Free-Body Diagram of the Group Behavior of a Pile Group under Compressive Loads

ties of individual piles. On the other hand, if the sand is so dense that the sand particles will dilate instead of undergo compaction, group efficiency may then be less than unity. In all cases, group efficiency will approach 100% if the piles are spaced far enough apart, i.e., group effects will be minimized.

Lo (1967) provided a summary on pile group efficiency versus pile spacings, which is shown in Fig. 3.19. The data confirm that piles driven into dense sand may have an efficiency less than one. Furthermore, it can be seen that piles driven into loose sand reach the maximum efficiency at a spacing of about two pile diameters. This maximum efficiency ranges between 1.8 to 2.2.

A rather extensive investigation on the behavior of pile groups in sand was conducted by Vesić (1969). He carried out a series of tests with 4-in-diameter (102 mm), 60-in-long (1.5 m) piles in four- and nine-pile groups, with and without caps, in sand. Two types of artificial sand deposits were used: 1) homogeneous, medium dense with relative density of about 65% 2) two-layer mass, consisting of an upper stratum of loose sand (relative density $\approx$ 20%), underlain by a stratum of dense sand (relative density $\approx$ 80%). Some of his test results are shown in Fig. 3.20. The test results indicate that grouping has practically no effect on ultimate point resistance. As shown in the figure, the point resistance efficiency remains constant at unity, independent of spacing. On the other hand, Vesić detected a significant increase of ultimate shaft resistance when

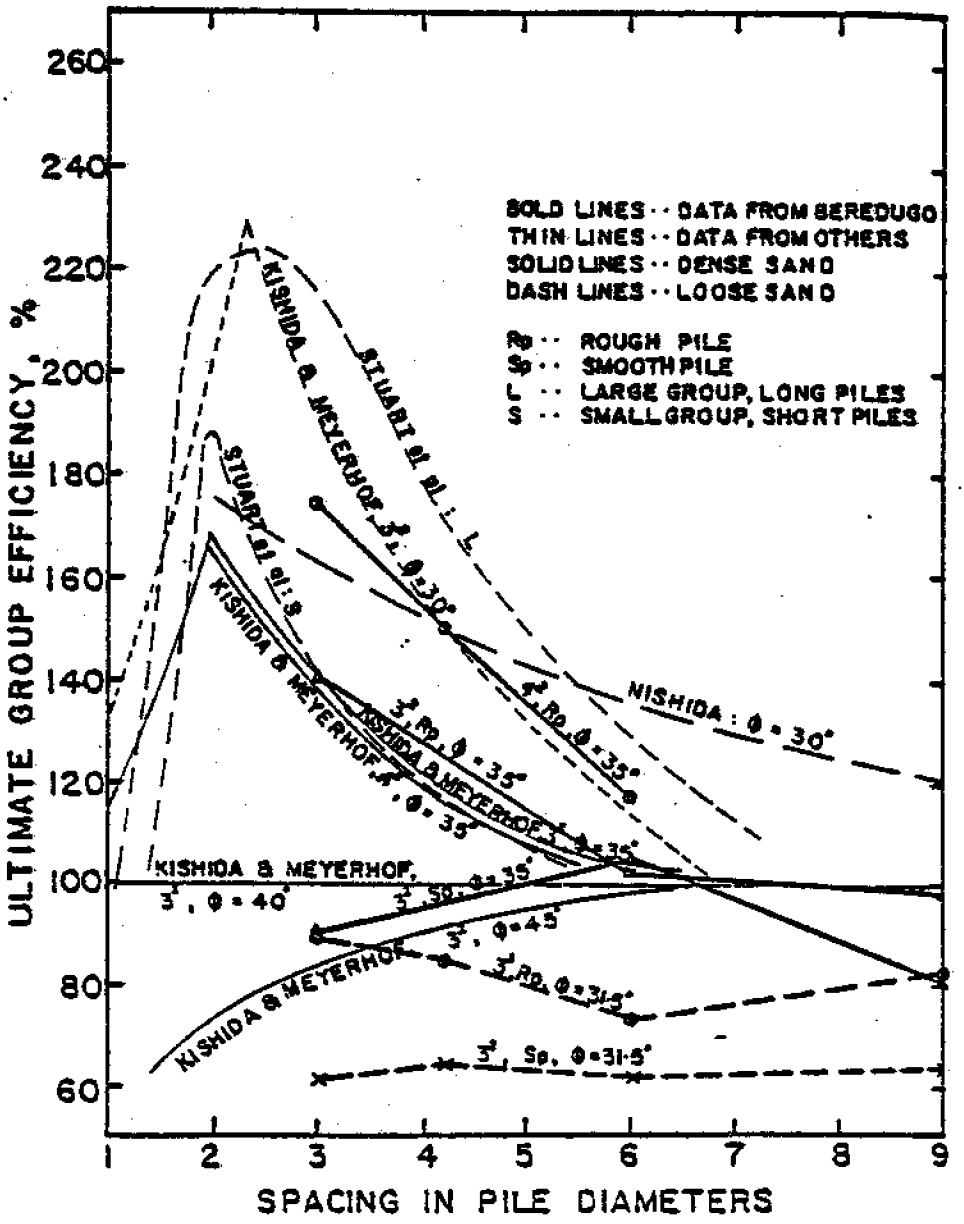

Fig. 3.19 Pile Group Efficiency (Lo, 1967)

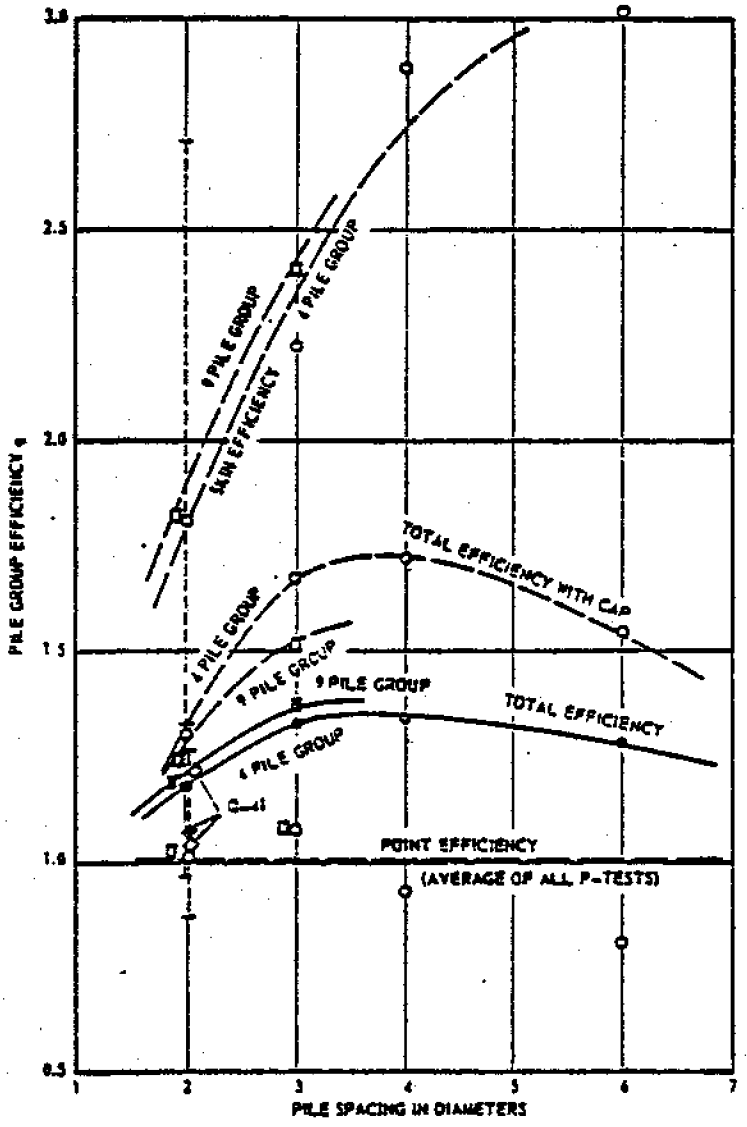

Fig. 3.20 Pile Group Efficiency (Vesić, 1969)

piles are placed in a group. Consequently, Vesić's finding does not support the idea that pile groups in sand can be analyzed through a comparison between individual pile failure versus block failure. Nevertheless, he pointed out that the procedures can be used reasonably well with respect to ultimate shaft resistance.

As can be seen from Fig. 3.20, pile caps that sit on the surface of the soil can contribute significantly to the ultimate capacity of the group, particularly in the case of smaller, four-pile groups. Kishida and Meyerhof (1965) have suggested that the contribution of pile cap to the ultimate capacity of a pile group in sand should be evaluated based on the outer rim of the cap contact area (shaded area in Fig. 3.21) if block failure dominates or the entire contact area if piles fail individually. However, Vesić (1969) showed that the idea that only the outer rim of the cap contact area contributes to the ultimate capacity of a group applies equally well for both situations. Comparisons between back-calculated and theoretical values of the surface bearing capacity factor, N_γ, showed good agreement. However, if erosion or settlement of soil underneath the cap is anticipated, it is not a good idea to count on this increased capacity in design.

3.3 Settlement Analysis

It is well known that the total deformation of a soil mass under load does not occur instantaneously; instead it is a time-dependent process that may extend over long periods of time. A typical time-settlement plot is illustrated schematically in

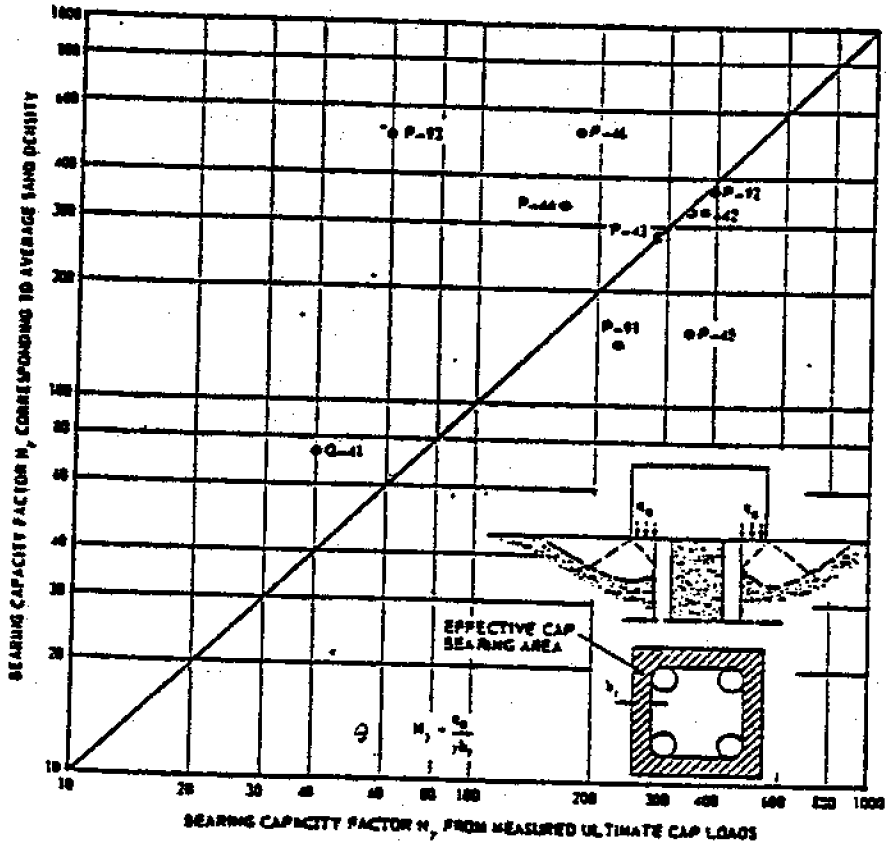

Fig. 3.21 Contribution of Pile Caps to Load Capacity of Group (Vesić, 1969)

Fig. 3.22. Three components of settlement can be identified on this plot:

1) immediate settlement

2) consolidation settlement

3) secondary settlement

Immediate settlement is the portion of the settlement that occurs "instantaneously" under the application of load. This arises from elastic compression of solids and water as well as air compression (if the soil is partially saturated). Consolidation settlement results from the dissipation of excess pore water stress and the consequent increase in effective stress. It is essentially completed when the excess pore water stress is completely dissipated (t_{100} on the curve). The final phase is secondary settlement, which is from the plastic deformation of solid particles and rupture of interparticle bonds. The relative magnitude of these three components of settlement vary over a wide range, depending upon the soil type, soil condition and the form of loading. General settlement behavior is discussed in detail in numerous textbooks on soil mechanics (e.g., Terzaghi and Peck, 1967; Sowers, 1979; Wu, 1976). Based on elasticity solutions, Poulos and Davis (1968) demonstrated that for pile foundations, immediate settlement is a predominant portion of the total final settlement.

Settlement of a pile foundation under load incorporates the following two factors:

1) elastic shortening of the pile

2) displacement of the pile point because of deformation

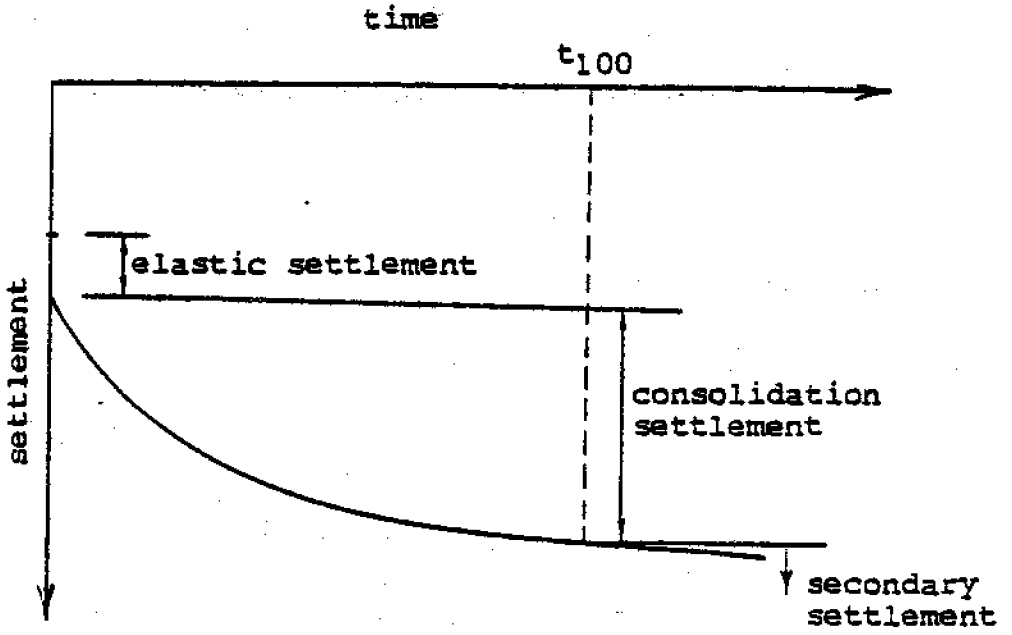

Fig. 3.22 Typical Time-Settlement Curve for Soil

of soil below the pile tip

The determination of these two factors requires sophisticated methods of analysis. It is beyond the scope of this study to discuss all these methods. If necessary, the reader can refer to the elastic solutions compiled by Poulos and Davis (1974) for estimation of pile settlement.

In contrast to shallow foundations (e.g., spread footings), settlement is rarely a controlling factor for the design of pile foundations. As pointed out by Tomlinson (1977), settlement for small diameter piles (up to 2 feet or 1.2 m) will be minimal ($\frac{3}{8}$ inch or 10 mm) under working load conditions if a safety factory of at least 2.5 is applied. In fact, settlement calculations are often ignored in design. This is particularly so for coastal structures in which the structural configurations are of simpler form than residential or commercial buildings.

It should be emphasized that the amount of displacement required to mobilize shaft resistance is small (0.25 to 0.50 inch) and is practically independent of the soil type as well as the diameter and length of the pile. On the contrary, the movement required to mobilize the base resistance is large and generally increases with the diameter of the pile. Therefore, under working load conditions, it is desirable to have full mobilization of shaft resistance for maximum efficiency. In other words, settlement can be reduced simply by increasing the

shaft area either by increasing the diameter or the length of the pile.

The settlement of a group of loaded piles is always greater than that of a single pile carrying the same load as that on each pile within the group. This occurs because the zone of soil stressed by a pile group has a much greater dimension than that of a single pile. This difference will become more distinct if the stressed zone of the pile group extends down to a soft compressible stratum that is beyond the influence of a single pile (Fig. 3.23). Therefore, extrapolation of load test results on the settlement of single piles to group behavior must take this possibility into consideration.

3.4 Summary

For piles embedded in clays, three major methods (α, β and λ-methods) have been proposed to evaluate the ultimate compressive load capacity. The α and λ-methods are largely based on empiricism, while the β-method has some theoretical basis. At the present time, there is no solid evidence that prefers one method over the others. All three approaches are widely adopted in practice. Therefore, it is recommended that all three methods should be examined for a particular design. For piles embedded in sands, the point resistance may reach a limiting value at some critical depth below the ground surface. This value can be computed either by a conventional approach using the effective vertical stress or by Vesić's approach using the mean normal effective stress. The evaluation of shaft resistance lies essentially in the determination of K and δ. Ideally,

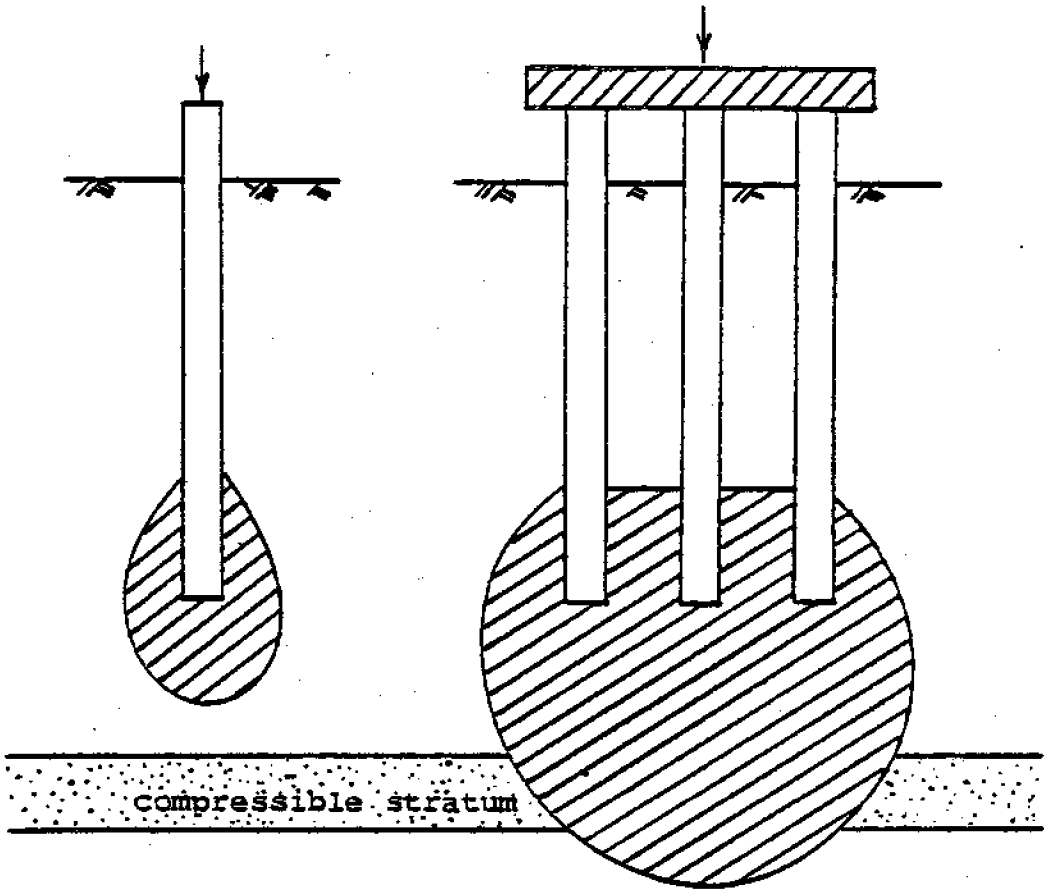

Fig. 3.23 Comparison between Stressed Zones of Single Piles and Pile Groups

these can be determined from load test results. If these are not available, the values shown in Table 3.2 can probably be used.

Two methods have been presented to estimate the group load capacity. The efficiency factors can provide a quick and rough estimate, but no consideration is given to the physical behavior of the system. Terzaghi and Peck's approach seems to be more reasonable and should be used for final computation of pile group capacity.

As indicated in Section 3.3, the settlement of pile foundations for coastal structures is often a minor consideration. In most cases, settlement under working loads will be minimal if an appropriate factor of safety is applied. Overdesign of the foundations to reduce the settlement of waterfront structures is normally not justified.

CHAPTER 4

DESIGN OF PILES FOR UPLIFT LOADS

Except for special types of structures (e.g., tall transmission towers, buildings founded on expansive clays), piles used on land are seldom subject to significant uplift forces. On the other hand, the design of piles for coastal structures (e.g., docks, piers) often requires consideration of uplift loads.

Uplift loads may result either from lateral forces or direct pull-out. While lateral forces may develop from waves, boat impact, ice impact, wind, etc., direct pull-out forces arise almost exclusively from ice grip on piles along with rise of water levels. In cold regions where there is large variation in water levels, the latter can dominate the design.

4.1 Ultimate Capacity of Single Piles

The determination of ultimate uplift capacity of single piles basically follows that adopted for calculation of ultimate compressive capacity. While the dead weight of the pile may become more significant in Equation 3.1, the point resistance is not applicable and should be omitted.

The uplift resistance of single piles is determined by three major factors:

1) geometry of failure surface
2) shear strength of soil
3) weight of pile

The geometry of the failure surface is probably the most diffi-

cult to evaluate. In most cases, this is not well-defined and an assumption has to be made with regard to the shape of the failure surface before mathematical formulation of the problem is possible.

4.1.1 Piles in Clay

For an isolated single pile in clay, the uplift failure surface is often assumed to be at the pile-soil interface. Strictly speaking, if the adhesion strength between the pile and the soil is larger than the undrained shear strength of the soil (which is possible for very soft clays), the failure boundary is likely to occur at some distance away from the pile surface. This point is often ignored in design and the maximum adhesion strength is taken to be equal to the undrained shear strength of the soil. The uplift resistance is simply expressed as:

$$T_{ult} = c_\alpha A_s + W_p \qquad (4.1)$$

in which: T_{ult} = ultimate uplift load

c_α = pile-soil adhesion

A_s = area of pile shaft embedded in soil

W_p = net weight of pile

= (dead weight of pile - hydrostatic uplift)

As shown by Equation 4.1, the uplift capacity of piles in clays is composed of shaft resistance and the dead weight of the piles minus any hydrostatic uplift. Although very few pulling tests have been performed for piles in clay, it seems that most designers agree to use the same pile-soil adhesion for both up-

lift and compressive loadings. According to the summary of pulling test results given by Sowa (1970) on cast in-situ concrete piles, the α-coefficient does show a general trend of decrease with increasing undrained shear strength and these values conform roughly with those suggested by Tomlinson (1957) for compressive loadings (Fig. 4.1). This concept is also confirmed by the λ-method proposed by Vijayvergiya and Focht (1972). Of the 47 load tests summarized by the investigators, 9 are pulling tests and it seems that these data do not show any sign of noticeable dissimilarity from the rest of the data points (Fig. 4.2).

In contrast to piles under compressive loads, piles under sustained uplift forces have capacities that decrease with time. It is believed that negative pore water stresses occur in clay during uplift. As these negative pore water stresses dissipate, the soils adjacent to the pile will decrease in strength and thus the long-term (drained) uplift capacity will be less than the short-term (undrained) capacity. As noted by Meyerhof and Adams (1968), this reduction is larger for piles in stiff clays with short embedded lengths. The latter idea is also pointed out by Tomlinson (1977), who suggested that the reduction will not be significant for a depth/diameter ratio of greater than 5. Furthermore, it should be mentioned that a major portion of the uplift force is transient, so the evaluation of long-term uplift capacity may not be necessary under these situations. However, if drained conditions are found to be critical, the uplift load capacity can be estimated by procedures outlined in Section 4.1.2 using the drained parameters of clays.

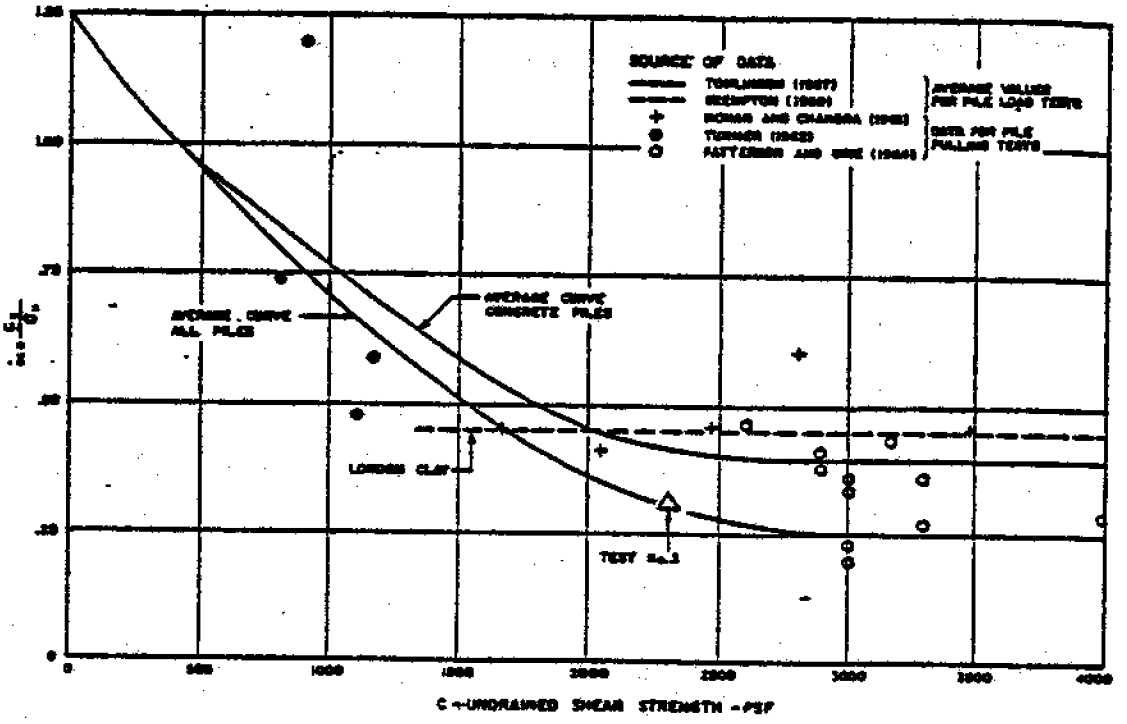

(See Preface for SI Conversions)

Fig. 4.1 Relationship between α and c_u for Pull-out Tests (Sowa, 1970)

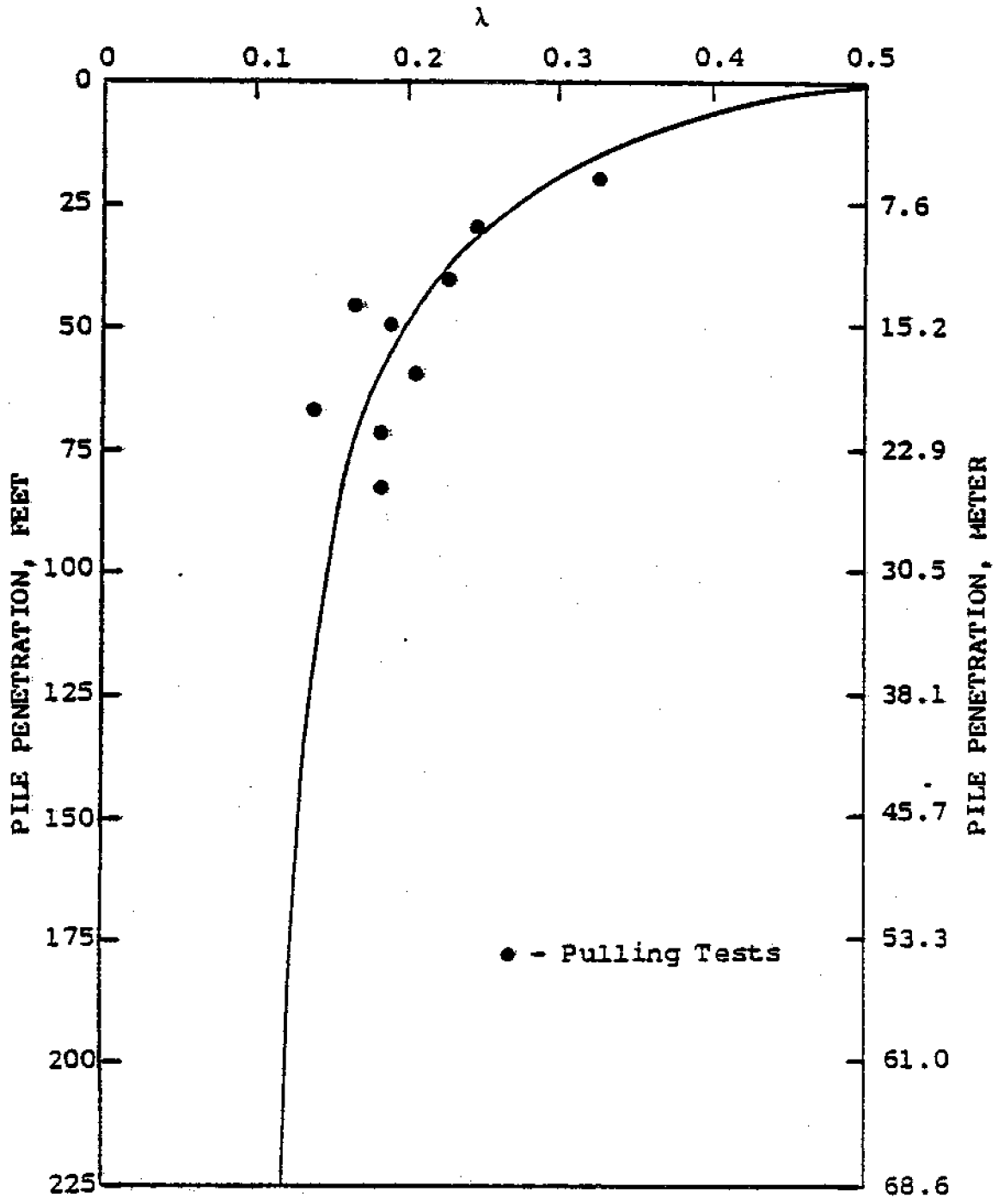

Fig. 4.2 Distribution of Pulling Tests Data Points Using the λ-method (data and curve from Vijayvergiya and Focht, 1972)

4.1.2 Piles in Sand

The uplift failure surface for an isolated single pile in sand is more complex than that of piles in clay, because it is often not well-defined. Depending on the roughness of the pile and the density of the sand, particles in the vicinity of the piles are often mobilized as the piles move upwards. Some of the uplift forces have to be dissipated in mobilizing these sand particles. In spite of this, a cylindrical failure surface close to the pile-soil interface is often used in design and the uplift capacity is given as:

$$T_{ult} = \frac{1}{2} \pi D L K_u \bar{\sigma}_{vp} \tan \bar{\phi} + W_p \qquad (4.2)$$

in which: T_{ult} = ultimate uplift capacity

L = length of embedment of pile

D = diameter of pile

$\bar{\phi}$ = effective angle of internal friction of soil

$\bar{\sigma}_{vp}$ = effective vertical stress at the pile tip

K_u = horizontal stress coefficient for uplift

Theoretically, there are at least two reasons that support different K values for uplift and compression. First, the Poisson effect of the pile under load tends to increase K during compression and reduce K during uplift. Second, arching of soil above the pile point will probably increase K during uplift and reduce K during compression. At present, there is not enough information to assess the extent of influence of these two phenomena. In spite of this, a lower value of K for uplift is often recommended (e.g., McClelland, et al., 1969; API, 1977). While this may not be of any significant effect to

piles governed by compressive loadings, such a recommendation may lead to an over-conservative design for piles subject to large uplift forces. Until further information can clarify this point, the K values for uplift and compression can probably be taken as the same value.

4.2 Ultimate Capacity of Pile Groups

In estimating the uplift capacity of pile groups, an approach similar to that adopted for compressive loads can be used. The ultimate uplift load for the group can be taken as the smaller of:

1) the sum of the ultimate uplift capacities of individual piles in the group.
2) the ultimate uplift capacity of the block defined by the failure surface of the group.

The ultimate capacities of individual piles in the group can be estimated by procedures outlined in Section 4.1. If the pile group behaves as a single large foundation, the uplift resistance is provided by the shear strength of the soil around the periphery of the block. Furthermore, the weight of the block, including the weight of the soil enclosed by it, will add to the uplift capacity of the large foundation (Fig. 4.3).

4.2.1 Groups in Clay

For pile groups in cohesive soils, the ultimate uplift load under undrained conditions is given as:

$$T_{ult} = 2L(L_g + B_g)\, C_u + W_T \qquad (4.3)$$

in which: L_g = length of pile group

B_g = width of pile group

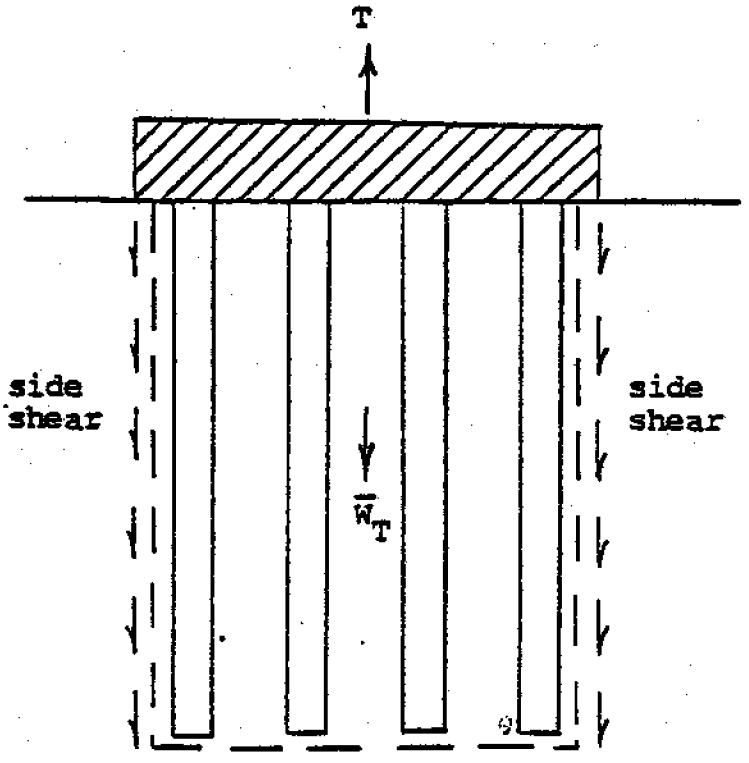

Fig. 4.3 Free-Body Diagram of the Group Behavior of a Pile Group under Uplift Loads

C_u = undrained shear strength of soil

W_T = weight of structure + weight of soil enclosed by pile group - hydrostatic uplift

The first term in Equation 4.3 gives the undrained shear resistance of soil around the equivalent single large foundation and the second term represents the total dead weight of the materials that the uplift forces have to overcome.

4.2.2 Groups in Sand

In the case of cohesionless soils, the failure surface of a group of closely-spaced piles is not well-defined. Nevertheless, a failure surface defined by the exterior piles in the group can probably be used for design purposes. The ultimate uplift load is given as:

$$T_{ult} = L(L_g + B_g)\, K_u\, \bar{\sigma}_{vp}\, \tan \bar{\phi} + W_T \qquad (4.4)$$

4.3 Summary

The determination of the ultimate uplift load capacity basically follows that for compressive loads. The point resistance is not applicable and the uplift loads are mainly counteracted by the shaft resistance and the dead weight of the piles. Therefore, uplift resistance can be increased either by employing a larger shaft area or by adding dead weight to the piles. The latter is usually not feasible, especially if the piles are required to carry alternating uplift and compressive loads.

For pile groups, the concept of individual-pile failure versus block failure is also adopted for the evaluation of the ultimate uplift capacity. For block failure, the uplift

load capacity incorporates two factors: 1) the shear resistance around the periphery defined by the exterior piles in the group and, 2) the net weight of the piles plus the weight of the soil enclosed by the group.

CHAPTER 5

DESIGN OF PILES FOR LATERAL LOADS

In addition to compressive and uplift loads, piles used for coastal structures are often subjected to significant lateral forces. Lateral loads arise from many sources, among which the more important ones are:

1) ship impact
2) ice
3) wind
4) waves
5) current
6) earthquake
7) soil stress
8) floating debris

These loads may or may not reinforce one another, depending upon the locations and the functions of the members.

The design of laterally loaded piles is one of the more difficult aspects of deep foundations. In the past, methodologies for design were largely based on the "rule-of-thumb" approach. One example of that is the recommendation made by McNulty (1956) on safe allowable lateral forces on vertical piles (Table 5.1). This type of approach may very often lead to underdesign or overdesign since the basic mechanics of the problem are not properly dealt with.

As indicated earlier, the design of piles for compressive loads has to meet the basic requirements of capacity and settle-

Free-end timber piles, 12-inch diameter

Medium sand	1500 pounds
Fine sand	1500 pounds
Medium clay	1500 pounds

Fixed-end timber piles, 12-inch diameter

Medium sand	5000 pounds
Fine sand	4500 pounds
Medium clay	4000 pounds

Free-end concrete piles, 16-inch diameter

Medium sand	7000 pounds
Fine sand	5500 pounds
Medium clay	5000 pounds

Fixed-end concrete piles, 16-inch diameter

Medium sand	7000 pounds
Fine sand	5500 pounds
Medium clay	5000 pounds

(See Preface for SI Conversions)

Table 5.1 Suggested Safe Allowable Lateral Forces on Vertical Piles (McNulty, 1956)

ment. Similarly, the design of piles for lateral loads must conform to two criteria: lateral capacity and deflection. The pile-soil system must be safe against lateral capacity failure. In addition, the piles should not undergo excessive deflection at service load conditions.

In this chapter, the behavior of piles and pile groups under lateral loads will be examined. It should be noted that most of the recent work on this subject matter is based on computer-aided techniques. These will not be described here. However, the reader can refer to Reese and Desai (1977) for a thorough discussion and a list of references on these approaches. The following discussions will emphasize methods that are suitable for rapid hand calculations.

5.1 Ultimate Capacity of Single Piles

In contrast to the ultimate capacity of piles under compressive loads, in which the strength of the pile-soil system is normally limited by the strength of the soil, the ultimate capacity of piles subjected to lateral loads may or may not be controlled by the strength of the soil. The bending moment induced in the pile may well exceed the yield moment and consequently the failure mode is determined by the structural capacity of the pile. Because of this, laterally loaded piles can be separated into rigid and flexible piles.

A pile behaves as a rigid unit if failure of the soil occurs before failure of the pile. On the other hand, a pile is considered to be a flexible member if failure of the pile occurs prior to failure of the soil. In other words, the capaci-

ty of a rigid pile is determined by the strength of the soil and that of a flexible pile is governed by the yield moment of the member. Whether a pile will behave as a rigid or a flexible member depends primarily upon three factors:

1) relative stiffness between pile and soil
2) length of piles
3) depth of penetration

To achieve maximum efficiency, the pile should be designed so that both the member and the soil can fail simultaneously. However, this is not always possible since there are numerous other factors involved in the design process.

Laterally loaded piles are further classified as free-headed or restrained piles. A free-headed pile is free to rotate at the pile head (Fig. 5.1); a restrained pile is fixed against rotation at the ground-line (Fig. 5.2). Piles that extend above the ground-line, and are fixed against rotation at the top, can be treated as free-headed members with the loads applied at some distance e above the ground-line (Fig. 5.3), where e is given as:

$$e = \frac{1}{2} (L_u - L_s) \qquad (5.1)$$

in which: e = distance of lateral loads above the ground-line

L_u = length of unsupported portion of piles (from the ground-line to the deck or cap)

L_s = equivalent length of embedded portion of pile

The equivalent embedded length, L_s, can be estimated according to procedures outlined in Section 6.2.

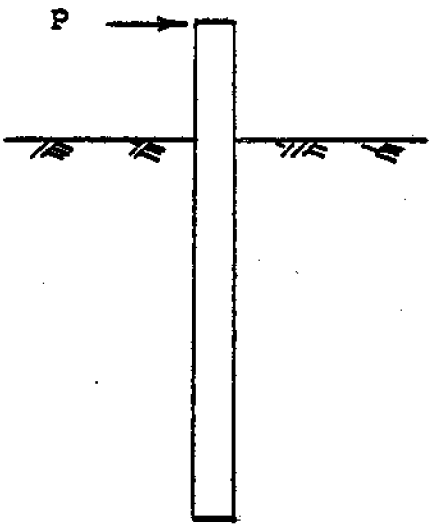

Fig. 5.1 Free-Headed Pile

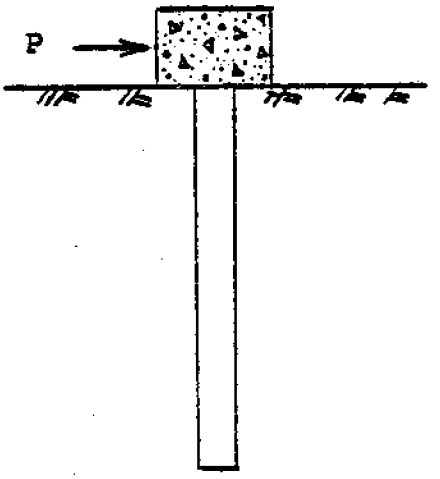

Fig. 5.2 Restrained Pile

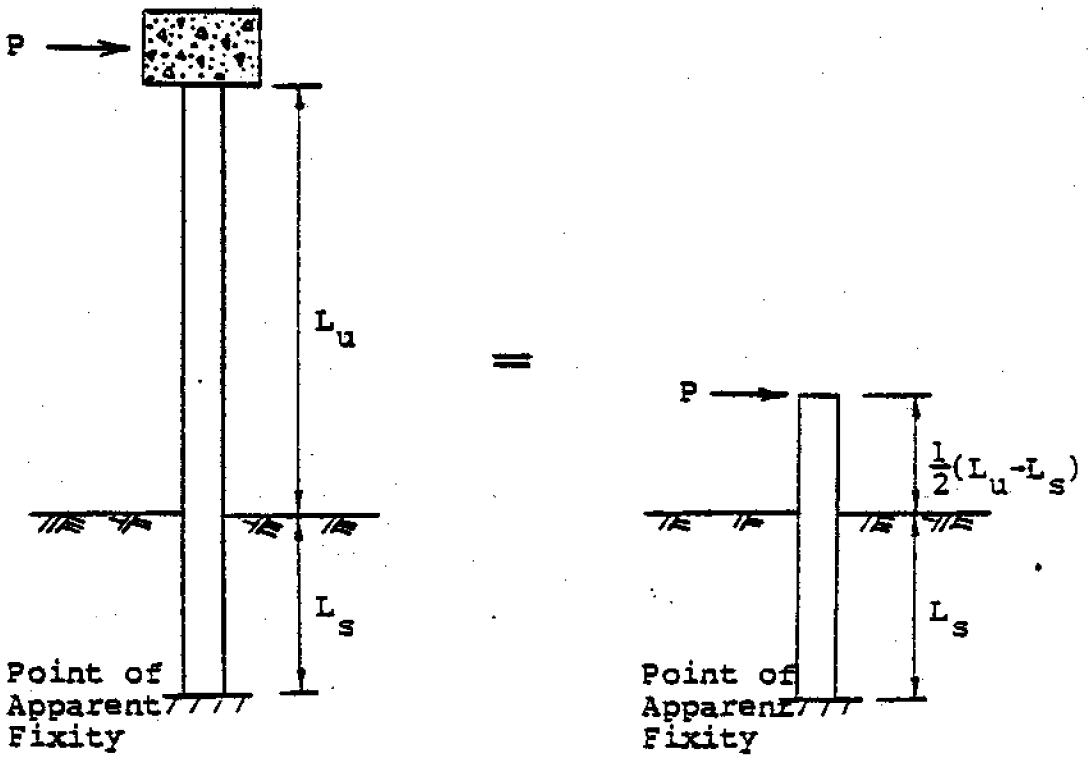

Fig. 5.3 Restrained Pile that Extends above the Ground Surface

Upon application of lateral loads, free-headed piles will undergo larger deflections and therefore are more desirable to be used as fender piles. On the contrary, piles fixed against rotation at the top have more rigidity and are more suitable for docks, piers or wharves where excess deformations of the structure cannot be tolerated.

Obviously, a free-standing pile with no pile cap is considered to be a free-headed pile. For other types of piles, the level of restraint depends upon the connections between the piles and the deck or cap (See Section 6.2.). To some extent, cross-bracing between adjacent members may also restrain rotational movement at the top and provide extra lateral rigidity to the system (Fig. 5.4).

Strictly speaking, the failure mode of laterally-loaded piles is three-dimensional. Thus, rigorous treatment of the problem requires a three-dimensional analysis. Analytical solutions are likely to be very difficult, if not impossible. Numerical procedures (e.g., finite element methods) with the advent of high-speed digital computers have thrown some light on this problem. However, the implementation of these procedures is expensive and may not be justified for simpler construction.

The procedures to estimate the ultimate lateral resistance of single piles will be outlined in this section. The method basically follows that proposed by Broms (1964). In each case, the capacities of piles at the ultimate stage will be evaluated. The allowable lateral load can be calculated by dividing

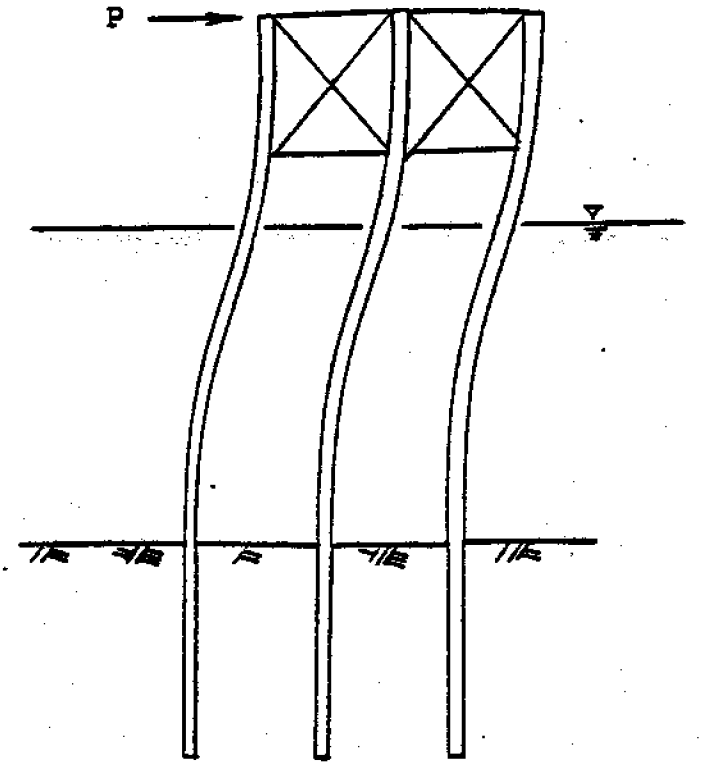

Fig. 5.4 Effect of Bracing on Rotational Movement at the Top of the Pile

the ultimate load with an appropriate factor of safety.

5.1.1 Piles in Clay

When a free-headed, rigid pile is loaded laterally, it will rotate as a unit with the center of rotation located at some distance below the ground surface. The soils in front of the pile near the ground surface will be pushed upwards while those at greater depth will be compressed in the direction of pile movements. In the case of a restrained pile, the member will translate horizontally with the soils in front of it being compressed.

Assuming the pile displacements to be large enough to mobilize the maximum soil reactions, Broms (1964a) simplified the distributions of soil reactions and pile moments at the ultimate stage to those shown in Figs. 5.5 and 5.6. The ultimate lateral resistance provided by the soil in front of the pile has been related to its undrained shear strength (c_u). Broms (1964a) suggested the use of $9c_u$ to be the maximum soil resistance. Soil reactions up to 1.5 D below the ground-line are ignored to account for the effect of soil moving above the ground-line as a result of lack of vertical restraint near the ground surface.

The soil reactive stress diagrams shown in Figs. 5.5 and 5.6 are in a state of plastic equilibrium, so the soils will deform indefinitely under loads and the system is on the verge of plastic failure. The maximum moments induced in the piles at this ultimate state are given as:

$$M_{max} = P_{ult}\left(e + 1.5\ D + \frac{0.5P_{ult}}{9c_u D}\right) \text{ for free-headed pile} \quad (5.2)$$

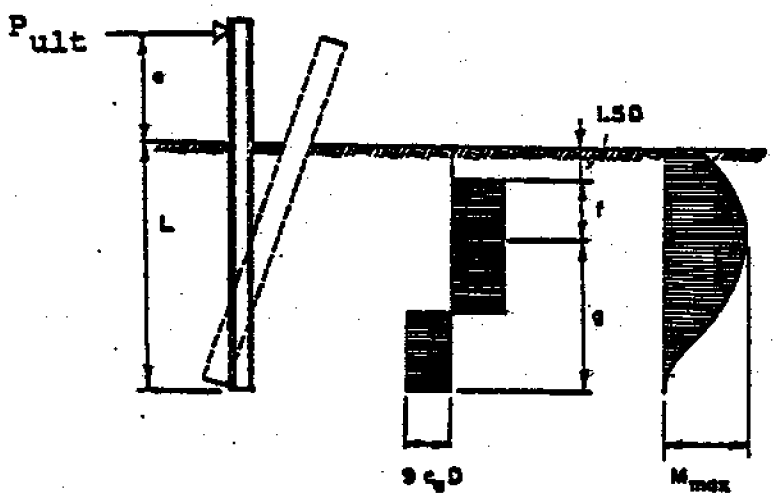

Fig. 5.5 Soil Reaction and Bending Moment Distribution for a Rigid, Free-headed Pile in Cohesive Soil (Broms, 1964a)

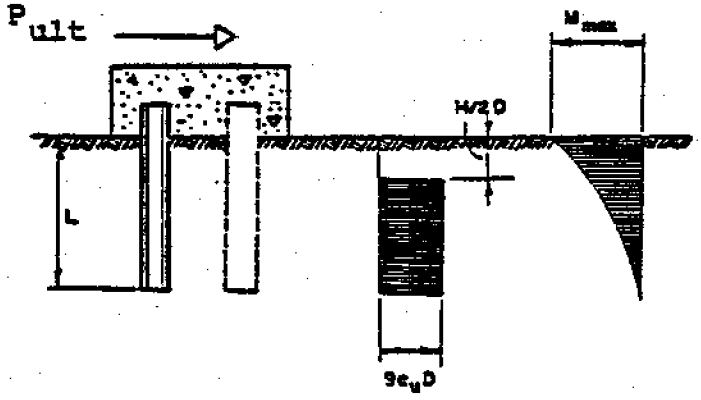

Fig. 5.6 Soil Reaction and Bending Moment Distribution for a Rigid, Restrained Pile in Cohesive Soil (Broms, 1964a)

$$M_{max} = P_{ult} (0.5\ L + 0.75\ D) \text{ for restrained pile} \qquad (5.3)$$

in which: M_{max} = maximum pile moment

P_{ult} = ultimate lateral load

D = diameter of pile

c_u = undrained shear strength of soil

L = length of embedment of pile

Based on statics considerations on the simplified distribution of maximum soil reactions shown in Fig. 5.5 and 5.6, Broms (1964a) developed a chart for determination of ultimate lateral capacities of rigid piles. This is shown in Fig. 5.7. It should be noted that this graphical relationship applies only for cases where M_{max} is less than M_{yield}, the yield moment of the pile (i.e., the pile behaves as a rigid member).

When a free-headed, flexible pile is loaded laterally, both the pile moments and the soil reactions along the pile will increase. By definition of flexible members, the ultimate lateral capacity of the pile-soil system is determined by the yield moment of the pile shaft. Failure occurs when a failure hinge (a section where the pile material has reached its ultimate strength) is formed somewhere along the pile. In the case of a restrained pile, one or two failure hinges may be formed, depending upon the length of the member. For an intermediate-length pile, the failure hinge will occur at the level of restraint; for a long pile, one failure hinge will be formed at the level of restraint and the other at some depth below the ground surface.

By assuming the soil reactions above the failure hinge to

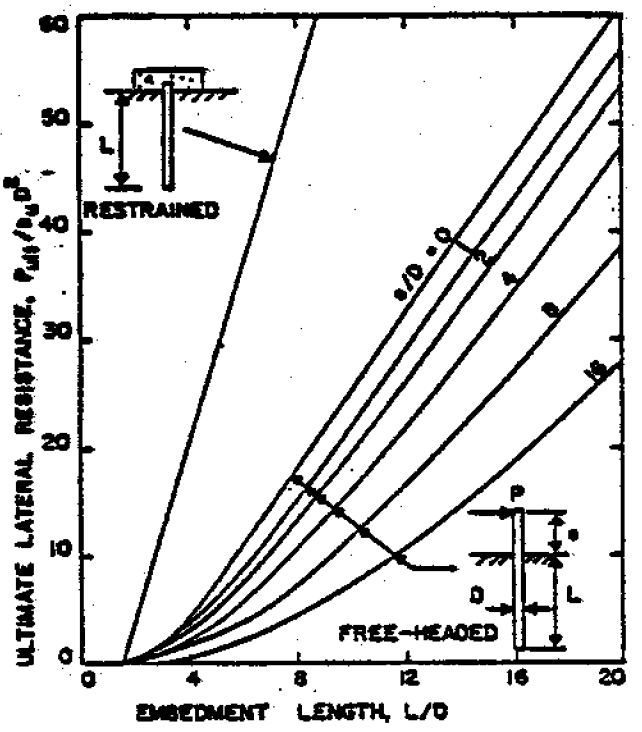

Fig. 5.7 Ultimate Lateral Resistance of Rigid Pile in Cohesive Soil (Broms, 1964a)

be fully mobilized, Broms (1964a) simplified the soil reaction and bending moment distributions for flexible piles in clays to those shown in Figs. 5.8, 5.9 and 5.10. Dimensionless solutions for these situations are shown in Fig. 5.11. It should be noted from the graph that the ultimate lateral capacity of a flexible pile is independent of the penetration depth and, therefore, there is no point in driving a pile down to a depth greater than that required for the pile to behave as a flexible member (except for cases where greater penetration depths are necessary to support axial loads).

Broms (1964a) has compared the maximum bending moments computed using the above approach with experimental values measured by various investigators and observed good agreement between the two values. Moreover, he pointed out that the calculated maximum bending moment value is not very sensitive to small variations in the assumed soil reaction distribution or the undrained shear strength values.

5.1.2 Piles in Sand

When a free-headed, rigid pile is loaded in the horizontal direction, the pile will rotate as a unit. The soils in front of the pile near the surface will move upwards and those at greater depth will be densified in the direction of pile movements. For a restrained pile, the member will translate horizontally. In both cases, the sands along the back of the pile will be loosened as a result of these pile movements.

Based on load test results, Broms (1964b) suggested that the horizontal soil stress which develops at lateral capacity

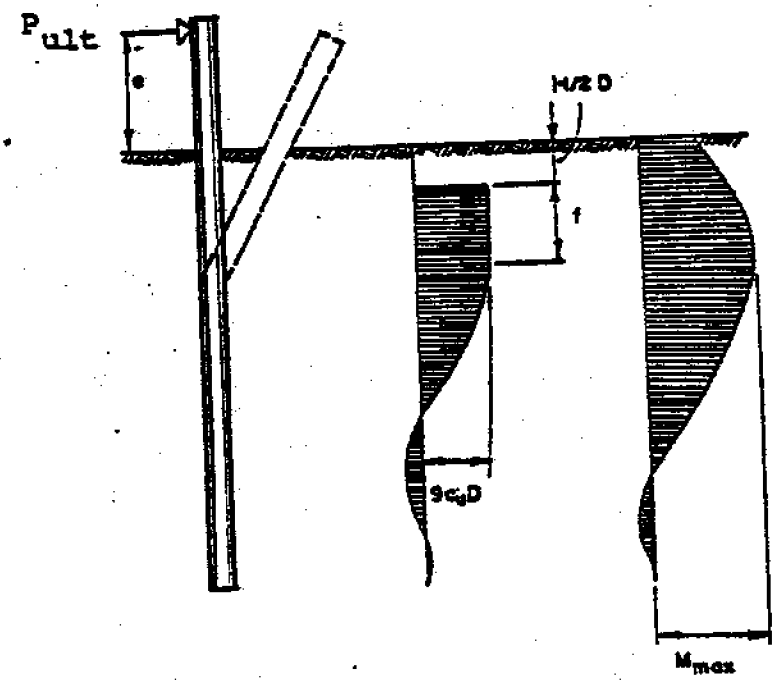

Fig. 5.8 Soil Reaction and Bending Moment Distribution for a Flexible, Free-Headed Pile in Cohesive Soil (Broms, 1964a)

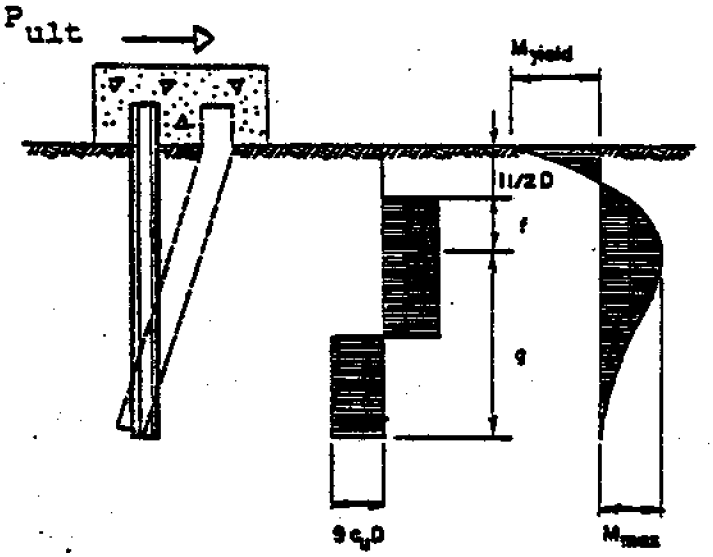

Fig. 5.9 Soil Reaction and Bending Moment Distribution for a Flexible, Restrained Pile (Intermediate Length) in Cohesive Soil (Broms, 1964a)

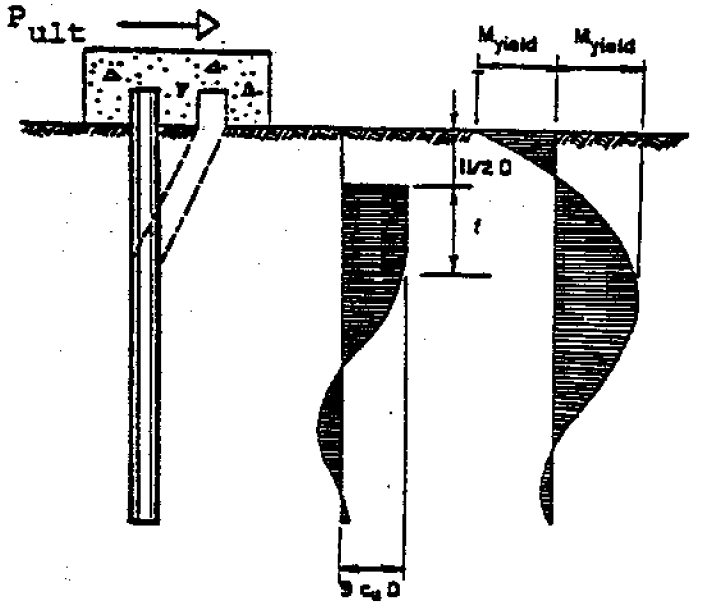

Fig. 5.10 Soil Reaction and Bending Moment Distribution for a Flexible, Restrained Pile (Long Length) in Cohesive Soil (Broms, 1964a)

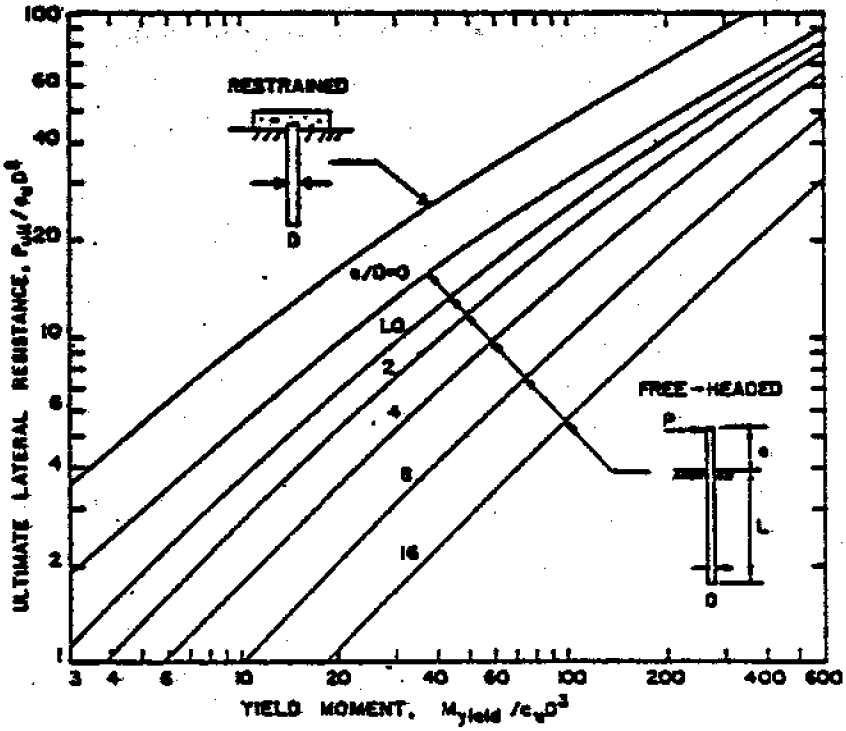

Fig. 5.11 Ultimate Lateral Resistance of Flexible Pile in Cohesive Soil (Broms, 1964a)

failure is approximately equal to three times the Rankine passive soil stress. The distributions of soil reactions and pile moments at the ultimate stage as proposed by Broms (1964b) are shown in Figs. 5.12 and 5.13. By assuming the maximum soil reactions to be fully mobilized at the ultimate stage and ignoring the active soil stress acting along the back of the pile, Broms (1964b) developed a chart to estimate the ultimate lateral capacities for rigid piles in sands and this is shown in Fig. 5.14. Again, the chart applies only when the maximum bending moment in the pile is less than the yield moment. The maximum moments at the ultimate states shown in Figs. 5.12 and 5.13 are given respectively as:

$$M_{max} = P_{ult} \left(e + 0.55 \sqrt{\frac{P_{ult}}{\bar{\gamma}_s D K_p}}\right) \quad \text{for free-headed pile} \qquad (5.4)$$

$$M_{max} = 0.67\, P_{ult}\, L \quad \text{for restrained pile} \qquad (5.5)$$

in which: $\bar{\gamma}_s$ = submerged unit weight of soil

K_p = passive soil stress coefficient

Using a similar logic as that for piles in clays, Broms (1964b) proposed soil reactions and pile moment distributions for flexible members in sands and these are shown in Figs. 5.15, 5.16 and 5.17. Dimensionless solutions obtained by Broms (1964b) for this category of laterally loaded piles are shown in Fig. 5.18.

Compared with the measured values of ultimate lateral capacities of piles in sands reported by various investigators, Broms (1964b) noted that the measured values generally exceed

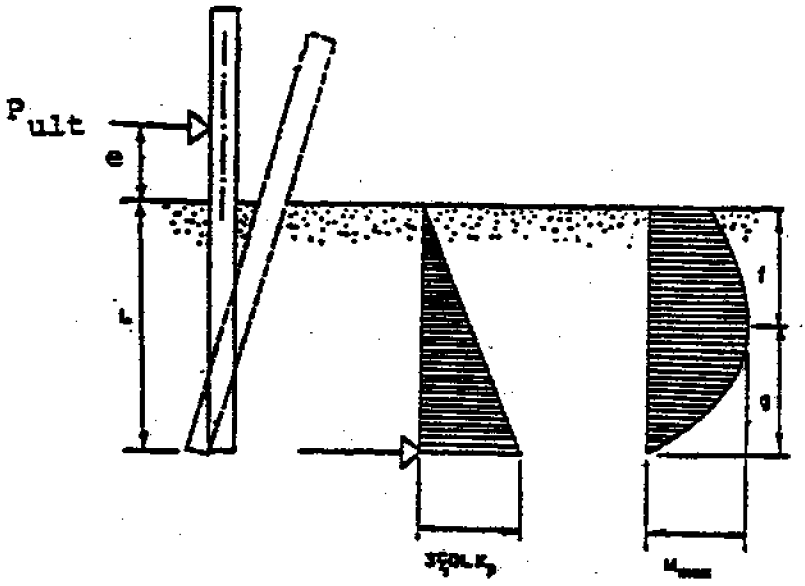

Fig. 5.12 Soil Reaction and Bending Moment Distribution for Rigid, Free-headed Pile in Granular Soil (Broms, 1964b)

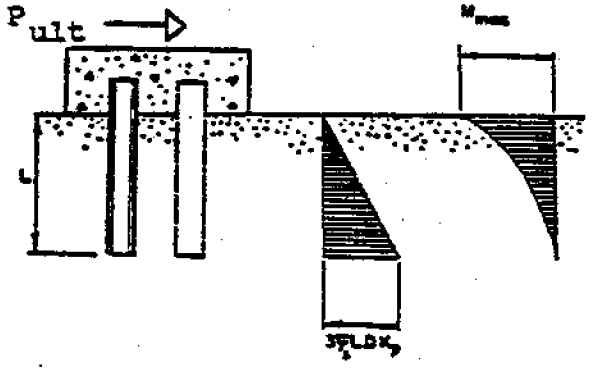

Fig. 5.13 Soil Reaction and Bending Moment Distribution for Rigid, Restrained Pile in Granular Soil (Broms, 1964b)

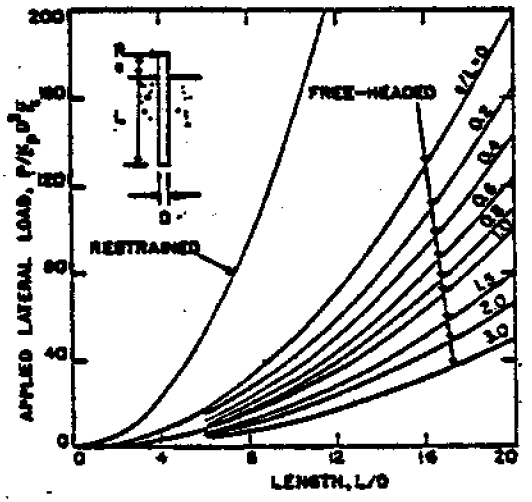

Fig. 5.14 Ultimate Lateral Resistance of Rigid Piles in Granular Soil (Broms, 1964b)

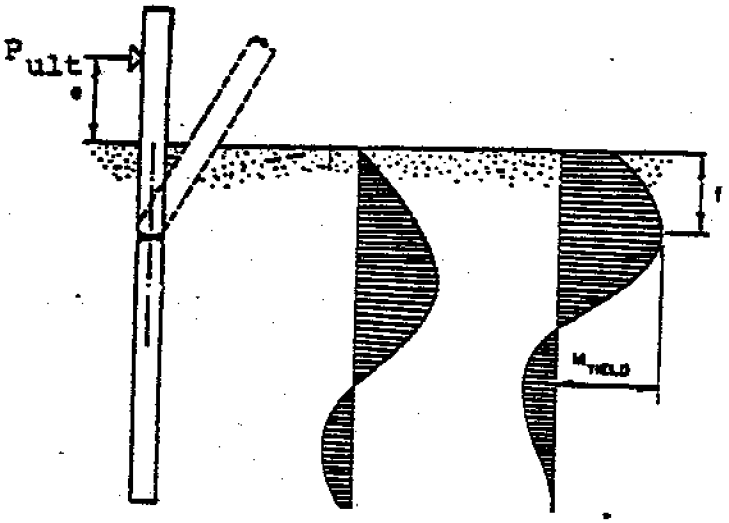

Fig. 5.15 Soil Reaction and Bending Moment Distribution for a Flexible, Free-Headed Pile in Granular Soil (Broms, 1964b)

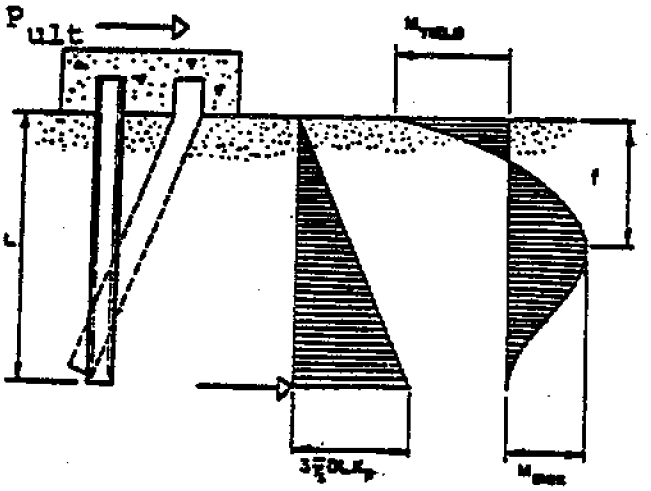

Fig. 5.16 Soil Reaction and Bending Moment Distribution for a Flexible, Restrained Pile (Intermediate Length) in Granular Soil (Broms, 1964b)

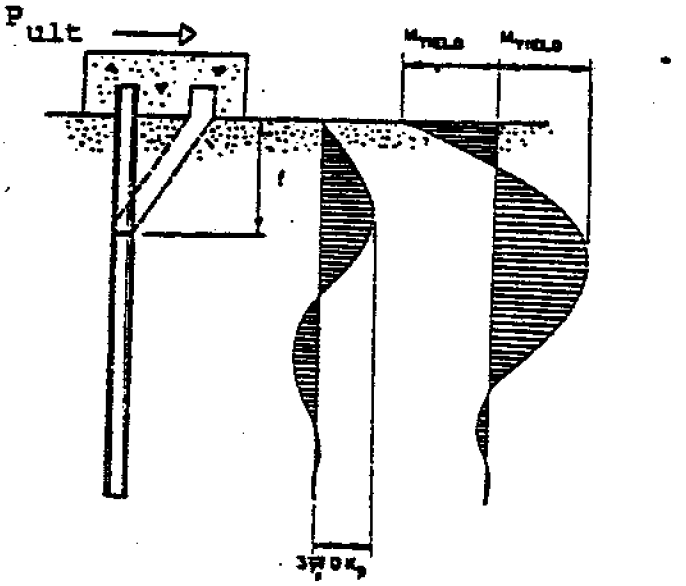

Fig. 5.17 Soil Reaction and Bending Moment Distribution for a Flexible, Restrained Pile (Long Length) in Granular Soil (Broms, 1964b)

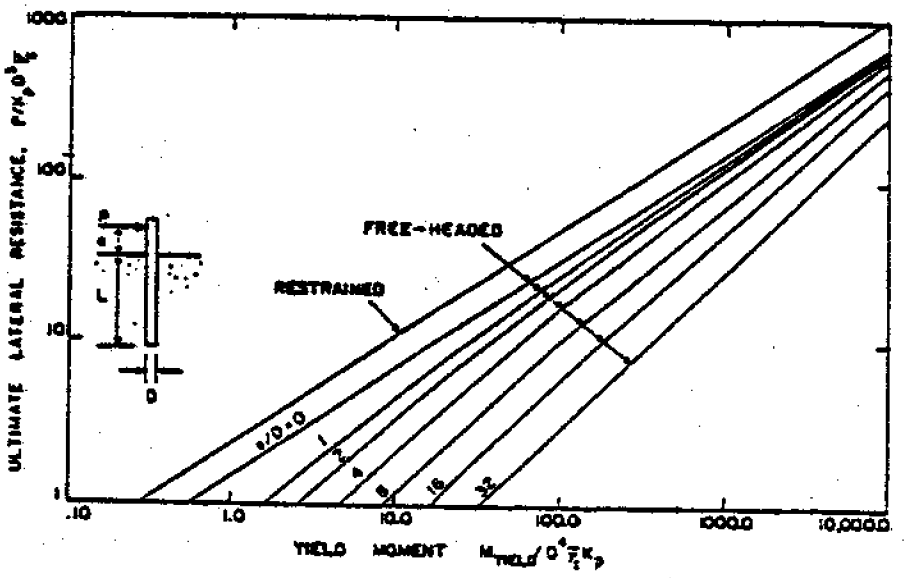

Fig. 5.18 Ultimate Lateral Resistance of Flexible Pile in Granular Soil (Broms, 1964b)

the calculated values by approximately 50%. The use of a factor of 3 for the Rankine soil stress at failure conditions is probably too conservative for the analysis.

5.2 Ultimate Capacity of Batter Piles

When large lateral loads are anticipated, it is common practice to use batter piles. Batter piles, sometimes called raking or inclined piles, are piles that are driven at an angle from the vertical. Common pile batters range from 1 horizontal : 12 vertical to 5 horizontal : 12 vertical (Bowles, 1977). It should be noted that installation of batter piles is likely to be more expensive and, in fact, construction limitations may sometimes prohibit the use of a large angle of inclination. These conditions should be thoroughly checked in the design phase.

One effective way of resisting lateral forces from either direction is to have piles battered in opposite directions as shown in Fig. 5.19. As the system is loaded, one pile will be in tension and the other in compression. Both piles will contribute resistance to lateral forces. This type of pile arrangement is commonly used for dolphins.

Simple procedures for determination of capacities of batter piles are not firmly established because of the complexity of this soil-structure interaction problem. Very limited load tests have been performed on batter piles. Results on model tests conducted by Awad and Petrasovits (1968) to determine the effects of pile inclination on load capacity are shown in Fig. 5.20. This can serve as a rough guide for estimation of load

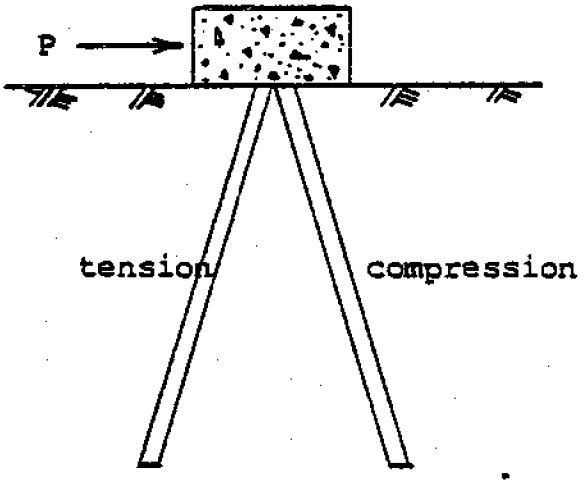

Fig. 5.19 Use of Batter Piles to Resist Lateral Forces

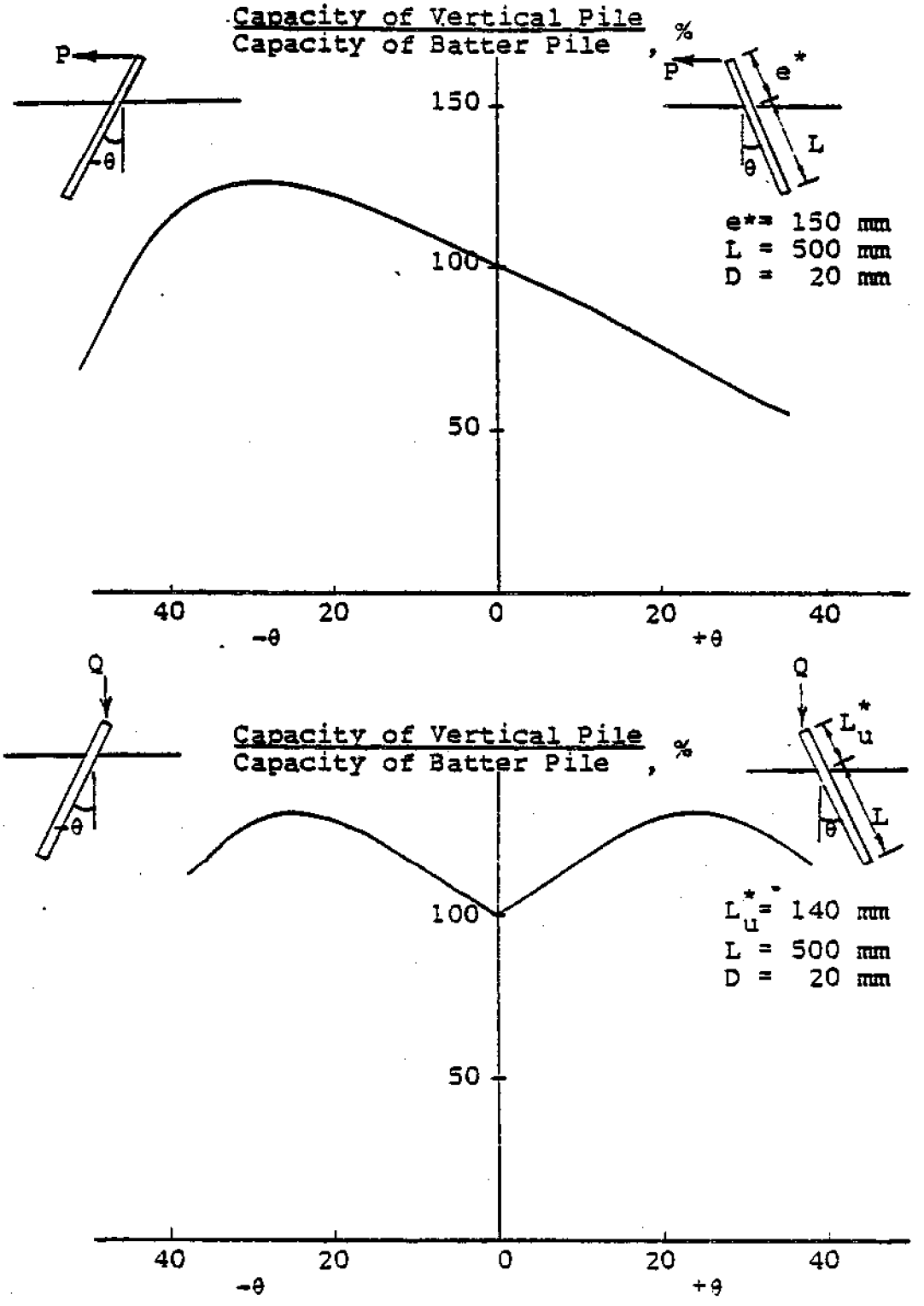

Fig. 5.20 Relative Ultimate Capacity for Different Angle of Inclination (after Awad and Petrasovits, 1968)

capacities of batter piles until more up-to-date information is available.

One major problem associated with the use of batter piles in compressible soil layers has been addressed by Broms (1976). The author pointed out that settlement of soil layers, because of self weight or surcharge load, may impose significant vertical loads along the inclined piles and induce large bending moments that can cause the pile to fail. His idea is further depicted in Fig. 5.21. Because of this, batter piles should not be used or the inclinations should be kept very small in areas where substantial settlements of the soil mass may occur.

5.3 Ultimate Capacity of Pile Groups

The evaluation of the lateral load capacity of a pile group is very complex. Lateral load tests performed on pile groups are rare and they are mainly restricted to small groups of piles. No simple method currently exists to deal with this problem. Some general guidelines will be provided here; they should be used cautiously, with good judgment. If possible, load tests should be performed to verify the computational results.

If the piles behave as rigid members, it will probably be reasonable to adopt an approach similar to that for axial loads. On this basis, the group lateral capacity is given as the smaller of:

1) the sum of lateral load capacities of individual piles.
2) the lateral load capacity of an equivalent single block defined by the exterior piles in the group.

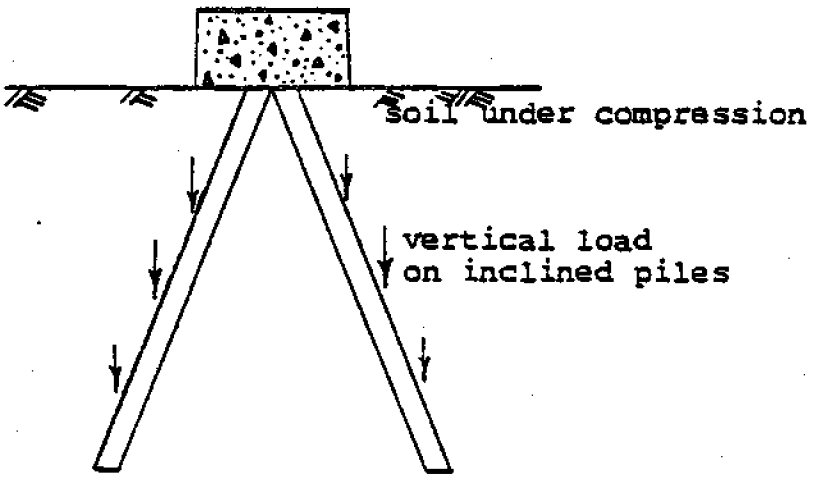

Fig. 5.21 Bending of Batter Piles because of Soil Settlement

The former can be obtained using procedures outlined in Section 5.1 The latter will include the ultimate soil resistance in front of the block plus the shear resistance acting along the two sides and the base of the block (Fig. 5.22).

The failure mode of the soil in the front end of the block (plane surface) will not be identical to that assumed for a circular surface. However, it is likely that the soil resistance acting on a plane surface will be higher than that acting on a curved surface. Therefore, the use of $9c_u$ (undrained case) and $3K_p\bar{\sigma}_v$ (drained case) as the ultimate soil reactions, as illustrated in Figs. 5.5, 5.6, 5.12 and 5.13, should give an approximate and conservative solution.

If the piles act as flexible members, the failure of the system is caused by yielding of the pile material rather than the soil. In such cases, block failure will be confined to the upper portion of the block located above the failure hinges and the group capacity can be estimated by summation of the lateral load capacities of individual members.

Davisson (1970) pointed out that, under most circumstances, piles behave as individual units if they are spaced more than 8 diameters apart in the direction of the loading and at least 2 1/2 diameters apart in the perpendicular direction.

5.4 Deflections of Vertical Piles

The design of laterally loaded piles may very often be governed by deflections rather than ultimate load capacity. Pile deflections lead to lateral displacements and tilt of the supported structures. This may lower the serviceability of the

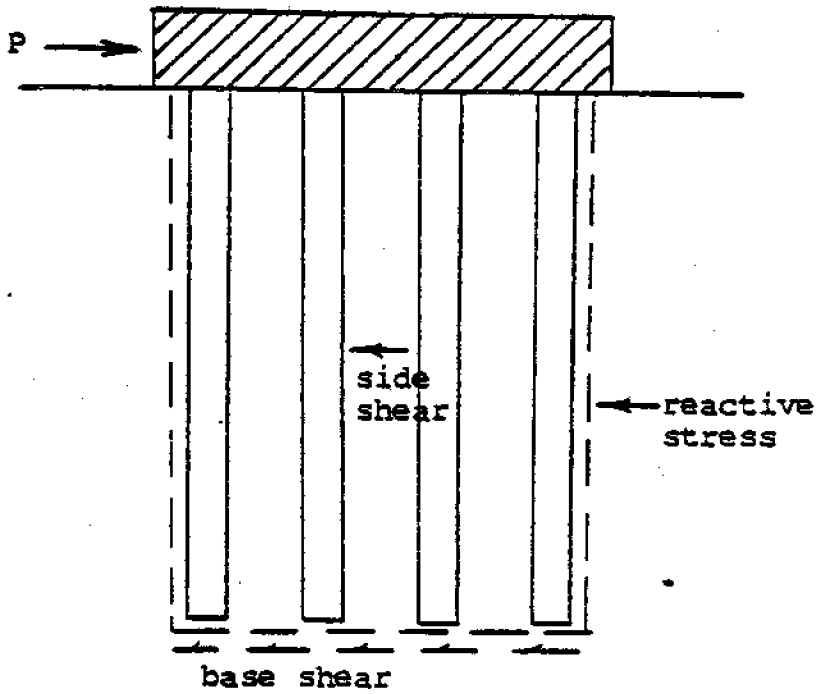

Fig. 5.22 Free-Body Diagram of the Group Behavior of a Pile Group under Lateral Loads

structure even though it may be 100% safe from a structural standpoint. The allowable deflection that can be tolerated at working load depends upon the function of the structure. Although large movements for docks or piers are not desirable, the deflections can be relatively large for fender piles or temporary structures.

The evaluation of lateral deflections of horizontally loaded piles has been based on the subgrade reaction model. This stems from a well-known class of problems in structural mechanics known as "beam on elastic foundation." The governing equation for this class of problems is given as:

$$E_p I_p \frac{d^4 y}{dz^4} = -p D \qquad (5.6)$$

in which: E_p = modulus of elasticity of pile material
I_p = moment of inertia of cross-section of pile
y = deflection of pile
p = soil reactive stress

Theoretically, if the magnitude and variation of the reactive stress are known, Equation 5.6 can be solved for deflection at any point along the pile.

Using the above concept, the soil reactions in front of a laterally loaded pile are simulated by a series of horizontal elastic springs (Fig. 5.23). The stiffness of these springs is represented by the horizontal subgrade reaction modulus, k_h; the reactive horizontal stress at any point along the pile is related to the amount of deflection at that same point. Studies have shown that this relationship is nonlinear (Davisson

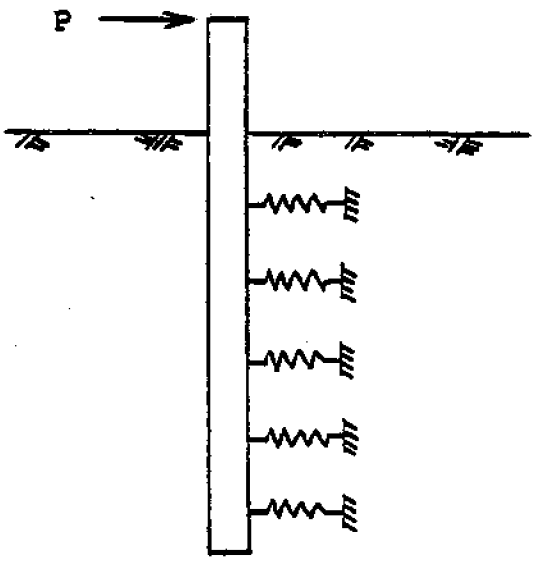

Fig. 5.23 Subgrade Reaction Model for Laterally Loaded Piles

and Prakash, 1963) and the horizontal subgrade reaction modulus for a given magnitude of deflection is given by the slope of the p-y curve at that magnitude of deflection (Fig. 5.24). The p-y curve for any pile-soil system is best derived from full-scale pile load tests and a nonlinear analysis of the problem can be performed by iterative techniques with the help of a computer.

As illustrated by the typical p-y curve shown in Fig. 5.24, the initial portion of the curve can be linearized without sacrificing much accuracy. Under most circumstances, this is valid as long as the load is less than 1/2 to 1/3 of the ultimate load, i.e., under most working load conditions. Assuming the springs to behave in a linear and elastic manner, the reactive horizontal stress at any depth along the pile can be expressed as:

$$p = -k_h y \tag{5.7}$$

in which: k_h = horizontal subgrade reaction modulus

The solution of Equations 5.6 and 5.7 requires a knowledge of the magnitude and variation of k_h with depth. These can be inferred through load test results on instrumented piles. A typical plot of k_h versus depth for overconsolidated clays is shown in Fig. 5.25. Granular soils and normally consolidated cohesive soils, on the other hand, exhibit a variation as shown in Fig. 5.26. For simplicity, a constant modulus is often used for the case of overconsolidated clays and a linearly increasing modulus with depth is assumed for normally

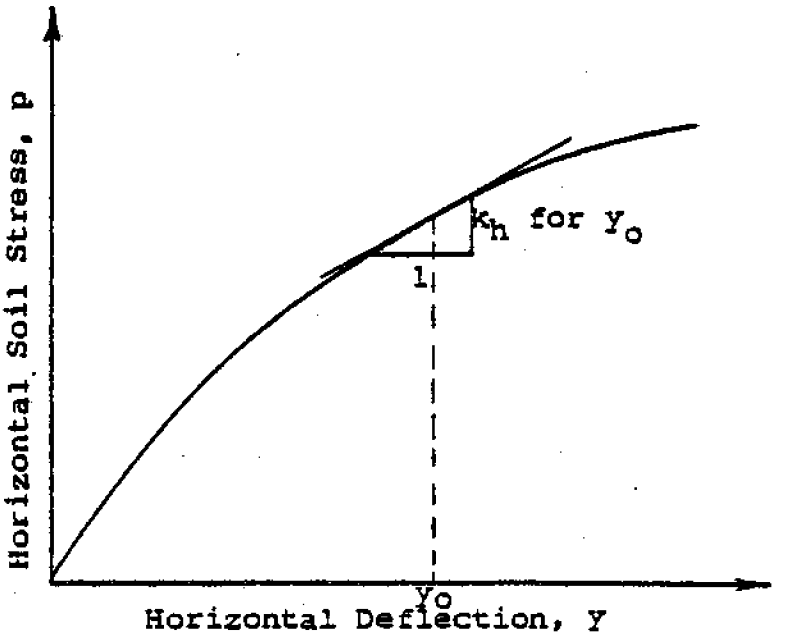

Fig. 5.24 Typical p-y Curve

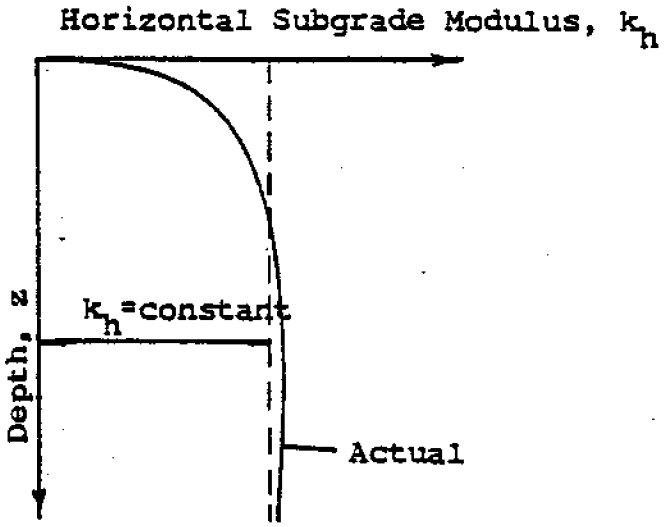

Fig. 5.25 Variation of k_h with Depth for Over-consolidated Clay (after Davisson, 1970)

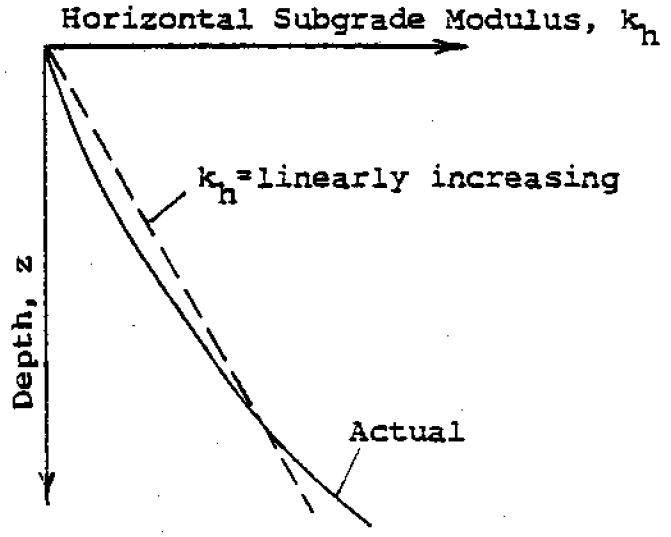

Fig. 5.26 Variation of k_h with Depth for Normally Consolidated Clay and Granular Soil (after Davisson, 1970)

consolidated cohesive soils and granular materials (Davisson, 1970).

Analytical closed-form solutions are readily available for the two conditions described below. For the case of a linearly increasing modulus, the stiffness of the "springs" is represented by a new constant parameter, n_h, which is related to k_h by:

$$k_h = n_h \frac{z}{D} \tag{5.8}$$

in which: n_h = coefficient of horizontal subgrade modulus variation

z = depth below the ground surface

The two parameters, k_h for constant modulus and n_h for linearly increasing modulus, as suggested by various investigators, are shown in Tables 5.2 and 5.3.

By adopting the above concept, Broms (1964) developed charts to give the deflection of piles at ground surface under working load conditions. The charts for the two cases where k_h is constant with depth and is increasing linearly with depth are shown in Figs. 5.27 and 5.28, respectively. The use of these charts requires a knowledge of the dimensionless parameters, β and η, defined as:

$$\beta = \sqrt[4]{k_h D/4E_p I_p} \tag{5.9}$$

$$\eta = \sqrt[5]{n_h/E_p I_p} \tag{5.10}$$

In cases where repeated loadings can occur, Davisson (1970) suggested that k_h (or n_h) be reduced to 30% of the value used for sustained loadings. He attributed this to degradation of

Type of Clay	Stiff	Very Stiff	Hard
c_u lb/ft^2 kN/m^2	2000 - 4000 96 - 192	4000 - 8000 192 - 383	> 8000 > 383
k_h lb/ft^3 kN/m^3	100,000 15,700	200,000 31,400	400,000 62,800

Table 5.2 Values of Horizontal Subgrade Modulus for Over-consolidated Clay (Terzaghi, 1955)

For Sands:

Source	Loose		Medium		Dense		Units
	dry	submerged	dry	submerged	dry	submerged	
Terzaghi (1955)	14000 2200	8000 1300	42000 6600	28000 4400	112000 17600	68000 10700	lb/ft^3 kN/m^3
Rowe (1956)	5000 790	–	–	–	160000 25100	–	lb/ft^3 kN/m^3
Reese, et al. (1974)	–	35000 5500	–	104000 16300	–	216000 33900	lb/ft^3 kN/m^3

For Normally Loaded Soils: (Davisson, 1970)

Organic Silt, 700 - 5000 lb/ft^3 (110 - 790 kN/m^3)

Peat, 350 lb/ft^3 (55 kN/m^3)

Clay, 67 c_u/D lb/ft^3 (11 c_u/D kN/m^3)

Table 5.3 Values of Coefficient of Modulus Variation

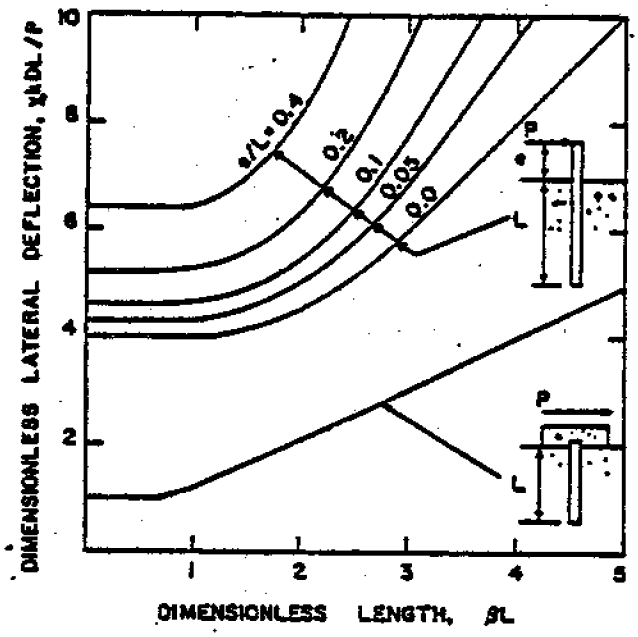

Fig. 5.27 Lateral Deflection at Ground Surface - Subgrade Modulus Constant with Depth (Broms, 1964a)

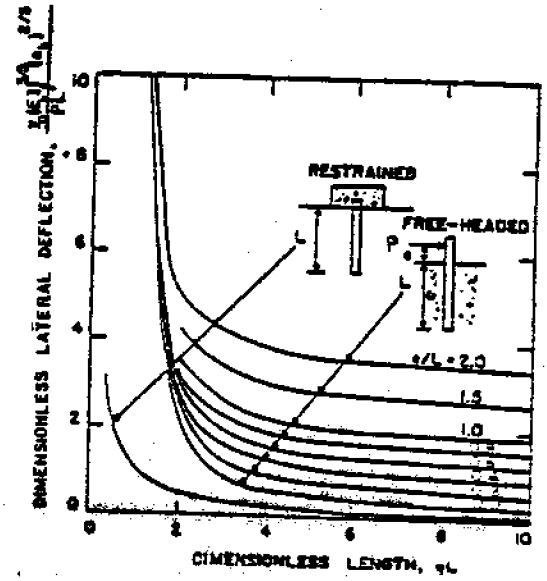

Fig. 5.28 Lateral Deflection at Ground Surface - Subgrade Modulus Increasing Linearly with Depth (Broms, 1964b)

soil reactions caused by repeated loadings.

When the subgrade reaction model is applied to predict group movements, a reduction in k_h (or n_h) should also be used, as shown in Table 5.4.

5.5 Summary

The design of laterally loaded piles is one of the more complicated aspects of pile foundations. Very few load tests have been reported in the literature. Most of the recent work is based on computer techniques. Nevertheless, hand calculation methods can provide a rapid and rough estimate of the solution.

It has been pointed out that the lateral capacity of the pile-soil system may be limited by the strength of either the pile or the soil. The former is a flexible pile and the latter is a rigid pile. A designer should understand the fundamental differences in behavior and application between these two types of piles to achieve a proper design. The degree of end restraint may also significantly influence the lateral capacity of the system and therefore should be thoroughly examined.

Batter piles are commonly used to resist large lateral forces. However, construction limitations or field conditions may very often prohibit the use of a large angle of inclination. The occurrence of any potential problem should be investigated in the design phase. Guidelines are provided to estimate the capacities of batter piles. These are based on very limited model test results and should be used cautiously.

Pile Spacing in the Direction of Loading	Effective k Values for Pile Groups
8D	1.00 k_h
7D	0.85 k_h
6D	0.70 k_h
5D	0.55 k_h
4D	0.40 k_h
3D	0.25 k_h

Note Pile spacing normal to the direction of loading has no influence if it is greater than 2.5 D.

Table 5.4 Subgrade Reaction Modulus of Pile Groups (after Davisson, 1970)

The best approach to analyze a laterally loaded pile group is by pile load test. If this is not economically feasible, the approximate procedures outlined in Section 5.3 can probably be used.

Similar to piles under compressive loads, piles subjected to lateral forces must also conform to deformation requirements, as well as ultimate capacity. The method presented herein to predict the amount of deflection upon application of loads is based on the subgrade reaction theory. Although this theory has some inherent limitations (e.g., fails to recognize the continuity of soils), it is widely used in practice and can be adopted under working load conditions.

In situations where the lateral loads are significant and batter piles cannot or should not be used, various methods suggested by Broms (1976) can be employed to increase the lateral resistance of vertical piles. These are shown in Fig. 5.29. Most of these methods are intended to increase the stiffness of the piles near the ground surface.

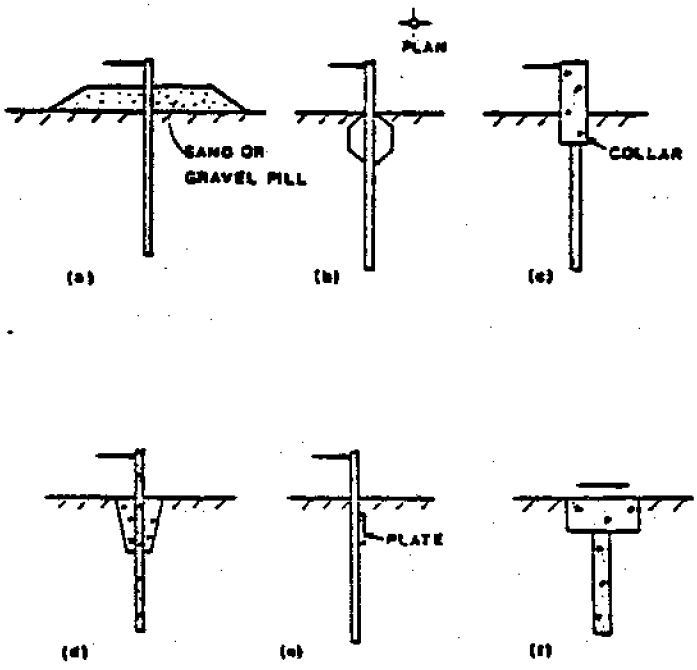

Fig. 5.29 Methods to Increase the Lateral Resistance of Vertical Piles (Broms, 1976)

CHAPTER 6

OTHER CONSIDERATIONS

In addition to the load carrying capacities, the design of pile foundations often incorporates factors that form a major portion of the design considerations. Some of the more common of these will be described in this chapter. The degree of importance of these factors depends upon the foundations, the site conditions and the applied loads. Other considerations may also influence the design of pile foundations at a given site; these have to be left to the ingenuity of the designer since it is impossible to discuss every possibility in this report.

6.1 Scour Around Pile Foundations

Scour can be defined as a process which involves the removal of granular material on the sediment bed. It occurs around any obstacle that obstructs the normal water-flow patterns. This erosive action around pile foundations has always been a concern for the design of coastal structures. The formation of a scour pit (depression surrounding an obstruction) as a result of this erosion reduces the lateral capacity of the pile. Moreover, the unsupported length of the pile will increase, thus reducing the frictional resistance of the pile under axial loadings. If not properly taken into account in the design phase, this phenomenon may markedly reduce the life of the structure.

Scour may result from currents, waves, ship motion or rise

of water level. The factors that are likely to control are currents and waves. Current and wave-induced scour are dominated by parameters such as velocity of flow, wave characteristics, water depth, pile diameter and the geological history of the site. Scour that occurs as a result of rise of water level is important at sites where large floods occur frequently, especially if the rise occurs in a very short period of time.

Earlier methods to predict scour depth were largely based on experience and a large number of parameters related to the problem were ignored. Kuhn and Williams (1961) suggested the scour depth to be the depth where there is a sudden increase in penetration resistance. While this may be adequate to locate the depth of the loose deposit layer, the scour depth can have a large deviation, depending upon the current velocity and the dimensions of the obstacles. Terzaghi and Peck (1967) proposed the maximum scour depth for design to be four times the amount of water level rise anticipated. This proposal is impractical in places where there is a large fluctuation (e.g., 8 ft) in water level.

Later investigations on the problem were mainly conducted in laboratory flumes. The primary objective of these investigations is to establish criteria and guidelines by which designers can assess the depth of scour under certain given conditions. Important factors are identified with varying degrees of success. However, the results obtained are qualitative rather than quantitative.

Palmer (1969) observed oscillatory wave-induced scour and

developed a schematic view of the general hydrodynamics in the vicinity of an obstruction (Fig. 6.1). He considered the pattern of secondary flow or turbulence to be a major factor in the removal of granular material around an obstacle. He suggested the main scouring force to be the primary vortex that develops in front of the cylinder.

Laursen (1962) studied the phenomenon of scour in a laboratory flume and demonstrated that there is an equilibrium or limiting depth of scour for any given set of conditions. He also pointed out that the depth of scour for a group of piles does not depend upon the proximity of adjacent piles unless the scour pits overlapped, in which case the depth of scour can be estimated by the solution for contraction of a river channel. This will probably accelerate the formation of scour pits. Similar investigations by Palmer (1969) showed that the pit diameter is proportional to the diameter of the pile, but is largely independent of surge velocity. He further noted that scour pits caused by inclined piles are of equal dimensions to those caused by identical vertical piles.

Machemehl and Abad (1975) investigated scour phenomenon caused by the combined effect of oscillatory waves and unidirectional current around a model cylindrical pile foundation. They studied the effects of current velocity, wave characteristics and diameter of piles on extent of scour. They concluded that:

1) the increase of water particle velocity adjacent to the pile is the main scouring mechanism.

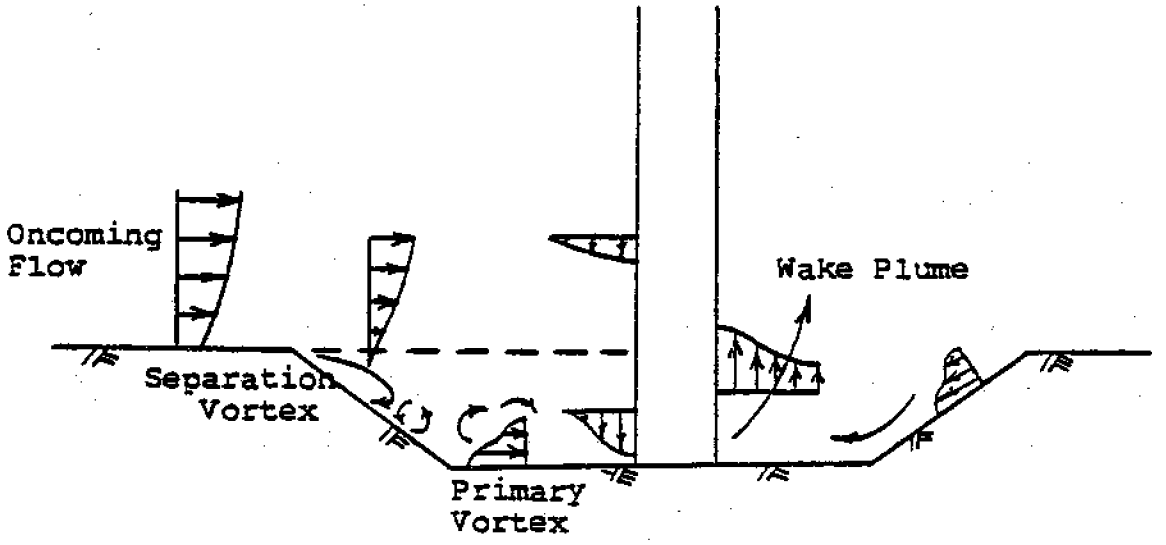

Fig. 6.1 Mechanism of Scour (after Palmer, 1969)

2) the addition of oscillatory waves in a unidirectional flow field increases the rate of scour development.
3) waves with long wavelength produce scour pits at a faster rate as compared with that produced by waves of short wave length.
4) scour effect is directly proportional to the diameter of the pile.

Since the severity of scour is very site-specific, the best approach to estimate the scour pit dimensions is to consult professionals with local experience. If this is not possible, a large margin of safety should be used. Allowances for this effect should be made in the selection of pile embedment so that adequate penetration will remain after scour.

6.2 Buckling of Fully and Partially Embedded Piles

It is well known that only very short members can be stressed to their yield point under compression; the usual situation is that buckling, or sudden bending as a result of instability, occurs prior to development of full material strength of the member. The buckling strength of a pile depends upon the end conditions, the properties of the pile, and the amount of horizontal support.

Early studies of the buckling of piles showed that the occurrence of buckling for fully embedded piles is a remote possibility, even in soft soils. Under most circumstances, minimal horizontal support will be able to prevent the piles from buckling under compressive forces. Bjerrum (1957) has shown that buckling of fully embedded piles in a soil with a constant

modulus need be considered only in cases where:

$$\frac{I_p}{A^2} \leq \frac{\sigma^2_{max}}{4k_h D E_p} \tag{6.1}$$

in which: I_p = moment of inertia for weak axis bending

A = cross-sectional area of pile

σ_{max} = yield stress of pile material

k_h = subgrade reaction modulus

D = diameter of pile

E_p = modulus of elasticity of pile material

In general, the above restraint can be satisfied except for very slender piles in soft soils.

Davisson (1963) presented theoretical solutions to evaluate the buckling potential of fully embedded piles for various boundary conditions shown in Fig. 6.2. These boundary conditions represent idealized situations for design. For total fixity at the top, the deck or cap must be rigidly attached to the piles; for total fixity at the bottom, the soil must be a firm material into which the piles are driven a considerable depth. Whether or not the ends can translate depends largely upon the structural configuration. Horizontal stability can be provided by diagonal bracing, shear walls, adjacent structures, pile caps, etc.. For most real situations, the degree of rotational and translational restraints do not exist at these extremes. However, analyses made can provide bounding solutions for designers. An appropriate choice of end conditions is based on the judgment of the designer.

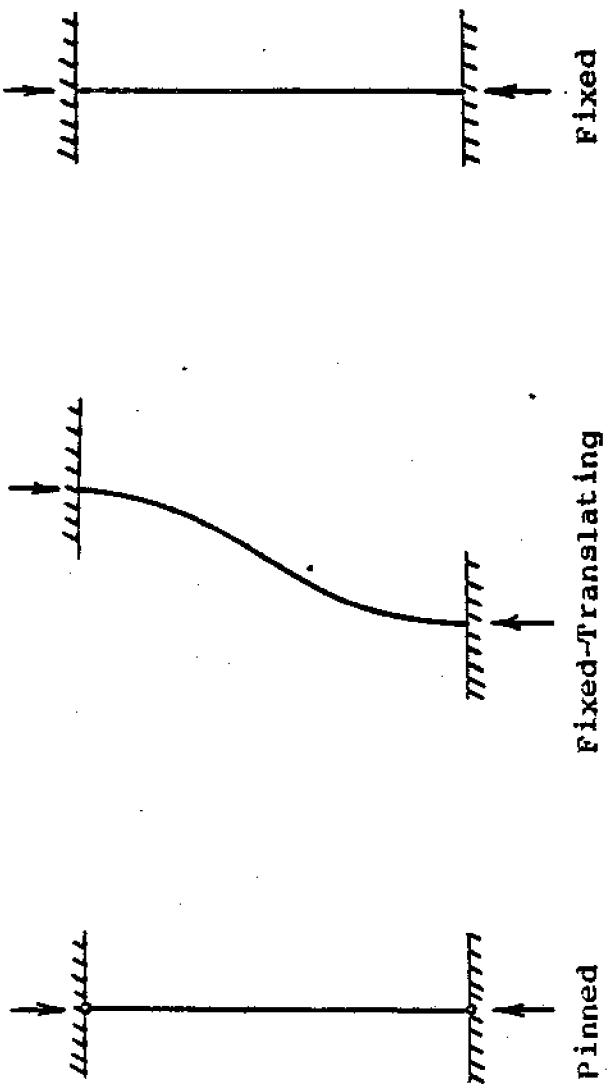

Fig. 6.2 Different Boundary Conditions for Piles (after Davisson, 1963)

For the case of constant subgrade reaction modulus with depth, Davisson (1963) derived the following equation to estimate the elastic pile buckling loads for fully embedded piles:

$$Q_{cr} = U_{cr} \frac{E_p I_p}{R^2} \tag{6.2}$$

in which: Q_{cr} = critical buckling load

U_{cr} = dimensionless buckling parameter for fully embedded piles in soils with constant modulus

$$R = \sqrt[5]{E_p I_p / k_h D} = \sqrt[5]{E_p I_p / k}$$

The dimensionless parameter, U_{cr}, can be obtained from Fig. 6.3 and is a function of both the end conditions and the dimensionless length parameter, ℓ_{max}, defined as:

$$\ell_{max} = \frac{L}{R} \tag{6.3}$$

in which: ℓ_{max} = dimensionless length parameter for fully embedded piles in soils with constant modulus

L = length of embedment of pile

It can be seen in Fig. 6.3 that the pile boundary conditions can have a strong influence on the critical buckling load. The lowest value of Q_{cr} is associated with piles that have no restraint with both the upper and lower ends.

With a linearly increasing subgrade reaction modulus, Davisson (1963) obtained the following equation to compute the critical buckling load for fully embedded piles:

$$Q_{cr} = V_{cr} \frac{E_p I_p}{T^2} \tag{6.4}$$

in which: V_{cr} = dimensionless buckling parameter for fully em-

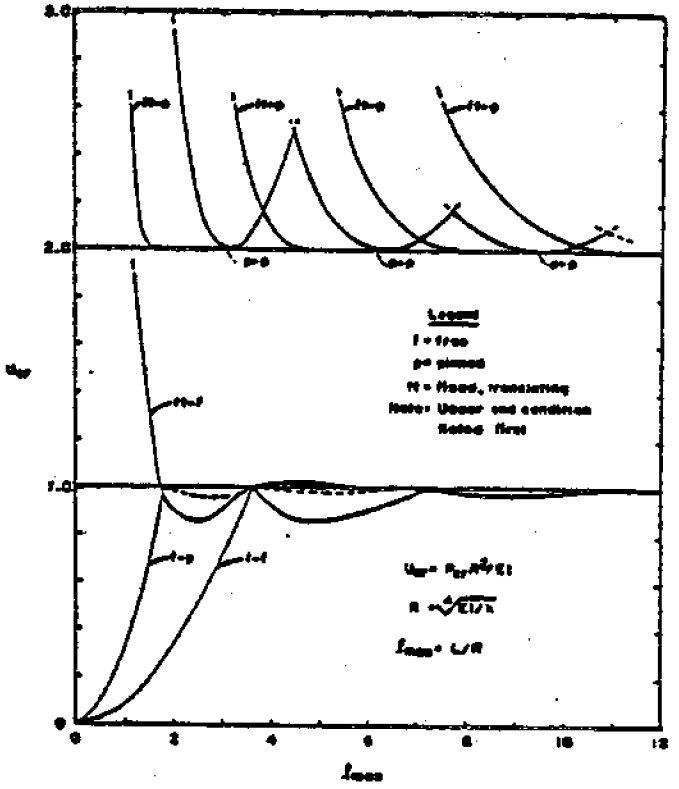

Fig. 6.3 Buckling Load Versus Length for Constant Modulus (Davisson, 1963)

bedded piles in soils with linearly increasing modulus

$$T = \sqrt[5]{E_p I_p / n_h}$$

The dimensionless buckling load parameter, V_{cr}, is shown in Fig. 6.4 as a function of both the end conditions and the dimensionless length parameter, z_{max}, defined as:

$$z_{max} = \frac{L}{T} \tag{6.5}$$

in which: z_{max} = dimensionless length parameter for fully embedded piles in soils with linearly increasing modulus

Partially embedded piles that extend through water are commonly used for coastal structures such as docks and piers. The buckling potential of these piles is larger than that of fully embedded piles. An approximate procedure to deal with this problem was developed by Davisson and Robinson (1965). The buckling load is estimated through an analysis of an "equivalent" system under which the pile is assumed to be free-standing with a fixed base located at some distance below the ground surface. The distance from the ground surface to the point of fixity is directly related to the strength of the soil. The lower the strength value, the deeper will be the point of fixity. This concept is further illustrated in Fig. 6.5.

The critical buckling load for the "equivalent" system shown in Fig. 6.5 can be computed from the following equations:

$$Q_{cr} = \frac{\pi^2 E_p I_p}{4(L_u+L_s)^2} = \frac{\pi^2 E_p I_p}{4L_e^2} \text{ for free-head condition} \tag{6.6}$$

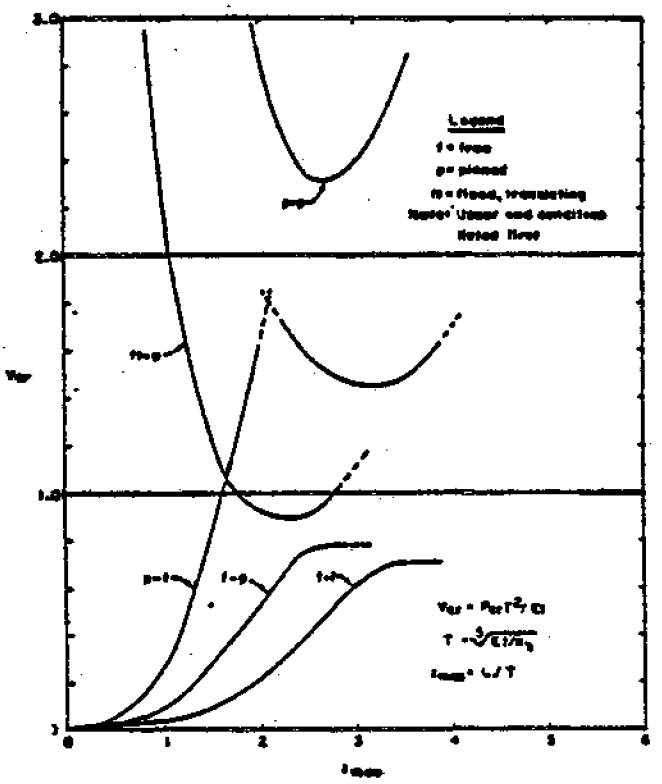

Fig. 6.4 Buckling Load Versus Length for Linearly Increasing Modulus with Depth (Davisson, 1963)

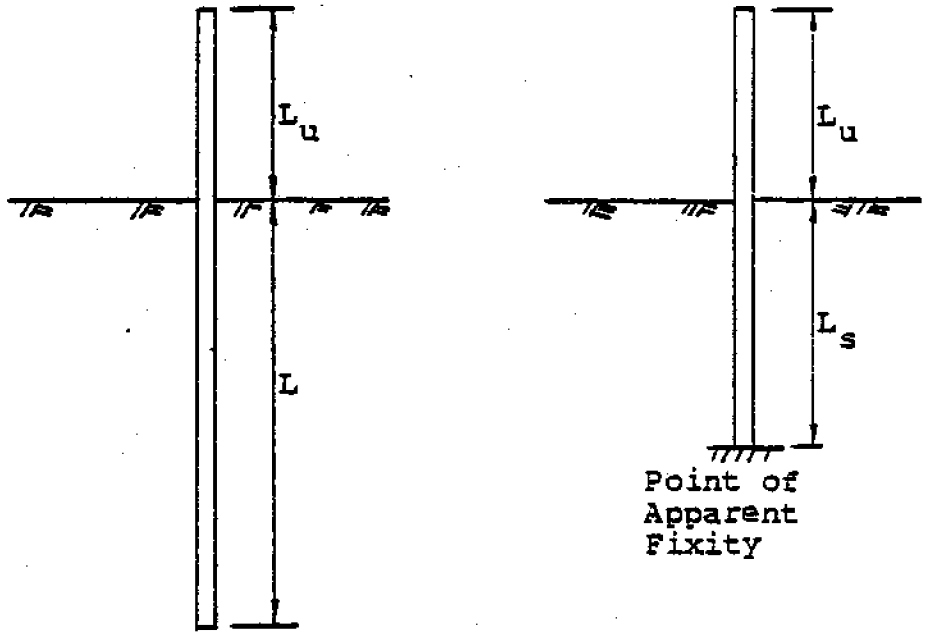

Fig. 6.5 Point of Fixity Method

$$Q_{cr} = \frac{\pi^2 E_p I_p}{(L_u+L_s)^2} = \frac{\pi^2 E_p I_p}{L_e^2} \quad \text{for fixed-translating head condition} \quad (6.7)$$

in which: L_u = length of unsupported portion of pile

L_s = equivalent length of embedded portion of pile

L_e = equivalent length of the pile

Therefore, the problem lies essentially in the determination of L_s.

Davisson and Robinson (1965) presented the solution in non-dimensional form. In the case of a constant modulus with depth, Fig. 6.6 can be used to obtain L_s. In the figure, J_R and S_R are given respectively as:

$$J_R = \frac{L_u}{R} \quad (6.8)$$

$$S_R = \frac{L_s}{R} \quad (6.9)$$

in which: J_R = dimensionless parameter for unsupported portion of piles in soils with constant modulus

S_R = dimensionless parameter for embedded portion of piles in soils with constant modulus

Once the equivalent length is known, the buckling load can be estimated from Equations 6.6 and 6.7.

In the case of a linearly increasing modulus with depth, Fig. 6.7 can be used. The parameters in the plot are defined as follows:

$$J_T = \frac{L_u}{T} \quad (6.10)$$

$$S_T = \frac{L_s}{T} \quad (6.11)$$

in which: J_T = dimensionless parameter for unsupported portion

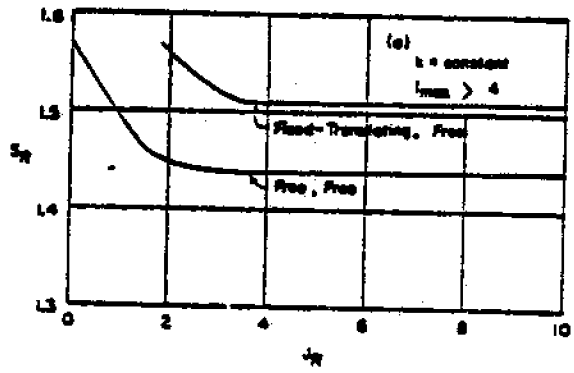

Fig. 6.6 Depth of Fixity for Buckling in Soils with Constant Subgrade Modulus (Davisson and Robinson, 1965)

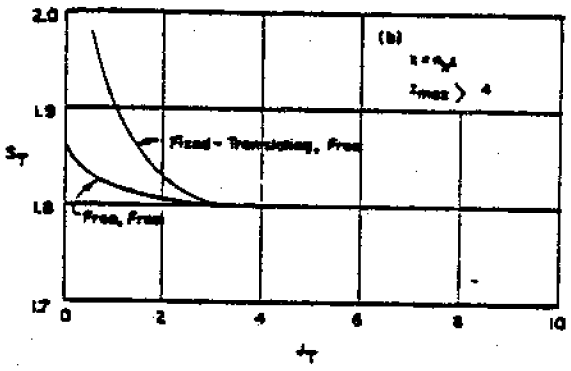

Fig. 6.7 Depth of Fixity for Buckling in Soils with Linearly Increasing Modulus with Depth (Davisson and Robinson, 1965)

of piles in soils with linearly increasing modulus

S_T = dimensionless parameter for embedded portion of piles in soils with linearly increasing modulus

Again, the critical buckling load can be estimated from Equations 6.6 and 6.7.

Although the method appears to be sound, the point of fixity method does not have any theoretical justification and in fact it violates the principles of equilibrium and compatibility. Nevertheless, Davisson and Robinson (1965) stated that for most practical purposes, the replacement of a partially embedded pile by an equivalent fixed base pile with no horizontal support can be used as long as ℓ_{max} is greater than 4 (soil modulus constant with depth) or z_{max} is greater than 4 (soil modulus linearly increasing with depth). According to the investigators, these requirements can be met under most practical situations.

6.3 Axial Capacity of Initially Bent Piles

Piles are often bent during driving, particularly when long slender piles are driven into soils that contain rock fragments. This results in reduced capacity under compressive load from that predicted for a concentric load on a straight pile. Failure of a bent pile under compressive load will occur when either the maximum bending stress in the pile reaches the yield strength of the pile material or the maximum soil reaction reaches the yield strength of the soil surrounding the pile. The tolerance level for this type of loading condition depends upon three fac-

tors:

1) soil properties

2) pile properties

3) magnitude of applied load

Methods for estimating the probable load capacity of bent piles have been proposed by Johnson (1962) and Broms (1963). The procedures as proposed by Johnson (1962) are rather tedious without the accessibility of a high-speed computer and will not be described here. However, his study revealed some of the more important points with regard to axial capacity of bent piles and these are stated as follows:

1) the reduction in capacity for bent end-bearing piles is greater than for bent friction piles.

2) a sharp bend is more detrimental than a long sweep.

3) the reduction in capacity is greater if the bent portion of the pile is located in soft soils.

The method as proposed by Broms (1963) is more suitable for hand calculation and will be presented in this section.

By expressing the deflection curve of the pile as a series of sine functions and assuming the soil to be an elastic Winkler medium (soil reaction at any point along the pile bears a linear relation with its horizontal deflection at the same point), Broms (1963) derived the following equation to estimate the maximum soil reaction along the bent pile under compressive loadings:

$$p_{max} = k_h \left(\frac{Q}{Q_{cr} - Q}\right) y_{max} \qquad (6.12)$$

in which: p_{max} = maximum soil reaction along the deflected pile

k_h = subgrade reaction modulus

Q = applied compressive load

Q_{cr} = critical buckling load

y_{max} = maximum horizontal deflection of pile

Values of subgrade reaction modulus can be found in the chapter on lateral loadings and the estimation of the critical buckling load is presented in Section 6.2.

Broms (1963) noted that the lateral soil reactions caused by pile deflections reach their ultimate values at approximately $9c_u$ for cohesive soils and three times the Rankine passive stress for cohesionless soils. Thus, using a factor of safety of three, Broms (1963) suggested the following allowable soil reaction values for design:

$$p_{all} = 3c_u \qquad \text{for cohesive soils} \tag{6.13}$$

$$p_{all} = \bar{\sigma}_v K_p = \bar{\sigma}_v \frac{1 + \sin \bar{\phi}}{1 - \sin \bar{\phi}} \qquad \text{for cohesionless soils} \tag{6.14}$$

in which: p_{all} = allowable soil reaction stress

c_u = undrained shear strength of soil

$\bar{\sigma}_v$ = effective vertical stress

$\bar{\phi}$ = effective angle of internal friction of soil

K_p = passive soil stress coefficient

Based on Broms's recommendations, the allowable axial load that can be applied to a bent pile without overstressing the soil is given as:

$$Q_{all} = \frac{p_{all} Q_{cr}}{k_h y_{max} + p_{all}} \tag{6.15}$$

in which: Q_{all} = allowable compressive load

Besides overstressing the soils, compressive loadings on bent piles may also induce axial and bending stresses in the pile that may well exceed the yield strength of the pile material. Broms (1963) derived the following equation to compute the maximum bending moment on a bent pile under an applied load Q:

$$M_{max} = \frac{Q_{cr}}{Q_{cr} - Q} E_p I_p \frac{(\theta_a - \theta_b)_{max}}{\Delta L} \tag{6.16}$$

in which: M_{max} = maximum bending moment in a pile

E_p = Young's modulus of pile material

I_p = moment of inertia of the cross-section of pile

$(\theta_a - \theta_b)_{max}$ = maximum difference between inclination (in radians) of a pile between two points a and b, which are ΔL apart

Therefore, the maximum stress (axial + bending) that occurs in the pile can be computed from:

$$\sigma_{max} = \frac{Q}{A} + \frac{M_{max}}{Z} \tag{6.17}$$

in which: σ_{max} = maximum stress in pile

A = cross-sectional area of pile

Z = section modulus of the cross-section of pile

This maximum stress should be less than the allowable stress that can be imposed on the pile material.

6.4 Downdrag of Piles

When piles are embedded in soils that are undergoing settlement, downdrag forces will be developed along the shaft as

the soils move downwards relative to the pile. The skin friction developed as a result of this relative downward movement of the soil is called negative skin friction. As the term implies, this skin friction will increase the magnitude of the axial downward load on the pile and can have serious effects on pile performance if not properly accounted for in design.

The magnitude of downdrag forces is a function of the relative displacement between the pile and the soil. For cohesive soils, settlement takes place mainly because of consolidation; therefore the development of downdrag forces will be a time-dependent process. Rigorous analysis to determine the interrelationship between downdrag and settlement is possible by means of numerical methods. However, assuming sufficient relative settlement has occurred to mobilize the ultimate shaft resistance, the maximum downdrag force on a single isolated pile can be estimated from the following equation:

$$Q_d = \int_0^L \tau_a \pi D \, dz \tag{6.18}$$

in which: Q_d = maximum downdrag force

τ_a = maximum pile-soil adhesion per unit area

D = diameter of pile

L = length of embedment of pile

Bjerrum (1973) has stated that the drained shear strength should be used to evaluate the downdrag load. He showed that if the rate of relative movement between the soil and the pile is negligible, τ_a in Equation 6.17 can be expressed as:

$$\tau_a = K\bar{\sigma}_v \tan \bar{\phi} \tag{6.19}$$

in which: K = horizontal stress coefficient

$\bar{\sigma}_v$ = effective vertical stress

$\bar{\phi}$ = effective angle of internal friction of soils

Values of K and $\bar{\phi}$ for various types of clays as suggested by Bjerrum (1973) are tabulated in Table 6.1.

It should be realized that Equation 6.18 is not applicable for batter piles. Based on model test results, Koerner and Mukhopadhyay (1972) have measured substantially larger values of negative skin friction for batter piles. For batter angles commonly used in practice, the authors reported values that are twice that of vertical piles (Fig. 6.8).

Negative skin friction can also occur on piles installed in groups, but the downdrag forces are likely to be less severe than that calculated for isolated single piles. Results of model tests conducted by Koerner and Mukhopadhyay (1972) showed that group effects reduce downdrag loads. The investigators reported a sharp decrease in negative skin friction at a spacing of about 2.5 D on a 3X3 group. This reduction was observed at all values of soil surface settlement (Fig. 6.9).

With a knowledge of the soil properties and the dimensions of the pile, the downdrag forces can be estimated and incorporated into the design. However, in cases where the allowable loads have to be reduced significantly to account for this effect, application of methods to minimize the downdrag forces may be more economical.

Downdrag loads can often be effectively reduced by predrilling through the soils contributing to the downdrag, there-

Type of Clay	K	$\bar{\phi}$
Silty	0.45	30°
Low Plasticity	0.50	20°
Plastic	0.55	15°
High Plasticity	0.60	10°

Table 6.1 Values of K and $\bar{\phi}$ for Negative Skin Friction (Bjerrum, 1973)

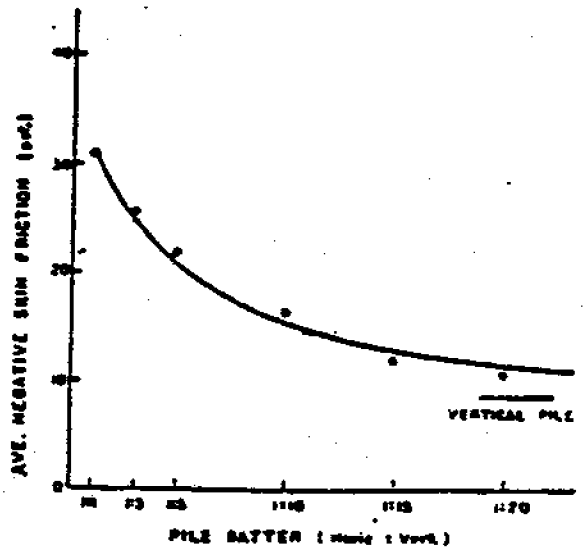

Fig. 6.8 Effect of Pile Batter on Average Negative Skin Friction (Koerner and Mukhopadhyay, 1972)

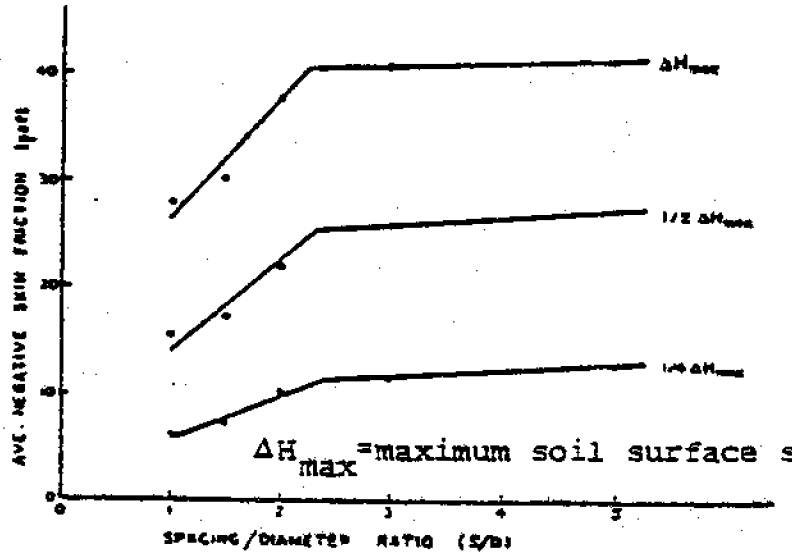

Fig. 6.9 Effect of Pile Group Spacing on Average Negative Skin Friction (Koerner and Mukhopadhyay, 1972)

by reducing the frictional drag of the settling soil on the pile. Downdrag could also be theoretically eliminated by enclosing the portion of the pile which extends through the settling soil in a sleeve with a diameter larger than the pile. This would separate the pile completely from the soil in the zone contributing to the downdrag loads. However, the economic feasibility of such a procedure is questionable and such sleeves often hang up on the piles, thereby defeating the purpose of their use (AWPI, 1966).

Besides the two methods described above, surface coatings have also been used to minimize negative skin friction. Koerner and Mukhopadhyay (1972) demonstrated that asphalt coatings can reduce the amount of downdrag load transfer to the pile. They indicated that the reduction will be larger if the asphalt coatings are thicker and softer. Claessen and Horvat (1974) also discovered significant reductions (by about one-half) in downdrag loads with the use of a slip layer (about 0.375 inch or 10 mm thick) of bitumen coatings on a concrete pile.

6.5 Load Distribution in Pile Groups

It has often been assumed that all piles in a group carry an equal share of load. As noted by Bowles (1977), this assumption is valid only when the following conditions are met:

1) the pile cap is in contact with the ground.
2) the piles are all vertical.
3) the load is applied at the center of the pile.
4) the pile group is symmetrical.

For free-standing pile groups in clays, the load distribu-

tion among piles has been studied by Whitaker (1957) using model tests. The investigator reported that for 3X3 groups with spacings of 2 D and 4 D, the piles at the corners of the group carry the largest proportion of load while the center pile carries the smallest proportion under working load conditions. However, as the pile group is loaded to its ultimate capacity, the order of driving starts to play a significant role in distribution of load among piles. The test results indicated that piles that are driven first carry the least share of load while those driven last carry the largest share. Whitaker further noted that at spacings of 8 D, under which individual pile failure governs, the load distribution among piles is essentially uniform, i.e., all piles carry an equal share of load, regardless of position or order of driving. His results are summarized in Fig. 6.10a and 6.10b. For 5X5 groups at spacings of 2 D and 4 D, experimental results showed that the load distribution basically follows that of 3X3 groups except that the variation of load distribution is greater in this case (Fig. 6.11).

For pile groups in sand, a rather extensive investigation on load distribution using model tests has been conducted by Beredugo (1966). The author identified four stages of loadings at which the load distributions are quite different. These four stages are described as follows:

1) at a small percentage of the ultimate load, the load distribution appears to be random.
2) as the load increases, load distribution among piles

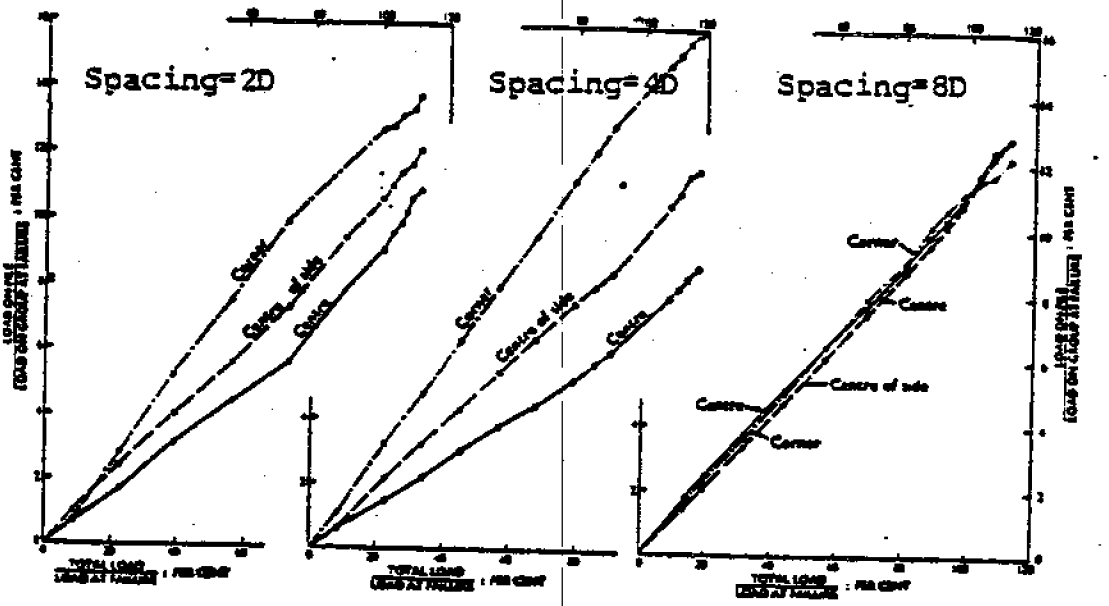

Fig. 6.10a Load Distribution in 3X3 Groups of Piles: Center Pile Driven First, Corner Piles Last (Whitaker, 1957)

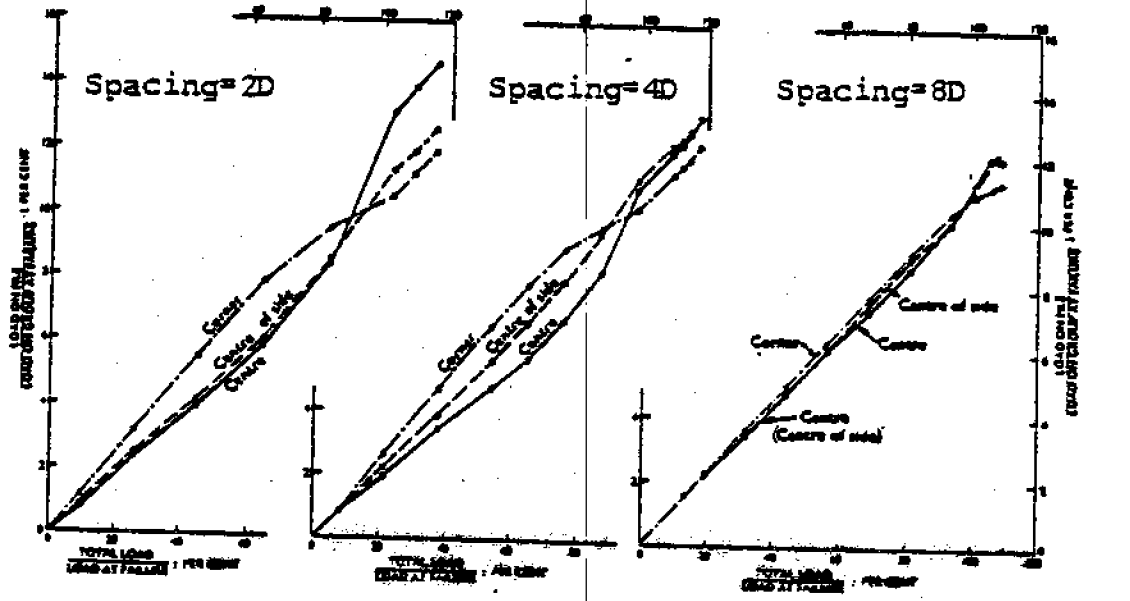

Fig. 6.10b Load Distribution in 3X3 Groups of Piles: Corner Piles Driven First, Center Pile Last (Whitaker, 1957)

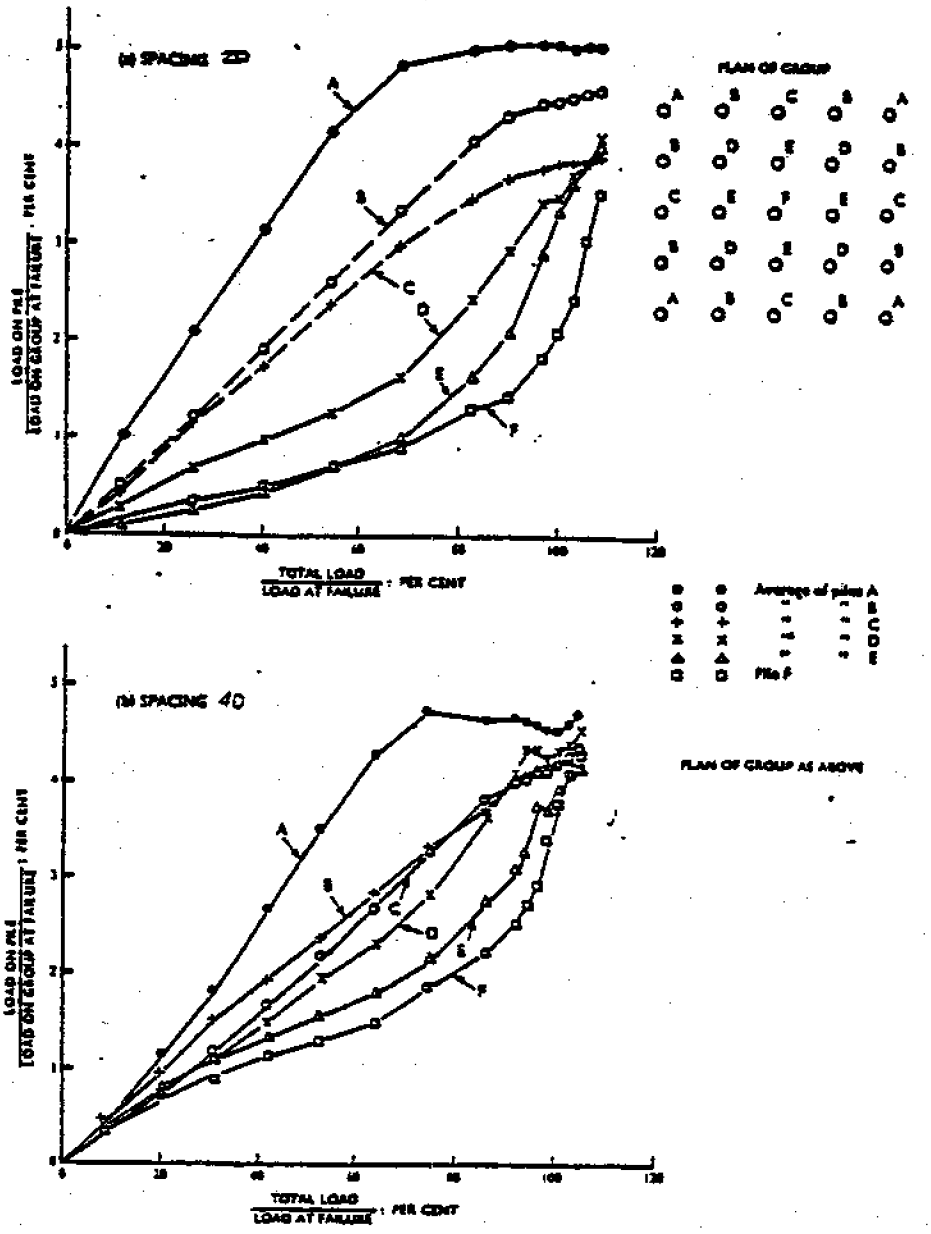

Fig. 6.11 Load Distribution in 5X5 Groups of Piles: Center Pile Driven First, Corner Piles Last (Whitaker, 1957)

is mainly governed by the driving order (piles that are driven last carry a greater share of the load).

3) at or near the ultimate load, load distribution is determined by the position of the pile in the group with the center pile carrying the greatest proportion of the load and the corner piles carrying the least proportion.
4) for loading beyond failure, there will be a uniform distribution of load among the piles.

Typical results of Beredugo's experimental investigation can be seen in Fig. 6.12. He also noted that as the spacings between piles increase, the load carried by each pile will tend to equalize, a case similar to that of pile groups in clay.

Vesić (1969) has also performed a detailed study on load distribution of pile groups in sands. The typical load distribution measured is shown in Fig. 6.13. According to the figure, the center pile carries the greatest share of load and the corner piles carry the least.

6.6 Pile Groups under Eccentric Loadings

Often it is necessary to consider the effects of eccentric loadings on pile groups. This is common for piles used in docks, piers, etc.. Rigorous analysis of this problem usually follows the procedures for three-dimensional structural analysis with computer-aided solutions. However, for simpler construction, the discussion below will provide some general guidelines to analyze the problem.

For pile groups in clays, Meyerhof (1963) carried out model tests on pile groups loaded eccentrically. He reported that

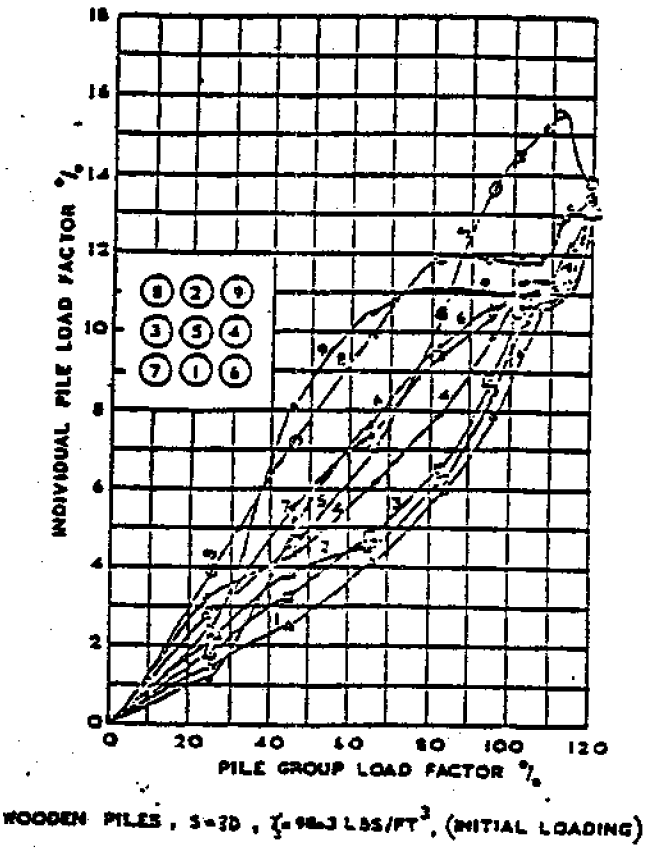

Fig. 6.12 Load Distribution Curves for 3X3 Group (Beredugo, 1966)

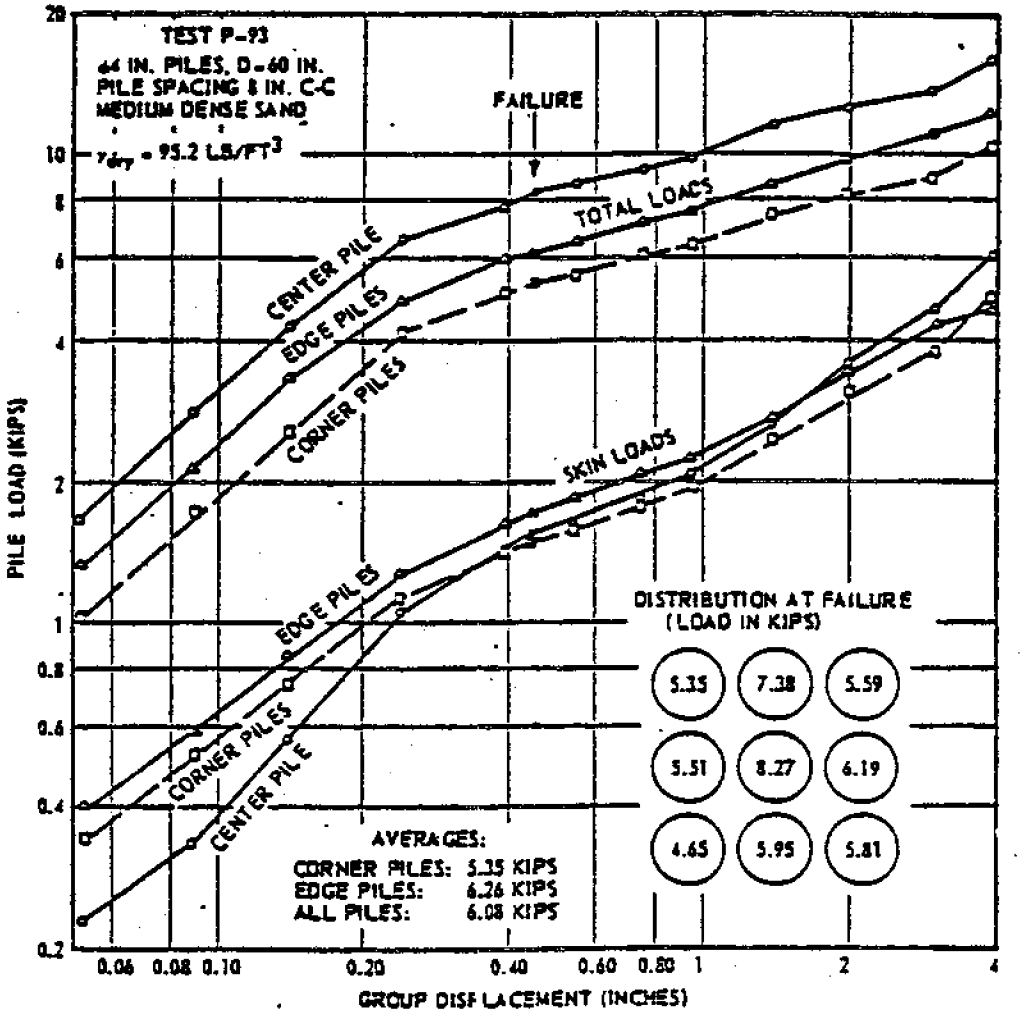

(See Preface for SI Conversions)

Fig. 6.13 Distribution of Loads among Piles (Vesić, 1969)

for eccentricities up to half the group width, the group capacity is not noticeably affected and can be evaluated using the same procedures as for centrally applied axial loads. This is explained by the fact that the reduced point resistance because of eccentric loading is offset by an increase in shaft resistance on the side of the group. However, it was pointed out that if the width of the group is equal to or greater than the depth of penetration of the piles, the effects of horizontal soil stress will be relatively small and thus the shaft resistance should be ignored with the point resistance calculated in the same manner as for a shallow foundation. In other words, the piles in the tension region of the group are ignored and an equivalent group width is used (Fig. 6.14), given as:

$$B'_g = B_g - 2\bar{e} \tag{6.20}$$

in which: B'_g = equivalent group width

B_g = group width

$\bar{e}$ = eccentricity of loading

The effects of eccentric loading on the bearing capacity of pile groups in sand have been studied by Kishida and Meyerhof (1965) using a series of model tests. Their results showed that for small eccentricities, the bearing capacity of the group is not significantly affected. The induced moment is resisted by the horizontal resistance on the side of the group until the maximum passive soil stress is reached. Within this limit, a slight increase in the ultimate capacity of the group over that of a centrally applied load is possible. However, beyond this limit, the difference has to be balanced by an ec-

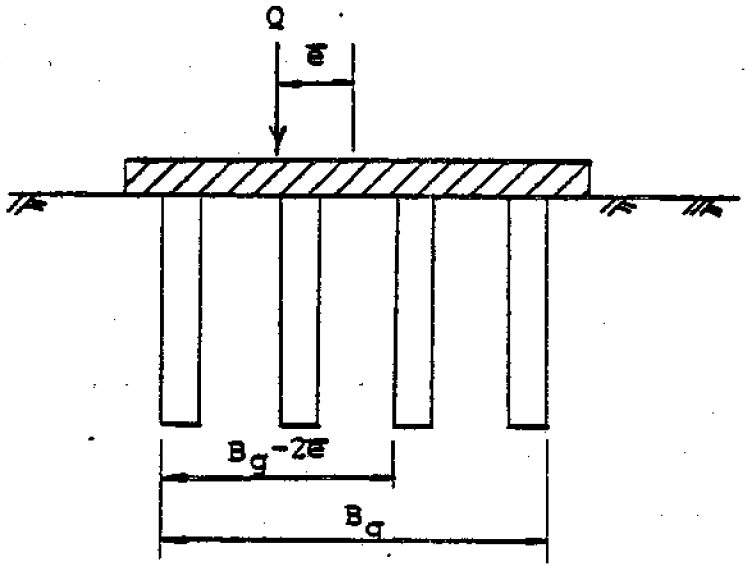

Fig. 6.14 Effect of Eccentric Loadings on Bearing Capacity of Pile Groups

centric point resistance or uplift resistance of piles, depending on whether block failure or individual pile failure governs. This results in a decrease of group capacity with increasing eccentricities.

6.7 Summary

In addition to the load carrying capacities requirement, the design of pile foundations must also take into account other factors that may significantly influence the performance of the foundations under loads. The considerations presented in this chapter are typical problems that are commonly encountered in real situations. These should be studied carefully and incorporated into the design, if applicable.

CHAPTER 7

MATERIALS FOR PILES

A wide variety of materials has been employed for construction of waterfront structures. At present, the materials used for pilings are normally restricted to:

1) concrete
2) steel
3) wood

Discussions in this chapter will be limited to the above materials. The performance of these materials, as well as other types of recently developed materials, has been discussed by Hubbell and Kulhawy (1979). No attempt will be made to repeat this information; however, some of the more important points relevant to piles will be discussed herein. The reader should refer to Hubbell and Kulhawy (1979) for more detailed information.

The selection of material type for a given structure should not be based on minimum initial total cost; factors such as delivery, installation, maintenance, replacement, durability and protective measures required throughout the design life of the structure should also be taken into consideration. For facilities such as recreational playgrounds, aesthetics or public preference may also influence the choice of material type.

Although the material type will not greatly affect the computational design procedures for pile foundations, its determination should not be made after the whole design process has

been completed. Instead, different options should be constantly examined throughout the analysis-design cycles to select the best material appropriate for a given project.

7.1 Material Deterioration in the Coastal Environment

Material deterioration has always been a major concern for all types of coastal facilities. Many structures have been rendered useless as a result of this process. Deterioration often is expressed in the form of reduced cross-sectional area. If not properly taken into account in the design phase, the load-carrying capacities of the members may be significantly reduced with subsequent failure of the structure.

Material deterioration involves an interaction between the material and the aggressive components of the environment. The rate at which this occurs is very site-specific and it varies with the location of the material with respect to different environmental zones. Five zones can be identified in the coastal regime:

1) atmospheric
2) splash
3) submerged
4) erosion
5) embedded

These are best illustrated by a pile free-standing in water, as shown in Fig. 7.1. While the deterioration in the atmospheric, submerged and embedded zones is determined by the environmental conditions, the degradation processes in the splash and erosion zones are dominated by wave action and abrasive action

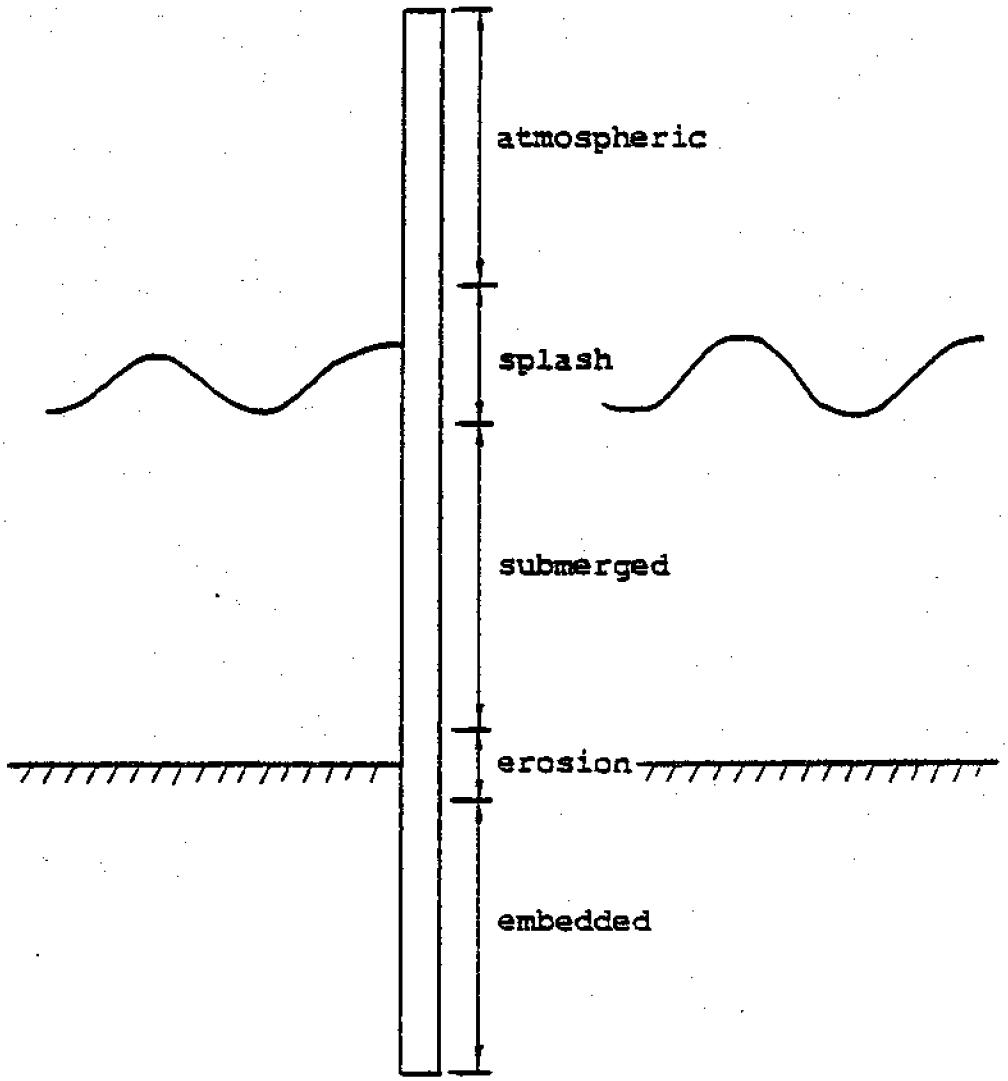

Fig. 7.1 Different Environmental Zones of Attack in the Coastal Environment

of sea bed sediments, respectively. Each of these zones has its own characteristics with regard to deterioration. Under most circumstances, the splash zone is likely to be the critical region that governs the design because high rates of deterioration usually occur in this zone.

An understanding of the local environment is essential to study the nature and extent of material deterioration. A complete evaluation of the problem should include a study of the atmosphere, the water and the soil. Atmospheric attack depends largely upon climatic conditions and the presence of airborne destructive elements. A complete analysis of water properties includes type (fresh or salt), oxygen content, pH values, resistivity and bacterial counts. Soil factors that may influence material deterioration are type (sandy or clayey), location of ground water table, mineral composition and the corrosiveness of the gaseous phase of the soils.

Instead of the detailed analyses mentioned above, the severity of deterioration can very often be estimated by a thorough observation of any existing piles at the site. If necessary, old piles can be pulled from the ground for this purpose.

7.2 Concrete

Plain concrete is composed of water, fine aggregate, coarse aggregate, cement and, frequently, admixtures. When properly proportioned and thoroughly mixed, these constituents will form a plastic mass which can be cast into any predetermined shape and size. Upon a hydration reaction between the water and the cement, the plastic mass will solidify and become hardened con-

crete.

Concrete is a material that is strong in compression, but weak in tension. Because of this, concrete piles are often reinforced with steel for bending and uplift, where significant tensile stresses can be developed. In cases where the formation of cracks is strictly prohibited, prestressed concrete piles can be used.

Concrete piles are relatively durable and can withstand a harsh environment. They can carry heavy compressive loads and have long life. On the other hand, concrete piles are susceptible to cracking under tensile forces (e.g., uplift, frost heave) and can be expensive. They require time for curing and special equipment for handling. Furthermore, a predetermined length is almost necessary as cutting or splicing is likely to be expensive.

Concrete exposed to air is subject to the weathering processes of the atmosphere. They may result either from thermal expansion/contraction caused by changes in atmospheric temperature or chemical weathering caused by airborne destructive elements. Abrasive action by wind-carrying particles may also cause damage to piles in the atmospheric zone. In general, the rate of deterioration under this environmental condition is minimal and does not require much attention. However, these processes may lead to the formation of small cracks on the surface of the piles. Subsequently, water may penetrate through these cracks and cause spalling and rusting of the reinforcing bars.

In an extensive investigation of long-term behavior of concrete structures in the marine environment, Browne and Domone (1974) discovered that disintegration of concrete piles is most severe in the splash zone, a region that is constantly subjected to pounding of waves and abrasive action of floating debris or ice. The investigators also reported no deterioration in the portion of the piles that is permanently submerged. They attributed this to the lack of oxygen supply in the submerged zone.

In the erosion zone, the severity of attack by abrasive action of the sea bed sediments depends upon the current velocity and the characteristics of the sea bed sediments. Damage may be appreciable in places where current velocity is fast and particle abrasive action is strong.

The embedded portion of concrete piles is generally considered permanent. However, this assumption may not be valid when the soils or groundwater contain destructive alkalis, acids or sulphate salts that can cause damage to concrete. According to Chellis (1961), this effect is more pronounced in sandy soils than in clays because large pore space permits rapid leaching and provides more air for deterioration to take place.

In the atmospheric zone, concrete may be subjected to dramatic changes in temperature. The durability of concrete with respect to temperature changes is measured by the number of freeze-thaw cycles required to produce a specified amount of deterioration. Laboratory tests conducted by the PCA (1968)

on concrete specimens have shown that high durability is associated with the use of air-entrainment and a low water-cement ratio, as illustrated in Fig. 7.2

Abrasion can be a serious problem in the splash and erosion zones where floating debris and shifting sea bed sediments may cause rapid loss of material from the pile surface. Test results provided by the PCA (1968) have indicated that the resistance of concrete to abrasion is directly related to the compressive strength of the material. Concrete with low compressive strength is found to be more vulnerable to attack than concrete with high compressive strength. Fig. 7.3 shows results of abrasion tests on concrete specimens with different compressive strength.

As the compressive strength of concrete is dependent upon the water-cement ratio and the length of moist curing period, it is obvious that a low water-cement ratio and long curing period will develop higher resistance to abrasion.

Sulphate attack is also a major cause of concrete deterioration. Concrete piles can be attacked very rapidly by sulphates occurring naturally in soils and in sea water.

The amount of sulphates in the soils can be measured by the sulphate content of the ground water, if the sulphates are soluble; otherwise, chemical analyses of soil samples can be performed. When determining sulphate concentrations, seasonal and topographic effects must be taken into consideration. Samples should be retrieved after a long period of dry weather to obtain the best representative samples. The concentrations

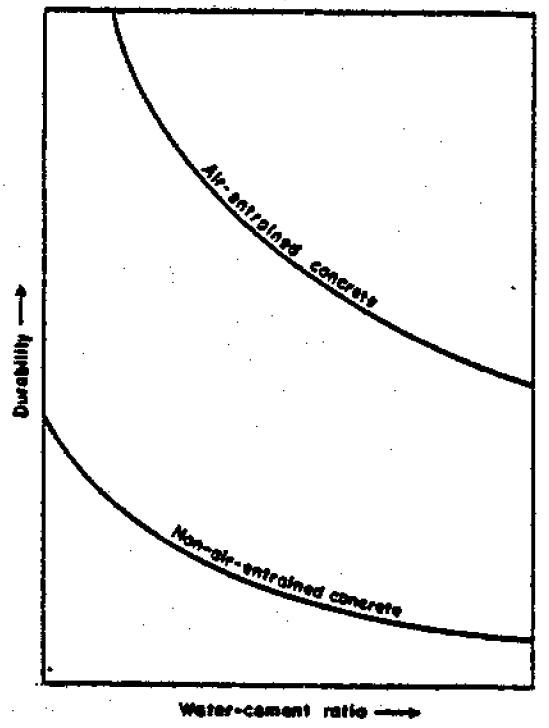

Fig. 7.2 Relationship between Freeze-thaw Resistance and Water-cement Ratio for Air-entrained and Non-air-entrained Concretes (PCA, 1968)

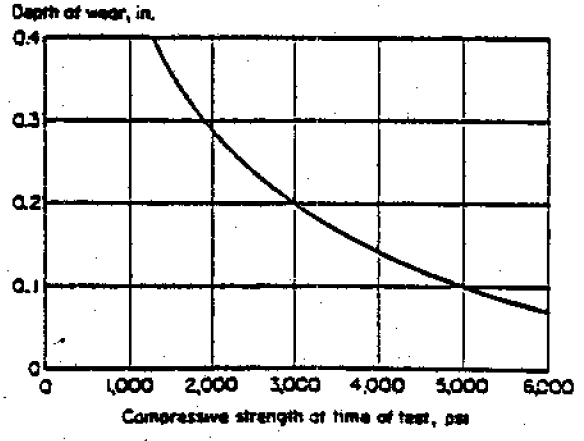

(See Preface for SI Conversions)

Fig. 7.3 Effect of Compressive Strength on the Abrasion Resistance of Concrete (PCA, 1968)

of sulphates and the relative degree of attack are described by Hubbell and Kulhawy (1979).

Although sea water typically has a sulphate content of about 230 parts per 100,000, the presence of sodium chloride has an inhibiting or retarding effect on its reaction with ordinary Portland cement (Tomlinson, 1977). Therefore, sulphate attack in the submerged zone in sea water may not be a concern for design.

The problem of sulphate attack can be overcome by a proper choice of cement type. In the United States, information on properties of various types of cement can be obtained from the Portland Cement Association. In cases where sulphate attack is moderate, ASTM Type II cement is recommended. When sulphate action gets severe, ASTM Type V cement should be used. It should be noted that these two types of cement gain strength more slowly than Type I or normal cement and thus a longer period of curing should be anticipated.

To some extent, all concretes are permeable to water. This allows water to penetrate through the surface and leads to subsequent corrosion of the steel reinforcement. In addition, entry of soluble sulphates into the pore space of the concrete piles can cause disintegration of the member.

Permeability of concrete depends upon numerous factors including water-cement ratio, air-entrainment, aggregate grading and period of curing. PCA (1968) indicated that the watertightness of the material depends principally on the water-cement ratio used and the length of the moist curing period.

Their test results on non-air-entrained mortar disc specimens subjected to 20 psi (138 kN/m^2) water pressure are shown in Fig. 7.4. It can be seen that watertightness increases with increasing moist curing period and decreasing water-cement ratio. PCA (1968) further noted that the permeability will decrease with addition of air-entrainment and that honeycombs or cracks should be avoided to ensure a low porosity.

7.3 Steel

The term "steel" usually refers to carbon steel with the following maximum content of elements other than iron: carbon, 2.0%; manganese, 1.65%; copper, 0.6%; and silicon, 0.6% (Hornbostel, 1978).

The properties of steel are determined not only by the chemical composition, but they are influenced to a great extent by the type of heat treatment and mechanical working during manufacturing.

Overall, steel is a strong material that can carry heavy loads. Unlike concrete, it is strong in both tension and compression. Steel piles can be expensive; however, they have great versatility. They can be driven to great depth and through hard materials. Furthermore, they are found to be particularly useful in cases (e.g., in sensitive clays) where small displacement piles must be used.

Frye (1970) examined the corrosion profile of steel pilings in the offshore envrironment. Fig. 7.5 shows the relative loss in metal thickness of steel piling with five years expo-

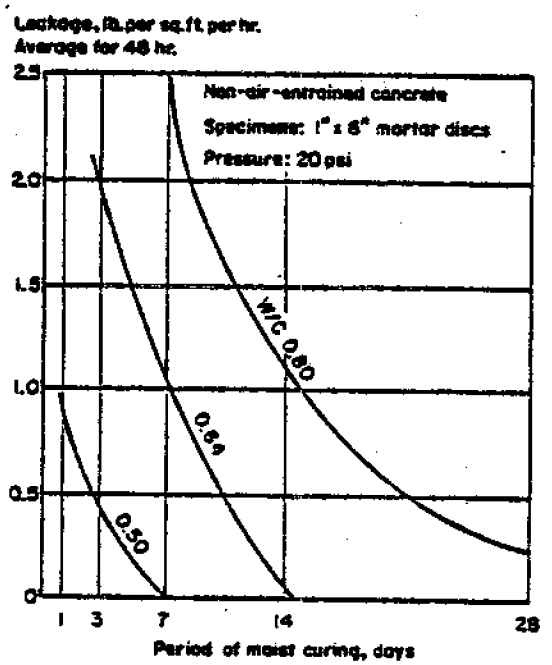

(See Preface for SI Conversions)

Fig. 7.4 Effect of Water-cement Ratio and Curing on Watertightness (PCA, 1968)

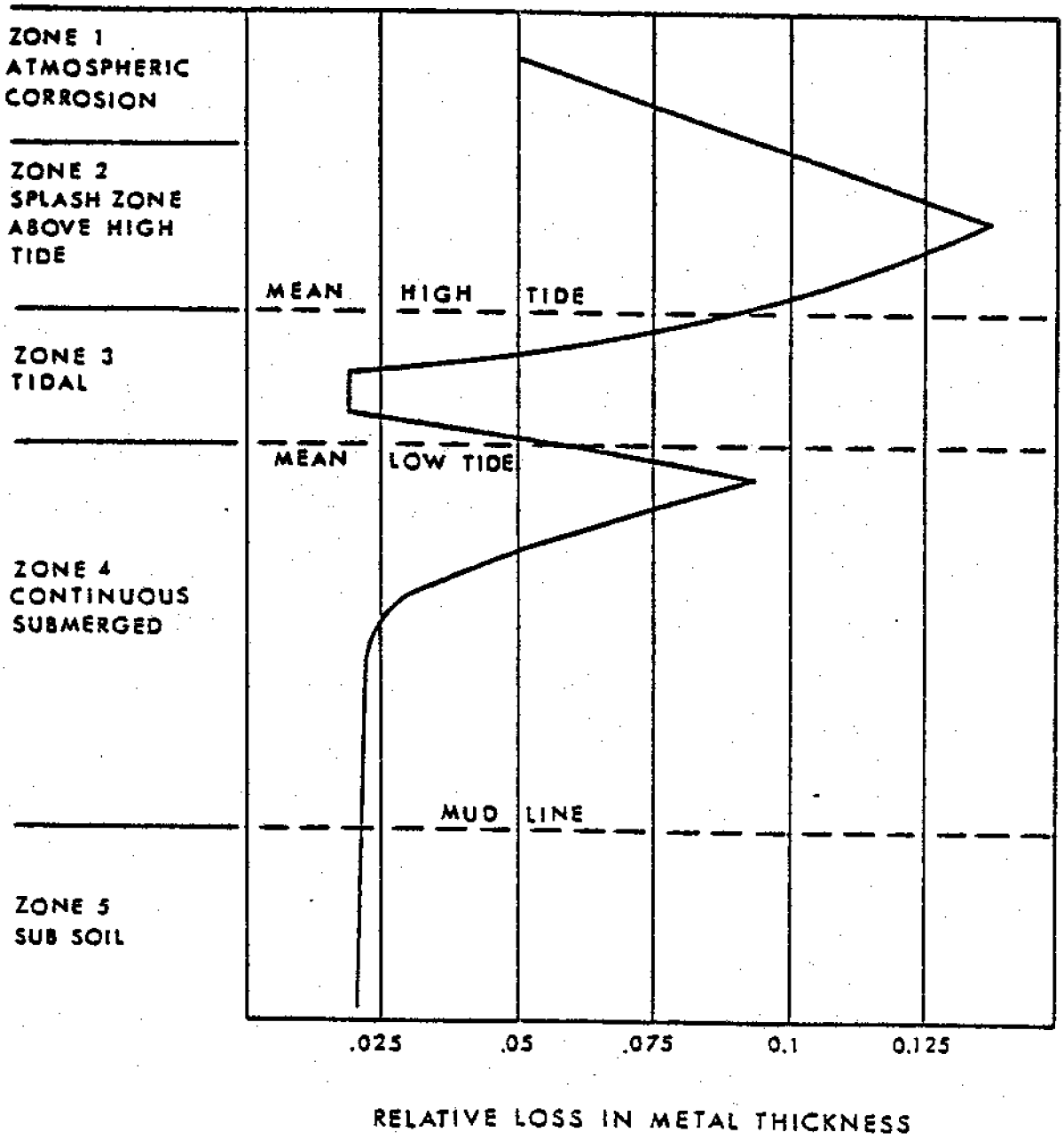

Fig. 7.5 Typical Corrosion Profile of Steel Piling with Five Years Exposure in Sea Water (Frye, 1970)

sure in sea water on the North Carolina Coast. This is a typical corrosion profile for steel piles free-standing in water subjected to attack by aggressive components in various corrosive zones.

In the uppermost zone where the steel surface is normally dry, the material is subjected to atmospheric corrosion and the deterioration rate is not very significant.

In the splash zone, the pile is under severe attack and the loss in metal thickness is larger than anywhere else in the pile. Similar to concrete piles, this is a critical portion which usually requires special attention. Added thickness or other preventive measures are almost necessary in this region.

The corrosion rates in the tidal and submerged zones are minimal except in the upper area of the submerged region. Frye (1970) attributed this to the difference in oxygen concentrations between the air in zone 3 and the water in zone 4, resulting in electrochemical corrosion.

An erosion zone along the mud-line was not identified. This is probably because of the high strength of steel, which provides strong resistance against abrasive action of the shifting sea bed sediments.

In the embedded zone, Frye (1970) discovered that no serious deterioration had occurred. This may not be true in general. According to Chellis (1961), the rate of corrosion of steel piles embedded in soils may be significant, depending on the texture and composition of the soils, depth of embedment and moisture content. He further pointed out that bacterial

activities in the soils may cause corrosion of steel embedded in the ground.

A corrosion study on steel piles conducted by Romanoff (1962) indicated that no appreciable corrosion occurs in steel piles driven into undisturbed natural soils, regardless of the soil properties. The study was conducted at a site with soil types that ranged from well-drained sands to impervious clays, with soil resistivities that ranged from 300 ohm-cm to 50200 ohm-cm and soil pH which varied between 2.3 to 8.6. Romanoff (1962) attributed the non-aggressive behavior to the lack of oxygen in undisturbed soils and concluded that properties of soil will not affect the extent of corrosion of steel piles driven in undisturbed soils.

It is well known that corrosion of metals is largely electrochemical in nature and that the presence of oxygen in some forms is necessary for this process to take place. Chellis (1961) described electrochemical corrosion as "...the result of a difference in potential between two points in a conductor exposed to an electrolyte, with material moving from the anode, which in this case is the surface corroding, to the cathode, or noncorroding material. Corrosion cells are formed on piles between areas of different aeration. The steel surface plentifully supplied with oxygen is cathodic with respect to the portions of the pile less accessible to oxygen."

Frye (1970) noted the following three requirements for corrosion of metals to take place:

1) there must be an anode and a cathode.

2) there must be an electrical potential between the anode and cathode.

3) there must be an electrolyte that is capable of conducting electric current by ionic flow.

Thus, electrochemical corrosion can essentially occur under all types of environmental conditions (air, water or soil) as long as there is a nonuniform distribution of oxygen content and an appropriate electrolyte.

The damage may be either general or localized depending upon the relative size of the anodic and cathodic areas for a given difference in potential between the two areas. If the anodic area is relatively large compared to the cathodic area, the corrosion current will be small and the little damages to the anodic area can be distributed over a large area, thus resulting in uniform corrosion. On the other hand, if the anodic area is relatively small compared with the cathodic area, corrosion will be localized and severe damages may result in the form of pitting (Romanoff, 1962).

Cathodic protaction is often used as a remedy to curtail or eliminate electrochemical corrosion. This countermeasure operates on the basic principles of electrochemical corrosion described earlier. Two methods of cathodic protection are generally used:

1) impressed-current

2) galvanic

These two methods have been discussed by Hubbell and Kulhawy (1979).

As pointed out by Frye (1970), cathodic protection is more effective for corrosion in the submerged zone. There is little reduction in corrosion in the region above mean high water level, as shown in Fig. 7.6. Also, this method may not be applicable in fresh or pure water, which is a very weak electrolyte.

Paints and coatings are also used as an alternative or supplement to cathodic protection. A stable coating can serve as a physical as well as a chemical barrier against corrosive attack. Protection can be applied throughout the length of the member or just in the portion of greatest corrosion.

Some of the more common types of coatings that are used by the marine industry are summarized in Table 7.1. The choice of these coatings depends upon factors such as (Petersen and Soltz, 1975):

1) surface preparation possible
2) environment
3) material cost
4) weather condition at time of application
5) surface abrasion expected during service life
6) life desired from the system
7) type of metal being coated
8) type of worker available for applying the coatings

The effectiveness of some of the coatings mentioned above has been described by Hubbell and Kulhawy (1979). It should be realized that paintings or other types of coatings applied prior to driving may not be totally reliable because portions of coatings removed by abrasion or handling may serve as areas of at-

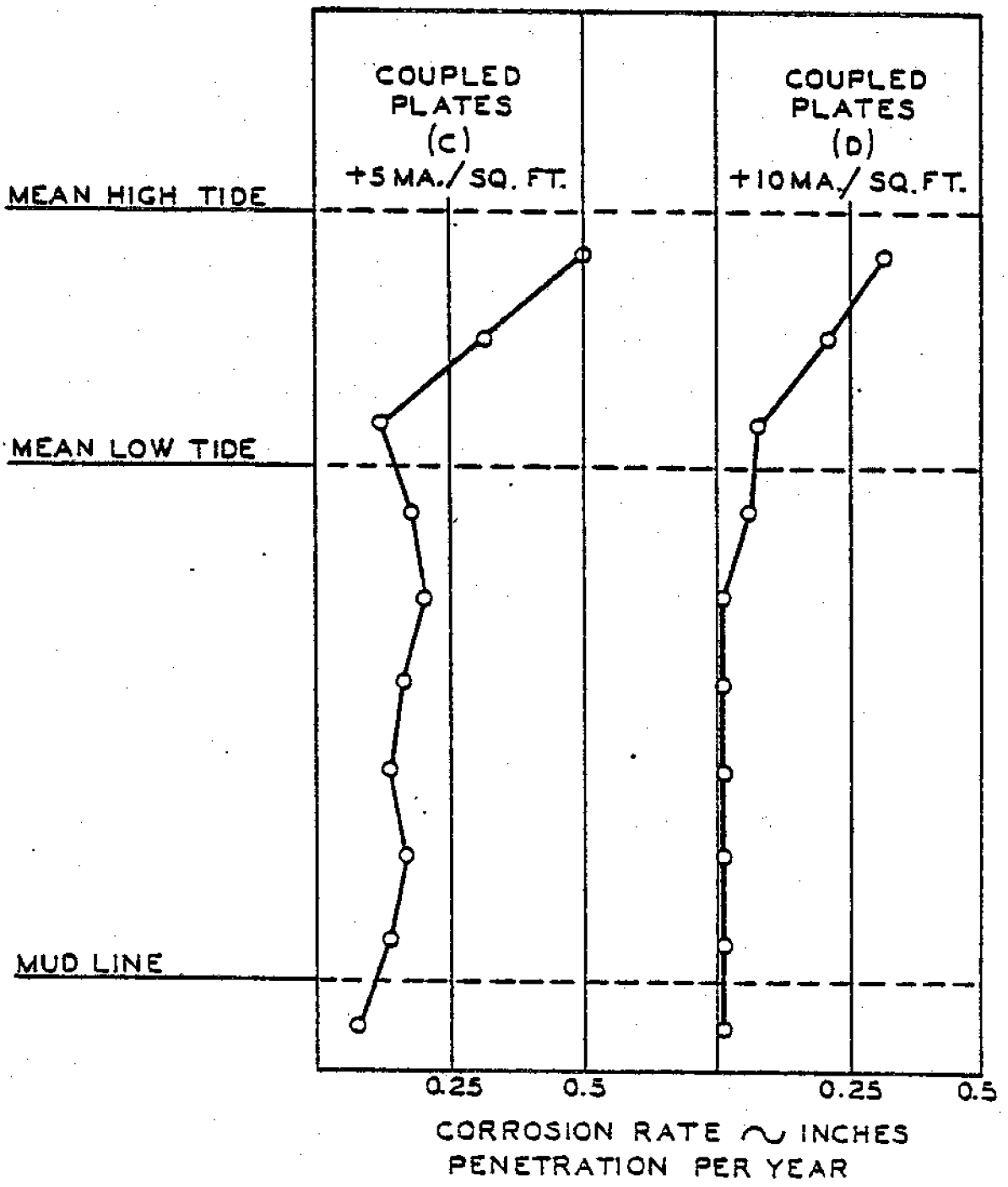

Fig. 7.6 Effect of Cathodic Protection on Steel Piling (Frye, 1970)

1. Oil paints—based on natural oils from plants and fish:
   a. Easy to apply.
   b. Relatively inexpensive.
   c. May require longer drying times.
   d. Permeable and recommended only for mild atmosphere.
2. Alkyd paints—resins obtained from the reaction of glycerin and phthalic anhydride:
   a. Have to be baked to dry (unless combined with oil paints).
   b. More corrosion-resistant than oil paints, but still not suitable for chemical service.
3. Emulsion or water-base paints—resin in a water vehicle:
   a. Little odor.
   b. Easy to apply.
   c. Easy to clean up.
4. Urethane paints—reaction of isocyanates with polyols:
   a. Good toughness and abrasion resistance.
   b. Corrosion resistance may approach that of vinyls and epoxies.
5. Chlorinated rubber—natural rubber chlorinated:
   a. Does not wet well.
   b. Dries quickly.
   c. Resistant to water and many inorganics.
   d. Temperature maximum—150°F.
   e. May be painted for better protection.
6. Vinyl paints—polymerization of compounds containing vinyl groups:
   a. More corrosion-resistant than oil or alkyd-based paints.
   b. Resistant to a variety of aqueous acids and alkaline media.
   c. Temperature maximum—150°F.
   d. Adherence and wetting can be poor.
   e. Adherence for the first 24 h or so is suspect.
7. Epoxy paints—reaction of polyphenols with epichlorohydrin:
   a. Amine-hardened epoxy coatings (hardness and resin—most resistant to chemicals).
   b. Polyamide-hardened epoxy is less resistant to acids but is tougher and more moistureproof.
   c. Epoxy-ester less corrosion-resistant but easier to apply.
   d. Coal tar-epoxy has good resistance to water, soil, and inorganic acids.
8. Silicone paints—high-temperature service (with modification up to 1200°F):
   a. Not very good against chemicals.
   b. Are water-repellent.
9. Coal tars—applied hot; used especially in underground applications
10. Zinc paint—metallic zinc dust in an organic or inorganic vehicle:
    a. Used in galvanic protection by the zinc to prevent pitting at holes in the coating.
    b. Effective in neutral and slightly alkaline solutions.
    c. Organic zinc paint requires less surface preparation and is easier to topcoat than inorganic counterpart is.
    d. Inorganic is more heat-resistant, however.

Table 7.1 Paints and Coatings (Petersen and Soltz, 1975)

tack by various corrosive agents.

In the splash zone where the deterioration of steel is most severe, concrete encasements are commonly used. To be effective, the concrete has to be durable and watertight. The jacket should be of adequate thickness and length. Chellis (1961) suggested such encasements to be at least 2 feet (0.61 m) below mean low water and 3 feet (0.91 m) above mean high water levels. Besides the splash zone, encasements can also be used through water for protection. In this case, Chellis (1961) recommended a penetration of encasement of at least 4 feet (1.22 m) into the soil. With regard to the thickness of the encasements, Watkins (1969) suggested a minimum of 4 inches (102 mm) to be used under normal corrosive conditions.

7.4 Wood

Wood is one of the oldest construction materials. It is a biological compound of trees and is composed of approximately 49% carbon, 44% oxygen, 6% hydrogen and 1% ash (Brady and Clauser, 1977).

Compared with steel and concrete, wood has a higher strength to weight ratio. In addition, its high energy-absorbing capabilities has made it an excellent material for use in fendering devices.

Timber piles are cut from tree trunks. They are relatively cheap and easy to handle. Moreover, they are readily available in most areas and can be cut to any desired length with little difficulties. However, in projects where long piles are required, it may be difficult to obtain such piles and splicing

is a necessity.

Because of different growth conditions, wood exhibits a wide range of properties. The characteristics and applications of various species of wood can be found in Chellis (1961) or U.S. Forest Product Laboratory (1974).

Decay, insects and marine borers are the primary causes of wood deterioration. These have been adequately discussed by Hubbell and Kulhawy (1979) and, therefore, only a brief description will be provided herein. The reader should refer to Hubbell and Kulhawy's work for more detailed information on these aspects as well as their appropriate treatment procedures.

Decay is caused by fungi, which are microscopic plants that obtain their food supply from organic materials. These microorganisms require food, moisture, oxygen and a favorable temperature to survive. Deprival of any of these essential elements will deter or eliminate the decay of wood.

The food supply for the decay-producing fungi is the cellulose and lignin of the wood. Therefore, it is possible to poison the material with some form of preservatives to curtail the growth of fungi.

Wood that is exposed to the atmosphere is normally too dry to support fungus growth and wood that is permanently submerged under water is too high in moisture content to promote decay. The moisture content for fungus growth should be greater than 20%, but less than the fiber saturation point (Hubbell and Kulhawy, 1979).

Fungus growth requires sufficient oxygen from the air. For

piles embedded in clays, this will be limited to within a few feet below the ground surface. However, for piles embedded in sands where air circulation is likely to be better, it is possible that decay can occur to a great depth.

Temperature will also affect fungus growth. Decay will be slow when the temperature is below 50°F (10°C) or above 90°F (32°C) and it will essentially stop when temperature drops below 32°F (0°C) or rises above 100°F (38°C) (U.S. Forest Product Laboratory, 1974).

In general, fungus damage is caused by the following three major factors (U.S. Forest Product Laboratory, 1974):

1) lack of appropriate protective methods when storing logs or bolts.
2) improper seasoning or handling of the wood after storage.
3) failure to take simple precautions in using the final product.

Insects are another major form of attack for timber piles. Among them, termites cause the most destructive damage to wood. Termites can be classified into two types according to their habitations:

1) subterranean termites
2) nonsubterranean termites

The distribution of these two types of termites in the United States is shown in Fig. 7.7. The subterranean termites are ground-inhabiting and build their tunnels through earth to reach their food supply. They cause the most severe insect damage to wood in the United States, particularly in the south-

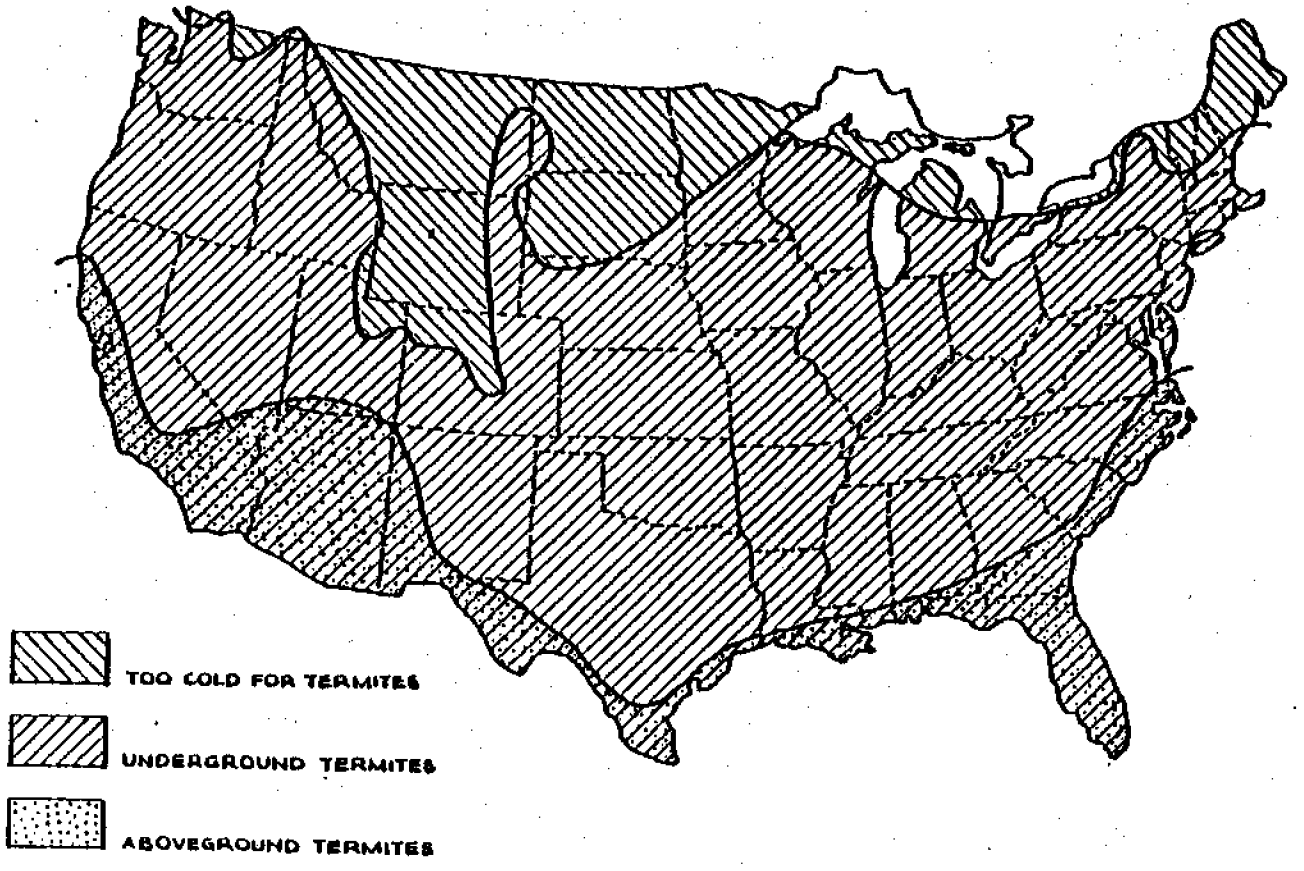

Fig. 7.7 Distribution of Termites in the United States (Hornbostel, 1978)

ern part. The nonsubterranean termites enter the wood from the ground and are wood-inhabiting. They are found only in the southern part of the United States.

Marine borers have also caused severe damage to waterfront structures. They are inhabitants of salt or brackish waters and can be found throughout the world. They can attack susceptible wood very rapidly. Major species of marine borers and appropriate protection methods are discussed by Hubbell and Kulhawy (1979) and will not be repeated here.

7.5 Summary

Three commonly used materials (concrete, steel and wood) for piles have been discussed. Each of these materials has its advantages and disadvantages for a given project. The factors that determine the final choice of material type have been outlined at the beginning of the chapter. They should be examined carefully, and the relative importance between various factors should be noted.

Piles used in the coastal environment are often subject to nonuniform deterioration. In the general case, five environmental zones can be identified. These are described in the chapter. Under most circumstances, the splash zone is of major concern since high rates of deterioration usually occur in this region.

Concrete is a durable material and can withstand a harsh environment. However, the formation of cracks is very common because of the weak tensile capacity of the material. The durability of concrete with respect to the freeze-thaw process is

directly related to the water-cement ratio and the use of air-entrainment. The abrasive resistance of concrete is proportional to the compressive strength of the material. Sulphate attack can be a serious problem and can be overcome by a proper choice of cement type. High permeability concrete is undesirable and proper precautions should be used.

Steel is a material that is strong in both tension and compression. Steel piles can be expensive; however, they are adaptable to many types of conditions and requirements. It was noted that corrosion of steel piles in undisturbed natural soils is negligible and rarely needs consideration. Corrosion of steel is an electrochemical process, which can take place in all types of environmental conditions. Cathodic protection and/or protective coatings are often used as remedies to retard the corrosion of the material.

Wood is a biological compound of trees. It has a high strength to weight ratio and is proven to be an excellent material for fender piles because of its high energy-absorbing capabilities. Deterioration of wood is principally caused by decay, insects and marine borers. These various forms of attack can be avoided with appropriate preventive measures and treatment procedures.

CHAPTER 8

INSTALLATION OF PILES

The operation of driving piles into the ground is a complicated construction process that requires skills and experience. Supervision by an experienced person is necessary for all pile-driving jobs. The appropriate degree of supervision depends upon the nature of the project, the variability of the ground conditions and any anticipated installation problems. During the driving operation, any peculiar conditions should be noted and the driving history should be properly recorded for future references.

The method of installation of a pile can influence its behavior under loads significantly. It may also determine the degree of disturbance on the soil properties and adjacent structures. Thus, the installation operations should be carefully examined in the design phase. The persons who are responsible for designing the pile foundations should have a sound understanding of the construction procedures and limitations in the field.

Piles may be installed by driving with hammers through impact or vibration, or by jetting, augering or other methods that are capable of driving the piles down to the required penetration without damaging the piles or nearby structures.

In this chapter, some of these installation methods will be described. The effect of time on pile capacity because of installation loads will also be discussed.

8.1 Pile Handling

Concrete piles are probably the most difficult to handle among the three materials considered. The low tensile capacity of concrete often leads to the formation of cracks because of bending moment induced by the dead weight of the member during lifting. This is highly undesirable, especially for piles that are used in a corrosive coastal environment. Therefore, in handling these piles, great care must be exercised during pickup. Long piles should be picked up at several points to reduce the unsupported lengths. The maximum bending moment induced for various points of pickup is shown in Fig. 8.1. The bending stresses developed from lifting should be accounted for in the design phase and the corresponding pickup points should be clearly marked.

Although the handling of steel and timber piles does not require special attention, the members should be lifted as carefully as possible, especially for piles that have been treated surficially to deter material deterioration. Removal of protective coatings as a result of negligence in handling can very possibly lead to future problems of corrosion.

8.2 Pile-Driving Rigs

The driving rig is one of the most important pieces of equipment for pile installation, and a wide variety of these rigs is available. The range in dimensions and capabilities of the equipment is too wide to be fully described in this section. Detailed information can be obtained from manufacturer's literature.

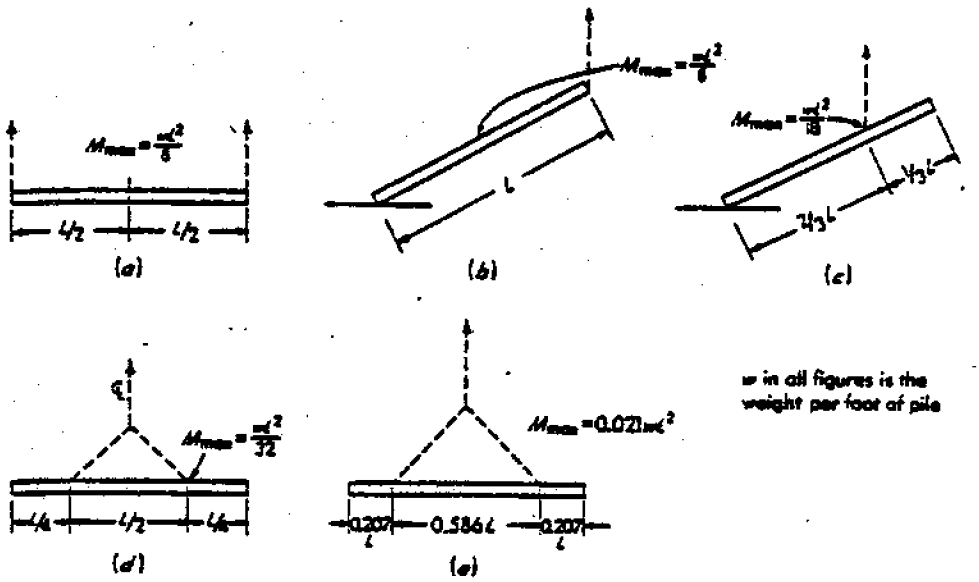

Fig. 8.1 Location of Pickup Points for Precast Piles, with the Indicated Resulting Bending Moments (Bowles, 1977)

A typical driving rig is shown in Fig. 8.2. The most essential component of a driving rig is the leads, which are connected to the boom and serve as tracks for the hammer during the driving operation. They are made of stiff members of solid, channel, box or tubular section and stiffened by trussing (Tomlinson, 1977). The leads are attached to the crane by the spreader, which is adjustable in length to permit driving of batter piles.

The pile is located under the hammer within the leads. Lateral support is provided by sliding guides placed in the leads at the mid-point or quarter-points of the pile (Sowers, 1979). When it is necessary to drive piles below the base of the crane, extension leads can be bolted to the bottom of the main lead (Tomlinson, 1977).

Prefabricated leads commonly in use can be separated into two categories (Hunt, 1979):

1) fixed leads which are rigidly attached to the tip of the boom.
2) hanging (or swinging) leads which are not attached to the boom but are suspended by a cable from the boom tip.

Fixed leads can align a pile more rapidly and are preferred in cases where a large number of vertical piles are to be driven. On the other hand, hanging leads are found to be more efficient for batter piles and hard-to-reach areas (Hunt, 1979).

8.3 Driving Hammers

Piles are commonly driven into the ground by hammers. These

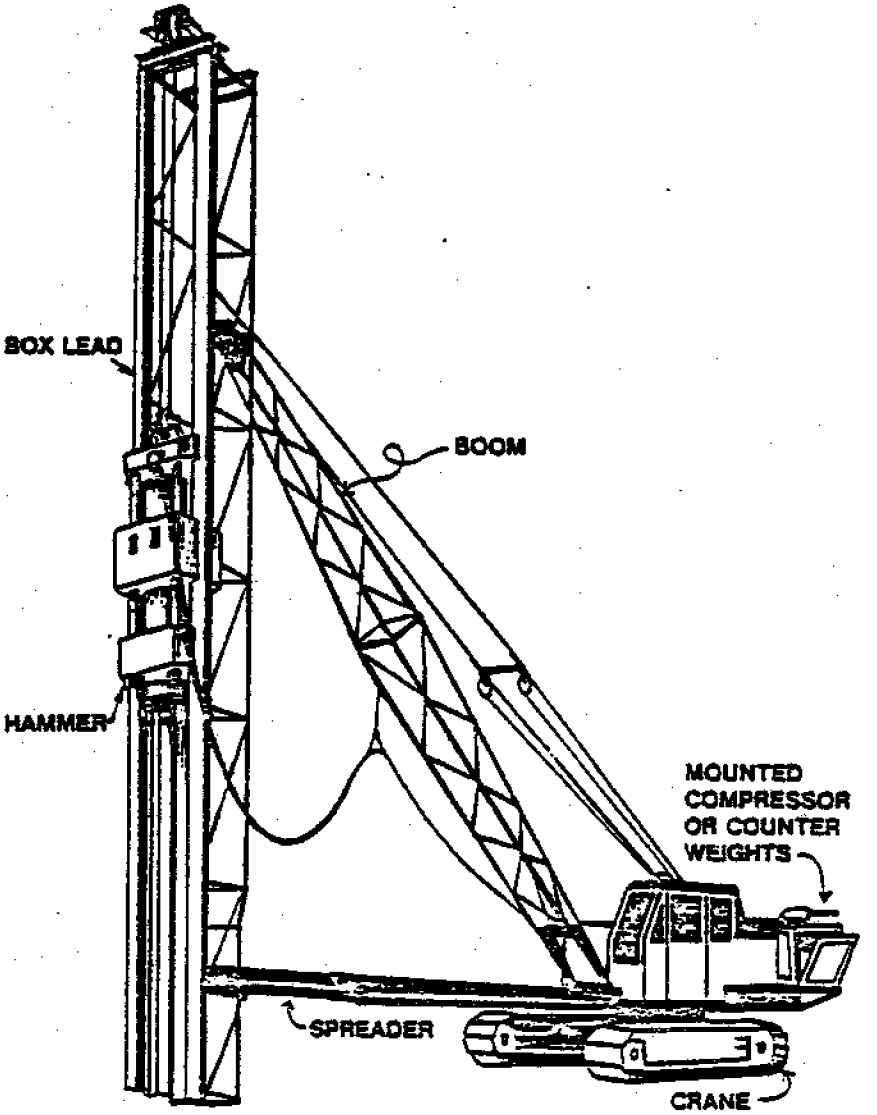

Fig. 8.2 Typical Driving Rig (DFI, 1979)

hammers are heavy rams that derive their energy either by free fall or through some form of external excitation. The energy is usually transmitted through a pile helmet (also called pile cap) and a pile cushion resting on top of the pile, as illustrated in Fig. 8.3.

Many types of hammers are used in practice. The final determination of the hammer to be used in a pile-driving job depends upon the size and type of piles, the number of piles, the characteristics of the soil, the location of the project, the topography of the site, the type of rig available, etc. (Peurifoy, 1979).

The merits and limitations of some of the major types of hammers are described below. The materials are essentially extracted from Gilbert (1970) and Peurifoy (1979), unless otherwise stated.

8.3.1 Drop Hammer

A drop hammer operates on the simple mechanical principles in which the ram is raised by a rope, released and then allowed to fall freely on to the pile (Fig. 8.4a). The weight of a typical drop hammer ranges from 500 to 3000 lbs (2225 to 13350 N), while the height of fall normally varies between 5 to 20 ft (1.52 to 6.10 m).

Drop hammers are cheap, simple and easy to operate. However, it has an extremely slow blow count of 1 to 4 per minute, and therefore is uneconomical to use except at remote sites where the delivery of heavy driving equipment is difficult. One potential problem in using a drop hammer is overstressing and

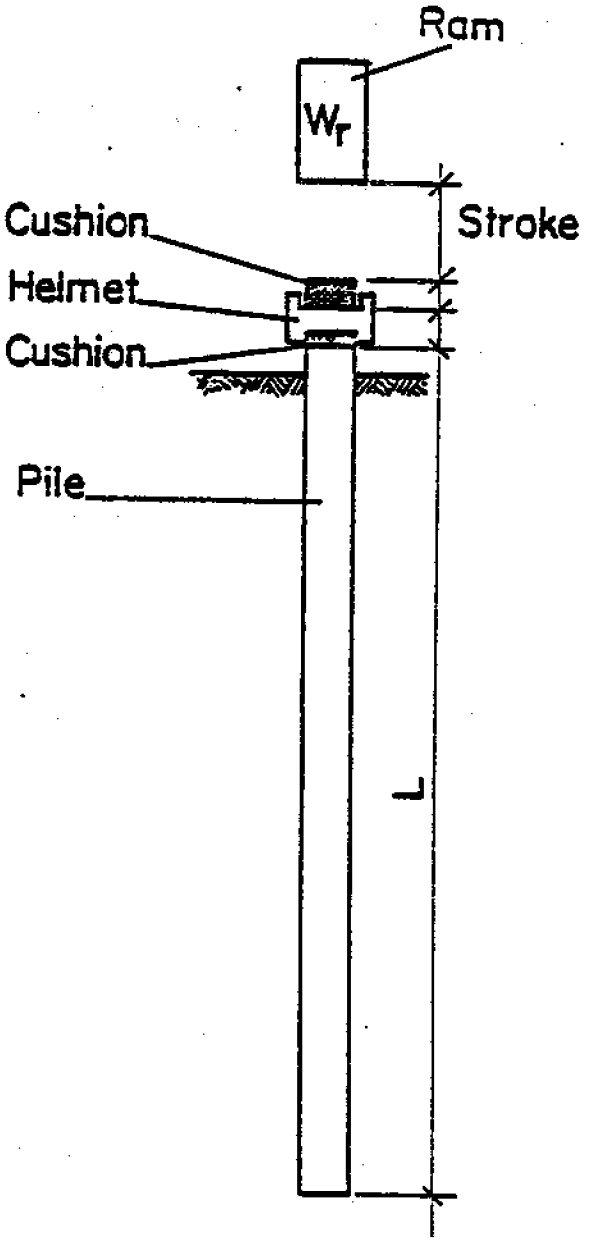

Fig. 8.3 Pile Driving Operation (Vesić, 1977)

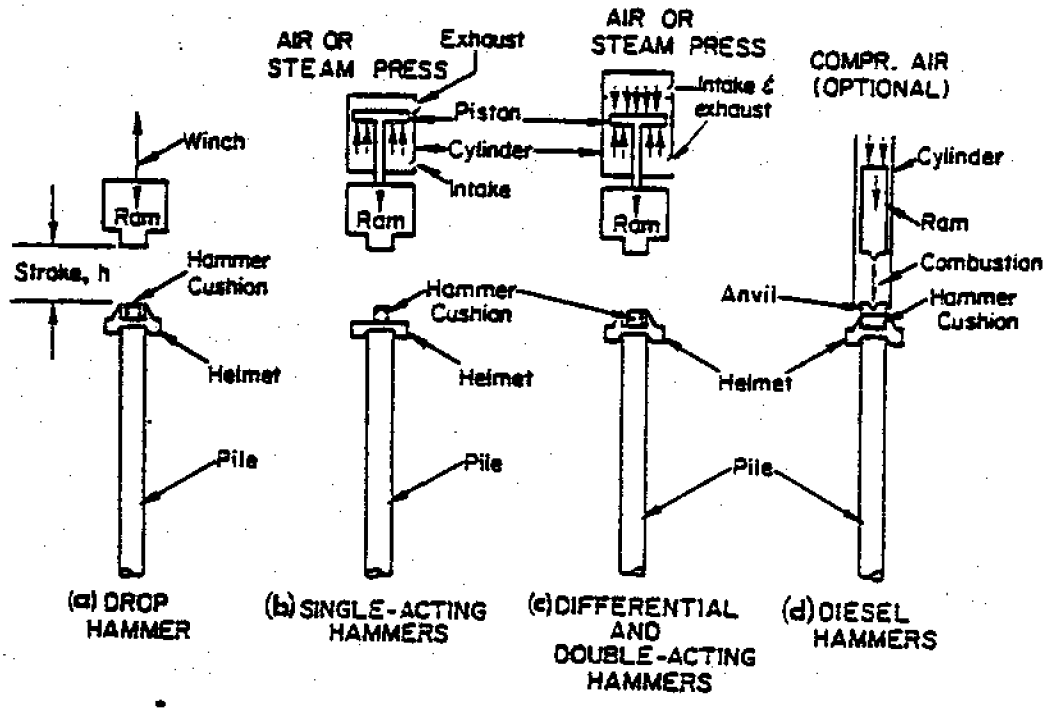

Fig. 8.4 Driving Hammers (Vesić, 1977)

damaging the piles by lifting the hammer too high.

8.3.2 Single-Acting Hammer

A single-acting hammer is the simplest powered hammer. The ram is lifted by steam or compressed air and is allowed to drop freely by the pull of gravity (Fig. 8.4b). The energy is derived from a limited fall (2 to 3 feet or 600 to 900 mm (Sowers, 1979)), and thus the impact velocity is low. This type of hammer may strike 50 to 70 blows per minute.

As compared with a drop hammer, the single-acting hammer can deliver a greater number of blows per minute and requires a shorter driving time. Moreover, with the higher frequency of impact, the shaft resistance is reduced, permitting easier penetration in subsequent driving. On the other hand, this type of hammer is more complicated and requires higher capital investment and maintenance costs.

This type of hammer can operate in all soils conditions, but is most effective in driving piles through stiff clays.

8.3.3 Double-Acting Hammer

Double-acting hammers operate on the same principle as single-acting hammers, except that during the downward stroke, steam or compressed air is applied at the top to accelerate the ram in its downward stroke (Fig. 8.4c). It delivers from 90 to 150 blows per minute.

As compared with single-acting hammers, double-acting hammers deliver a greater number of blows per minute and therefore require shorter driving time. One of the main disadvantages of this type of hammer is the vibration that may result from the

relatively light weight and high velocity of the ram. Therefore, the use of double-acting hammers should be avoided in driving heavy piles through soils that have high frictional resistance, especially if there are many adjacent structures around the site.

Overall, the hammer performs best in sandy soils, but also performs well in both sands and clays.

8.3.4 Diesel Hammer

A diesel hammer is a self-contained unit that does not require the use of an external source of energy. The complete unit consists of a cylinder, ram, anvil block and simple fuel injection system (Fig. 8.4d). It is basically a one cylinder, two-cycle diesel engine in which the piston acts as the ram of the hammer. The range of blows is 48 to 105 per minute, with ram weights from 1000 to 3855 lbs (4450 to 17155 N).

Since a diesel hammer requires no external source of energy, it is highly mobile and proves to be desirable to operate at remote sites. Furthermore, the hammer is light in weight and has low fuel consumption. It can function in cold weather where it may be difficult to use steam. The major drawback of this type of hammer is that it is not suitable for use in soft ground because sufficient driving resistance is necessary to activate the ram. In addition it is difficult to determine the impact energy per hammer blow because it varies with the pile resistance.

8.4 Vibratory Pile Drivers

Vibratory drivers are operated by a pair of counter-rotating eccentric weights (Fig. 8.5). The horizontal impulses from

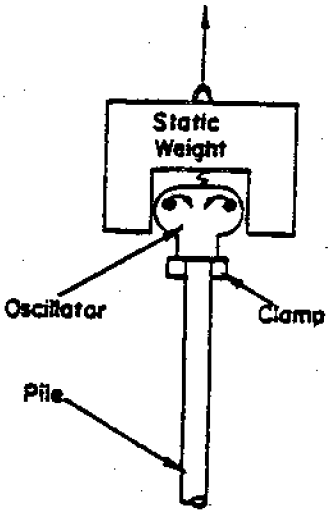

Fig. 8.5 Vibratory Pile Drivers (Vesič, 1977)

these weights will cancel one another, but the vertical impulses will reinforce each other to produce a pulsating load on the pile at a rate of 16 to 24 cycles per second (Gilbert, 1970).

The driving of piles into the ground is accomplished by vibrations that loosen the soil in the vicinity of the pile to behave as a viscous fluid. These drivers are most effective for piles driven into saturated sands. Fair results are obtained for silty and clayey soils. Driving in stiff clays or soils with boulders with vibratory drivers is not possible at present (Bowles, 1977).

There are at least three major advantages of vibratory drivers (Bowles, 1977):

1) less vibrations as compared with impact hammers
2) lower noise level
3) greater speed of penetration

8.5 Jetting

Jetting is often used to facilitate driving operations through hard strata. This is performed by applying a high pressure stream of water (air has also been used) to cause displacement and agitation of the soil particles. The process may be applied before driving starts or it can be employed simultaneously as driving proceeds. In the latter case, two jets should be attached to the pile point on opposite sides to avoid drifting of the pile in one direction (Fig. 8.6).

Jet pipes commonly used vary in size from 2 to 4 inches (51 to 102 mm) in diameter, depending upon the volume of discharge required. The nozzle diameter ranges from $\frac{1}{2}$ to $1\frac{1}{2}$ inch

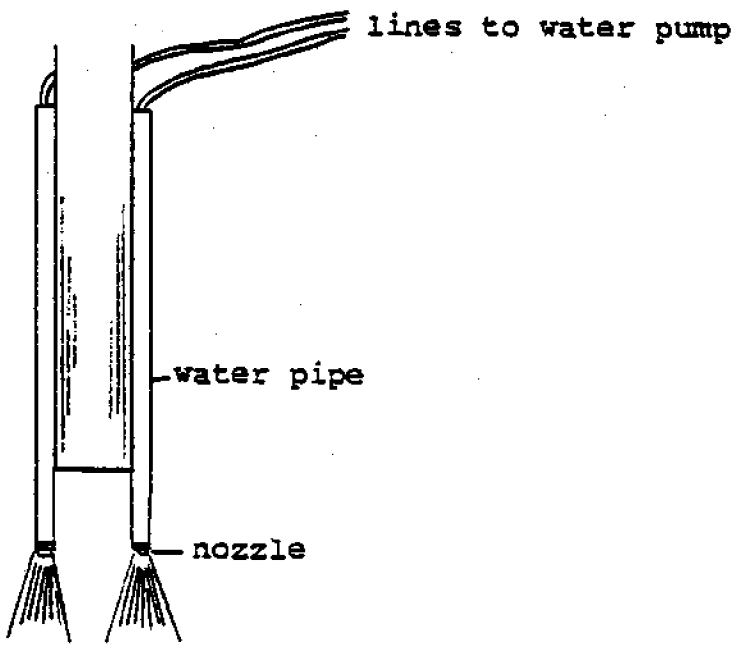

Fig. 8.6 Jetting of Piles by Water Pipes (after AWPI, 1966)

(13 to 38 mm). Water pressure is normally maintained between 100 to 300 psi (690 to 2070 kN/m^2) (Peurifoy, 1979).

The method is usually applied to sands; however, good results have also been reported in silty sands and in fine gravels (AWPI, 1966).

Care must be exercised to avoid disturbance by the water jet to previously driven piles. The zone of influence usually extends to $2\frac{1}{2}$ or 3 feet (0.76 to 0.91 m) away from the pile, which is smaller than the normal spacings commonly used for pile groups (AWPI, 1966). It should also be noted that jetting should be avoided when the pile is driven close to its final position; otherwise, the point resistance may be reduced by the water jet action.

8.6 Preaugering

When a stiff stratum is encountered at an upper level, preaugering is sometimes used to drill through it so the piles can be driven much easier down to a bearing stratum. For many projects, this is cheaper and faster than trying to drive the piles through the upper firm material.

8.7 Effect of Time on Pile Capacity

Most of the studies on time effects deal only with piles driven in clays. For sands where drained conditions normally govern, the effect of time on pile capacity is negligible and rarely needs consideration.

It is well known that driving of piles into normally consolidated and lightly overconsolidated clays (contractive soils) generates excess pore water stresses in the soils. These pore

stresses will dissipate with time and the clay undergoes consolidation. During the process of consolidation, the soils adjacent to the piles will experience an increase in strength. This increase in strength with time, as caused by dissipation of positive pore water stresses, has been confirmed experimentally by Seed and Reese (1957) and is shown in Fig. 8.7. On the other hand, when piles are driven into heavily overconsolidated clays (dilative soils), negative pore water stresses will be induced. As these negative stresses dissipate with time, the clays will experience a reduction in strength and the pile capacity will decrease.

The rate of consolidation depends upon the properties of the soils and the dimensions of the piles. It has also been found that for normally consolidated or lightly overconsolidated clays, the gain in load capacity is more rapid for concrete or timber piles than for steel piles. Depending upon these variables, the maximum capacity can be reached in several weeks to several months. This phenomenon is often referred to as "set-up."

Soderberg (1962) attributed this set-up phenomenon for piles in contractive clays to radial dissipation of pore water stresses initiated by pile-driving. He indicated that the time required to attain the maximum pile capacity is proportional to the square of the diameter of the pile and inversely proportional to the horizontal coefficient of consolidation. This implies that the horizontal dimension of the pile is more significant than the properties of the soils in the determination of the

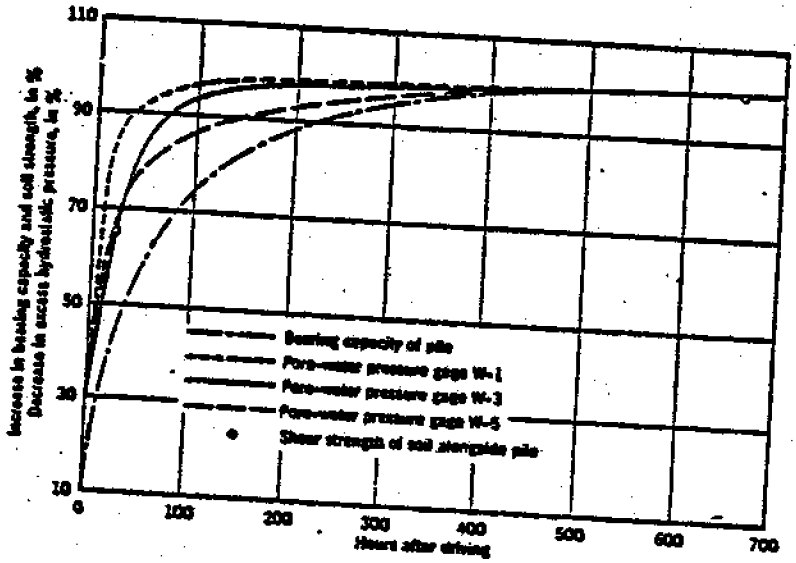

Fig. 8.7 Comparison of Rate of Change of Bearing Capacity, Excess Pore Water Stresses and Soil Shear Strength (Seed and Reese, 1957)

time effect. Soderberg's (1962) work is based on the following assumptions:

1) vertical flow is assumed to be negligible as compared with horizontal flow.
2) the horizontal coefficient of consolidation is not altered by pile-driving.

Vesić (1977) further demonstrated that piles driven in a group have a much slower gain in capacity than individual piles, as illustrated in Fig. 8.8. This point should be remembered for interpretation of time effects on group capacity.

8.8 Summary

The method of installation can have a strong influence on the behavior of piles under loads. The pile capacities may be significantly reduced because of faulty construction skills and techniques. All pile-driving operations should be supervised by an experienced person. A proper driving record should be kept and any peculiar conditions should be noted.

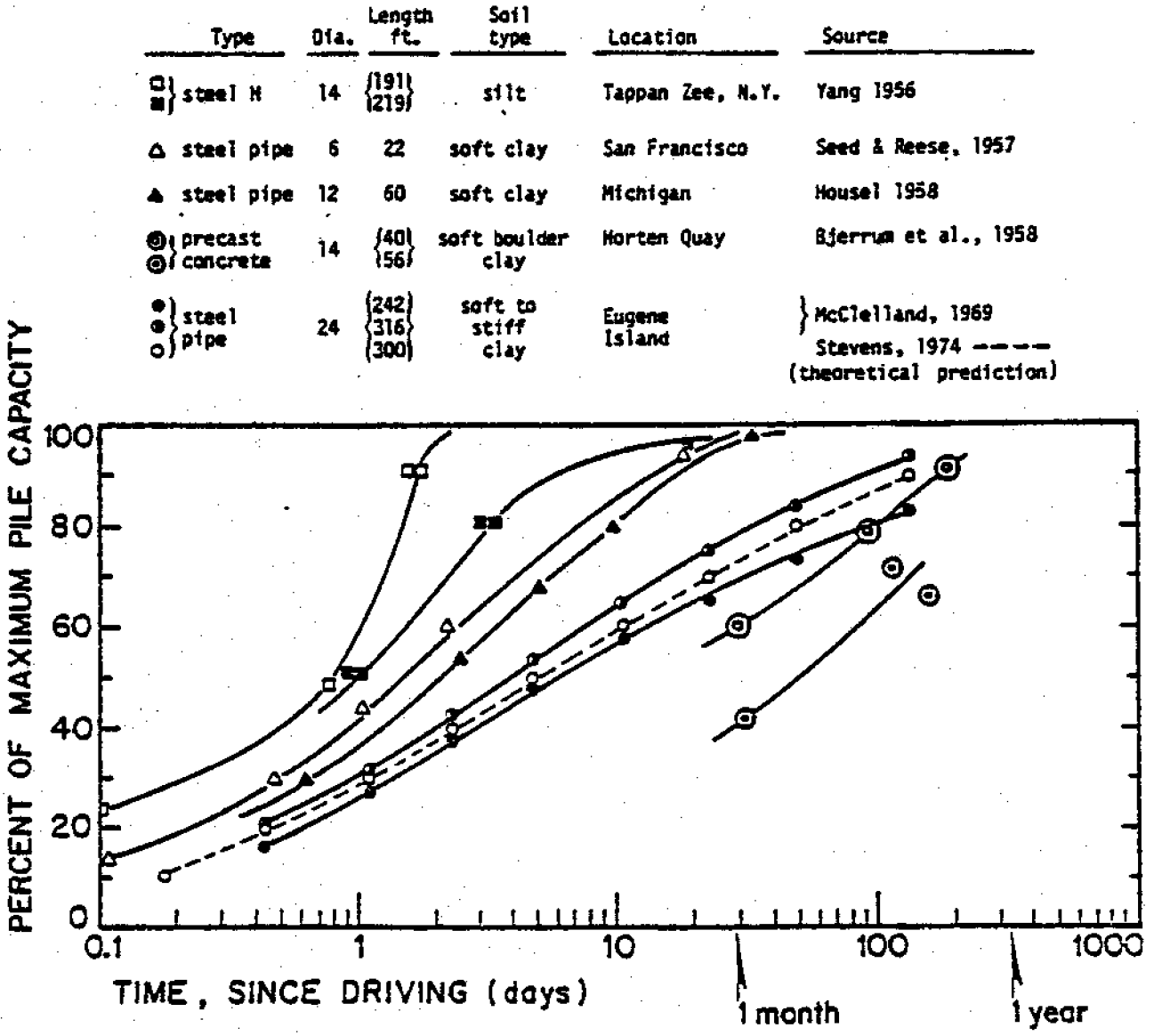

Fig. 8.8 Field Data on Increase of Bearing Capacity with Time for Friction Piles in Clay (Vesić, 1977)

CHAPTER 9

SUMMARY AND CONCLUSIONS

The design of pile foundations depends upon many parameters. It is impossible to cover all types of conditions that may be encountered in actual practice. No set of simple standard rules or procedures is available to deal with all the situations that can influence a pile foundation. Therefore, the designer must understand the design objectives, the design methodologies and the site conditions to develop a proper design.

The determination of the magnitude of loads, the design methodologies for various forms of loadings, material evaluation and the construction procedures have all been described in various chapters throughout this report. Although these aspects are presented in separate sections, they are not to be treated separately; rather, the different factors should be examined together and the interaction among them should be identified.

Five forms of loadings (waves, currents, ice, earthquakes and ship impact) have been discussed in Chapter 2. They represent the most common loading conditions for piles used in the coastal regime. The evaluation of wave forces is largely based on Morison's equation, which assumes the total force to be composed of an inertial and a drag component. Forces resulting from currents are similar to those for wave-associated flows and can be superimposed on the wave forces, if applicable. Ice loads can be a dominant factor in cold regions. Drifting ice may cause significant impact forces, and ice grip on piles can

pose large uplift loads on the member upon a sudden rise of water level. Loadings from earthquakes are complex and may induce large lateral forces on a structure. Rigorous treatment of the problem requires a dynamic analysis; nevertheless, simplified design procedures using a pseudo-static analysis can be used to approximate the behavior of the system under earthquake excitation forces. Design for ship impact forces is important for fender piles. The magnitude of these forces depends largely upon the energy-absorbing capabilities of the system.

Various conventional methods to predict compressive load capacity of piles are presented in Chapter 3. These are based largely on theory and empiricism with the empirical factors often back-calculated from load test results. For pile groups, the compressive capacity can be determined either by empirical efficiency formulae or by Terzaghi and Peck's approach. The latter seems to be more reasonable and should be used for final computation of ultimate group capacity. Settlement is often a minor consideration for coastal structures. Under most circumstances, costly solutions to reduce settlement are not justified.

The methods to evaluate the ultimate uplift load capacity of pile foundations basically follow those adopted for compressive loads. However, the point resistance does not exist and the net weight of the piles may be significant in computation of the ultimate load capacity.

The design of laterally loaded piles is one of the more difficult areas of deep foundations. Recently developed procedures are largely based on computer-aided techniques. The

methods proposed by Broms are suitable for rapid hand calculations and are outlined in Chapter 5. The failure mode of the soil in front of the pile is assumed to be two-dimensional and the resistance provided by the soil is obtained from empirical data. The estimation of the deflection of piles under lateral loads is discussed in Section 5.4 and is based on the subgrade reaction model.

In addition to the requirement of load capacities, the design of pile foundations often incorporates other considerations that may strongly influence the performance of the foundations under loads. Some of the major problems such as scour, downdrag, etc., are highlighted in Chapter 6. They are not by all means exclusive, but they do represent the problems that are commonly encountered in practical situations.

The choice of material type for piles is discussed in Chapter 7. Each of the three commonly used materials (concrete, steel and wood) has its own advantages and disadvantages. Although the choice of material type will not greatly affect the computational design procedures, the determination should not be made after the design process is completed; instead, different possibilities should be reviewed throughout the analysis-design cycle.

The methods of installation, as described in Chapter 8, can have a marked influence on the actual performance of the pile foundations. Very often, construction limitations may prohibit the implementation of a certain design. Therefore, a designer should have considerable field experience before a good design

can be achieved.

Although the discussions presented herein cover a relatively wide range of topics, they are not by all means exhaustive. Good judgment must be exercised and every factor that can influence the results should be identified. Also, every design methodology has its own inherent assumptions and it is imperative that the designer has a sound understanding of any limitations involved in employing certain procedures for design.

The ultimate goal of all design is to achieve an optimum solution to properly defined objectives. On one hand, underdesign will lead to premature failure of the structure and on the other, overdesign can pose unnecessary financial hardship on the client. Both of these extremes should be avoided. The more complex the design, the more difficult it is to achieve the optimum solution.

Finally, it should be realized that analysis methods and techniques are advancing at a rapid rate; therefore, the designer should ensure that the most up-to-date information is available.

REFERENCES

American Petroleum Institute (1977), Recommended Practice for Planning, Designing and Constructing Fixed Offshore Platforms, Report 2A, 9th Edition, Washington, D.C., November.

American Wood Preservers Institute (1966), Pressure-Treated Timber Foundation Piles, prepared by Dames & Moore, Washington, D.C., February.

Awad, A. and Petrasovits, G. (1968), "Considerations on the Bearing Capacity of Vertical and Batter Piles Subjected to Forces Acting in Different Directions," Proceedings, 3rd Budapest Conference on Soil Mechanics and Foundation Engineering, Section 3, Budapest, pp. 483-497.

Beredugo, Y. O. (1966), "An Experimental Study of the Load Distribution in Pile Groups in Sand," Canadian Geotechnical Journal, Vol. 3, No. 3, August, pp. 145-166.

Berezantzev, V. G., Khristoforov, V. S. and Golubkov, V. N. (1961), "Load Bearing Capacity and Deformation of Piled Foundations," Proceedings, 5th International Conference on Soil Mechanics and Foundation Engineering, Vol. 2, Paris, pp. 11-15.

Bjerrum, L. (1957), "Norwegian Experiences with Steel Piles to Rock," Geotechnique, Vol. 7, No. 2, June, pp. 73-96.

Bjerrum, L. (1973), "Problems of Soil Mechanics and Construction on Soft Clays," Proceedings, 8th International Conference on Soil Mechanics and Foundation Engineering, Vol 3, Moscow, pp. 111-159.

Bowles, J. E. (1977), Foundation Analysis and Design, 2nd Edition, McGraw-Hill Book Company, New York.

Brady, G. S. and Clauser, H. R. (1977), Materials Handbook, McGraw-Hill Book Company, New York.

Broms, B. B. (1963), "Allowable Bearing Capacity of Initially Bent Piles," Journal of the Soil Mechanics and Foundations Division, ASCE, Vol. 89, No. SM5, September, pp. 73-90.

Broms, B. B. (1964a), "Lateral Resistance of Piles in Cohesive Soils," Journal of the Soil Mechanics and Foundations Division, ASCE, Vol. 90, No. SM2, March, pp. 27-63.

Broms, B. B. (1964b), "Lateral Resistance of Piles in Cohesionless Soils," Journal of the Soil Mechanics and Foundations Division, ASCE, Vol. 90, No. SM3, May, pp. 123-156.

Broms, B. B. (1966), "Methods of Calculating the Ultimate Capacity of Piles - A Summary," Sols-Soils, No. 18-19, pp. 21-32.

Broms, B. B. (1976), "Pile Foundations - Pile Groups," Proceedings, 6th European Conference on Soil Mechanics and Foundation Engineering, Vol. 2.1, Vienna, pp. 103-132.

Browne, R. D. and Domone, P. L. J. (1974), "The Long Term Performance of Concrete in the Marine Environment," Proceedings, Conference on Offshore Structures, Institution of Civil Engineers, London, pp. 31-41.

Burland, J. B. (1973), "Shaft Friction of Piles in Clay - A Simple Fundamental Approach," Ground Engineering, Vol. 6, No. 3, May, pp. 30-42.

Chandler, R. J. (1968), "The Shaft Friction of Piles in Cohesive Soils in Terms of Effective Stress," Civil Engineering and Public Works Review, Vol. 63, January, pp. 48-51.

Chappelear, J. E. (1959), "Wave Forces on Groups of Vertical Cylinders," Journal of Geophysical Research, Vol. 64, No. 2, February, pp. 199-208.

Chellis, R. D. (1961), Pile Foundations, 2nd Edition, McGraw-Hill Book Company, New York.

Claessen, A. I. M. and Horvat, E. (1974), "Reducing Negative Friction with Bitumen Slip Layers," Journal of the Geotechnical Engineering Division, ASCE, Vol. 100, No. GT8, August, pp. 925-944.

Clark, J. I. and Meyerhof, G. G. (1973), "The Behavior of Piles Driven in Clay," Canadian Geotechnical Journal, Vol. 10, No. 1, February, pp. 86-102.

Coastal Engineering Research Center (1977), Shore Protection Manual, U.S. Army Corps of Engineers, Fort Belvoir, Virginia.

D'Appolonia, D. J., Poulos, H. G. and Ladd, C. C. (1971), "Initial Settlement of Structures on Clay," Journal of the Soil Mechanics and Foundations Division, ASCE, Vol. 97, No. SM10, October, pp. 1359-1377.

Davisson, M. T. (1963), "Estimating Buckling Loads for Piles," Proceedings, 2nd Pan-American Conference on Soil Mechanics and Foundation Engineering, Vol. 1, Sao Paulo, pp. 351-371.

Davisson, M. T. and Prakash, S. (1963), "A Review of Soil-Pile Behavior, Record No. 39, Highway Research Board, Washington, D.C., pp. 25-48.

Davisson, M. T. and Robinson, K. E. (1965), "Bending and Buckling of Partially Embedded Piles," Proceedings, 6th International Conference on Soil Mechanics and Foundation Engineering, Vol. 2, Montreal, pp. 243-246.

Davisson, M. T. (1970), "Lateral Load Capacity of Piles," Record No. 333, Highway Research Board, Washington, D.C., pp. 104-112.

Deep Foundations Institute (1979), Inspector's Manual for Pile Foundations, Springfield, New Jersey.

Degenkolb, H. J. (1970), Earthquake Forces on Tall Structures, Bethlehem Steel, Pittsburgh, Pennsylvania.

de Mello, V. F. B. (1969), "Foundations of Buildings on Clay," State-of-the-Art Volume, 7th International Conference on Soil Mechanics and Foundation Engineering, Mexico City, pp. 44-136.

Esrig, M. I. and Kirby, R. C. (1979), "Soil Capacity for Supporting Deep Foundation Members in Clay," STP 670 - Behavior of Deep Foundations, ASTM, pp. 27-63.

Flaate, K. and Selnes, P. (1977), "Side Friction of Piles in Clay," Proceedings, 9th International Conference on Soil Mechanics and Foundation Engineering, Vol. 2, Tokyo, pp. 517-522.

Frye, S. C. (1970), "Protection of Piling," in Design and Installation of Pile Foundations and Cellular Structures, Ed. by H. Y. Fang and T. D. Dismuke, Envo Publishing Company, Lehigh Valley, Pennsylvania, pp. 191-207.

Gilbert, S. P. (1970), "Pile Alignment and Selection of Hammer," Pile Foundation Know-how, American Wood Preservers Institute, Washington, D.C., pp. 50-53.

Hall, M. A. (1958), "Laboratory Study of Breaking Wave Forces on Piles," Technical Memorandum No. 106, U.S. Army Corps of Engineers, Beach Erosion Board, Fort Belvoir, Virginia.

Hornbostel, C. (1978), Construction Materials, John Wiley & Sons, New York.

Hubbell, W. D. and Kulhawy, F. H. (1979), Environmental Loads for Coastal Structures, New York Sea Grant Institute, Albany, New York.

Hubbell, W. D. and Kulhawy, F. H. (1979), Coastal Construction Materials, New York Sea Grant Institute, Albany, New York.

Hunt, H. W. (1979), Design & Installation of Driven Pile Foundations, Associated Pile and Fitting Corp., Clifton, New Jersey.

Johnson, S. M. (1962), "Determining the Capacity of Bent Piles," Journal of the Soil Mechanics and Foundations Division, ASCE, Vol. 88, No. SM6, June, pp. 65-79.

Kishida, H. and Meyerhof, G. G. (1965), "Bearing Capacity of Pile Groups Under Eccentric Loads in Sand," Proceedings, 5th International Conference on Soil Mechanics and Foundation Engineering, Vol. 2, Montreal, pp. 270-274.

Koerner, R. M. and Mukhopadhyay, C. (1972), "Behavior of Negative Skin Friction on Model Piles in Medium-Plasticity Silt," Record No. 405, Highway Research Board, Washington, D.C., pp. 34-44.

Kuhn, S. H. and Williams, A. B. (1961), "Scour Depth and Soil Profile Determinations in River Beds," Proceedings, 5th International Conference on Soil Mechanics and Foundation Engineering, Vol. 1, Paris, pp. 487-490.

Laird, A. D. K. (1962), "Wave Forces on Flexible Oscillating Cylinders," Journal of the Waterways and Harbors Division, ASCE, Vol. 88, No. WW3, August, pp. 125-137.

Laursen, E. M. (1962), "Scour at Bridge Crossings," Transactions, ASCE, Vol. 127, Part 1, pp. 166-209.

Lo, M. B. (1967), Discussion to Paper by Y. O. Beredugo, Canadian Geotechnical Journal, Vol. 4, No. 3, August, pp. 353-354.

Machemehl, J. L. and Abad, G. (1975), "Scour around Pile Foundations," Proceedings, 7th Annual Offshore Technology Conference, Vol. 2, Houston, pp. 691-702.

McClelland, B., Focht, J. A. and Emrich, W. J. (1969), "Problems in Design and Installation of Offshore Piles," Journal of the Soil Mechanics and Foundations Division, ASCE, Vol. 95, No. SM6, June, pp. 1419-1514.

McClelland, B. (1974), "Design of Deep Penetration Piles for Ocean Structures," Journal of the Geotechnical Engineering Division, ASCE, Vol. 100, No. GT7, July, pp. 705-747.

McNulty, J. F. (1956), "Thrust Loading on Piles," Journal of the Soil Mechanics and Foundations Division, ASCE, Vol. 82, No. SM2, April, Paper No. 940, 25 pp.

Meyerhof, G. G. (1951), "The Ultimate Bearing Capacity of Foundations," Geotechnique, Vol. 2, No. 4, December, pp. 301-332.

Meyerhof, G. G. (1963), "Some Recent Research on the Bearing Capacity of Foundations," Canadian Geotechnical Journal, Vol. 1, No. 1, February, pp. 16-26.

Meyerhof, G. G. and Adams, J. I. (1968), "The Ultimate Uplift Capacity of Foundations," Canadian Geotechnical Journal, Vol. 5, No. 4, November, pp. 225-244.

Meyerhof, G. G. (1976), "Bearing Capacity and Settlement of Pile Foundations," Journal of the Geotechnical Engineering Division, ASCE, Vol. 102, No. GT3, March, pp. 195-228.

Morison, J. R., O'Brien, M. P., Johnson, J. W. and Schaaf, S. A. (1950), "The Forces Exerted by Surface Waves on Piles," Petroleum Transactions, American Institute of Mining, Metallurgical and Petroleum Engineers, Vol. 189, TP2846, pp. 149-154.

Muga, B. J. and Wilson, J. F. (1970), Dynamic Analysis of Ocean Structures, Plenum Press, New York.

Murphy, D. J. (1974), "Pile Foundations Capacity and Settlement Potential," Paper presented at Piletalk Foundation Seminar on Current Practices in Pile Design and Installation, Saddle Brook, New Jersey, February.

Nair, K. (1969), "Dynamic and Earthquake Forces on Deep Foundations," STP 444 - Performance of Deep Foundations, ASTM, pp. 229-261.

Nordlund, R. L. (1963), "Bearing Capacity of Piles in Cohesionless Soils," Journal of the Soil Mechanics and Foundations Division, ASCE, Vol. 89, No. SM3, May, pp. 1-35.

Newmark, N. (1956), "The Effect of Dynamic Loads on Offshore Structures," Proceedings, 8th Texas Conference on Soil Mechanics and Foundation Engineering, Austin, Texas, September, 30 pp.

Palmer, H. D. (1969), "Wave-induced Scour on the Sea Floor," Proceedings, Civil Engineering in the Oceans II, Miami Beach, Florida, pp. 703-716.

Petersen, C. and Soltz, G. (1975), "Ocean Corrosion," Chapter 5 in Introduction to Ocean Engineering, Ed. by H. Schenck, McGraw-Hill Book Company, New York.

Peurifoy, R. L. (1979), Construction Planning, Equipment and Methods, 3rd Edition, McGraw-Hill Book Company, New York.

Portland Cement Association (1968), Design and Control of Concrete Mixtures, 11th Edition, Skokie, Illinois.

Poulos, H. G. and Davis, E. H. (1968), "The Settlement Behavior of Single Axially-Loaded Incompressible Piles and Piers," Geotechnique, Vol. 18, No. 3, September, pp. 351-371.

Poulos, H. G. and Davis, E. H. (1974), Elastic Solutions for Soil and Rock Mechanics, John Wiley & Sons, New York.

Quinn, A. D. (1972), Design and Construction of Ports and Marine Structures, 2nd Edition, McGraw-Hill Book Company, New York.

Reese, L. C., Cox, W. R. and Koop, F. B. (1974), "Analysis of Laterally Loaded Piles in Sand," Proceedings, 6th Annual Offshore Technology Conference, Vol. 2, Houston, pp. 473-483.

Reese, L. C. and Desai, C. S. (1977), "Laterally Loaded Piles," Chapter 9 in Numerical Methods in Geotechnical Engineering, Ed. by C. S. Desai and J. T. Christian, McGraw-Hill Book Company, pp. 297-325.

Romanoff, M. (1962), "Corrosion of Steel Piling in Soils," National Bureau of Standards Monograph 58, U.S. Department of Commerce, Washington, D.C.

Rowe, P. W. (1956), Discussion to Paper by K. Terzaghi, Geotechnique, Vol. 6, No. 2, June, pp. 94-98.

Saffery, M. R. and Tate, A. P. K. (1961), "Model Tests on Pile Groups in a Clay Soil with Particular Reference to the Behavior of the Group When It Is Loaded Eccentrically," Proceedings, 5th International Conference on Soil Mechanics and Foundation Engineering, Vol. 2, Paris, pp. 129-134.

Seed, H. B. and Reese, L. C. (1957), "The Action of Soft Clay Along Friction Piles," Transactions, ASCE, Vol. 122, pp. 731-754.

Seed, H. B. and Whitman, R. V. (1970), "Design of Earth Retaining Structures for Dynamic Loading," Proceedings, ASCE Specialty Conference on Lateral Stresses in the Ground and Design of Earth Structures, Cornell University, Ithaca, New York, pp. 103-147.

Soderberg, L. (1962), "Consolidation Theory Applied to Foundation Pile Time Effects," Geotechnique, Vol. 12, No. 3, September, pp. 217-225.

Sowa, V. A. (1970), "Pulling Capacity of Concrete Cast in Situ Bored Piles," Canadian Geotechnical Journal, Vol. 7, No. 4, November, pp. 482-493.

Sowers, G. F., Martin, C. B., Wilson, L. L. and Fausold, M. (1961), "The Bearing Capacity of Friction Pile Groups in Homogeneous Clay from Model Studies," Proceedings, 5th International Conference on Soil Mechanics and Foundation Engineering, Vol. 2, Paris, pp. 155-159.

Sowers, G. F. (1979), Introductory Soil Mechanics and Foundations: Geotechnical Engineering, 4th Edition, MacMillan Publishing Company, New York.

Terzaghi, K. (1955), "Evaluation of Coefficients of Subgrade Reaction," Geotechnique, Vol. 5, No. 4, December, pp. 297-326.

Terzaghi, K. and Peck, R. B. (1967), Soil Mechanics in Engineering Practice, 2nd Edition, John Wiley & Sons, New York.

Tomlinson, M. J. (1957), "The Adhesion of Piles Driven in Clay Soils," Proceedings, 4th International Conference on Soil Mechanics and Foundation Engineering, Vol. 2, London, pp. 66-71.

Tomlinson, M. J. (1971), "Some Effects of Pile Driving on Skin Friction," Proceedings, Conference on Behavior of Piles, Institution of Civil Engineers, London, pp. 107-114.

Tomlinson, M. J. (1977), Pile Design and Construction Practice, Viewpoint Publications, London.

U. S. Department of Commerce (1973), Earthquake History of the United States, U. S. Government Printing Office, Washington, D.C.

U. S. Department of Commerce and U. S. Department of the Interior (annual), United States Earthquake, U. S. Government Printing Office, Washington, D.C.

U. S. Forest Product Laboratory (1974), Wood Handbook, U. S. Department of Agriculture, Forest Service, Agricultural Handbook No. 72, Washington D.C.

Vesić, A. S. (1965), "Ultimate Loads and Settlements of Deep Foundations in Sand," Proceedings, Symposium on Bearing Capacity and Settlement of Foundations, Duke University, Durham, North Carolina, pp. 53-68.

Vesić, A. S. (1967), "A Study of Bearing Capacity of Deep Foundations," Final Report, Project B-189, School of Civil Engineering, Georgia Institute of Technology, Atlanta, Georgia.

Vesić, A. S. (1969), "Experiments with Instrumented Pile Groups in Sand," STP 444 - Performance of Deep Foundations, ASTM, pp. 177-222.

Vesić, A. S. (1977), Design of Pile Foundations, National Cooperative Highway Research Program, Synthesis of Highway Practice No. 42, Transportation Research Board, Washington, D.C.

Vijayvergiya, V. N. and Focht, J. A. Jr. (1972), "A New Way to Predict the Capacity of Piles in Clay," Proceedings, 4th Annual Offshore Technology Conference, Vol. 2, Houston, pp. 865-874.

Wade, B. G. and Dwyer, M. (1976), "On the Application of Morison's Equation to Fixed Offshore Platforms," Proceedings, 8th Annual Offshore Technology Conference, Vol. 3, Houston, pp. 1181-1190.

Watkins, L. (1969), "Corrosion and Protection of Steel Piling in Seawater," Technical Memorandum No. 27, U. S. Army Corps of Engineers, Coastal Engineering Research Center, Fort Belvoir, Virginia.

Whitaker, T. (1957), "Experiments with Model Piles in Groups," Geotechnique, Vol. 7, No. 4, December, pp. 147-167.

Wiegel, R. L. (1964), Oceanographical Engineering, Prentice-Hall Book Company, New York.

Wu, T. H. (1976), Soil Mechanics, 2nd Edition, Allyn and Bacon, Inc., Boston.

APPENDIX

EXAMPLE PROBLEMS

EXAMPLE PROBLEM 2.1

DESIGN DATA: Wave period, $T = 8$ sec

Pile diameter, $D = 1.5$ ft (0.46 m)

Water depth, $d = 10$ ft (3.05 m)

PROBLEM STATEMENT: Can force calculations be based on Morison's Equation?

SOLUTION: $\frac{d}{gT^2} = \frac{10}{(32.2)(8)^2} = 0.0049$

From Fig. 2.2,

$$L_o = 5.12\ T^2 = 5.12(8)^2 = 328 \text{ ft}$$

$$\frac{L_A}{L_o} = 0.40$$

$$L_A = 0.40(328) = 131 \text{ ft}$$

$$\frac{D}{L_A} = \frac{1.5}{138} = 0.01$$

According to Equation 2.4,

Morison's Equation can be used.

EXAMPLE PROBLEM 2.2

DESIGN DATA: Pile diameter, D = 1 ft (0.3 m)

Maximum horizontal velocity at still water level, u_{max} = 3 ft/sec (0.9 m/sec)

Kinematic viscosity of water, $\upsilon = 1X10^{-5}$ ft^2/sec ($9.3X10^{-7}$ m^2/sec)

PROBLEM STATEMENT: Determine the inertial and drag coefficients.

SOLUTION: From Equation 2.8,

$$R_e = \frac{u_{max}D}{\upsilon} = \frac{(3)(1)}{1X10^{-5}} = 3X10^5$$

From Equation 2.6,

$$C_M = 2.5 - \frac{R_e}{5X10^5}$$

$$= 2.5 - \frac{3X10^5}{5X10^5}$$

$$= \underline{1.9}$$

From Fig. 2.3,

$$C_D = \underline{0.98}$$

EXAMPLE PROBLEM 2.3

DESIGN DATA: Wave height, H = 20 ft (6.10 m)

Wave period, T = 10 sec

Pile diameter, D = 2 ft (0.6 m)

Water depth, d = 80 ft (24.4 m)

Drag coefficient, $C_D = 0.7$

Inertial coefficient, $C_M = 1.5$

PROBLEM STATEMENT: Determine the maximum wave force on the pile.

SOLUTION: $\frac{d}{gT^2} = \frac{80}{(32.2)(10)^2} = 0.025$

From Fig. 2.2,

$$\frac{L_A}{L_o} = 0.82$$

$$L_o = 5.12\ T^2 = 5.12(10)^2 = 512 \text{ ft}$$

$$L_A = 0.82(512) = 420 \text{ ft}$$

$$\frac{D}{L_A} = \frac{2}{420} = 0.0048 < 0.05 \text{ (Equation 2.4)}$$

$\therefore$ Morison's Equation is valid.

From Fig. 2.8,

$$\frac{H_b}{gT^2} = 0.018$$

$$H_b = 0.018(32.2)(10)^2 = 58 \text{ ft}$$

$$\frac{H}{H_b} = \frac{20}{58} = 0.34$$

From Figs. 2.4 and 2.5,

$$K_{im} = 0.42$$

$$K_{Dm} = 0.27$$

From Equations 2.15 and 2.16,

$$F_{im} = C_M \gamma \frac{\pi D^2}{4} H K_{im}$$

$$= (1.5)(64)\frac{\pi(2)^2}{4}(20)(0.42)$$

$$= 2533 \text{ lbs}$$

$$F_{Dm} = C_D \frac{1}{2} \gamma D H^2 K_{Dm}$$

$$= (0.7)(0.5)(64)(2)(20)^2(0.27)$$

$$= 4838 \text{ lbs}$$

From Equation 2.21,

$$W = \frac{C_M D}{C_D H}$$

$$= \frac{(1.5)(2)}{(0.7)(20)}$$

$$= 0.21$$

$$\frac{H}{gT^2} = \frac{20}{(32.2)(10)^2} = 0.0062$$

Interpolating between Figs. 2.10 and 2.11,

$$\phi_m = 0.17$$

From Equation 2.22,

$$F_m = \phi_m \gamma C_D H^2 D$$

$$= (0.17)(64.0)(0.7)(20)^2(2)$$

$$= \underline{\underline{6090 \text{ lbs}}} \quad (27 \text{ kN})$$

EXAMPLE PROBLEM 2.4

DESIGN DATA: Same as Example Problem 2.3.

PROBLEM STATEMENT: Determine the maximum moment on the pile.

SOLUTION: Interpolating between Figs. 2.14 and 2.15,

$$\alpha_m = 0.12$$

From Equation 2.23,

$$M_m = \alpha_m \gamma C_D H^2 D$$

$$= (0.12)(64.0)(0.7)(20)^2(2)$$

$$= \underline{4300 \text{ lb-ft}} \ (5830 \text{ N-m})$$

EXAMPLE PROBLEM 2.5

DESIGN DATA: Same as Example Problem 2.3.
Two piles that are spaced 60 ft apart in the direction of wave propagation.

PROBLEM STATEMENT: Determine the maximum total force acting on the two piles (use Airy theory).

SOLUTION: From Equations 2.19 and 2.20,

$$F_I = F_{Im} \sin\theta = 2533 \sin\theta$$

$$F_D = F_{Dm} \cos\theta\,|\cos\theta| = 4838 \cos\theta\,|\cos\theta|$$

$$F_T = F_I + F_D = 2533 \sin\theta + 4838 \cos\theta\,|\cos\theta|$$

The variation of F_T with θ is plotted in Fig. A.1

The phase difference between the two piles,

$$\theta = \frac{s}{L_A} \times 360^\circ$$

$$= \frac{60}{420} \times 360^\circ$$

$$= 51.4^\circ$$

The curve in Fig. A.1 can be shifted by 51.4° to represent the force variation on the second pile.

The sum of these two curves represents the variation of the total force acting on the two piles.

The maximum value of the total force as read directly from the curve is

$$[F_T]_{max} = \underline{9000 \text{ lbs}} \ (40 \text{ kN})$$

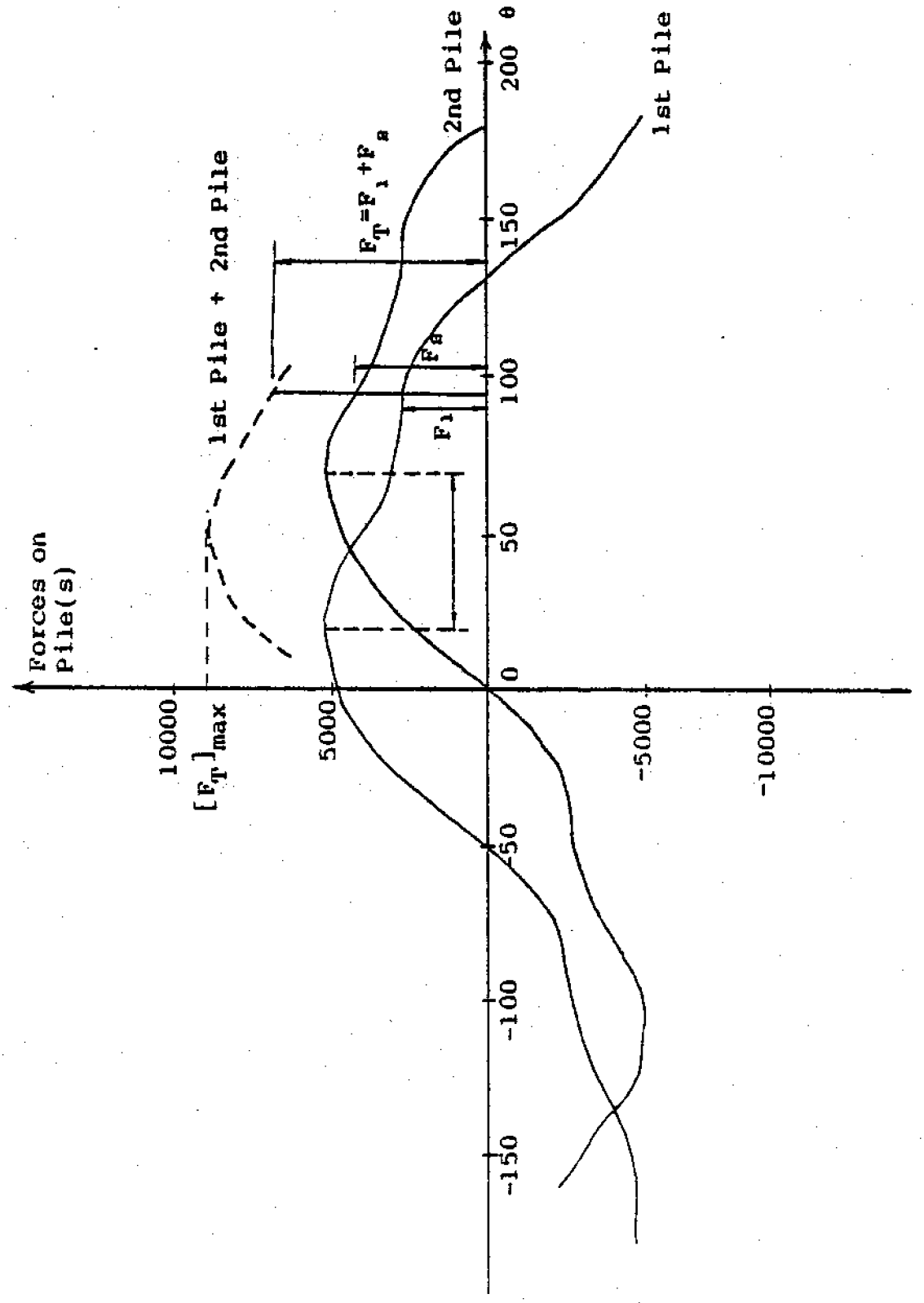

Fig. A.1 Variation of Forces on Single Piles and Pile Groups

EXAMPLE PROBLEM 2.6

DESIGN DATA: Same as Example Problem 2.3.

The pile is battered at an angle of 60° with the sea bed.

PROBLEM STATEMENT: Determine the maximum inertial and drag forces acting on the pile 40 ft below the the still water level (use Airy theory).

SOLUTIONS: From Equations 2.2 and 2.6,

$$f_{im} = C_M \frac{\gamma}{g} \frac{\pi D^2}{4} \frac{g\pi H}{L} \frac{\cosh[2\pi(z+d)/L]}{\cosh[\pi d/L]}$$

$$= 1.5 \frac{64.0}{32.2} \frac{\pi(2)^2}{4} \frac{(32.2)\pi(20)}{(420)} \frac{\cosh[2\pi(-40+80)/420]}{\cosh[2\pi(80)/420]}$$

$$= 45.1 \frac{\cosh(0.6)}{\cosh(1.2)}$$

$$= \underline{30 \text{ lb/ft}} \quad (438 \text{ N/m})$$

From Equations 2.3 and 2.5,

$$f_{Dm} = C_D \frac{1}{2} \frac{\gamma}{g} D \frac{H^2}{4} \frac{g^2T^2}{L^2} \left\{\frac{\cosh[2\pi(z+d)/L]}{\cosh[2\pi d/L]}\right\}^2$$

$$= (0.7)(0.5) \frac{64.0}{32.2} (2) \frac{(20)^2}{4} \frac{(32.2)^2(10)^2}{(420)^2} \left[\frac{\cosh(0.6)}{\cosh(1.2)}\right]^2$$

$$= 81.8 \left[\frac{\cosh(0.6)}{\cosh(1.2)}\right]^2$$

$$= \underline{35 \text{ lb/ft}} \quad (511 \text{ N/m})$$

EXAMPLE PROBLEM 2.7

DESIGN DATA: Diameter of pile, $D = 1$ ft (0.3 m)

Wave period, $T = 10$ sec

Wave height, $H = 20$ ft (6.1 m)

Drag coefficient $C_D = 0.7$

Maximum horizontal velocity at still water level,

$\bar{u}_{max} = 8$ ft/sec (2.4 m/sec)

PROBLEM STATEMENT: Determine the maximum lift force acting on a pile.

SOLUTION: $\frac{\bar{u}_{max}\, T}{D} = \frac{(8)(10)}{1} = 80$

$$\frac{H}{gT^2} = \frac{20}{(32.2)(10)^2} = 0.0062$$

From Fig. 2.19,

$\frac{\bar{u}_{max}\, T}{D} = 80$ is beyond the range of the figure.

$\therefore$ Take $C_L = C_D = 0.7$

From Example Problem 2.3,

$K_{Dm} = 0.27$

From Equation 2.25,

$$F_{Lm} = C_L \frac{1}{2} \gamma D H^2 K_{Dm}$$

$$= (0.7)(0.5)(64.0)(1)(20)^2(0.27)$$

$$= \underline{2420 \text{ lbs}} \ (10.8 \text{ kN})$$

EXAMPLE PROBLEM 3.1

DESIGN DATA: Concrete cylindrical pile in normally consolidated clay.

Diameter of pile, D = 1 ft (0.3 m)

Length of embedment, L = 50 ft (15.2 m)

Undrained shear strength of clay, c_u = 500 lb/ft^2 (24 kN/m^2)

Effective angle of internal friction of soil, $\bar{\phi} = 30°$

Submerged unit weight of soil, $\bar{\gamma}_s$ = 60 lb/ft^3 (9.4 kN/m^3)

Net weight of pile, $\bar{W}_p$ = 8000 lbs (35.6 kN)

PROBLEM STATEMENT: Determine the ultimate pile capacity under compressive loads.

SOLUTION: Area of pile shaft embedded in soil,

$$A_s = \pi D\, L = \pi(1)(50) = 157 \text{ ft}^2$$

Area of pile tip,

$$A_p = \frac{\pi D^2}{4} = \frac{\pi(1)^2}{4} = 0.79 \text{ ft}^2$$

(a) α - method

For soft clay, α = 1 (Fig. 3.3)

For normally consolidated clay, $N_c = 9$

From Equations 3.1, 3.5, 3.6 and 3.9,

$$Q_{ult} = \alpha c_u A_s + N_c c_u A_p - \bar{W}_p$$

$$= (1)(500)(157) + (9)(500)(0.79) - 8000$$

$$= \underline{74000 \text{ lbs}} \text{ (330 kN)}$$

(b) β - method

With $\frac{L}{D} = 50$ and $\bar{\phi} = 30°$, $N_q = 20$ (Fig. 3.12)

$= 0.30$ for normally consolidated soil

$(\bar{\sigma}_v)_{avg} = \bar{\gamma}_s \frac{L}{2} = (60)(\frac{50}{2}) = 1500$ lb/ft^2

$(\bar{\sigma}_v)_{tip} = \bar{\gamma}_s L = (60)(50) = 3000$ lb/ft^2

$Q_{ult} = \beta(\bar{\sigma}_v)_{avg} A_s + N_q (\bar{\sigma}_v)_{tip} A_p - \bar{W}_p$

$= (0.3)(1500)(157) + (20)(3000)(0.79) - 8000$

$= \underline{111,000 \text{ lbs}}$ (490 kN)

(c) λ - method

With L = 50 ft, $\lambda = 0.20$ (Fig. 3.9)

$Q_{ult} = \lambda[(\bar{\sigma}_v)_{avg} + 2c_u]A_s + N_c c_u A_p - \bar{W}_p$

$= 0.20[(1500) + 2(500)] (157) + (9)(500)$

$(0.79) - 8000$

$= \underline{74000 \text{ lbs}}$ (330 kN)

EXAMPLE PROBLEM 3.2

DESIGN DATA: Same as Example Problem 3.1, except:

Undrained shear strength of clay, c_u = 2500 lb/ft^2 (120 kN/m^2)

Overconsolidation ratio, OCR = 4

PROBLEM STATEMENT: Determine the α, β and λ coefficients.

SOLUTION: (a) α - coefficient

With $\frac{L}{D}$ = 50 and c_u = 2500 lb/ft^2

α = 0.70 (Fig. 3.5)

(b) β - coefficient

From Equation 3.13,

$$\beta = 0.3 \sqrt{OCR}$$

$$= 0.3 \sqrt{4}$$

$$= 0.6$$

(c) λ - coefficient

With L = 50 ft,

λ = 0.20 (Fig. 3.9)

EXAMPLE PROBLEM 3.3

DESIGN DATA: Timber pile in sand.

Diameter of pile, D = 1.5 ft (0.46 m)

Length of embedment, L = 45 ft (13.7 m)

Net weight of pile, $\overline{W}_p$ = 3000 lbs (13.4 kN)

Submerged unit weight of soil, $\overline{\gamma}_s$ = 55 lb/ft^3 (8.6 kN/m^3)

Effective angle of internal friction of soil, $\overline{\phi}$ = 27°

Rigidity Index, I_r = 80

PROBLEM STATEMENT: Determine the ultimate compressive load.

SOLUTION: From Equations 3.2 and 3.3,

Area of pile shaft, $A_s = \pi(1.5)(45) = 212$ ft^2

Area of pile tip, $A_p = \frac{\pi(1.5)^2}{4} = 1.8$ ft^2

With $\overline{\phi}$ = 27°, $\frac{L_c}{D} = 6$ (Fig. 3.13)

$L_c = 6(1.5) = 9.0$ ft

With $\frac{L}{D} = 30$ and $\overline{\phi}$ = 27°, $N_q = 10$ (Fig. 3.12)

From Equations 3.15 and 3.17,

$q_p = N_q \overline{\sigma}_{vp} = (10)(9X55) = 4950$ lb/ft^2

Average effective vertical stress along the pile,

$\overline{\sigma}_v = \overline{\gamma}_s(\frac{L}{2}) = (55)(\frac{45}{2}) = 1238$ lb/ft^2

Horizontal soil stress coefficient, K = 1.5 (Table 3.2)

Friction angle between pile and soil, $\delta = \frac{2}{3}(27) =$ 18° (Table 3.2)

From Equation 3.16,

$$f_s = K\bar{\sigma}_v \tan \delta$$

$$= (1.5)(1238)\tan 18°$$

$$= 603 \text{ lb/ft}^2$$

From Equation 3.1,

$$Q_{ult} = f_s A_s + q_p A_p - W_p$$

$$= (603)(212) + (4950)(1.8) - 3000$$

$$= \underline{134,000 \text{ lbs}} \ (595 \text{ kN})$$

EXAMPLE PROBLEM 3.4

DESIGN DATA: Same as Example Problem 3.3.

PROBLEM STATEMENT: Determine the ultimate compressive load capacity using Vesić's (1977) approach.

SOLUTION: From Equation 3.12,

$$K_o = 1 - \sin \bar{\phi} = 1 - \sin 27° = 0.55$$

Mean normal effective stress at the pile tip,

$$\bar{\sigma}_o = \frac{1+2K_o}{3} \bar{\sigma}_{vp}$$

$$= \frac{1+2(0.55)}{3} (55)(45)$$

$$= 1733 \text{ lb/ft}^2$$

Assuming little volume change, $I_{rr} = I_r = 80$

With $I_{rr} = 80$ and $\bar{\phi} = 27°$, $N_\sigma = 35$ (Fig. 3.15)

From Equation 3.18,

$$q_p = (35)(1733) = 60660 \text{ lb/ft}^2$$

From Equation 3.1,

$$Q_{ult} = f_s A_s + q_p A_p - \bar{W}_p$$

$$= (603)(212) + (60660)(1.8) - 3000$$

$$= \underline{234,000 \text{ lbs}} \text{ (1040 kN)}$$

EXAMPLE PROBLEM 3.5

DESIGN DATA: Same as Example Problem 3.1.

Width of block, B_g = 7 ft (2.1 m)

Length of block, L_g = 7 ft (2.1 m)

Center-to-center spacing of piles, s = 3 ft (0.9 m)

3X3 Group

PROBLEM STATEMENT: Determine the ultimate compressive capacity of the group.

SOLUTION: (a) Converse-Labarre Formula

From Equation 3.23,

$$\eta = 1 - \phi \left\{\frac{(n-1)m + (m-1)n}{90\ mn}\right\}$$

$$= 1 - \arctan\left(\frac{1}{3}\right) \left\{\frac{(3-1)3 + (3-1)3}{(90)(3)(3)}\right\}$$

$$= 1$$

From Equation 3.23,

Group capacity = 9X74000 lbs

= 666,000 lbs (2960 kN)

(b) Terzaghi and Peck's approach

Block failure, from Equation 3.24,

$$Q_{ult} = B_g L_g c_u N_c + 2D(B_g + L_g) c_u$$

$$= (7)(7)(500)(9) + 2(50)(7+7)(500)$$

$$= 920,500 \text{ lbs}$$

Individual pile failure,

$$Q_{ult} = 9X74000 = 666,000 \text{ lbs}$$

∴ Group capacity = 666,000 lbs (2960 kN)

EXAMPLE PROBLEM 4.1

DESIGN DATA: Same as Example Problem 3.1

PROBLEM STATEMENT: Determine the ultimate uplift capacity.

SOLUTION: (a) α - method

From Equation 5.1,

$$T_{ult} = c_\alpha A_s + \bar{W}_p$$

$$= (1)(500)(157) + 8000$$

$$= \underline{86500 \text{ lbs}} \ (385 \text{ kN})$$

(b) β- method

$$T_{ult} = \beta \bar{\sigma}_v A_s + \bar{W}_p$$

$$= (0.3)(1500)(157) + 8000$$

$$= \underline{78650 \text{ lbs}} \ (350 \text{ kN})$$

(c) λ- method

$$T_{ult} = \lambda(\bar{\sigma}_v + 2c_u)A_s + \bar{W}_p$$

$$= 0.20(1500 + 2X500)(157) + 8000$$

$$= \underline{86500 \text{ lbs}} \ (385 \text{ kN})$$

EXAMPLE PROBLEM 4.2

DESIGN DATA: Same as Example Problem 3.3.

PROBLEM STATEMENT: Determine the ultimate uplift capacity.

SOLUTION: $T_{ult} = f_s A_s + W_p$

$= (603)(212) + 3000$

$= \underline{130,800 \text{ lbs}}$ (582 kN)

EXAMPLE PROBLEM 4.3

DESIGN DATA: Same as Example Problem 3.5.

PROBLEM STATEMENT: Determine the ultimate uplift capacity of the group.

SOLUTION: Assuming the density of pile material is equal to that of the soil,

$\overline{W}_T$ = Volume of soil enclosed by group X submerged unit weight of soil

= (7X7X50)(60)

= 147,000 lbs

Block Failure, from Equation 5.3,

$$T_{ult} = 2D(L_g+B_g)c_u + \overline{W}_T$$

$$= 2(50)(7+7)(500) + 147,000$$

$$= 847,000 \text{ lbs}$$

Individual pile failure,

$$T_{ult} = 9(c_\alpha A_s + \overline{W}_p)$$

$$= 9(86500)$$

$$= 778,500 \text{ lbs}$$

∴ Group uplift capacity = 778,500 lbs (3460 kN)

EXAMPLE PROBLEM 5.1

DESIGN DATA: Free-headed pile in clay.

Diameter of pile, D = 2.0 ft (0.61 m)

Length of embedment, L = 30 ft (9.1 m)

Distance of lateral load above ground-line, e = 16 ft (4.9 m)

Undrained shear strength of clay, c_u = 1000 lb/ft^2 (48 kN/m^2)

Yield moment of pile, M_{yield} = 230,000 lb-ft (310 kN-m)

PROBLEM STATEMENT: Determine the ultimate lateral capacity of the pile.

SOLUTION: $\frac{L}{D} = \frac{30}{2} = 15$

$\frac{e}{D} = \frac{16}{2} = 8$

Assuming the pile to be rigid, from Fig. 5.7,

$$\frac{P_{ult}}{c_u D^2} = 24$$

$$P_{ult} = 24(1000)(2)^2 = 96000 \text{ lbs}$$

From Equation 5.2,

$$M_{max} = P_{ult}\left(e + 1.5D + \frac{0.5P_{ult}}{9c_u D}\right)$$

$$= 96000\left[16 + (1.5)(2) + \frac{0.5(96000)}{(9)(1000)(2)}\right]$$

$$= 208{,}000 \text{ lb-ft} < M_{yield}$$

$\therefore$ the pile is rigid.

P_{ult} = <u>96000 lbs</u> (430 kN)

EXAMPLE PROBLEM 5.2

DESIGN DATA: Same as Example Problem 5.1, except

Yield moment of the pile, M_{yield} = 170,000 lb-ft (230 kN-m)

PROBLEM STATEMENT: Determine the ultimate lateral capacity of the pile.

SOLUTION: From Example Problem 5.1,

$$M_{max} = 208{,}000 \text{ lb-ft} > M_{yield}$$

$\therefore$ the pile is flexible.

$$\frac{M_{yield}}{c_u D^3} = \frac{170{,}000}{(1000)(2.0)^3} = 21$$

From Fig. 5.11,

$$\frac{P_{ult}}{c_u D^2} = 2.2$$

$$\therefore P_{ult} = 2.2(1000)(2)^2$$

$$= \underline{\underline{8800 \text{ lbs}}} \ (39 \text{ kN})$$

EXAMPLE PROBLEM 5.3

DESIGN DATA: Restrained pile in sand.

Diameter of pile, D = 1.5 ft (0.46 m)

Length of embedment of pile, L = 12 ft (3.7 m)

Effective angle of internal friction of soil,

$\bar{\phi} = 30°$

Submerged unit weight of soil, $\bar{\gamma}_s = \gamma_s = 120$ lb/ft^3

(18.9 kN/m^3)

Yield moment of pile, $M_{yield} = 800{,}000$ lb-ft

(1085 kN-m)

PROBLEM STATEMENT: Determine the ultimate lateral capacity of the pile.

SOLUTION: $K_p = \frac{1+\sin \bar{\phi}}{1-\sin \bar{\phi}} = \frac{1+\sin 30°}{1-\sin 30°} = 3$ (Equation 6.14)

$\frac{L}{D} = \frac{12}{1.5} = 8$

Assuming the pile to be rigid, from Fig. 5.14,

$$\frac{P_{ult}}{K_p D^3 \gamma_s} = 95$$

$$P_{ult} = (95)(3)(1.5)^3(120)$$

$$= 115{,}400 \text{ lbs}$$

From Equation 5.5,

$$M_{max} = 0.67\, P_{ult}\, L$$

$$= 0.67\ (115{,}400)(12)$$

$$= 927{,}800 \text{ lb-ft} > M_{yield}$$

$\therefore$ the pile is flexible.

$$\frac{M_{yield}}{D^4 \gamma_s K_p} = \frac{800,000}{(1.5)^4 (120)(3)} = 439$$

From Fig. 5.18,

$$\frac{P_{ult}}{K_p D^3 \gamma_s} = 140$$

$$P_{ult} = (140)(3)(1.5)^3(120)$$

$$= \underline{170,100 \text{ lbs}} \ (760 \text{ kN})$$

EXAMPLE PROBLEM 5.4

DESIGN DATA: Free-headed pile in sand.

Length of embedment, L = 60 ft (18.3 m)

Distance of lateral load above the ground-line, e = 30 ft (0.91 m)

Modulus of elasticity of pile material, E_p = 30000 ksi (46.5 kN/mm^2)

Moment of inertia of cross-section of pile, I_p = 30000 in^4 (0.0125 m^4)

Horizontal load, P = 1,000,000 lbs (4450 kN)

Coefficient of modulus variation, n_h = 100,000 lb/ft^3 (15715 kN/m^3)

PROBLEM STATEMENT: Determine the pile deflection at ground-line.

SOLUTION: $E_pI_p = 6.25X10^9$ lb-ft^2

From Equation 5.10,

$$\eta = \sqrt[5]{\frac{n_h}{E_pI_p}} = \sqrt[5]{\frac{100000}{6.25X10^9}} = 0.11/\text{ft}$$

$$\frac{e}{L} = \frac{30}{60} = 0.5$$

From Fig. 5.28,

$$\frac{y_o(E_pI_p)^{3/5}(n_h)^{2/5}}{PL} = 1$$

$$y_o = \frac{(100000)(60)}{(6.25X10^{\ })^{3/5}(100000)^{2/5}}$$

$$= \underline{1 \text{ inch}} \ (25.4 \text{ mm})$$

EXAMPLE PROBLEM 6.1

DESIGN DATA: Pile pinned at top and bottom.

Length of embedment of pile, L = 50 ft (15.2 m)

Modulus of elasticity of pile material, E_p = 30000 ksi (46.5 kN/mm^2)

Moment of inertia of cross-section of pile, I_p = 30000 in^4 (0.0125 m^4)

Horizontal reactive stress, $k_h D$ = 200000 lb/ft^2 (9600 kN/m^2)

PROBLEM STATEMENT: Determine the critical buckling load.

SOLUTION:

$$R = \sqrt[4]{\frac{E_p I_p}{k_h D}} = \sqrt[4]{\frac{6.25X10^9}{200000}} = 13.2 \text{ ft}$$

From Equation 6.3,

$$\ell_{max} = \frac{L}{R} = \frac{50}{13.2} = 3.8$$

From Fig. 6.3,

$$U_{cr} = 2.15$$

From Equation 6.2,

$$Q_{cr} = U_{cr} \frac{E_p I_p}{R^2}$$

$$= (2.15) \frac{6.25X10^9}{(13.2)^2}$$

$$= \underline{77100 \text{ kips}} \text{ (343 MN)}$$

EXAMPLE PROBLEM 6.2

DESIGN DATA: Pile free at top and bottom.

Length of unsupported portion of pile, L_u = 30 ft (9.1 m)

Length of embedment, L = 60 ft (18.3 m)

Modulus of elasticity of pile material, E_p = 30000 ksi (46.5 kN/mm^2)

Moment of inertia of cross-section of pile, I_p = 30000 in^4 (0.0125 m^4)

Coefficient of modulus variation, n_h = 80000 lb/ft^3 (12.6 MN/m^3)

PROBLEM STATEMENT: Determine the critical buckling load.

SOLUTION:

$$T = \sqrt[5]{\frac{E_p I_p}{n_h}} = \sqrt[5]{\frac{6.25X10^9}{80000}} = 9.5 \text{ ft}$$

From Equation 6.10,

$$J_T = \frac{L_u}{T} = \frac{30}{9.5} = 3.2$$

From Equation 6.5,

$$z_{max} = \frac{L}{T} = \frac{60}{9.5} = 6.3 > 4$$

From Fig. 6.7,

$$S_T = 1.8$$

From Equation 6.11,

$$L_S = S_T T = (1.8)(9.5) = 17 \text{ ft}$$

From Equation 6.6,

$$Q_{cr} = \frac{\pi^2 E_p I_p}{4(L_u+L_s)^2}$$

$$= \frac{\pi^2(6.25X10^9)}{4(30+17)^2}$$

$$= \underline{7000 \text{ kips}} \text{ (31 MN)}$$

EXAMPLE PROBLEM 6.3

DESIGN DATA: Pile in clay.

Applied compressive load, Q = 20000 lbs (89 kN)

Critical buckling load, Q_{cr} = 1400000 lbs (6230 kN)

Horizontal subgrade modulus, k_h = 200000 lb/ft^3 (31.4 MN/m^3)

Undrained shear strength of clay, c_u = 1200 lb/ft^2 (57.5 MN/m^2)

Maximum horizontal deflection of pile, y_{max} = 0.5 ft (0.15 m)

PROBLEM STATEMENT: Will the bent pile overstress the soil?

SOLUTION: From Equation 6.12,

$$P_{max} = k_h \left(\frac{Q}{Q_{cr}-Q}\right) y_{max}$$

$$= 200000 \left(\frac{20000}{1400000-20000}\right)(0.5)$$

$$= 1450 \text{ lb/ft}^2$$

From Equation 6.13,

$$P_{all} = 3c_u$$

$$= 3(1200)$$

$$= 3600 \text{ lb/ft}^2 > 1450 \text{ lb/ft}^2$$

$\therefore$ the loading of the bent pile will not overstress the soil.

EXAMPLE PROBLEM 6.4

DESIGN DATA: Pile in high plasticity clay.

Diameter of pile, D = 1.5 ft (0.46 m)

Length of embedment, L = 35 ft (10.7 m)

Submerged unit weight of soil, $\bar{\gamma}_s$ = 60 lb/ft^3 (9.4 kN/m^3)

PROBLEM STATEMENT: Determine the maximum downdrag force on the pile.

SOLUTION: From Table 6.1,

$K = 0.60$

$\bar{\phi} = 10°$

Average effective vertical stress along the pile,

$$\bar{\sigma}_v = \bar{\gamma}_s \left(\frac{L}{2}\right) = (60)(17.5) = 1050 \text{ lb/ft}^2$$

From Equation 6.17,

$$Q_d = (\pi DL)(K\bar{\sigma}_v \tan\bar{\phi})$$

$$= \pi(1.5)(35)(0.60)(1050) \tan 10°$$

$$= \underline{67 \text{ kips}} \ (300 \text{ kN})$$